UCRL -9652

cy. 2

UNIVERSITY OF CALIFORNIA

Ernest O. Lawrence Radiation Laboratory

BIO-ORGANIC CHEMISTRY QUARTERLY REPORT
DEC. 1960 thru FEB. 1961

APRIL 1961

UCRL-9652 Cy 2

Please sign this card and return to Document Section, Tech. Info. Div., Bldg. 50, Rm. 110.

NAME	LOCATION	DATE
M. EDLUND	~~~	AUG 21 1961

UCRL-9652
UC-4 Chemistry-General
TID-4500 (16th Ed.)

UNIVERSITY OF CALIFORNIA

Lawrence Radiation Laboratory
Berkeley, California

Contract No. W-7405-eng-48

BIO-ORGANIC CHEMISTRY QUARTERLY REPORT

December 1960 through February 1961

April 1961

Printed in USA. Price $3.00. Available from the
Office of Technical Services
U. S. Department of Commerce
Washington 25, D.C.

BIO-ORGANIC CHEMISTRY QUARTERLY REPORT

December 1960 through February 1961

Contents

*Preceding Quarterly Reports: UCRL-9519, UCRL-9408.

F. ANIMAL BIOCHEMISTRY

UCRL-9652

BIO-ORGANIC CHEMISTRY QUARTERLY REPORT

December 1960 through February 1961

M. Calvin, Director
Edited by J. A. Bassham

Lawrence Radiation Laboratory and Department of Chemistry
University of California, Berkeley, California

April 1961

A. PHYSICAL CHEMISTRY

1. A PHOTOREFRACTOMETER USING A LIQUID LIGHT PIPE

Kenneth Sauer

Introduction

The current interest in the subject of fiber optics has brought about, among its many achievements, the development of a new technique for measuring refractive index. An instrument designed as a light-pipe refractometer or rod photorefractometer has been described by Kapany and Pike.[1] These authors have presented both a theoretical study of the phenomenon and experimental results arising from a prototype apparatus. The range of applicability of such a device is limited, however, by the availability of rod materials having suitable refractive indices. In particular, the available solid material which has the lowest refractive index and which is also transparent is fused quartz (n_D = 1.458). For reasons inherent in the geometry of the photorefractometer optics, the use of quartz rods does not permit high sensitivity of measurement on liquids having refractive index values less than 1.44. Aqueous solutions, therefore, are beyond the range of study of a system using solid rods. Kapany and Pike suggested the possibility of replacing the solid rod with a hollow cylindrical glass tube filled with a standard liquid. In this manner the effective refractive index of the light pipe is that of the reference liquid and can be varied over the complete range of refractive index for which liquids are available. Under these conditions the refractive index of the solid tube material now serves as an upper limit to the range of applicability. To date no experimental results using a hollow-tube refractometer have been reported, however.

In the study presented here a photorefractometer cell incorporating a liquid light pipe has been constructed, and experimental results are reported on solutions in both water and methanol as solvents. These solutions would not be capable of sensitive refractive index measurement using a solid-rod photorefractometer. In addition, some experiments have been carried out toward determining the refractive dispersion curves of colored substances, and some difficulties inherent in these measurements are discussed.

---

[1] N. S. Kapany and J. N. Pike, J. Opt. Soc. Am. 47, 1109 (1957).

General Principles

In order to describe the operation of the photorefractometer, let us first consider the simple case of a solid cylindrical rod surrounded by a liquid of lower refractive index, as shown in Fig. 1a. If the image of a point source of monochromatic light is focused on one of the polished ends of the cylindrical rod, the incident rays form a cone whose included angle is determined by the aperture and distance of the focusing lens. The rays entering the rod close to its axis pass down its length and emerge from the other end diminished only by the reflection losses at the rod ends. Other rays, at somewhat greater angles to the axis, are intercepted by the walls of the rod and totally reflected. These rays also eventually emerge from the other end of the rod. Still other rays, however, intercept the interface at an angle less than the critical angle, θ_c, measured relative to the normal to the surface, characteristic of the boundary. This critical angle is determined by the refractive indices of the rod and the sample liquid according to the equation

$$\sin \theta_c = n_s / n_r . \qquad (1)$$

Rays incident to the surface at less than the critical angle are refracted out of the rod, and therefore do not appear in the emergent light at the far end of the rod. Since, for a given rod material, the critical angle is determined solely by the refractive index of the liquid, the intensity of light transmitted through the far end of the rod is a measure of this refractive index. This, in brief, is the principle on which the photorefractometer depends. For a more detailed discussion of the theory, the reader is referred to the paper by Kapany and Pike.[1]

The case of the hollow-tube photorefractometer is illustrated in Fig. 1b. Here the situation is somewhat different, for the refractive index of the glass tube must be greater than that of either the reference or the sample liquid. In this case every ray that intercepts the inner surface of the glass tube is refracted into the glass and none is totally reflected immediately. At the outer surface of the rod, however, the light is passing from a medium of high refractive index toward one of lower refractive index. In this case the light is reflected as long as the angle of incidence is greater than the critical angle for this interface. These rays then pass back to the inner tube surface. If the two liquids should have the same refractive index ($n_r = n_s$) then the same situation would obtain at the inner boundary and the light would merely pass, by a succession of reflections, down inside the glass wall of the tube and eventually be absorbed at the end. If, however, the refractive index of the central reference liquid is somewhat greater than that of the sample liquid ($n_r > n_s$), then the critical angle for a ray in the glass rod incident on the inner surface is slightly greater than the critical angle for incidence at the outer surface. Consequently, some of the same rays which were at greater than the critical angle for the outer surface and were reflected, are at less than the (larger) critical angle for the inner surface and are therefore refracted into the central reference liquid. These rays eventually emerge from the end of the rod. In the glass wall rays whose angle of incidence is greater than the critical angles at both glass surfaces remain trapped in the wall, as in the case of all rays for $n_r = n_s$.

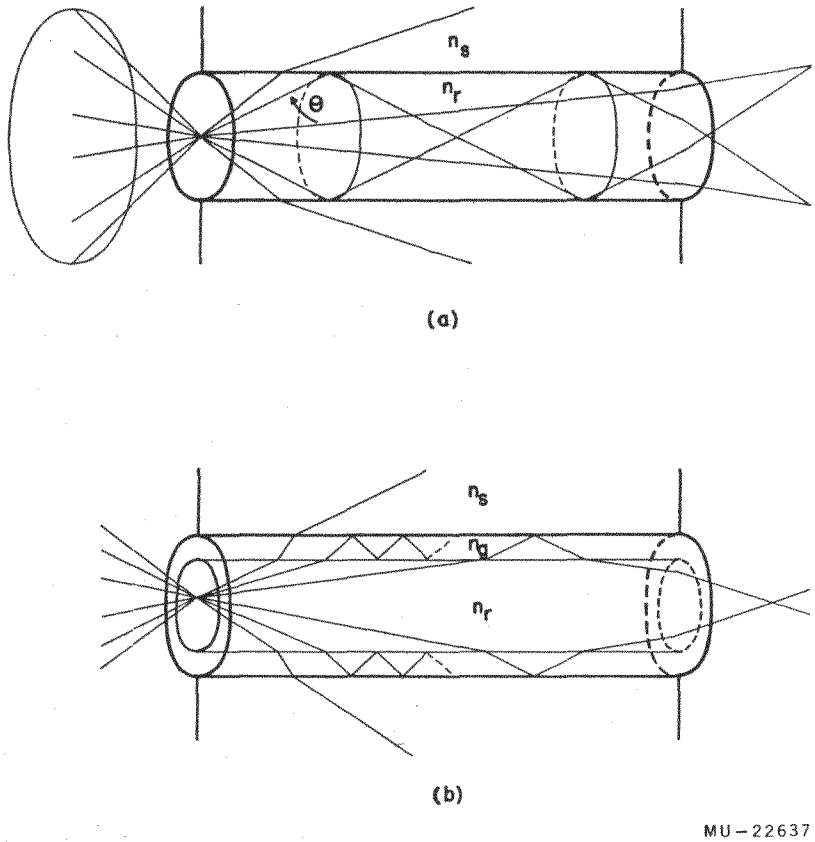

Fig. 1. Optical principles of photorefractometry using
(a) solid rod and
(b) liquid cylinder light pipes.

As in the solid rod photorefractometer, rays incident at the outer surface at a sufficiently small angle to the normal are refracted into the sample liquid and thereby lost to the measuring device.

It can be seem from this brief discussion of the hollow-tube photorefractometer that the intensity of the light emerging from the far end of the light pipe depends on the difference between the critical angles at the inner and outer surfaces of the glass tube -- consequently, on the difference in the refractive indices of the reference and sample liquids. The necessary refractive index relationship is $n_s \leqslant n_r < n_g$. For reasons discussed by Kapany and Pike, and also because of the finite wall thickness of the tubing, there is some loss in sensitivity for values of $\delta = n_r - n_s < 0.001$. This point is discussed later in connection with the experimental results.

Apparatus

The various components of the photorefractometer were mounted on an optical bench, as indicated diagrammatically in Fig. 2. A light source, focusing lenses, a lens stop, and neutral-density filters were aligned with the photorefractometer tube, and a monochromator and photomultiplier were used to monitor the emergent light intensity. The light source used was an Ediswan Pointolite rated at 150 candlepower and having a source diameter of about 2 mm. The light was collimated by a large-aperture short-focal-length lens and passed through one or more neutral-density filters, one of which had a 3-mm-diameter opaque spot which could be aligned precisely on the axis of the optical system. This beam-center stop served the purpose of blocking those rays which pass directly along the center of the liquid light pipe and therefore contain no information. The collimated beam was then focused by a lens identical to the first on a 2-mm-diam opening in the center of the cap on the photorefractometer cell. The included angle of rays incident on the end of the light pipe was 26 deg. The emergent beam was focused on the inlet slit of a Bausch and Lomb grating monochromator. The light from the outlet slit of the monochromator was collected by a short-focal-length lens system and caused to fall uniformly on the full face of a DuMont 6292 end-window photomultiplier. The photomultiplier was powered by a stabilized high-voltage supply and the output was recorded, for purposes of convenience, on a Varian Model G-10 Graphic Recorder (100 mv full scale). The photorefractometer was adjusted, either by changing the photomultiplier supply voltage or by introducing neutral density filters, so that the photomultiplier maximum average anode current rating was not exceeded.

A simple hollow-tube refractometer cell based on a standard polarimeter tube having a side-filling opening was constructed. A polarimeter tube 20 cm long and of 7 mm i.d. was used; however, others could be modified to suit the particular needs. A 20.15-cm length of ordinary borosilicate glass tubing (5 mm o.d., 3 mm i.d.) was centered in the polarimeter tube and sealed against the end windows by using standard O rings, as shown in detail in Fig. 3. Small brass ring spacers were used to keep the O rings centered during the assembly process. Before the second end cap and window were put on, the entire tube was filled with the reference liquid and the assembly then completed so as not to trap any bubbles of air. (No

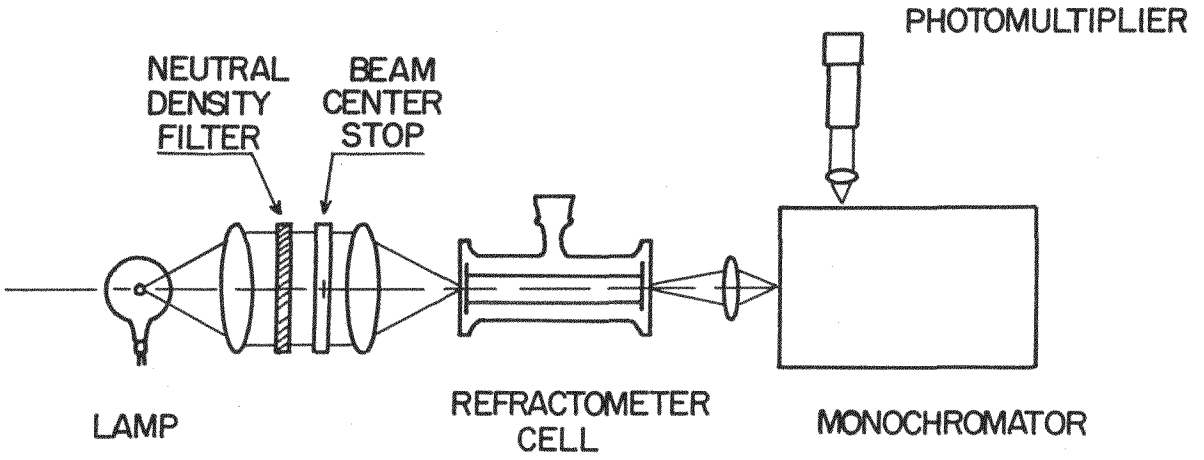

Fig. 2. Single-beam photorefractometer: schematic diagram.

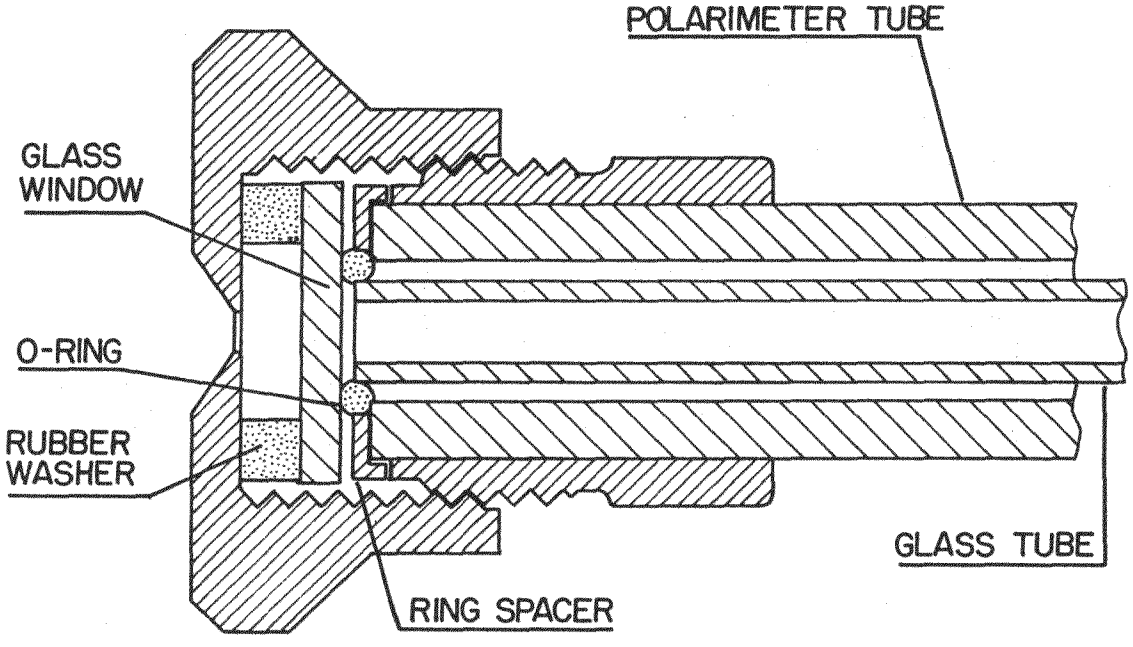

Fig. 3. Detail of assembly of the liquid cylinder photorefractometer cell.

precaution was taken to expel dissolved air from the liquid in advance. Consequently, a bubble usually formed in the tube after a few hours' use. If, on the next day, one end cap was removed and the air space filled with more of the reference liquid, no further trouble was encountered from this source. These tubes were then stable for weeks or months.)

After preparation of the liquid cylinder, the outer annular space was emptied through the side port and re-filled with the sample liquid under study. The 1-mm annular space is more than sufficient to obtain the full effect of the photorefractometer, which requires only about a 1-micron thickness of liquid. A thinner sample chamber would, however, make the process of introducing and removing the sample liquid more difficult, especially with regard to trapped air bubbles. The use of colored liquids in the sample chamber showed sensitively that there was no mixing of the annular sample liquid with the center reference liquid past the O-ring seals. Previous designs using machined teflon washers had given difficulty in this regard.

Results

Liquid Cylinder Photorefractometer Cell

An unlimited selection of reference liquids or solutions is available. The one chosen for these experiments was a 10% by volume solution of absolute ethanol in water. With this as reference, sample liquids in the region $n_D^{20°C} < 1.3370$, which is appropriate for dilute solutions in water or methanol, could be studied. A series of test solutions was prepared for purposes of calibrating the photorefractometer. In Fig. 4 is shown the transmitted light intensity at 589 mμ as a function of δ, the difference between the refractive index of the reference solution and that of the sample solution, for a series of solutions of ethanol in methanol (lower curve) and for a series of solutions of ethanol in water (upper curve). In both cases it can be seen that a linear relationship obtains between δ and transmitted intensity for values of δ essentially from 0 to 0.0080. The ethanol-water system shows some curvature for values of δ less than 8×10^{-4}. Both plots indicate considerably less sensitivity for negative values of δ; i.e., sample solutions having a greater refractive index than that of the reference liquid. For the lower curve, the beam intensity was reduced 50% from that in the upper by means of a neutral-density filter. In all experiments the sensitivity of the photorefractometer was held constant against the various slow drifts in the components by using a second cell containing a similar liquid light pipe and using a suitable fixed liquid in the sample chamber. This second cell was inserted into the beam between each pair of readings in a given set and the output was normalized by means of the fine adjustment on the photomultiplier supply voltage.

In both cases shown, the curve crosses the vertical axis ($\delta = 0$) considerably above the origin, indicating that an appreciable amount of light is falling on the photomultiplier even under conditions such that, in principle, none should be. This "zero intensity" prevents use of the technique to measure very much smaller values of δ sensitively. This point will be discussed later. When the beam-center stop is used, the large vertical intercept is still only partly (< 10%) due to light transmitted directly down the

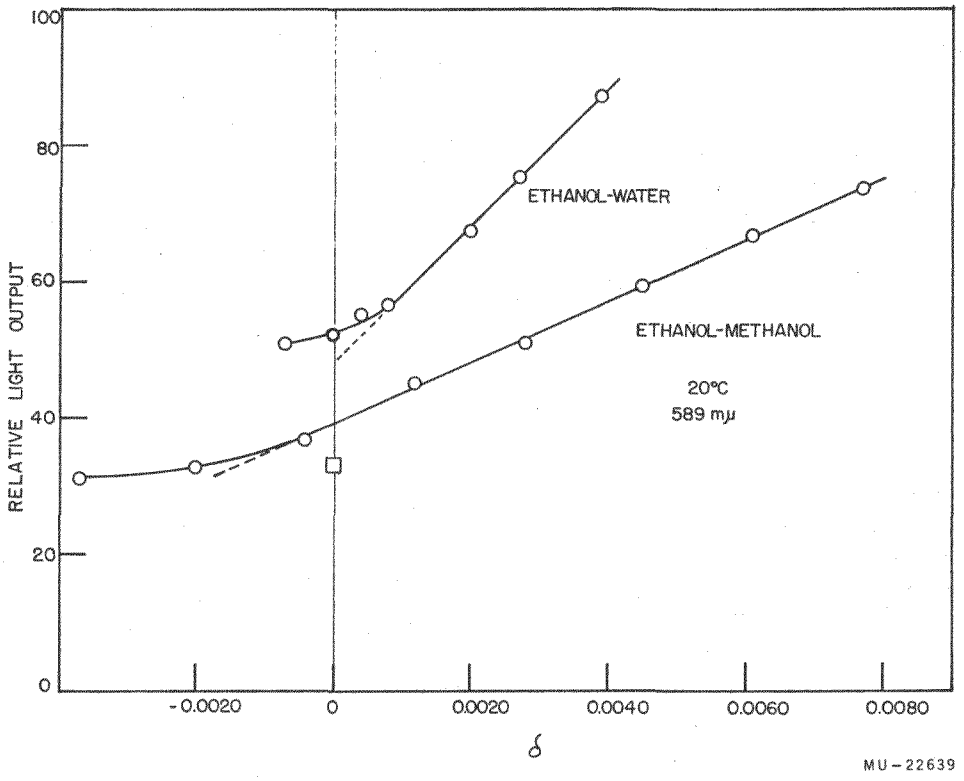

Fig. 4. Experimental results. Liquid light pipe: 10% ethanol in water ($n_D^{20°C}$ = 1.3370). Upper curve: solutions containing 0 to 12% ethanol in water. Lower curve: solutions containing 0 to 35 % ethanol in methanol; 50% neutral-density filter added in light path. Open square: sample solution of 10% ethanol in water, using 50% filter. Vertical scale is relative and is not exactly the same for the two sets of data.

center of the light pipe. The major portion results from internal reflections within the photorefractometer cell. The importance of these reflections is indicated by the fact that, in Fig. 4, the point (open square) corresponding to a measurement on a 10% ethanol-water solution does not fall on the curve for ethanol-methanol solutions. This is attributed to the differences in interfacial reflections of the two solvent systems, and emphasizes the need to perform a careful calibration using a liquid system similar to the one under study. These effects probably account for the observation that the points in the upper plot show curvature for small positive values of δ, whereas those of the lower are linear even through small negative values of δ. The former case is the more significant, as the same solution system is used as reference and as sample. Kapany and Pike[1] present reasons why liquid light pipes will give nonlinear relationships for small positive values of δ, although those authors indicate this will occur for values of less than 0.0015. Figure 4 indicates that the linear relationship holds down to about half this value for the ethanol-water system. Over most of the range studied, the points follow a much better straight line than was observed by Kapany and Pike. Undoubtedly as they point out, the nonlinearity of their measurements is associated with temperature effects resulting from their thermal method of changing the refractive index of the sample liquid.

The sensitivity of the method is best indicated in Fig. 4, upper curve, where a change of 10^{-4} in δ gave rise to a change of about 1 mv in the output signal. Since there was no observable noise, and long-term drifts and fluctuations were small owing to use of a stabilized voltage source for both the lamp and the power supply, these values are felt to represent the limits of sensitivity of the apparatus as described. A further increase in sensitivity--e.g., by removing the 5% transmission neutral-density filter present in the beam in all experiments-- was not feasible because of the large "zero intensity." Greater sensitivity could presumably be achieved by cancelling out the zero signal with an opposing potential, preferably from a second photomultiplier operating off the same power supply and monitoring the same light source. Such a double-beam apparatus is contemplated as a future modification. With adequate thermostating of the sample cell, it should permit the measurement of δ values as small as 10^{-6}.

Solid-Rod Photorefractometer

The useful range of the photorefractometer is indicated by the results shown in Fig. 5. In this case a solid fused quartz rod of 5 mm diameter is used in place of the liquid light pipe. Pure samples of benzene, carbon tetrachloride, chloroform, dioxane, and n-butanol were studied at 589 mμ. The figure shows that maximum sensitivity is attained for values in the range $0 < \delta < 0.012$. For values outside this range, the slope of the curve is less by a factor of at least 15. By comparison with Fig. 4, it is seen that this solid-rod refractometer would have at least 50-fold less sensitivity for dilute aqueous solutions ($\delta \approx 0.12$) than does the cell using a liquid light pipe.

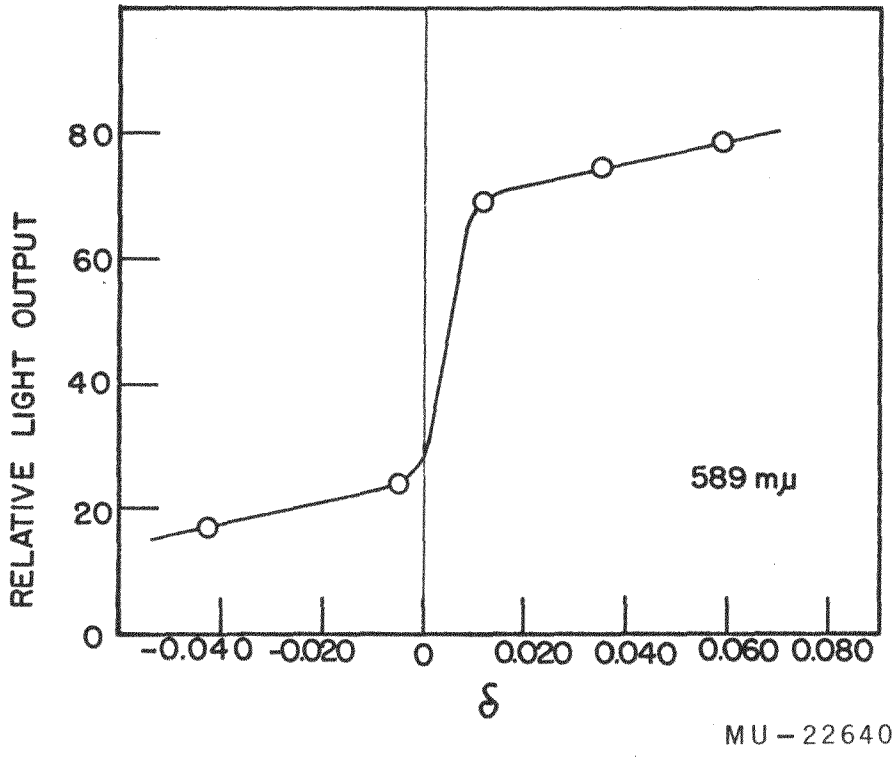

Fig. 5. Experimental results. Solid-rod light pipe: fused quartz (n_D = 1.458). Samples are various pure organic liquids.

Refractive Dispersion

Kapany[2] points out the advantages of using the photorefractometer for the measurement of relatively opaque or highly colored solutions. Since the reflection of the light at the boundary of the sample liquid involves penetration to a distance of approximately 1 wave length of the radiation used, there should be little reduction of the intensity of the light due to absorption. This would be in marked contrast with the situation arising from the use of the several types of conventional refractometers. Absorption is often found to reduce seriously the transmitted intensity, particularly for wave lengths in the vicinity of our absorption band. Through even a thin layer of sample such conventional refractive-dispersion measurements become impossible.

Experiments were conducted to determine the refractive-dispersion curves for colored solutions. In one series of experiments the measurements were made on solutions of methyl violet in n-butanol (n_D = 1.399) using the solid quartz rod light pipe (n_D for quartz is 1.458). As Fig. 5 shows, the sensitivity of the apparatus is low for $\delta = 0.06$, and it was necessary to use solutions containing about 1.4 mg/ml of methyl violet in n-butanol in order to observe a substantial refractive-index increment due to the solute. This solution had an optical density of 300 at 584 mμ, assuming Beer's Law holds from the 1000-fold more dilute soltuion actually measured in the Cary Model 14 spectrophotometer. For the measurement of the dispersion curve, at each wave-length setting of the monochromator the effects due to changing lamp intensity and photomultiplier sensitivity were corrected by changing the voltage of the photomultiplier power supply so as to give a fixed output reading when the second photorefractometer cell, containing only solvent in the sample chamber, was placed in the beam. In this way the readings were approximately normalized over the 350-to-780-mμ wave-length range studied. The curve of intensity of emergent light versus wave length for this solution was identical with the absorption spectrum of the solution, within the rather low sensitivity of the measurement. It did not at all resemble the expected dispersion curve. In the second series of experiments a much more favorable situation was utilized. The solution studied was one containing lamellar structures separated from sonicated spinach chloroplasts and suspended in water.[3] The resulting suspension had the appearance of a clear solution and did not settle on standing at 0°C overnight. The soltuion studied had an optical density of 45 at 680 mμ. A hollow-tube light pipe containing 10% ethanol in water was used. The apparent values of δ observed were between 2×10^{-4} and 2×10^{-3}, depending on the wave length. With reference to the solvent water ($n_D^{20^\circ C} = 1.3330$), these values represent increases in refractive index due to the solute of 4.2×10^{-3} to 5.8×10^{-3}. The plot of emergent light intensity versus wave length in this case gave a curve which was distorted from the absorption spectrum, yet was not obviously a simple dispersion curve. Jaffe, Goldring, and Oppenheim[4] point out that their measurements of infrared dispersion on absorbing substances, using the technique of critical-angle refractometry, give rise to curves from which a

---

[2] N. S. Kapany, Scientific American, November, 1960, p. 72.

[3] The author is indebted to Dr. Roderic B. Park of this Laboratory for furnishing this prepared sample.

[4] J. H. Jaffe, H. Goldring, and U. Oppenheim, J. Opt. Soc. Am. 49, 1199 (1959).

component resulting from absorption by the material must be subtracted in order to obtain the true dispersion curve. They present a theoretical treatment which shows that the critical angle for absorbing substances depends on the extinction coefficient as well as on the refractive index at any particular wave length.

The obvious result of the above measurements is that absorption by the colored solutions, even in the very thin reflecting layer, is the dominant factor in the change in the emergent light intensity. This situation can be improved by designing the light pipe in such a manner that rays at the critical angle for total reflection for the system will suffer only one such reflection, rather than many, during their passage through the cell. This will serve to decrease the effects due to absorption, which are cumulative, but will not affect the sensitivity of the refractive index measurement, which, in principle, is the same for a single reflection as for many. To achieve this goal it is necessary to have a large ratio of length to diameter of the light pipe and to adjust the refractive index of the reference liquid to be only slightly greater than that of the sample. Experiments in this direction are contemplated.

Photolysis of Chloroplast Fragments

The principal objective of the present experiments using the photorefractometer is to observe refractive index changes which occur upon illumination of photosynthetic materials. For this purpose experiments were carried out on the suspension of lamellar structures described above. The sample in the photorefractometer tube was illuminated from each side by two 1500-watt quartz-line lamps (General Electric 1500 T3Q/CL; 30,000 lumens) and the light was focused vertically on the tube by use of cylinder lenses. The incident intensity is estimated as 30,000 foot-candles; however, Corning 2404 sharp-cut filters in the beams permitted only wave lengths longer than about 620 mμ to enter the cell compartment. A shutter allowed the beams to be clocked without extinguishing the lamps. Measuring with the measuring radiation at 420, 430, 550, and 589 mμ, however, failed to show any sudden change (<1 sec) in refractive index when the shutters were opened or closed. Slow changes, undoubtedly due to temperature effects, were observed. The sample became quite warm to the touch when the light was left shining on it for several minutes. The sensitivity for measuring a sudden change is estimated as 0.00005 in terms of absolute refractive index; however, in terms of the contribution of the solute to the refractive index, the sensitivity is not better than 1 part in 100. Further experiments will be done using the greater sensitivity of a double-beam apparatus.

2. STUDIES ON THE GLASS ELECTRODE IN SOLUTIONS CONTAINING HYDROGEN ISOTOPES

Peter R. Hammond

The glass electrode method of measuring the hydrogen ion concentration of aqueous solutions has advantages over other methods in that it is simple and accurate to apply experimentally, hence it is widely used in biological research. The electrode is not easily poisoned or affected by oxidizing agents, reducing agents, or organic compounds, and it can be used with very small quantities of liquids.

The present availability of deuterium oxide is stimulating research on the deuterium isotope effects in chemistry and biology,[1] and an aspect that has received little attention is the convenient measurement of deuterium ion concentrations in heavy-water solutions. Methods that have been used rely on conductivity measurements,[2] spectrophotometry of acids with colored anions,[3] and measurements with deuterium gas[4] and quinhydrone electrodes.[5] For this reason a study of the behavior of glass electrode systems in solutions containing hydrogen isotopes was undertaken.

The emf across the glass membrane is said to result from the exchange of some of the cations of the glass with hydrogen ions in solution[6] to produce a pH-dependent potential difference[7] separately on each surface. Thus in the conventional glass electrode circuit it is the hydrogen ions that carry the current across the glass-solution interface. However, in the body of the glass it appears that the cations present are responsible[8] for carrying the largest fraction of the current.

Two problems, therefore, arise in applying the glass electrode to measuring deuterium ion concentration in solution. Firstly, does a surface exchange occur to give a similar pD-dependent emf, and, secondly, does the hydrogen ion alone, or solvated, carry current across the glass membrane? If hydrogen can cross the membrane, a protium oxide solution buffer placed in the interior of the glass electrode will change when measurements are taken in deuterium oxide solutions and an alteration in pD response will occur.

---

[1] Ann. N. Y. Acad. Sci. 84, 573 (1960) (Conference on Deuterium Isotope Effects in Chemistry and Biology).

[2] G. N. Lewis and P. W. Schutz, J. Am. Chem. Soc. 56, 1913 (1934); P. Ballinger and F. A. Long, J. Am. Chem. Soc. 81, 2347 (1959).

[3] D. C. Martin and J. A. V. Butler, J. Chem. Soc. 1939, 1366.

[4] Abel, Bratu, and Redlich, Z. physik. Chem. A173, 353 (1935).

[5] C. K. Rule and V. K. LaMer, J. Am. Chem. Soc. 60, 1974 (1938).

[6] K. Horovitz, Z. Physik 15, 369 (1923).

[7] M. Dole, J. A. Chem. Soc. 53, 4260 (1931).

[8] G. Haugaard, J. Phys. Chem. 45, 148 (1941).

Tritium Experiment

The first experiment was designed to investigate the transport of the current across the glass membrane. The evidence that the cations of the glass were mainly responsible came from the studies by Haugaard,[8] who passed an electric current across the membrane between dilute acid solutions on both sides of it. He found that the decrease in acid concentration on either side and the increase of residue left after evaporation on the cathode side (attributed to sodium chloride from the sodium-based glass) were equivalent to the amount of silver deposited in a silver coulometer in series with the cell. An increase in resistance of the glass with time during the electrolysis he attributed to the formation of two layers in which B, the layer containing hydrogen ions, had a lower conductance than the cations replaced. The layers are shown in Fig. 6(i), where A represents the layer still containing cations and B represents a layer in which replacement of cations with hydrogen ions during the electrolysis has occurred.

Haugaard's weights were on the order of 0.1-milligram equivalents and were not quoted to better than 1% accuracy. The agreement in weights was such that a conductance of 4% by hydrogen ions could not have been detected.[9] Also the resistance showed a linear relationship with time over 1000 hours. No limiting value that could be attributed to the conductance by the hydrogen ion was reached. Hence the possibility of a small transference of hydrogen ions across the membrane has not been eliminated by this experiment.

Electrolysis across the glass membrane was performed by using a solution of high tritium activity on the anode side, and the cathode compartment was analyzed after 130 hours.

Experimental Procedure

A miniature glass electrode (124138 of the Leeds and Northrup Company) constructed from a lithium-based glass and having a low sodium error at high pH, was used. It was suitable for electrolysis in small volumes of tritiated water. Also, the contents of the electrode could be easily interchanged.

Standard hydrochloric acid (0.02 N) made up in de-ionized water was placed in the interior of the electrode and a platinum wire in contact with this solution was sealed into the upper stem of the glass. A platinum anode was sealed into a glass tube and, together with the glass electrode, fitted tightly into a teflon stopper. These were contained in a small round-bottomed tube into which was placed hydrochloric acid (1.0 ml, 0.02 N, containing 58 mC tritium oxide). The cell was placed in an oil bath at $25 \pm 0.3^{\circ}C$, and was connected in series by means of shielded wires with a 5.0×10^5-ohm resistor and a 300-v dry battery. See Fig. 6 (ii). The voltage drop across the resistor was measured on a Cary Vibrating-Reed Electrometer.

[9] Author's interpretation.

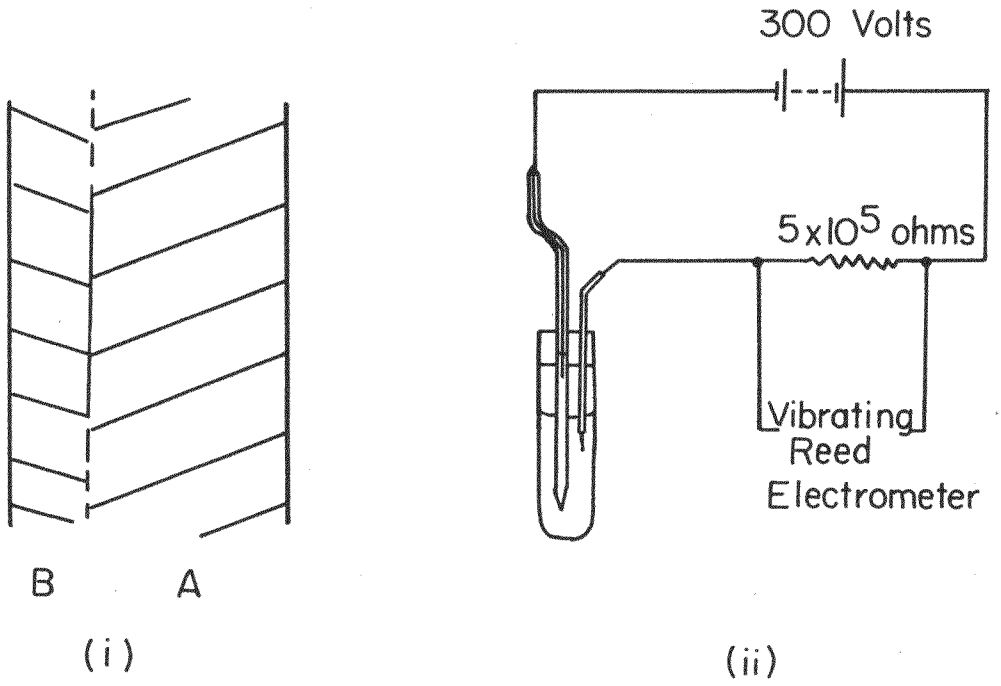

Fig. 6. (i) Composition of electrode glass during electrolysis
(ii) Electrolysis across membrane of glass electrode.

The cell resistance at the beginning of the experiment was 97 megohms, and showed marked temperature and voltage dependence. The deviations from a smooth curve of a plot of current against time during the electrolysis (Fig. 7) were in accord with temperature fluctuations about 25°C, but an increase of resistance with time clearly occurs.

The total current passed after 130 hours (0.49 coulombs) was obtained from the ratio of weights of the graph paper under the curve to the total paper. At the end of the experiment the electrode was carefully washed and cracked open and the contents (130 mg) was counted in scintillator solution No. 2 at -10°C.[10] For comparison, an equal weight of the original acid was counted under similar conditions and the counting efficiency was obtained from a standard sample.

Results

The counts obtained, together with standard deviations and efficiencies, are:

Electrode solution	308.5 ± 19	Efficiency 6% on thirty 10-minute counts.
Background	305.5 ± 15	
Electrode solution	4,245±60	Efficiency 7% on thirteen 100-minute counts
Background	4,218±69	

Thus no activity in the electrode solution has been detected, hence one cannot expect transfer of deuterium ions across the glass membrane under the conditions of measuring deuterium ion concentration (where emf's of less than a volt are concerned).

Extra activity equal to the standard deviation of the counts could have been detected, hence as little as 1.7×10^{-16} gram atom of tritium could have been found. Thus under the conditions of the experiment, hydrogen carried less than 2×10^{-6} of the total current through the glass, assuming no isotope effect for tritium/protium. This effect is likely to decrease the sensitivity of the experiment, for if the movement of a hydrogen ion in the body of the glass is considered as a continual association and dissociation of the ion with silica molecules making up the network, then the mobility of the hydrogen and tritium ions will be a function of K_H/K_T (the ratio of the dissociation constants in protium and tritium oxides) for silicic acid. K_H/K_D for an acid as weak as silicic is approximately 4, hence a ratio of 10 for K_H/K_T is not improbable. However, assuming an isotope effect even as great as 100, it can be said that the hydrogen ion carried less than 2×10^{-4} of the total current through the glass.

The tip of the glass electrode was carefully washed seven times in distilled water, dried with tissue paper, and counted in scintillator solution

[10] 2.0 l toluene, 2.0 l dioxane, 1.2 l absolute ethanol, 260 g naphthalene, 26 g 2,5-diphenyloxazole, 0.5 g 1,4-bis-(2(5-phenyloxazolyl)) benzene.

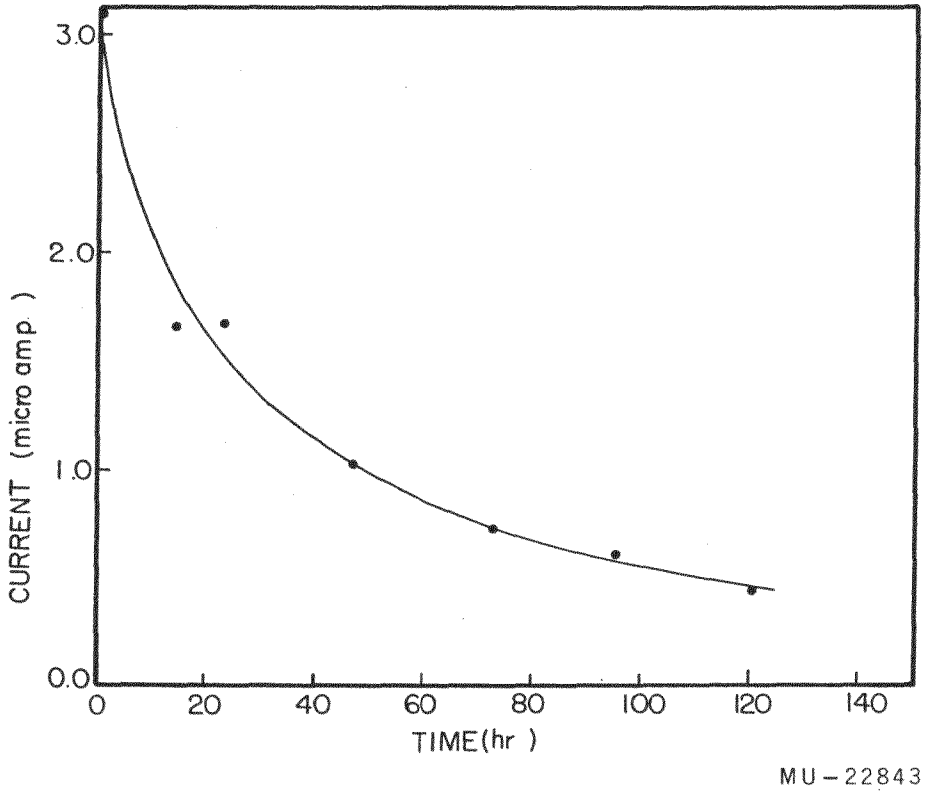

Fig. 7. Electrolysis current variation with time.

at room temperature. A high activity was found (first point of Fig. 8).

Complete exchange of the surface molecules of the glass with tritium together with an absorbed water layer two to three molecules thick could account for the high activity found, although, in view of the washing procedure, this was unlikely. Exchange of the surface silicate molecules only would have given a count estimated in the region of 35/min.[11] For comparison, a pyrex rod was immersed in tritiated water (58 mC/ml) for 5 min, dried with tissue paper, and washed seven times in distilled water as above. The count in scintillation solution was 261, whereas immersion in boiling water for 5 min reduced the count to 135 (the order of background). Also a similar glass electrode was immersed in dilute hydrochloric acid (0.02 N, 58 mC/ml) for 130 hr and was washed and treated as above. The first count was 3,000 counts/min and this was reduced to 250 by boiling the tip for 5 min in distilled water. Assuming that all the cations leaving the glass were replaced by hydrogen ions during the electrolysis, then a maximum possible count of 2×10^6 was to be expected.[12] The electrode tip was placed in boiling water and its activity against time of boiling was plotted (Fig. 8).

These results are interpreted to mean that considerable penetration of the glass by tritium ions had occurred under the conditions of the experiment. The boiling procedure was removing the ions nearest to the surface, and the residual activity found on prolonged boiling represented the ions inaccessible to water exchange.[13]

---

[11] This estimation may be out by a factor of a hundred either way because of the uncertainties in the assumptions involved. Nevertheless, the activity found is still too high to be accounted for just in terms of surface exchange. The following are assumed:
(a) K_H/K_T for silicic acid is as high as 10; hence the surface concentration is ten times the solution concentration in contact with it.
(b) The area occupied by each silicate group on the glass surface (0.4 cm^2) is 10 A^2 (compare W.H. Zachariasen, J. Am. Chem. Soc. 54, 3841 (1932); B.F. Warren, Chem. Revs. 26, 237 (1940)).
(c) Each silicate group on the surface has one position available for exchanging with hydrogen ions in solution.
(d) Tritium counting efficiencies are 6% (half normal), because of the limited 2π geometry of solution available to surface molecules.
Activity arising from tritium on the inside glass surface was neglected, as the solution inside the electrode had not been active.

[12] Assumptions: (a) K_H/K_T for silicic acid is 10, (b) mobility for a tritium ion in the glass is as high as for a proton, and (c) counting efficiency, 5%.

[13] Here a decrease in counting efficiency is also to be expected.

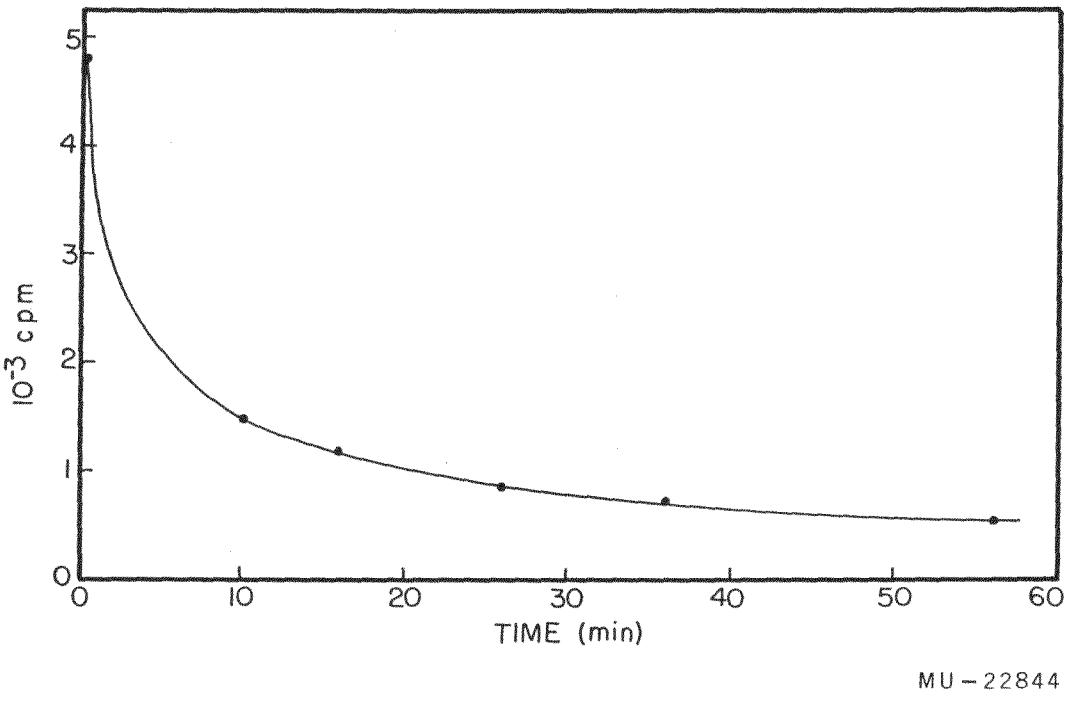

Fig. 8. Variation of activity in glass electrode membrane with time of boiling.

Deuterium Ion/emf Response

The second experiment was to investigate the deuterium ion/emf response. In view of the experiments by Hubbard and Cleek[14] a linear relationship and a pD dependence of 59 mv/pD was possible. These authors investigated the emf response for a number of glasses in solutions made up from deuterium oxide, phosphorus pentoxide, and calcium oxide, making use of the tribasic phosphoric acid to provide a wide range of pD values. The following criticisms of the principle of this experiment are made. Phosphorus pentoxide dissolved in water gives only a low concentration of ortho phosphoric acid (about 10%), [15] and mainly polyphosphoric acids are produced. No mention is made of the difference in the dissociation constants for the deuterio and protio phosphoric acids and of the unknown increase K_H/K_D ratio for the less acidic hydrogens.

The deuterium ion emf response was investigated for the following cells:

Cell I

Ag; AgCl,	NaCl Na_2HPO_4 NaH_2PO_4 Protium oxide	Glass	Deuterium oxide, Buffer solution	KCl, AgCl;Ag in D_2O

Cell II

Ag; AgCl,	NaCl Na_2HPO_4 NaH_2PO_4 Deuterium oxide	Glass	Deuterium oxide Buffer solution	KCl, AgCl; Ag in D_2O

The buffer solutions were made from acids whose dissociation constants in deuterium oxide have been measured. [16]

[14] D. Hubbard and G. W. Cleek, J. Res. Natl. Bur. Standards, U.S. 49, 267 (1952).

[15] See for example, E. Thilo and W. Wieker, Z. anorg. u. allgem. Chem., 277, 27 (1954).

[16] References 2, 3, 4, and 5. For a complete list, see R. P. Bell, The Proton in Chemistry, Methuen Monographs, 1959, p. 188.

Experimental Procedure

A stream of dry CO_2-free nitrogen was passed overnight through deuterium oxide (1.5 liters, previously distilled, 0.4% of the total hydrogen as protium). Deionization was achieved by passing the heavy water down a column composed of a mixture of the deuterated Dowex-50 and Dowex-1 resins in their acid and basic forms, respectively. In order to convert these resins (70 g each) from their protio forms, they were first filtered, washed with acetone, and dried. Then both resins were heated to 50°C overnight, after which the Dowex-1 was placed in a vacuum desiccator over phosphorus pentoxide, and the Dowex-50 was heated to 105°C for 3 hr. Finally, both were stored in this desiccator for a day, after which deuterium oxide (50 ml) was added to the dry powders. Heat was evolved in both cases.

The first two 50-ml samples of D_2O coming from the columns composed of these resins were analyzed for protium content by comparison of water and standard dioxane peaks in the NMR spectrometer. The values of 6%, 2%, and 0.5%, the last for the bulk of the heavy water collected, were found.

The electrodes mentioned above, together with their silver—silver-chloride reference cells, were used in the experiment. The solutions placed inside the glass electrode had the following composition:[17] NaCl, 0.004 M; NaH_2PO_4, 0.031 M; Na_2HPO_4, 0.031 M. Potassium chloride, 0.2 M, was used in the reference cells, and the slow leakage of this solution never added more than 4×10^{-4} M of the salt during the experiment.

Buffers 0.01 M in acid and anion were made by weighing sufficient acid to make 0.02 M acid concentration in 10 ml of D_2O and adding 1.00 ml of 0.100 N sodium deuteroxide in heavy water. (For the carbonate buffers, however, $NaHCO_3$ and Na_2CO_3 were weighed separately.) The entire protium thus added was about 0.03%. Compounds having water of crystallization were evaporated down with 2.0 ml of deuterium oxide prior to making up the solution. Analytical-grade reagents were used throughout. Chloracetic acid, 2, 6-dinitrophenol, and benzoic acid (corrected melting points, 55.0 to 57.3° C, 62.5 to 62.8°C and 122.5 to 122.9°C) were purified by crystallization; 2.6-dinitrophenol and benzoic acid buffers had to be diluted to bring all the material into solution.

Whenever deuterium oxide solutions were used, equilibration at least overnight was allowed for the silver chloride and for the glass electrodes.

The emf's were determined on a Beckman Model G potentiometric pH meter. Glass cells containing the buffer solutions were immersed in a bath at 25 ± 0.02°C and the electrodes, fastened into a glass cap by means of paraffin wax, were introduced into the solutions. Temperature equilibration was achieved within 10 min, and readings were taken after 15, 20, and 25 min. Deviations no greater than a millivolt were obtained. Emf's for a series of cells were thus measured, and the experiment was repeated. The greatest discrepancy found during the repetition was 2 mv.

[17] R. G. Bates, Electrometric pH Determinations (John Wiley and Sons, New York, N. Y., 1954), p. 247.

Results

The results in deuterium oxide are shown in the accompanying Table I and Fig. 9. Cell 1 (protium oxide) gave a straight line of slope 59.0 ± 1.3, and Cell 2 followed it so closely that it was not possible to plot its response on the same graph paper. Thus a surface exchange on the glass electrode does occur in deuterium oxide solutions, giving a pD-dependent emf similar to the protium counterport.

Table I. Emf/pD response for glass electrodes No. 1 and No. 2

			Anion		Emf	
Acid buffer	Anion	Acid	Log acid	pD	1	2
Deuterium chloride 0.01 N				2.00	420	424
Chloracetic acid	0.0100	0.0109	-0.04	3.16	346	350
2,6-Dinitro-phenol	0.00100	0.00100	0.00	4.03[a]	279	282
Benzoic acid	0.00500	0.00513	-0.01	4.70	256	260
Acetic acid	0.0100	0.00803	+0.10	5.36	204	208
Monosodium phosphate	0.0100	0.0101	0.00	7.75	85	89
Sodium bicarbonate	0.0199	0.0196	+0.01	10.86	-114	-118

[a] Although this measurement had been taken at 18 ± 2° C (Ref. 3), no alteration of pK_H at 25° C is recorded (International Critical Tables, Vol. VI, p. 271)

A final, accurate measurement with the glass electrode in deuterium oxide solutions will come from the study of the cell.

Pt; D_2, Deuterium test solution Glass ‖ Buffer, ‖ Reference electrode.

If, as appears likely, the cell emf does follow pD to a greater accuracy than the accuracy of the measurement, the deviation of points about the straight line must be accounted for in terms of experimental error (estimated to be no more than 0.02 pD unit, thus a plot in protium oxide solutions against standard commercial buffers was better than this) and, in terms of the error of the dissociation constants for the few acids that have been measured in deuterium oxide. For the low concentrations used, the ratio of the activity coefficients for the anion to the acid was assumed to be unity.

Many interesting possibilities exist, both of applying the glass electrode to measuring deuterium systems and of applying radioactive isotopes to further investigations of the mechanism of the glass electrode.

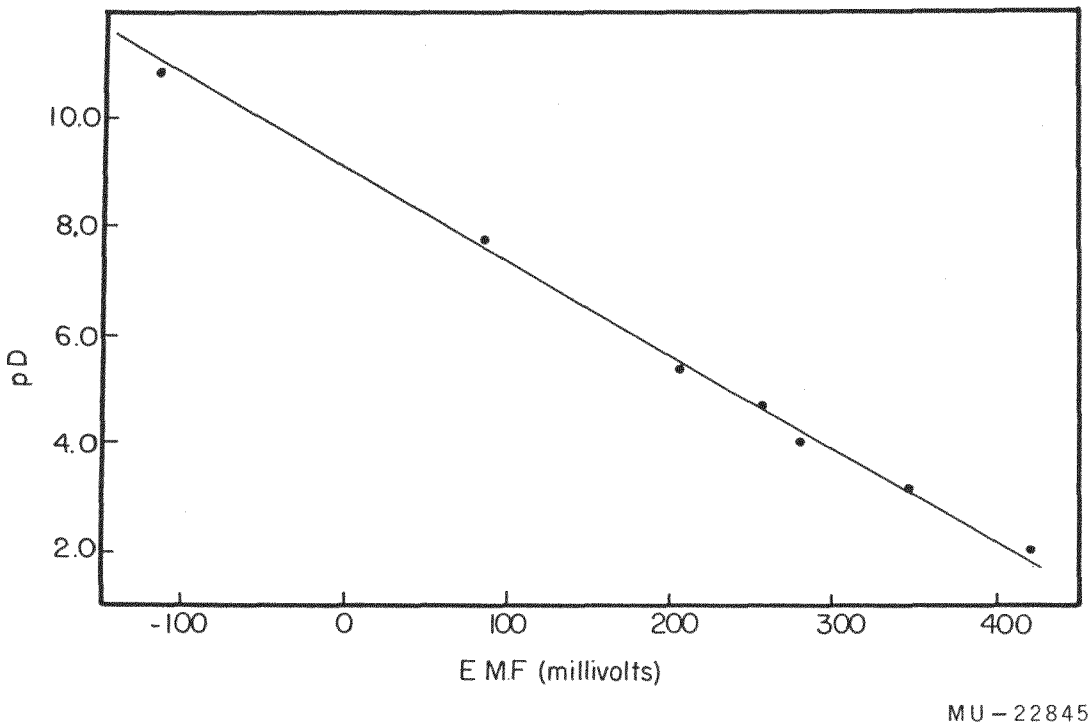

Fig. 9. Emf variation with deuterium ion concentration in Cell I.

3. ISOTOPE-EXCHANGE MEASUREMENT USING NUCLEAR MAGNETIC RESONANCE

Peter R. Hammond

Introduction

Nuclear magnetic resonance techniques have been applied successfully to the study of rapid exchange reactions[1] where the reacting species have lifetimes comparable with the thermal relaxation time of the observed nuclear resonance. On the other hand, little has been described of the straightforward appearance and disappearance of spectra peaks arising from isotope exchange.

Measurements of NMR spectra can be expected to supplement other more precise exchange determinations, such as the application of radioactive isotopes, and analysis of chemical products with the aid of the mass spectrometer. The method permits study of the elements for which radioactive isotopes of suitable half lives do not exist, for example, lithium, boron, nitrogen, and oxygen. In addition to being simpler experimentally, this method gives results which may be more directly interpreted than those frequently obtained with the mass spectrometer. Also, the position of resonance for a particular nucleus depends on the chemical environment, hence independent exchanges of an element on different parts of a molecule may be followed.

Figure 10A shows the proton signal obtained on a 60-Mc Varian spectrometer for a solution of a hydrogen compound 1 M in protium. Down to one-tenth of this concentration, peaks could be distinguished from back ground noise and measured. This represents the limit available[2] with existing machines The relative sensitivity of other nuclei are known at constant field[3] and at constant frequency.[4] Of the elements above, the spectra of lithium, boron, and oxygen, for the same frequency, exhibit a stronger response than protium, whereas many nitrogen studies have been reported despite a lesser sensitivity.

---

[1] See, for example, (a) J. D. Roberts, Nuclear Magnetic Resonance (McGraw-Hill Book Co., New York, N. Y., (1959), Chapter 4; (b) J. A. Pople, W. G. Schneider, and H. J. Bernstein, High Resolution Nuclear Magnetic Resonance (McGraw-Hill Book Co., New York, N. Y., 1959), Chapter 10.

[2] A. M. J. Mitchell and G. Phillips, Brit, J. Appl. Phys. 7, 67 (1956).

[3] Reference 1a, Page 19; see also Reference 4.

[4] Varian Associates, Table of NMR Properties, reproduced in Reference 1b, Page 480.

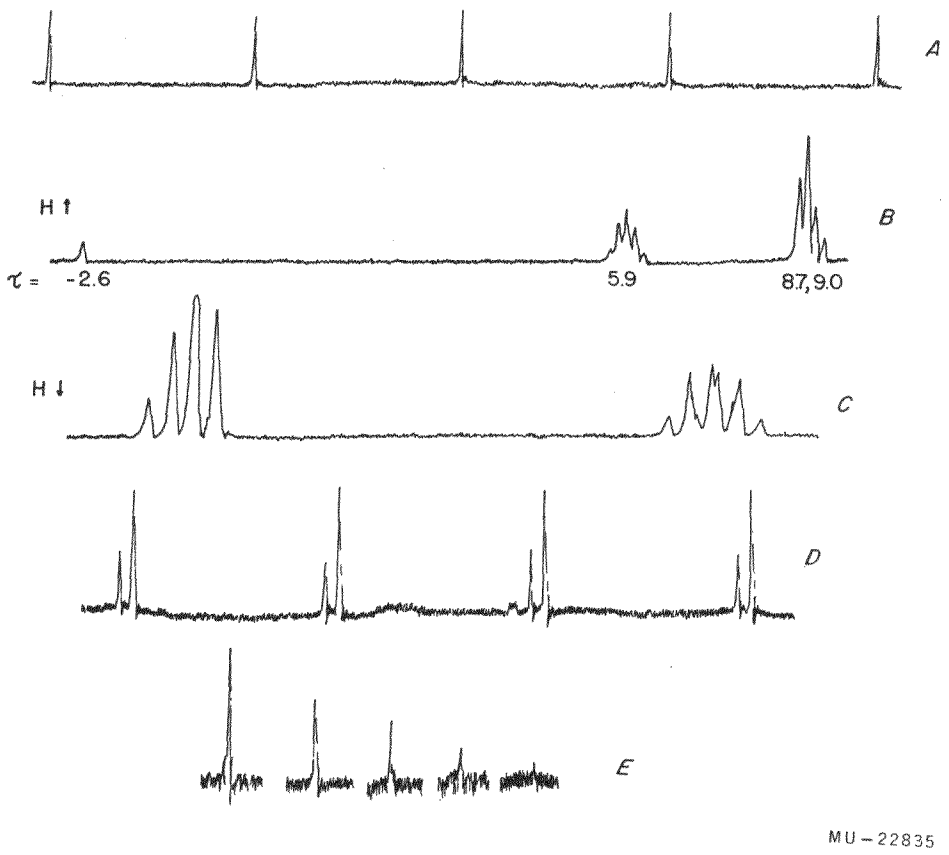

Fig. 10. A. Spectrum obtained from solution containing 1 M protium.
B. Diethyl phosphonate full spectrum.
C. Expanded portion of diethyl phosphonate spectrum.
D. Reference peak from dioxan in deuterium oxide. Smaller peak arises from protium oxide impurity.
E. Decrease in peak height with time.

Basis of Method

The basis of the method is that the area under a resonance peak is proportional to the number of nuclei contributing to the signal, and that these nuclei are exchanging with isotopes whose position of resonance does not occur in the region studied. For this proportionality to be achieved, stable, homogeneous field conditions are required[5] and the radio-frequency power must be below the limit of saturation. Because these conditions are not always easy to obtain, it is necessary to check the proportionality, using standard solutions.

The signal studied should preferably be sharp, well isolated from the rest of the system, and not subjected to spin-spin splitting with other nuclei. As it is convenient to measure signal height of a sharp signal, factors altering signal width must be minimized. For this reason identical conditions of rf power, speed of sweep, and sample spinning are used on each run. Conditions under which isotope exchange may be followed (half life from 3 min upwards) cannot be expected to alter the width of the observed peak. This follows from the approximate relationship for fast exchange[6] of a nucleus between two positions, where collapse of individual peaks occurs when

$$\tau \sim \frac{1}{(\nu_A - \nu_B)} ,$$

where τ is the mean lifetime for a stay on either site, ν_A and ν_B are the positions of resonance (frequencies). Thus, even for the most rapid reaction to cause line broadening, the signal disappearing from ν_A must reappear at ν_B less than 0.006 cycle away, in which case the peaks will be unresolved by existing machines.

Experimental

In the exchanges studied, the height of a disappearing peak was compared at frequent intervals with peaks from a standard solution. The variations of the reference (Fig. 11) make it evident that a comparison procedure is necessary. The following are possible:

(a) Comparison of changing peak with static neighboring peaks of the compound studied.
(b) Comparison with added internal reference.
(c) Comparison with reference placed in concentric tube.
(d) Comparison at frequent intervals with peaks from standard solution.
(e) Comparison with a peak obtained by side-banding a static peak remote from the position studied.

Considerable attention was paid to tube stability in order to reduce background noise, and it was found that measuring for one direction of sweep only reduced errors arising from slight drift of the field. The precise conditions used were automatic sweep, sweep frequency 1 by 6, sweep field 1 by 1, 70 db, attenuation x1, frequency response 4.

[5] See, for example, A.B. Williams, Ann. N.Y. Acad. Sci. 70, 890 (1958) and Reference 1b, Page 458.

[6] H.S. Gutowsky and C.H. Holm, J. Chem. Phys., 25, 1228 (1956). See also reference 1b, Page 223.

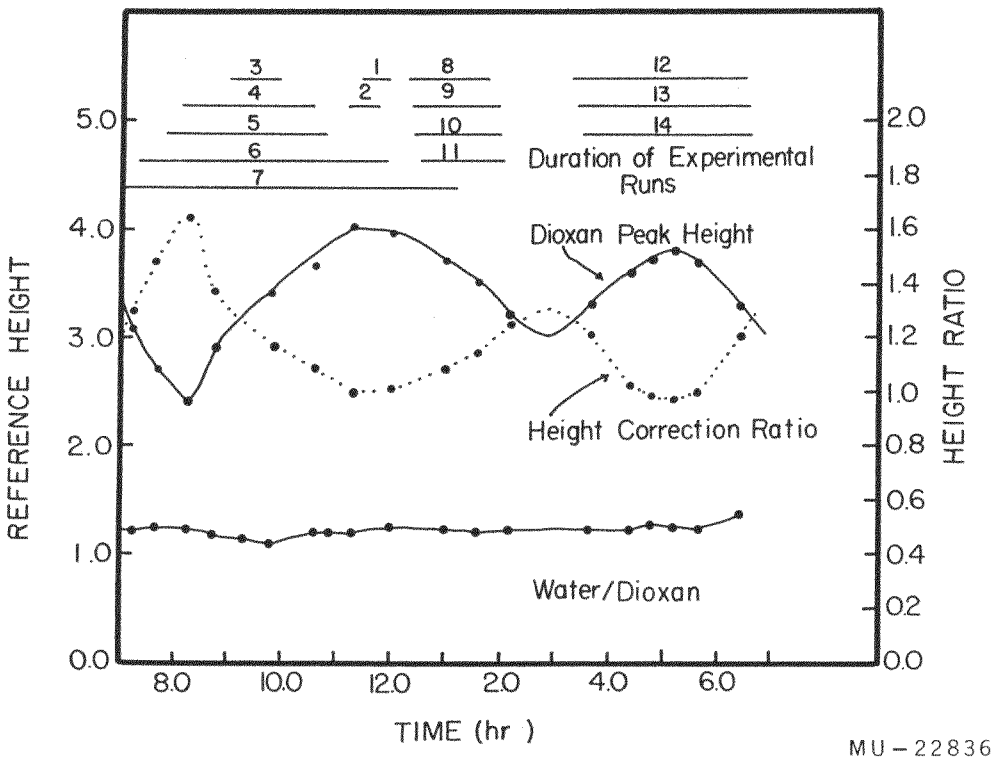

Fig. 11. Variation in reference peaks.

For each measurement, the spectrum was repeated five times, the heights above the middle of the background were measured, and the average of the heights was considered to occur at the average of the time for the five peaks. The standard deviations were dependent on the quality of the back ground, but ± 5% was typical value.

Application to Protium-Deuterium Exchange

The acid-catalyzed exchange of the P-H bond in diethyl phosphonate

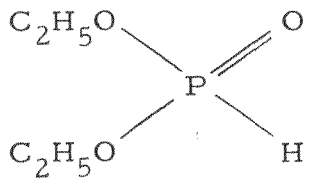

was studied. The proton spectrum of this compound is shown in Figs. 10B and 10C.

The peaks arising from the P-H hydrogen occur at τ values (with respect to the silicon tetramethyl scale) of -2.6 and 9.0 (partially obscured by the ethyl triplet but visible in the expanded spectrum--Fig. 10C), and arise from coupling of the P^{31} nucleus with the proton (j = 694 cycles[7]). The complex structure in the region of the ethyl quadruplets persists on careful purification and is attributed to coupling with the phosphorus atom (j = 6 cycles).

The isolated peak at τ = -2.6 was suitable for study, but as it arose by splitting from the phosphorus atom, 2 M solutions had to be used. The peak height was proportional to the concentrations of prepared solutions.

No convenient comparison peak was present in the spectrum, an internal reference of dioxane was obscured by the ethyl resonance, and a concentric tube containing sulfuric acid increased the background noise. The spectrum was therefore compared at frequent intervals with a 1 M solution of dioxane in deuterium oxide. (Fig. 10D) (Trimming of the spectrometer was unnecessary as the comparison solution was similar to the ones measured.) From the variations in peak height with time, a correction curve was plotted and was applied to all measurements. The second (lower) peak in all reference spectra came from the small percentage of water present in the D_2O. The ratio of these two peaks is plotted against time (Fig. 11), and it may be seen that an internal comparison method is subject to only small fluctuations, even when the height fluctuations are large.

Experimental peaks may be seen in Fig. 10E(run 9), plots of peak heights H against time in Fig. 12 a and b (Runs 1 and 5) and plots of

[7] Compare phosphorus measurements, H. Finegold, Ann. N.Y. Acad. Sci. 70, 875 (1954).

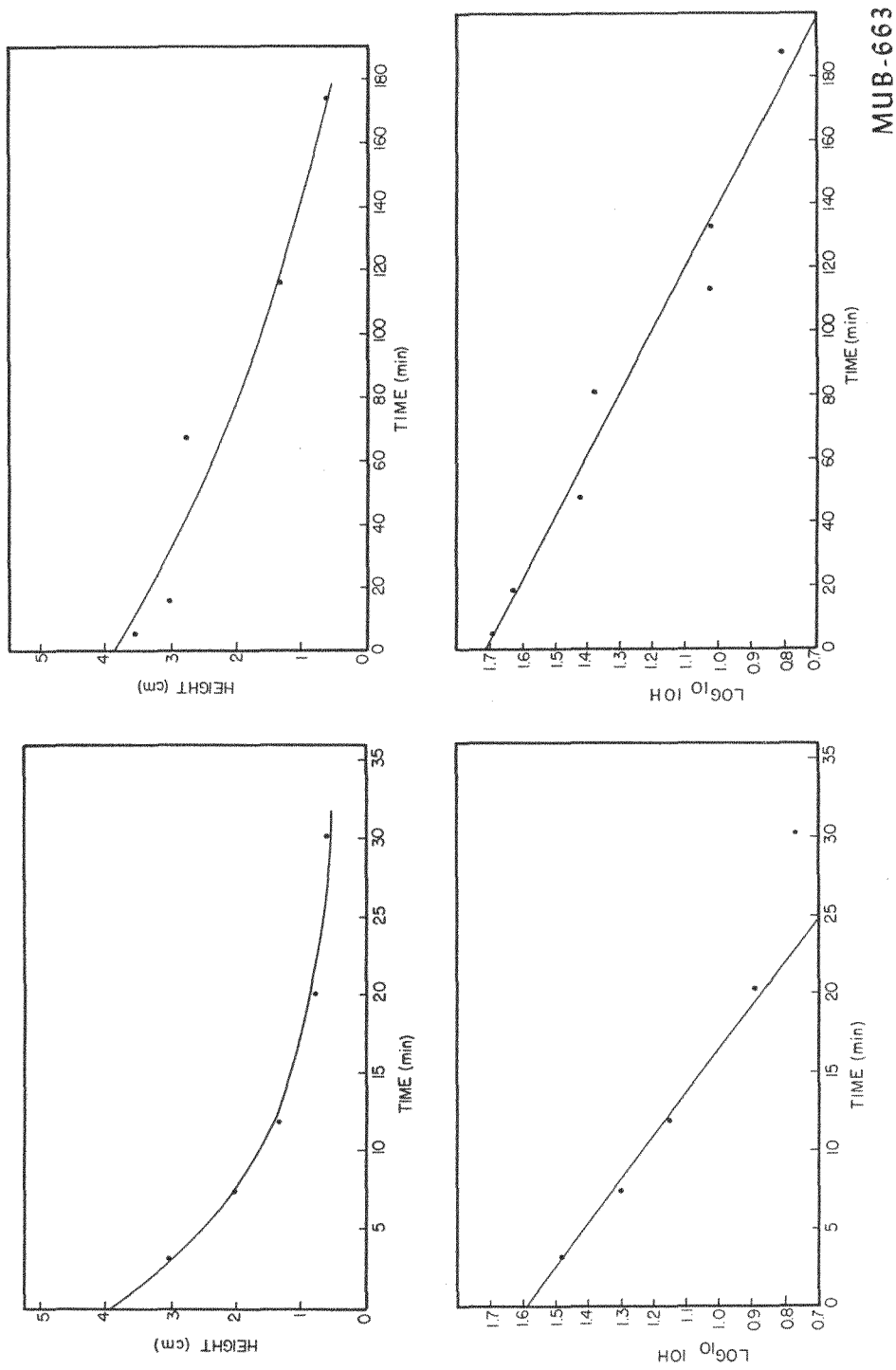

Fig. 12. Experimental plots of peak-height variation, (a) Run 1. (b) Run 5. (c) Run 1. (d) Run 14.

Log_{10} H against time in Fig. 14 c and d (Runs 1 and 14). The duration of the experiments is shown in Fig. 11. For the short runs (30 min) the reactions are clearly not zero-order, whereas for the longer (for example, run 5, Fig. 13), zero order is improbable. Logarithmic plots against time give acceptable straight lines with slopes (obtained by the method of least squares) and therefore, first-order rate constants having standard errors varying between ±10 and ±15%.

The Determination of Protium in Deuterium Oxide

The size of the smaller peak in Fig. 10D was altered by adding water, and was proportional to the quantity of water added, up to 0.6 M (in hydrogen). The heights were equal when 0.50 mole had been added. The solution was made up by diluting 0.110 ml (1.03 moles of protium) of dioxane (sodium dried) to 10 ml in deuterium oxide. The peak ratio obtained was 0.49 ± 0.02, hence the molarity of protium was 0.5 ± 0.02. This method may be used for concentrations of 0.1 M protium upwards. A departure from proportionality has been reported for resonance absorption much above 0.9 M solutions.[2]

B. PHYSICAL ORGANIC CHEMISTRY

1. ACID CATALYSIS OF THE IONIZATION OF THE P-H BOND IN DIETHYL PHOSPHONATE

Peter R. Hammond

Previous studies[1] on the exchange of the hydrogen of the P-H bond of diethyl phosphonate (A) with deuterium in deuterium oxide solutions

A

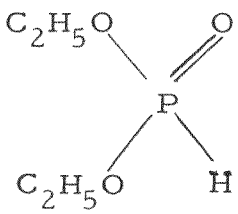

showed that the exchange exhibited general base catalysis and that the reaction velocity could be best expressed as a linear function of base-catalyst concentration, although the accuracy of the measuring technique (with NMR) did not allow precise assignments to the Bronsted coefficients for the buffers used.

The acid-catalyzed exchange, on the other hand, did not follow a similar simple relationship, and could be interpreted either as a decrease of catalytic coefficient with increasing deuterium ion concentration, or as a fractional-order relationship. The following experiment was designed to investigate the acid catalysis further.

Experimental Procedure

Deuterium Chloride Solutions

Hydrogen chloride gas, dried over concentrated sulfuric acid, was absorbed in deuterium oxide (15 ml) to give an approximately 4 N solution. All deuterium chloride solutions, Runs 1 to 11, were made by diluting this solution. This added a further protium concentration equal to the acid concentration for all the experiments. The maximum addition was in Run 1, a further 0.9% to the already existing 0.4%. The acid concentration was determined by running 1-ml samples into 20 ml of distilled tap water and titrating with 0.1 N sodium carbonate. A series of solutions was prepared with the acid and 4 M sodium chloride so that the addition of diethyl phosphonate to 2 M concentration gave 1-ml samples with the concentrations outlined (2M concentration was necessary in order to have a peak measurable above background noise for a suitable period). It was found that adding 0.25 ml of diethyl

[1] P.R. Hammond, Ionization of the P-H Bond. I. Diethyl Phosphonate, J. Chem. Soc. (in press).

[2] G.N. Lewis and P.W. Schutz, J. Am. Chem. Soc. 56, 1913 (1934); G. Dahlgren and F.A. Long, J. Am. Chem. Soc. 82, 1303 (1960).

phosphonate to 0.75 ml of the acid solutions (Runs 6 and 7 were tried) produced no volume change; hence all runs were started by making up 0.75ml of solution to 1 ml. Runs 12, 13, and 14 were prepared from analytical-grade chloracetic and maleic acids. Their dissociation constants in deuterium oxide have been measured.[2] The run with the anion (Run 13) of chloracetic acid was prepared by adding the equivalent of a standard deuterium oxide solution of sodium hydroxide to chloracetic acid.

After the phosphonate had been added, the solutions were thoroughly mixed, and a sample was transferred to a suitable glass tube for measuring in the NMR spectrometer. The top of the tube was sealed with plasticene.

Details of the experimental procedure have been given elsewhere. The time to record each point was about 1 min. The automatic time marker of the instrument together with an electric clock having a second hand gave the time measurement to a considerably greater accuracy than required.

Throughout the experiment, room temperature, taken as the temperature of the reaction, drifted upwards from 27.3° C to 27.8°C.

Results

Plots of corrected peak height against time clearly indicated in the faster runs, 1-4, 8-11, that the reaction was not zero-order. In the longer runs, where presumably fluctuations in the machine have more opportunity to make themselves apparent, the exchanges were probably not zero-order.[3] Logarithmic plots of peak height against time gave acceptable straight lines where the negative gradients ($\underline{m}$) and therefore first-order rate constants ($\underline{k}$) had a standard error of between ±10 and ±15:

$$\underline{m} = \underline{k} \log \underline{e} .$$

The solutions studied and the rate constants obtained are as tabulated (Table II) and are plotted in Fig. 13. For comparison the rate in deuterium oxide solution alone (k_w) was $0.6\ 10^{-3}$ min^{-1}. The contribution to the hydrolysis rate constant by hydrogen ions in protium oxide under similar conditions of salt concentration and temperature has been reported.[4]

HCl concentration	0.50	0.20	0.10	0.05	0.02	0.01
10^3 $\underline{k}$ (min^{-1})	3.28	1.57	0.85	0.45	0.19	0.09

The product, ethyl hydrogen phosphonate (B) ($K_h = 1.6 \times 10^{-1}$)

B 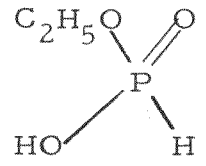

[3] Preceding article; the method of least squares was used.

[4] P. Nylen, Svensk Kem. Tidskr. 49, 29 (1937).

Table II. Rate constants for the disappearance of the P-H bond of diethyl phosphonate (2 M) in deuterium oxide solution

Run No.	1	2	3	4	5	6	7	8	9	10	11
DCl concentration	1.00	0.60	0.30	0.10	0.03	0.01	0.001	0.10	0.10	0.10	0.10
NaCl concentration	0.50	0.90	1.20	1.40	1.47	1.49	1.50	0.10	0.20	0.50	1.00
10^3 k (min^{-1})	83	69	44	14	10	6.9	2.3	17	17	19	19

Run No.	12	13	14
Chloracetic acid	0.10	0.00	0.00
Sodium chloroacetate	0.00	0.10	0.00
Maleic acid	0.00	0.00	0.10
Sodium chloride	1.49	1.40	1.48
10^3 k (min^{-1})	6.0	3.7	12

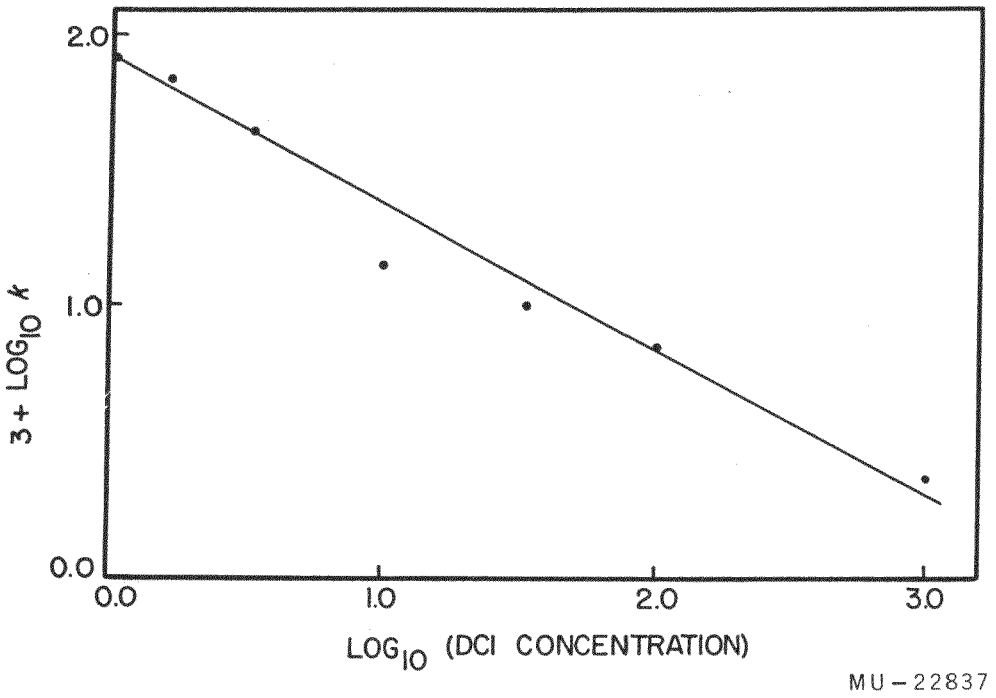

Fig. 13. Variation in first-order rate constants with deuterium chloride concentration.

was expected to catalyze the exchange also. Assuming similar rates of hydrolysis in deuterium oxide, as much as 0.007 M of the monoester was present at the end of Experiment 7, hence the rate measured occurred at an effective deuterium ion concentration of more than 10^{-3}. In comparison with the acid already present, the monoester would have had less effect at higher concentrations and, particularly in deuterium oxide, its ionization would be partially suppressed. The true curve for the exchange therefore falls away from the line drawn in the graph at low acid concentrations. As the data are only semiquantitative, and as the dissociation constant of B and the hydrolysis rate of A in deuterium oxide solutions are unknown, further calculation is not justified. The maximum concentration of the monoester obtained during the exchanges (Run 1, giving 0.2 M after 30 min) was just at the limit of detection. Neither this nor other intermediates were in fact seen. The catalysis by chloracetic and maleic acids (Runs 12 and 14) is considered to mean that the exchange shows catalysis by acids other than the deuterium ion.

Conclusions

The acid-catalyzed ionization of the P-H bond of A follows the graph shown except at low acid concentration. Here extra catalysis by the hydrolysis product, the monoester produces an over-all rate too high for just the acid added, and the true curve falls away from the line plotted. More detailed information will come from kinetic measurements with tritium-containing solutions, but it can be said the results above probably indicate a decrease in catalytic coefficient for the deuterium ion with increasing concentration. This is, in fact, the result to be expected for the equilibrium shown,

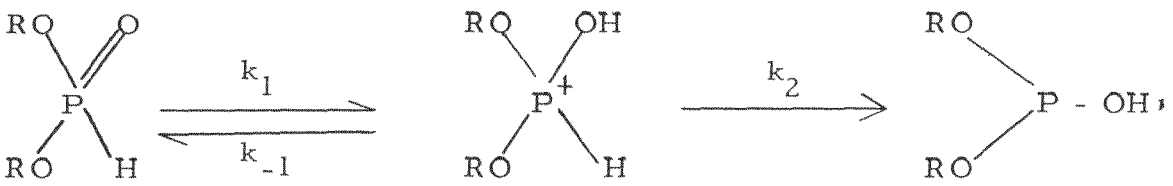

(A) C

where $k_1 \approx k_{-1} >> k_2$ and where the over-all rate[5] is in the form

$$k = \frac{\sum \pi_i K_i (A_i)}{(D^+) + K_c} .$$

[5] R. P. Bell, The Proton in Chemistry (Methuen and Company, London, 1959), p. 143.

2. ESR OF THERMAL IMPERFECTIONS IN SOME COMPLEX ORGANIC SOLIDS

John W. Eastman and Melvin Calvin

Preparation

When o-chloranil is dissolved with an equivalent amount of perylene in hot ethylene dichloride, shining black needles are precipitated on cooling. Chemical analyses for carbon and chlorine give results which agree well with the composition predicted for a 1:1 complex of perylene with o-chloranil.

The unit cell of the crystal is 7 by 17 by 16 A, and its symmetry is monoclinic or triclinic. If one assumed nearly square angles for the unit cell, it would contain two molecular complexes.

Physical appearance of the crystals, their chemical analysis, and the definition of x-ray photographs indicate that the crystals are homogenous molecular solids. These solids contain an equimolar ratio of hydrocarbon and quinone bound by charge-transfer forces (see below).

Black needles of the following have been prepared:

pyrene:o-chloranil (pyrene:$oQCl_4$),
pyrene:$oQBr_4$,
perylene:$pQCl_4$,
perylene:$pQBr_4$, perylene:$oQCl_4$,
perylene:$oQBr_4$,
coronene:$oQCl_4$.

In all cases the solids are 1:1 combinations of hydrocarbon and quinone.

There are at least two ways of recovering the components of the complex solids. A rapid (flash) sublimation of the complex in a thermal gradient produces separations. The more volatile $oQBr_4$ and $oQCl_4$ have been separated from perylene in this way. Perylene and $oQCl_4$ have been separated on a silicic acid column with ethylene dichloride and petroleum ether as the solvents. Also chloroform leaches $oQBr_4$ from the perylene:$oQBr_4$ complex. Again, one is led to the conclusion that the solids are indeed only complexes and that none of the original chemical bonds have been broken.

Nonmagnetic Properties

The presence of charge-transfer binding is demonstrated by the intense color of the solids. Their color is different from the color of the components. It is due to charge-transfer absorption of the complex solid. The absorption spectrum in a KBr disk of perylene:$oQBr_4$ has this very broad absorption with its maximum at 930 ± 25 mμ, with an extinction coefficient about 10^3 to 10^4 (mol. complex/liter KBr)$^{-1}$ cm^{-1}.

The infrared spectrum of perylene:$pQCl_4$ is nearly identical to the superimposed spectra of the individual components. There are slight shifts

in frequency which reflect the molecular association. Also in the region 1125 to 1275 cm^{-1} the spectrum of the complex solid is different from that of the components. However, the characteristic quinone frequency of 1690 cm^{-1} remains essentially unchanged. At least the carbonyl bonds have not been altered in the complex solid. It seems most likely that no intramolecular bonds have been changed during formation of the complex.

ESR of Imperfections

Formation of Imperfections

The purpose of this work was to determine the conditions for which ESR absorption could be observed in the hydrocarbon:quinone complexes. ESR absorption has been observed in all the complexes prepared. However, quantitative measurements of unpaired-spin concentration showed the absorption to be very irreproducible. With certain recipes it is possible to prepare complexes nearly free of ESR absorption. We conclude that the hydrocarbon: quinone complex solids which we have prepared are not themselves paramagnetic.

Given above was evidence from which we deduced that the crystals were near-perfect ordered homogeneous solids. Now we assign ESR absorption to imperfections in the solids. Some of these imperfections have been subjected to quantitative measurements in order to determine their structure.

The concentration of imperfections in ortho-quinone complexes may be increased by several orders of magnitude by heating the complex solid. ESR absorption of the para-quinone complexes does not increase when the solid is heated to 125°C. This may be because of structural differences or because of differences in the susceptibility to chemical reactivity (see below). At any given temperature the concentration of unpaired electrons is time-dependent. Data from a typical heating experiment are shown in Fig. 14. For reasons which will soon become evident, we divide the time scale into two periods. There is at first a rapid rise in ESR absorption (Period 1). Following, there occurs a decrease in ESR absorption that is in comparison very slow (Period 2) (Fig. 14a).

The original absorption is symmetric. It slowly becomes asymmetric (Fig. 14b). It appears that there are, in the solid, two individual absorbing imperfections. One is produced rapidly, then disappears; the other follows at a slower rate. As the second species appears (Fig. 14c), the observed total absorption becomes skewed, the width narrows, and the observed average g value shifts (Fig. 14c).

In Fig. 15, the observed asymmetric ESR absorption has been constructed from two symmetrically absorbing species.

Impurities

Since aromatic hydrocarbons do react with quinones in solution, it would not be surprising to discover solid-state reactions in our complex solids.

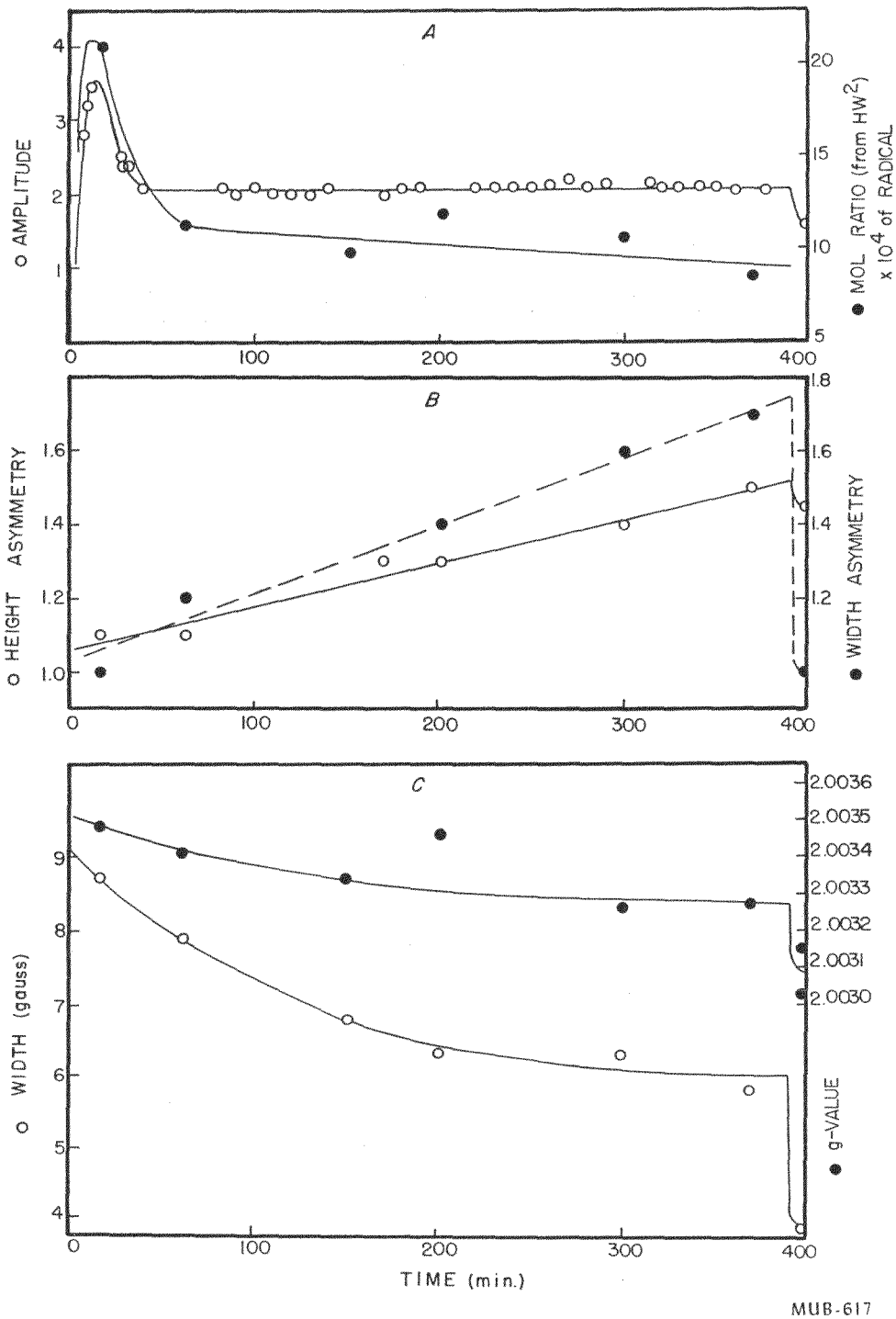

Fig. 14. ESR of solid perylene-$oQBr_4$ at about 100°C. (a) signal amplitude and concentration of unpaired electrons; (b) asymmetry; ratio of high-field amplitude to low-field amplitude, and ratio of low-field width to high-field width of the derivative of ESR absorption; (c) g value and width. The discontinuity at 400 min resulted from cooling the sample to 25°C.

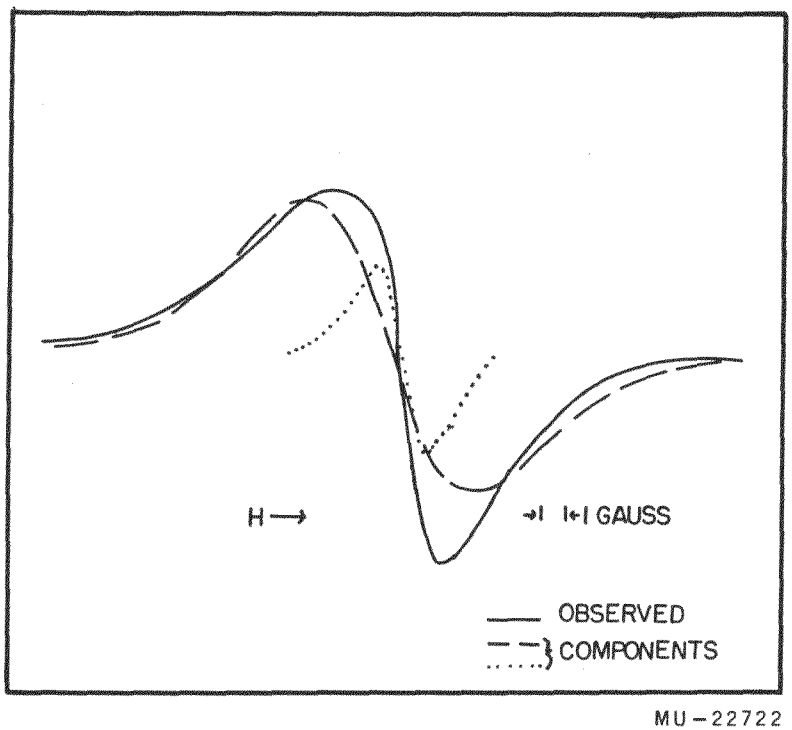

Fig. 15. Construction of the observed asymmetric ESR absorption from two hypothetical overlapping components.

Viewing again our typical experiment (Fig. 14), we note that distinct changes occur when the hot solid is cooled. The original broad symmetric signal (g = 2.0035), dominant at high temperatures, decreases in concentration while the other narrow signal begins to dominate the absorption. Thus the width, symmetry, and g value change on cooling. The narrow signal dominates the absorption after a relatively long heating time and at reduced temperatures.

We assume the narrow signal to be a trapped free-radical intermediate in the reaction between hydrocarbon and ortho-quinone. Quantitative kinetics of optical, infrared, and ESR absorptions should illuminate the mechanism of reaction. This mechanism must be consistent with the fact that para-quinones do not react similarly. In addition, the reactants and products can be separated by chromatography and identified. A correlation with observed solution reactions should strengthen the conclusions.

We have not continued this very preliminary investigation. Rather, we have attempted a more detailed study of the original ESR absorption which appears rapidly on heating (during Period 1).

Structural Defects

Examine for a moment the methods of preparation. Perylene and $oQBr_4$, for example, precipitate from most solvents as a brown and apparently amorphous solid. This solid usually contains about 10^{18} unpaired electrons per gram (s/g). When equimolar ratios of the components are crystallized from 25% ethylene dichloride—75% carbon tetrachloride, less than 10^{16} s/g are present (assuming an ESR line width of 10 gauss). Thus the concentration of unpaired electrons is greater for an amorphous mixture than for the shining needles. X-ray analysis will demonstrate whether the brown material is really amorphous.

The ESR absorption of perylene:$oQCl_4$ could be reversibly eliminated by dissolving the complex in nitrobenzene. As the solid was dissolved or precipitated, the ESR absorption disappeared or reappeared.

It appears that ESR absorption depends intimately upon imperfection of the structure of the solid complex. The imperfections, in this case, seem to be defects in the crystal structure. In this way we explain why the method of precipitation affects the concentration of unpaired electrons.

In the literature, reported g values of absorption by complex solids are the same as g values observed in layered systems. By layered we mean that a layer of hydrocarbon is coated with a layer of quinone or other acceptor. In all cases, the g values are $2.0030 \pm .0005$. This suggests a similarity of the electronic states. New g values measured are perylene:$oQCl_4$, $g = 2.0030 \pm .0005$; perylene:$oQBr_4$, $g = 2.0035 \pm .00005$.

We have assumed that the chemical reactivity of the component molecules is unimportant. The arguments have been physical. There occur only about 10^{-4} mole of unpaired electrons per mol of complex. Proof of nonreactivity would be very difficult.

Let us present a plausability argument to demonstrate whey the imperfections of a crystal structure may result in unpaired electrons (see Fig. 16). There have been determined crystal structures of many solids bound by charge-transfer forces. In all cases the donor molecules and acceptor molecules alternate throughout the solid. There is a balance of forces; on all sides of a given electron donor molecule there are acceptors, and ionization does not occur. Complete charge separation is inhibited. Rather, a partial (nonionized) separation occurs in three dimensions about each molecule.

This balance of forces is upset when the solid is heated. Figure 16 illustrates how interchanges, migrations, or dislocations might result in ionization within a complex solid.

There come to mind at least two possible reasons why para-quinones do not yield thermally produced imperfections. Para-quinones have higher melting points, and in complex situations they may have less tendency to migrate. On the other hand, there may be distinct structural differences between the complex solids of ortho- and para-quinones. An x-ray study would be in order.

As noted previously, the ESR absorption of this structural species decreased markedly as the temperature was lowered, contrary to Curie's Law. It appears that once they are introduced thermally, the imperfections exist in equilibrium. Quantitative temperature-concentration measurements will give valuable thermodynamic information about the equilibria.

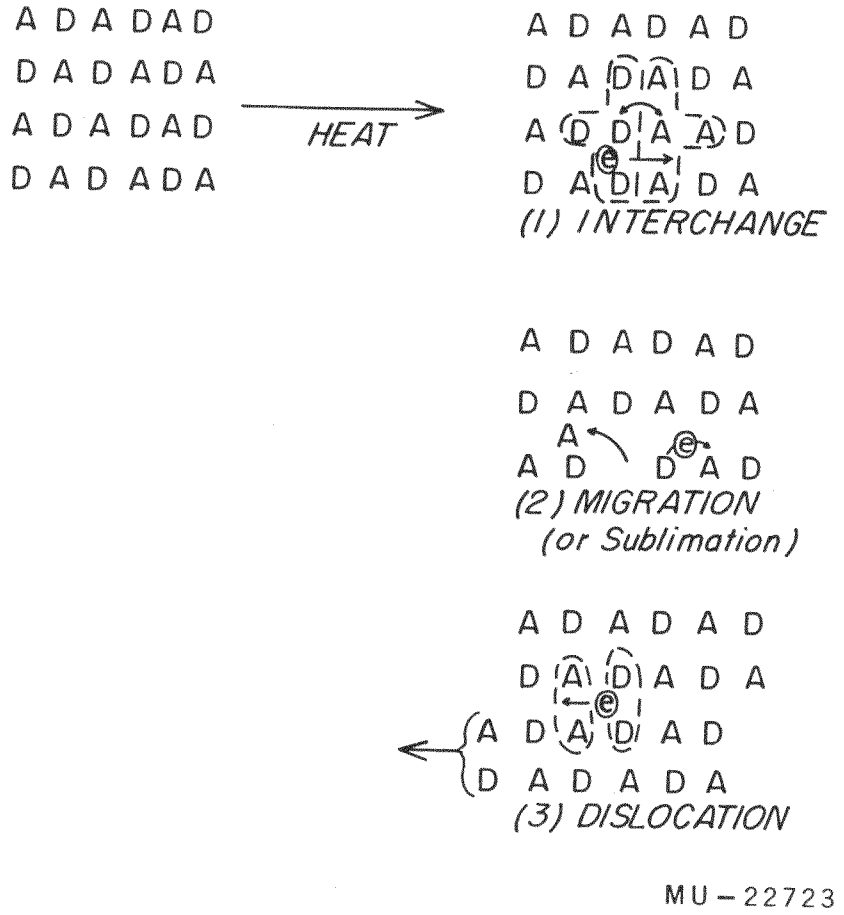

Fig. 16. Some proposals for thermally produced ionization in solids bound by charge-transfer forces.

3. VISIBLE SPECTRA OF ETIOPORPHYRIN I AND SOME METAL COMPLEXES OF ETIOPORPHYRIN I

Edward Markham and Gerrit Engelsma

We have prepared a number of metal complexes of etioporphyrin I in order to study their catalytic activity. Spectra have been taken, in the visible region, of solutions in chloroform and pyridine of etioporphyrin I; the Zn(II), Ni(II), Cu(II), and Co(II) complexes of etioporphyrin I; and Mn^{IV} etioporphyrin I diacetate. See Tables III, and IV and Figs. 17-19.

Table III. Analysis of the etioporphyrins for which spectra are given

Compound	Formula		C	H	N
Etioporphyrin I	$C_{32}H_{38}N_4$	Calc	80.6	7.6	11.8
		Found	80.2	7.8	11.9
Zinc(II) etioporphyrin I	$C_{32}H_{36}N_4Zn$	Calc	70.9	6.7	10.3
		Found	70.8	6.9	10.3
Copper(II) etioporphyrin I	$C_{32}H_{36}N_4Cu$	Calc	71.1	6.8	10.4
		Found	71.0	6.5	10.1
Cobalt(II) etioporphyrin I	$C_{32}H_{36}N_4Co$	Calc	71.7	6.8	10.5
		Found	71.5	6.8	10.8
Nickel(II) etioporphyrin I	$C_{32}H_{36}N_4Ni$	Calc	71.7	6.8	10.5
		Found	71.5	6.6	10.7
Manganese(IV) etioporphyrin I diacetate	$C_{34}H_{42}N_4O_4Mn$	Calc	67.4	6.7	8.7
		Found	67.5	6.5	8.5

Table IV. Wave lengths of peaks, with their absorption (s = shoulder)

Compound	In chloroform		In pyridine	
	λ (in mμ)	log ∑	λ (in mμ)	log ∑
Etioporphyrin I	375 s	4.977	376	4.903
	399	5.243	399	5.150
	470 s	3.496	471 s	3.432
	498	4.148	498	4.097
	502 s	4.124	503 s	4.062
	533	4.007	532	3.945
	-	-	558 s	3.305
	566	3.844	568	3.773
	572 s	3.765	576 s	3.658
	594	3.221	596	3.094
	-	-	611 s	3.160
	620	3.712	622	3.686
	650	2.702	652	2.382
Zinc(II) etioporphyrin I	330	4.245	337	4.382
	350 s	4.286	-	-
	383 s	4.780	396 s	4.717
	402	5.570	415	5.574
	466 s	3.288	-	-
	489	3.505	500 s	3.093
	532	4.159	543	4.229
	568	4.342	578	4.158
Copper(II) etioporphyrin I	329	4.271	331	4.235
	385 s	4.774	376 s	4.580
	408	5.658	399	5.428
	-	-	490 s	3.356
	526	4.157	527	4.057
	563	4.434	563	4.316

Table IV (Continued)

Compound	In chloroform		In pyridine	
	λ in mμ)	log ∑	λ in mμ	log ∑
Cobalt (II) etioporphyrin I	327	4.214	350 s	4.438
	392	5.387	393	5.092
	420 s	4.410	417	4.896
	518	4.045	532 s	4.126
	553	4.364	545	4.184
	-	-	605 s	3.074
	-	-	670	2.926
Nickel (II) etioporphyrin I	333	4.127	334	4.119
	392	5.289	392	5.263
	-	-	418	4.610
	470 s	3.388	470 s	3.394
	518	4.019	516	4.029
	554	4.477	551	4.500
Manganese (IV) etioporphyrin I diacetate	361	4.761	371	4.753
	395 s	4.378	395 s	4.512
	425	4.229	-	-
	472	4.480	471	4.513
	530	3.830	547	4.020
	553	3.947	-	-
	585	3.783	580 s	3.724
	655	3.398	653	3.441
	-	-	675	3.447
	-	-	742	3.486
	790	3.084	797	3.259

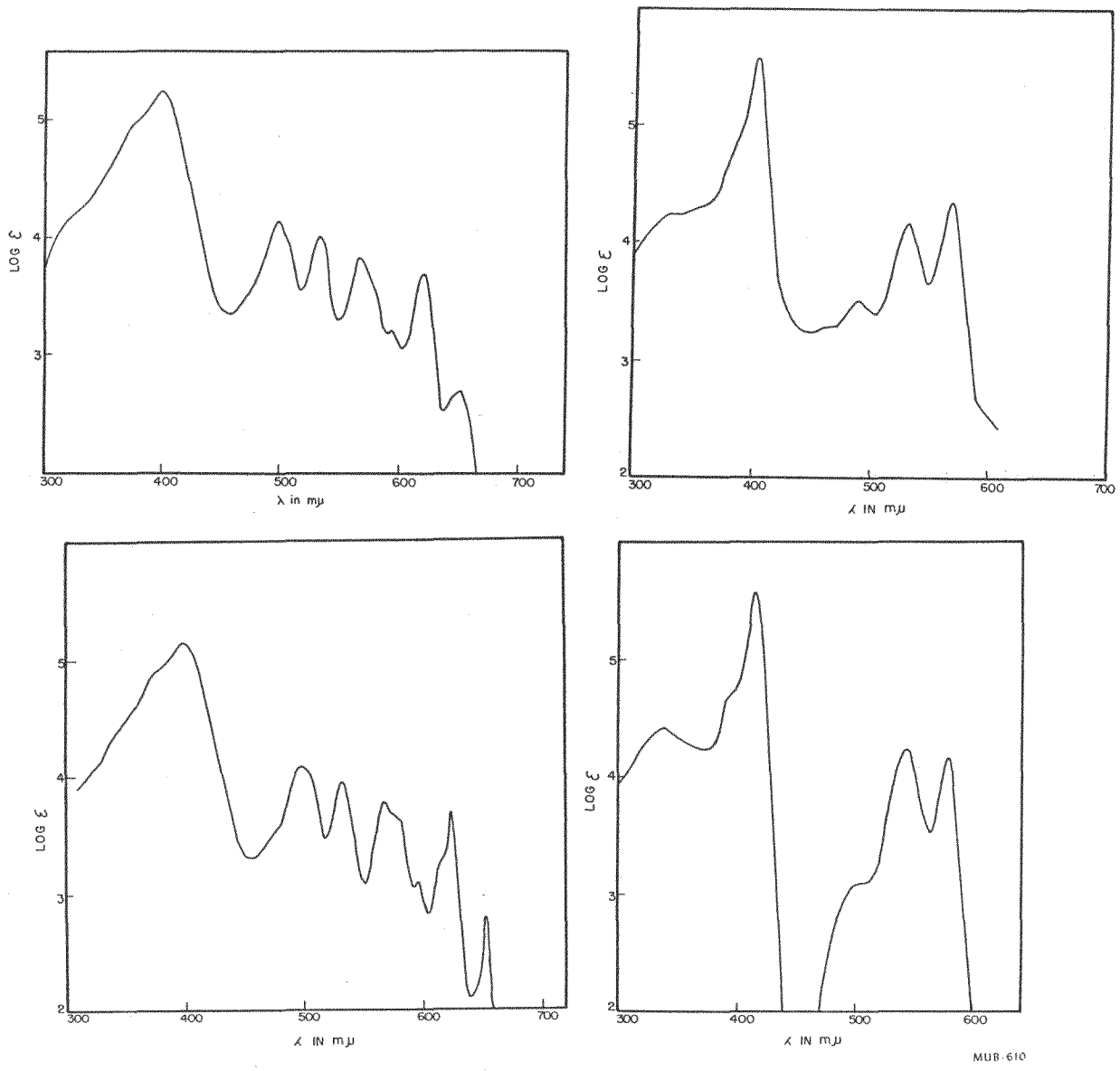

Fig. 17. Top left: Etioporphyrin I in chloroform.
bottom left: Etioporphyrin I in pyridine.
top right: Zinc II etioporphyrin I in chloroform.
bottom right: Zinc II etioporphyrin I in pyridine.

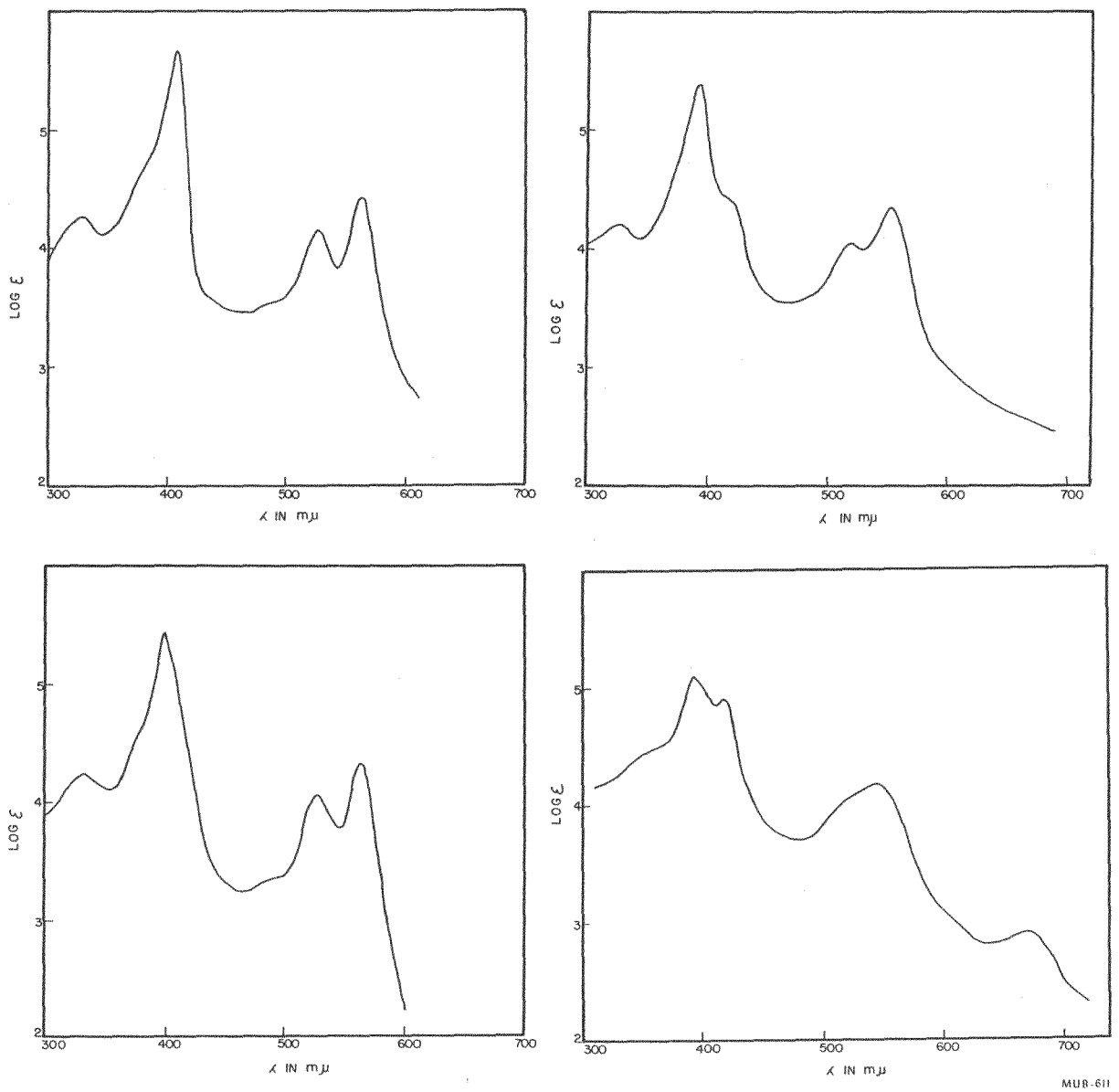

Fig. 18. Top left: Copper II etioporphyrin I in chloroform.
bottom left: Copper II etioporphyrin I in pyridine.
top right: Cobalt II etioporphyrin I in chloroform.
bottom right: Cobalt II etioporphyrin I in pyridine.

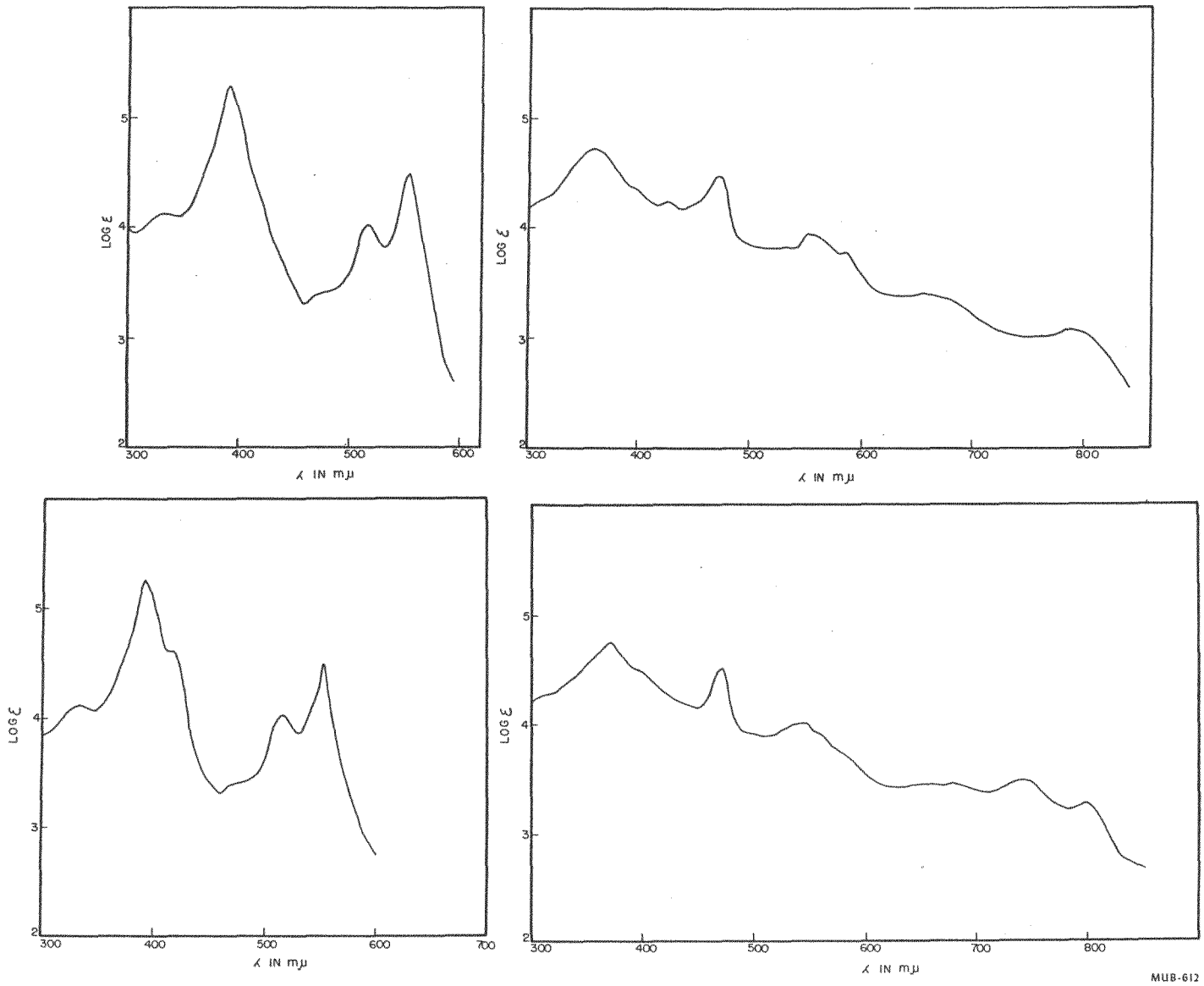

Fig. 19. Top left: Nickel II etioporphyrin I in chloroform.
bottom left: Nickel II etioporphyrin I in pyridine.
top right: Manganese IV etioporphyrin I diacetate in chloroform.
bottom right: Manganese IV etioporphyrin I diacetate in pyridine.

Etioporphyrin I was prepared by heating 20 g 5-brom-4, 3'-dimethyl-5'-brommethyl-3, 4' -diethylpyrromethene-hydrobromide (made by bromination of cryptopyrrole according to Fischer and Orth[1]) in 80 g succinic acid at 190 - 200°C for 1 hour. After cooling, the hard cake was powdered and the succinic acid was extracted with a 10% NaOH solution. The residue was then treated with chloroform to dissolve the etioporphyrin I. This solution was purified by chromatography over an aluminum oxide (Merck) column. The chloroform solution was then concentrated in vacuo and methanol was added to crystalize the etioporphyrin I.

The Ni(II), Zn(II), Co(II) and Cu(II) complexes of etioporphyrin I were prepared according to Fischer and Orth[2]).

Manganese(IV) etioporphyrin I diacetate, a compound not described by these authors, was made by extracting 500 mg etioporphyrin I from an extraction thimble into glacial acetic acid (100 ml), with 500 mg manganese chloride and 500 mg sodium acetate. The solution was concentrated to 25 ml , and the product that separated was washed with water and dried. The product was purified by sublimation under high vacuum at 350°C.

Only for cobalt(II) etioporphyrin I is there a big difference between the spectra in chloroform and in pyridine. The possibility that the complex in pyridine has been oxidized (or that an O_2-containing complex has been formed, or both) cannot be excluded.

C. ORGANIC CHEMISTRY

1. THE RADIATION DECOMPOSITION OF ADENINE

Cyril Ponnamperuma and Richard M. Lemmon

The action of ionizing radiation on a solution of adenine gives rise to two types of effects. In one case the purine ring is preserved, while in the other the ring structure is destroyed.

The conversion of adenine to hypoxanthine[1] is an example of the first type. An amino group in the sixth position is replaced by a hydroxyl group.

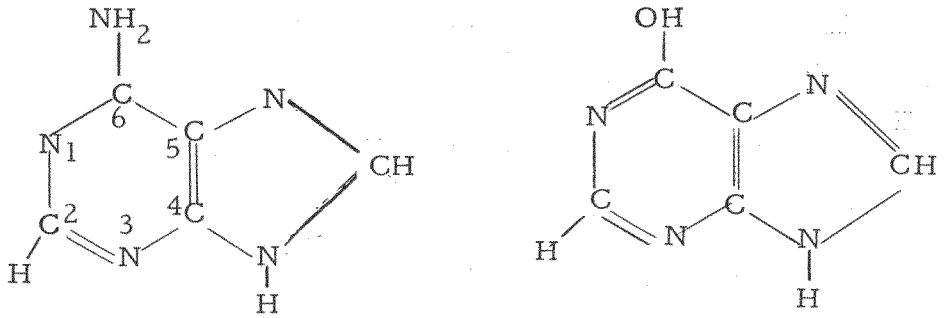

The extent of this conversion is small and the maximum effect observed was 1.9%. By analogy, however, to the deaminating action of HNO_2, which is a mutagenic agent,[2,3] the change from adenine to hypoxanthine under the influence of radiation is probably of great biological significance.[4]

The second type of radiation effect is characterized by severe damage to the molecule. Among the chief results observed are (a) the formation of water-insoluble volatile products, (b) the decrease in the optical density of the uv spectrum, and (c) the formation of two compounds in fair yield -- possibly formamidopyramidines.

Experimental Procedure

Adenine-2C^{14} of specific activity 1.3 mC/mmole was supplied by Isotope Specialties Inc., Burbank, Calif. The method of irradiation was the same as described in our earlier reports.[1] Two hundred and fifty µl of a 0.1% solution of adenine in water was sealed in vacuo. Dissolved oxygen had previously been expelled by bubbling nitrogen through the solution. The 1.5-kilocurie Co^{60} source was used for the irradiation. The intensity of radiation, calculated by Fricke ferrous sulfate dosimetry,[5] was 3.45×10^5 rads per hour.

---

[1] Cyril Ponnamperuma, Richard M. Lemmon, and Edward L. Bennett, in Bio-Organic Chemistry Quarterly Report, UCRL-9408, Sept. 1960.

[2] A. Gierer and K. W. Mundry, Nature 182, 1457 (1958).

[3] K. W. Mundy and A. Gierer, Z. Vererbungsforschung 89, 614 (1958).

[4] R. Lavalle, Compt. rend. 250, 1134 (1960).

[5] J. Weiss, A. O. Allen, H. A. Schwarz, in Proceedings of the International Conference on the Peaceful Uses of Atomic Energy, Geneva, 1955 (United Nations, New York, 1955), 14, 179.

To estimate the amount of volatile material formed, 25-μl portions of each of the irradiated solutions and of the control were diluted to 2 ml each. Aliquots (50 μl) of this solution were counted with a liquid scintillator using an internal standard.

The residual adenine was separated from the decomposition products of radiation by two-dimensional paper chromatography. Propanolammonia water was used as a solvent in one direction and butanol–propionic acid–water in the other.[6] Ten μl of each of the irradiated solutions was spotted on Whatman No. 4 paper, washed with oxalic acid. The uv-absorbing area was marked out and the spots eluted with 2 ml of 0.1% formic acid. The eluant was made up to 5 ml and 200 μl of each solution was counted with a liquid scintillator. The results are shown in Table V.

Table V. The radiation decomposition of adenine-2-C^{14}

Experiment	Dose (rads)	volatile C^{14} compounds (%)	Adenine destroyed (%)
Control	0	--	--
1	10^6	0	12.3
2	2×10^6	3.6	24.6
3	5×10^6	10.7	41.9
4	10×10^6	24.4	66.6
5	20×10^6	46.8	~ 100%

As the adenine used was labeled in the 2 position, most of the volatile material probably arose from the breakdown of the pyrimidine ring. At 20×10^6 rads no uv-absorbing spot was detected on the paper chromatogram, indicating complete disintegration of the ring structure.

Figure 20 shows the effect of irradiation on the uv absorption spectra of a 0.1% solution of adenine at pH 7. All measurements were made with a Cary recording spectrophotometer (Model 14). The optical density decreases with increasing radiation. At 20×10^6 rads there is no peak visible, confirming our findings by paper chromatography.

Figure 21 is a chromatogram of a 0.1% solution of adenine irradiated at 5×10^6 rads. Two well-defined areas of activity appear above the hypoxanthine spot. Hems[7,8] has reported that on irradiation purines

[6] E. L. Bennett, Biochim, Biophys. Acta 11, 487 (1953).

[7] G. Hems, Nature 181, 1721 (1958).

[8] G. Hems, Radiation Research 13, 777 (1960).

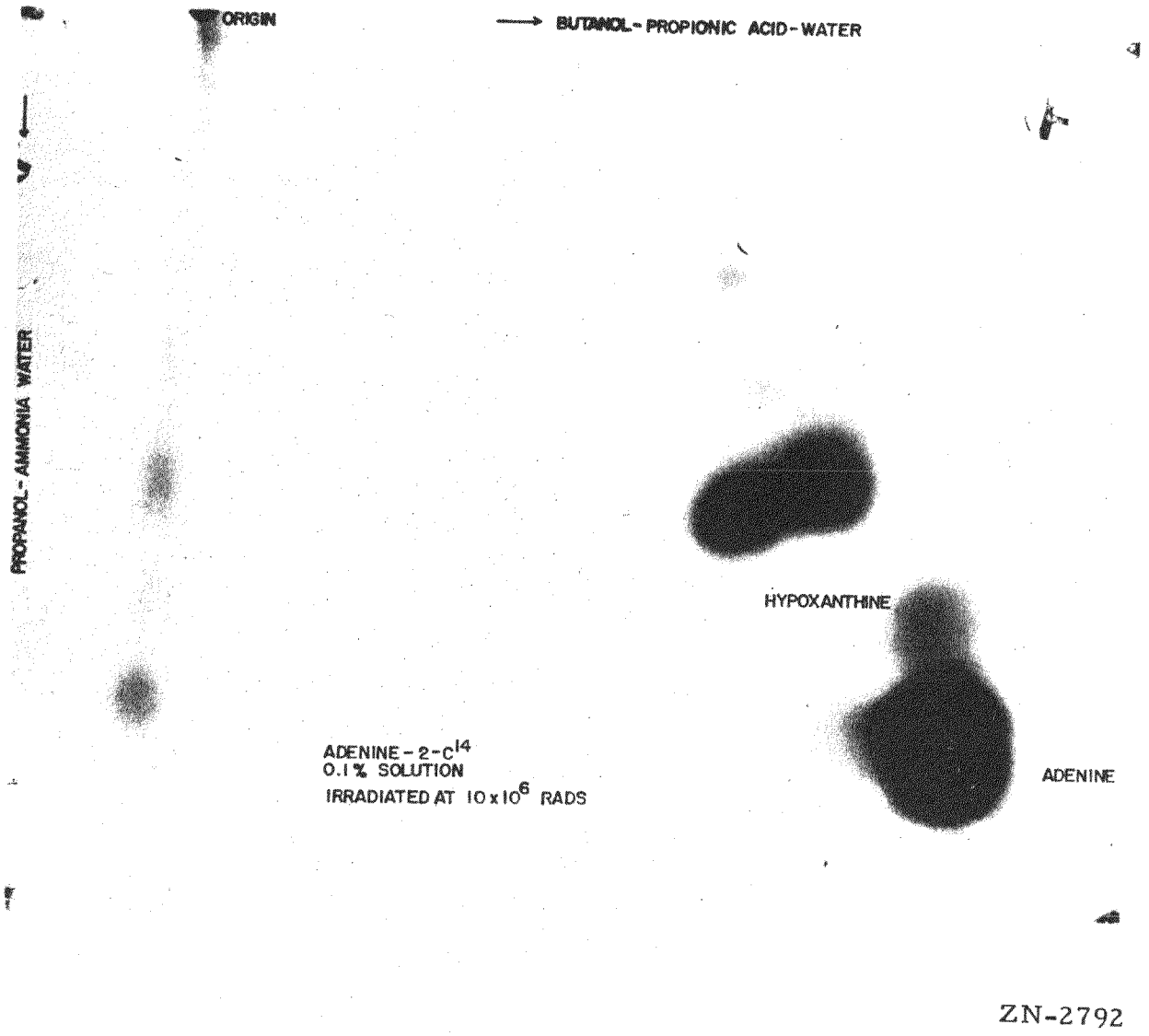

Fig. 20. Chromatogram of irradiated adenine-$2C^{14}$.

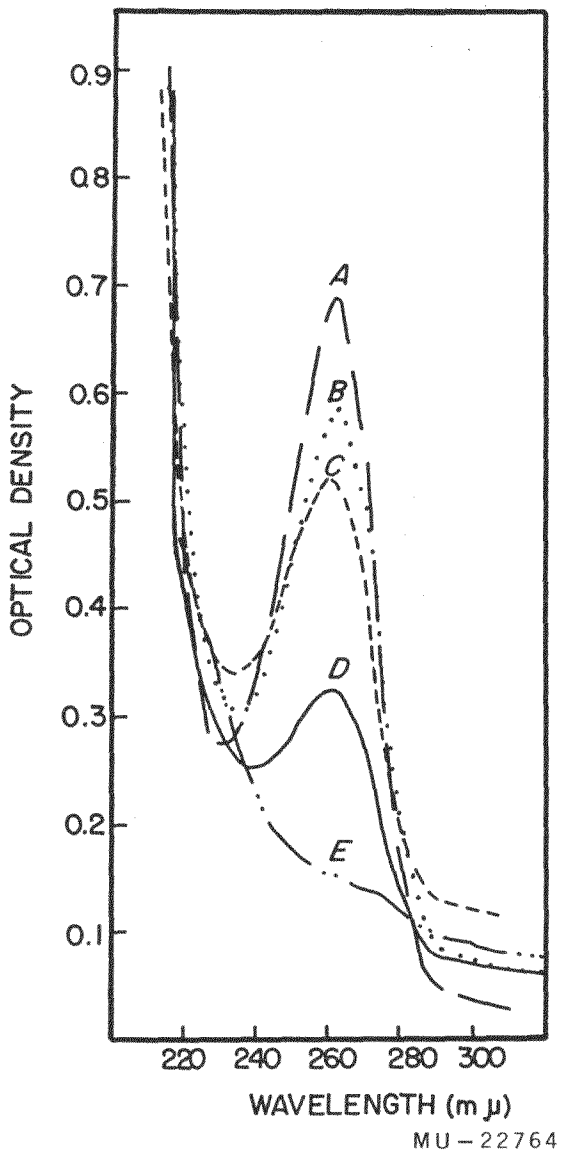

Fig. 21. Uv absorption spectra of irradiated adenine.

decomposed, with the fission of the imidazole ring, to give rise to formamidopyramidines. Thus, in adenine, a fission of the bond between C-8 and N-9 gives rise to a formamido compound of the structure

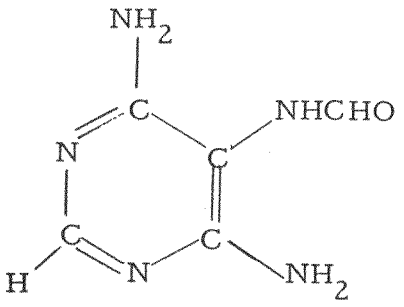

As no evidence is yet available for the mechanism of the fission of the imidazole ring under the influence of ionizing radiation, it may be supposed that ring opening could also take place by fission of the N-7—to—C-8 bond, giving rise to a formamido compound of the form

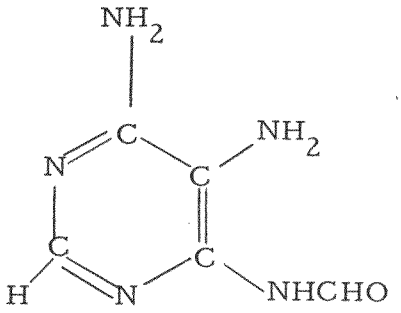

The two unidentified spots may be formamidopyramidines. The nature of these two compounds is now being studied.

2. STUDIES ON OXIDATION AND REDUCTION REACTION OF MANGANESE PHTHALOCYANINE COMPLEX

Akio Yamamoto

Introduction

It has been known that manganese plays an important role in photosynthesis, particularly in connection with the Hill reaction.[1-7] The study of oxidation and reduction reaction of manganese phthalocyanine complex was taken up in this laboratory with the hope of solving some of the key problems in the field of photosynthesis by studying this model compound.

Elvidge and Lever have reported that manganese (II) phthalocyanine can combine reversibly with oxygen in pyridine solution.[8] One molecule of oxygen is absorbed at room temperature per two molecules of manganese phthalocyanine. If the solution of the oxidized product is boiled, manganese(II) phthalocyanine is re-formed. Elvidge and Lever proposed the following scheme for the reactions

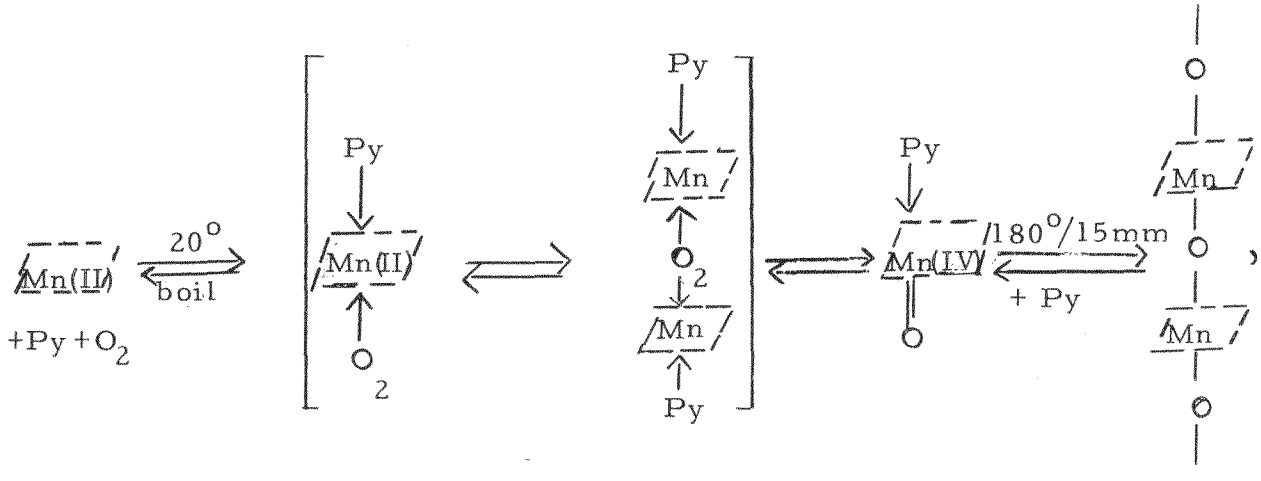

[1] E. Kessler, Planta 49, 435 (1957).

[2] E. Kessler, W. Arthur, and J.E. Brugger, Arch. Biochem. Biophys. 71, 326 (1957).

[3] T.E. Brown, H.C. Eyster, and H.A. Tanner, in Trace Elements p. 135, (Academic Press, Inc., New York, 1958).

[4] H.C. Eyster, T.E. Brown, and H.A. Tanner, in Trace Elements p. 157, (Academic Press, Inc. New York, 1958.

[5] H.A. Tanner, T.E. Brown, C. Eyster, and R.W. Treharne, Ohio J. Science 60 (4) 231 (1960).

[6] R.W. Treharne, T.E. Brown, H.C. Eyster, and H.A. Tanner, Biochem. Biophys. Research Communs. 3, 119 (1960).

[7] H.A. Tanner, T.E. Brown, C. Eyster, and R.W. Treharne, Biochem. Biophys. Research Communs. 3, 205 (1960).

[8] J.A. Elvidege and A.B.P. Lever, Proc. Chem. Soc., June-July, 195 (1959).

where $/\overline{Mn}/$ = PcMn = manganese phthalocyanine = $C_{32}H_{16}N_8Mn$, and Py = pyridine.

In this Laboratory, Markham has found that the absorption band at 7125 A previously ascribed by Elvidge and Lever to manganese (II) phthalocyanine is in fact due to an intermediate oxidation compound.[9] When a pyridine solution of manganese (II) phthalocyanine was prepared in the absence of air, a spectrum was obtained that had peaks at 880, 835, 660, 643, 596, and 557, and small peaks at 716 and 620 mμ. By introducing air to the solution, Markham observed an increasing band at 716 mμ which corresponds with Elvidge and Lever's band at 712.5 mμ. This band gradually built up to a maximum and then decreased, giving a spectrum with an absorption maximum at 620 mμ (Fig. 22). He ascribed the bands at 880, 835, 660, 643, 596, and 557 to manganese (II) phthalocyanine monoxide, and the transient band at 716 mμ to the peroxide of manganese (III) phthalocyanine with the structure:

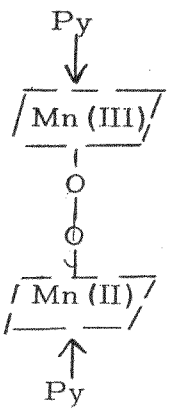

He also found that light breaks up the transient manganese (III) compound to form manganese (II) and manganese (IV) compounds. On the basis of these results the following scheme was proposed.

[9] Edward Markham, in Bio-Organic Chemistry Quarterly, UCRL-9041, Dec. 1959; UCRL-9208, June 1960; UCRL-9408, Sept. 1960.

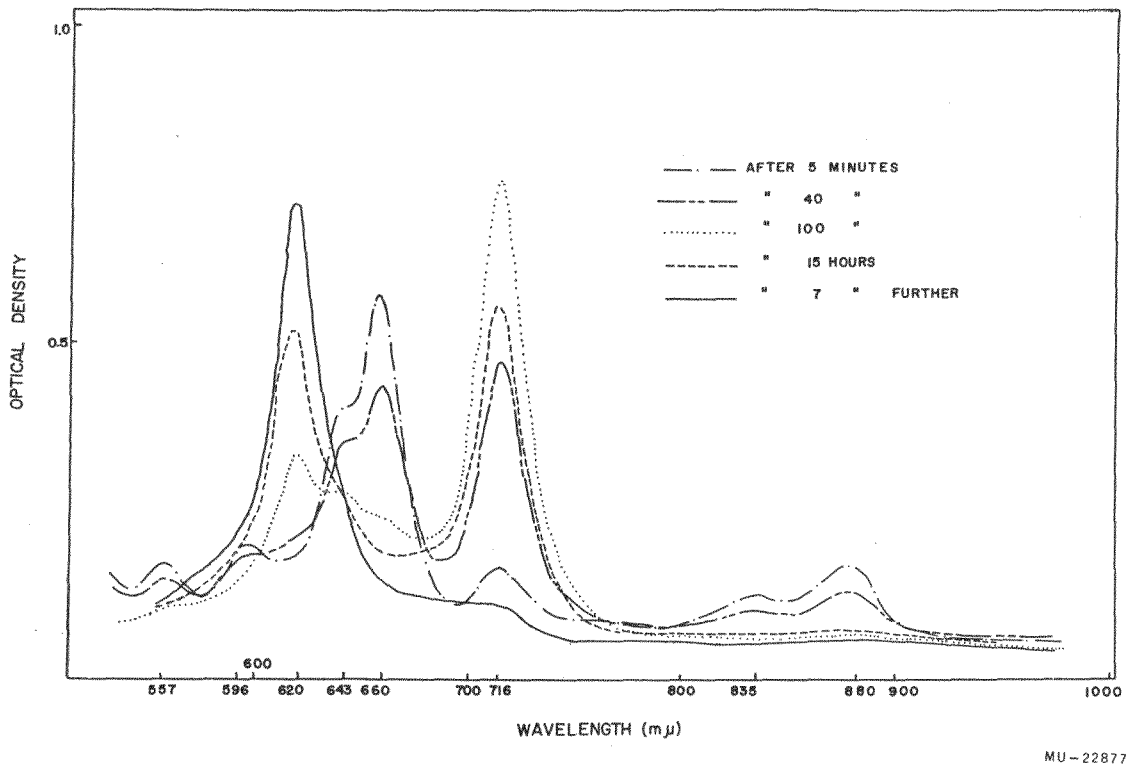

Fig. 22. Oxidation of manganese (II) phthalocyanine in pyridine solution.

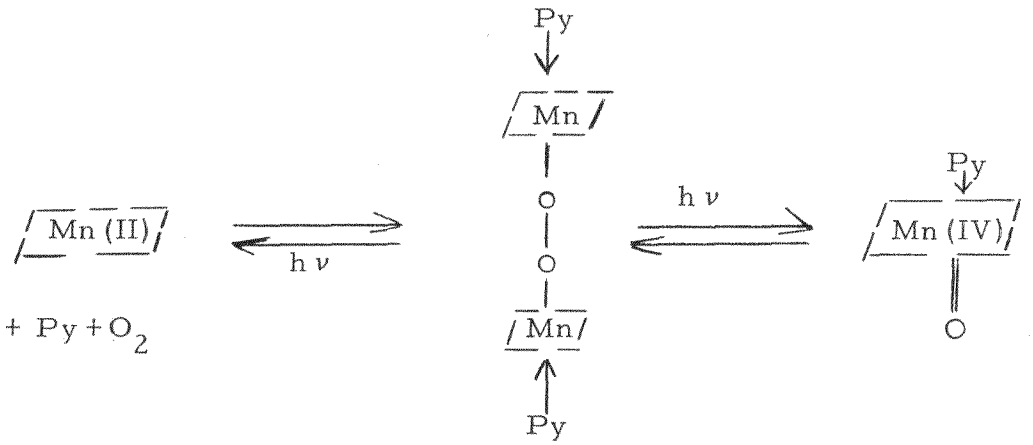

In order to test the validity of the mechanism, we found it necessary to study this reaction further with visible, uv, ir, and ESR spectroscopy. This report gives the results of this line of the investigation.

Experimental Procedure

Visible, uv, and Near-Infrared Spectra were measured by using a Cary 14 recording spectrophotometer. The technique used to prepare the solution in an optical cell in the absence of air was the same as Markham's.[9]

Infrared Spectra were measured by using a Beckman IR-7 spectrophotometer. Manganese phthalocyanine compounds were measured in KBr discs.

Electron Spin Resonance Spectra were measured with a Varian 100 Kc ESR Spectrometer.

Manganese phthalocyanine complexes were obtained by two methods. Manganese (II) phthalocyanine was prepared according to Rutter and McQueen's method[10] from manganese acetate and phthalonitrile in the yield of 52%. The product was purified by vacuum sublimation at $420^{o}/10^{-5}$ mm. Visible and ir spectra were compared that found by Markham for a product prepared according to the method of Barrett, Dent, and Linstead[11] from manganese dioxide and phthalocitrile. The two samples were found to be identical.[12] Figure 23 shows the ir spectrum of the manganese (II) phthalocyanine.

---

[10] H. A. Rutter, Jr., and J. D. McQueen, J. Inorg. Nuclear Chem. 12, 362 (1960).

[11] P. A. Barrett, C. E. Dent, and R. P. Linstead, J. Chem. Soc. 1936, 1719.

[12] Rutter and McQueen have stated in their report that their sample showed the absorption band at 620 mμ in pyridine solution. In view of our present knowledge, their pyridine solution used for the measurement is considered to have been oxidized to Mn (IV) phthalocyanine oxide.

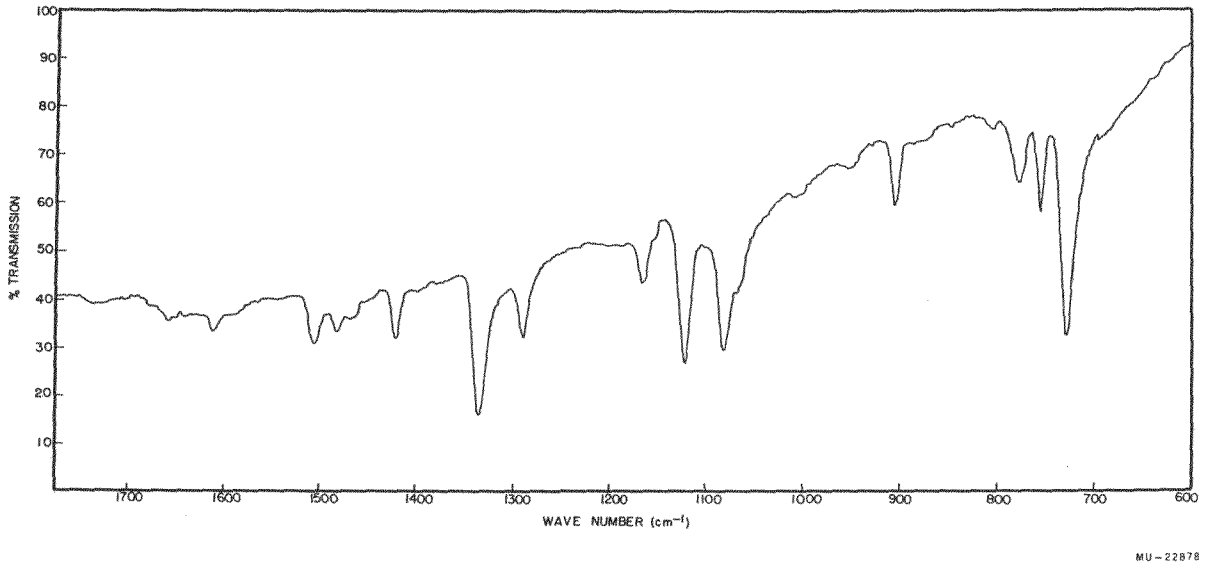

Fig. 23. Infrared spectrum of manganese (II) phthalocyanine.

Pyridine Manganese (IV) Phthalocyanine Monoxide was prepared from manganese (II) phthalocyanine by oxidation in air. The crystals of manganase (II) phthalocyanine were dissolved in pyridine at room temperature and the solution was allowed to stand for a few days exposed to air. Purple rhombs of pyridine manganese (IV) phthalocyanine oxide deposited and were collected. Figure 24 shows the ir spectrum of the sample. An absorption band is observed at 1100 cm^{-1} which is ascribed by Elvidge and Lever[8] to Mn = 0 linkage, although the intensity is not as strong as they stated.

Results and Discussion

Reduction of Manganese (IV) Phthalocyanine in Pyridine.

Although Elvidge and Lever have stated in their report[8] that the pyridine solution of manganese (IV) phthalocyanine oxide (λ_{max} 620 mμ) is reduced by boiling to a green solution of manganese (II) phthalocyanine, they apparently have not studied the reaction spectroscopically. Refluxing the solution of manganese (IV) phthalocyanine oxide in a stream of argon gave the spectrum of manganese (II) phthalocyanine at 880, 835, 660 mμ and soon as well as the band at 716 mμ. However, the reduction was not complete, and the band of the intermediate oxidation compound at 716 mμ did not disappear. The complete reduction of manganese (IV) phthalocyanine oxide to manganese (II) phthalocyanine was accomplished as follows. The optical cell containing a pyridine solution of manganese (IV) phthalocyanine oxide was cooled in liquid N_2 and evacuated to 10^{-5} mm, after which the system was closed and was heated at 60°. This process was repeated several times. The color of the solution changed from blue to green and the spectrum shown in Fig. 25, Curve 1 was obtained. This solution is photosensitive, the band near 720 mμ being suppressed and the bands at 660 and 880 mμ and soon increased by light. The change is carried out even with the light in the spectrophotometer. (In the Cary 14 spectrophotometer, all the light from the ir source passes through the sample before it is resolved by the monochromater.)

The spectral change was observed after certain time intervals, and is graphically shown in Fig. 26, in which the optical density of the peak at 660 and 725 mμ is plotted against time. The band near 720 mμ disappeared completely after 4 hours, and the genuine spectrum of manganese (II) phthalocyanine (probably its pyridine complex) was obtained for the first time; no band at 620 mμ was observed (Fig. 27). The interesting feature is the change of the band near 720 mμ. It appears that this band is a composite one, and after the band at 720 mμ had been suppressed by light, the band at 730 mμ remained but was then also suppressed completely (see Fig. 25).

Oxidation of Manganese (II) Phthalocyanine in Pyridine by Air

When a small amount of air was introduced into this reduced manganese (II) phthalocyanine solution, nearly inverse behavior of the reduction reaction was observed except for the appearance of the band at 620 mμ. The bands due to manganese (II) phthalocyanine decreased with the increase of the oxidation product. The composite peak near 720 mμ was observed in this case, too (Fig. 28). These observations suggest the presence of two intermediate oxidation compounds as follows.

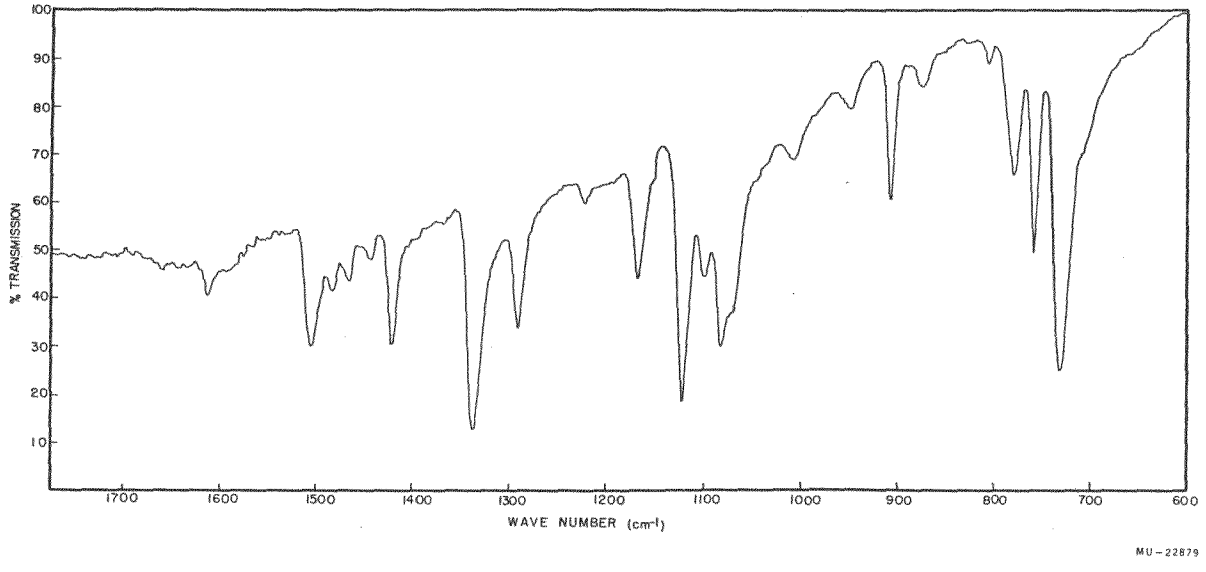

Fig. 24. Infrared spectrum of pyridine-manganese (IV) phthalocyanine oxide.

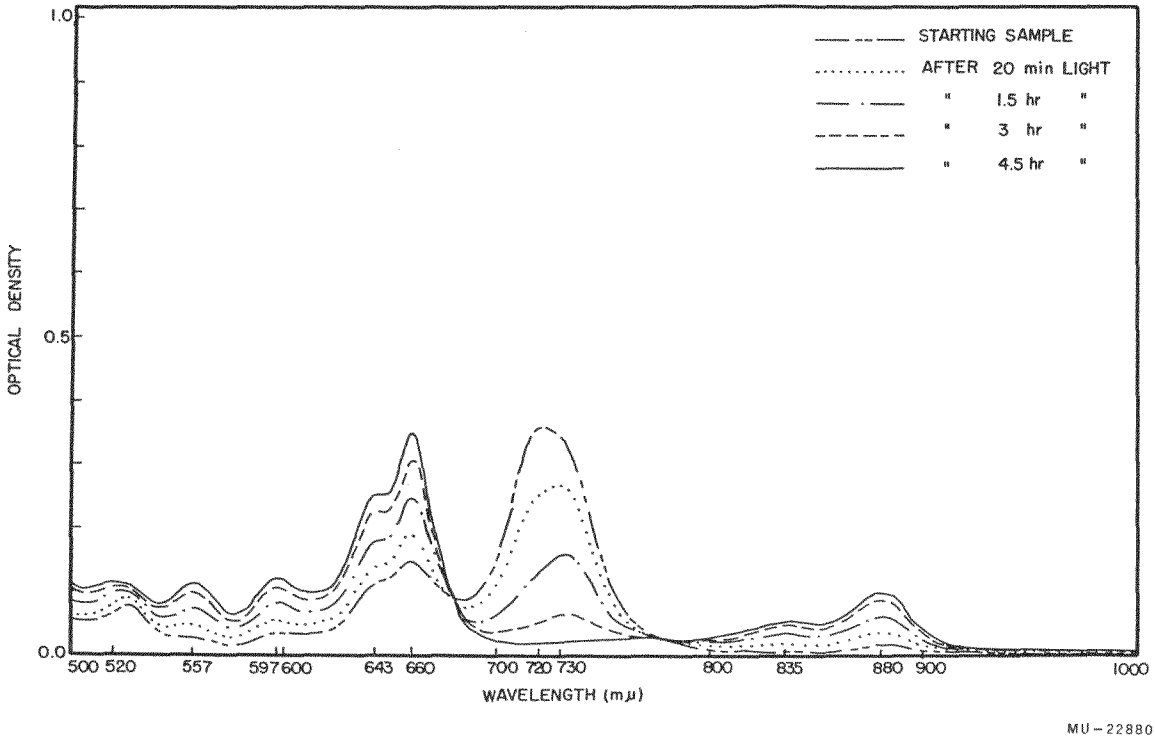

Fig. 25. Reduction of manganese (IV) phthalocyanine oxide to manganese (II) phthalocyanine in pyridine solution.

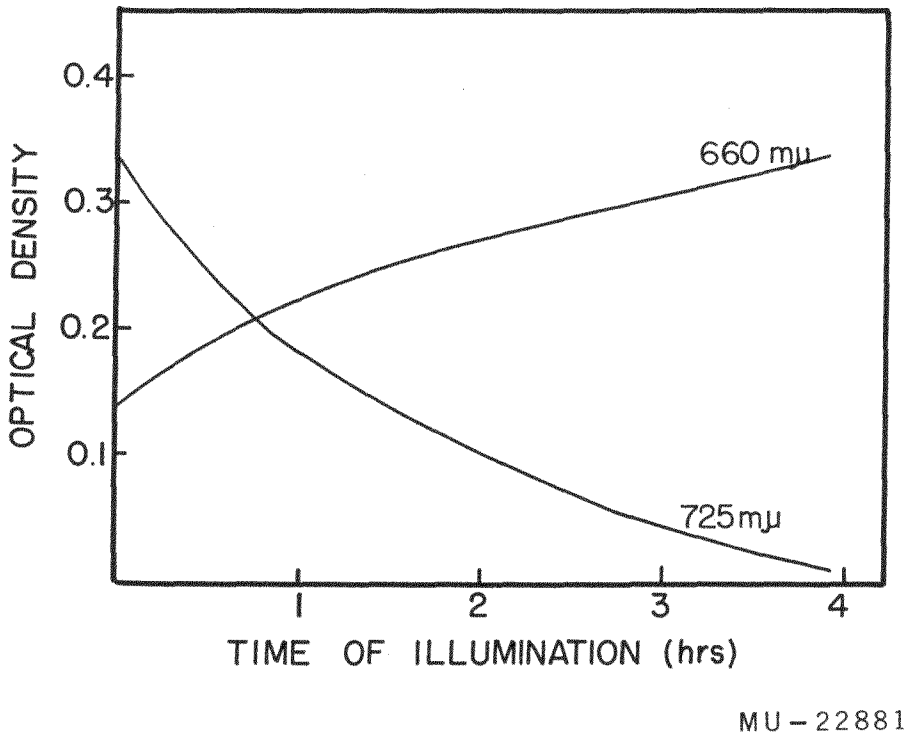

Fig. 26. Change of the optical densities of the bands at 660 and 725 mμ.

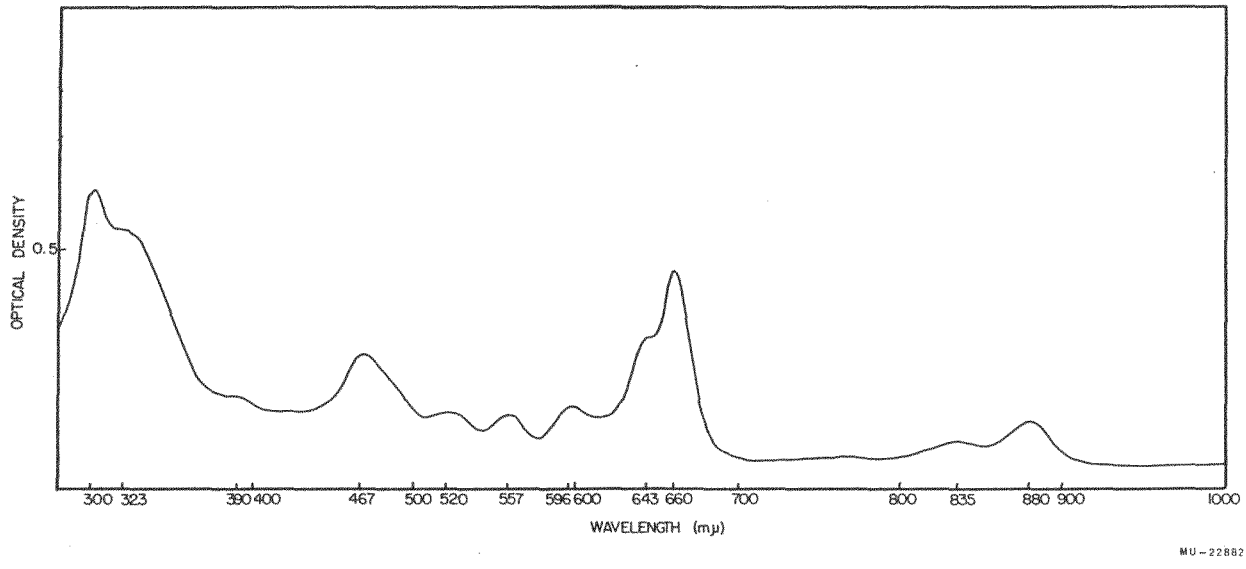

Fig. 27. Spectrum of manganese (II) phthalocyanine in pyridine.

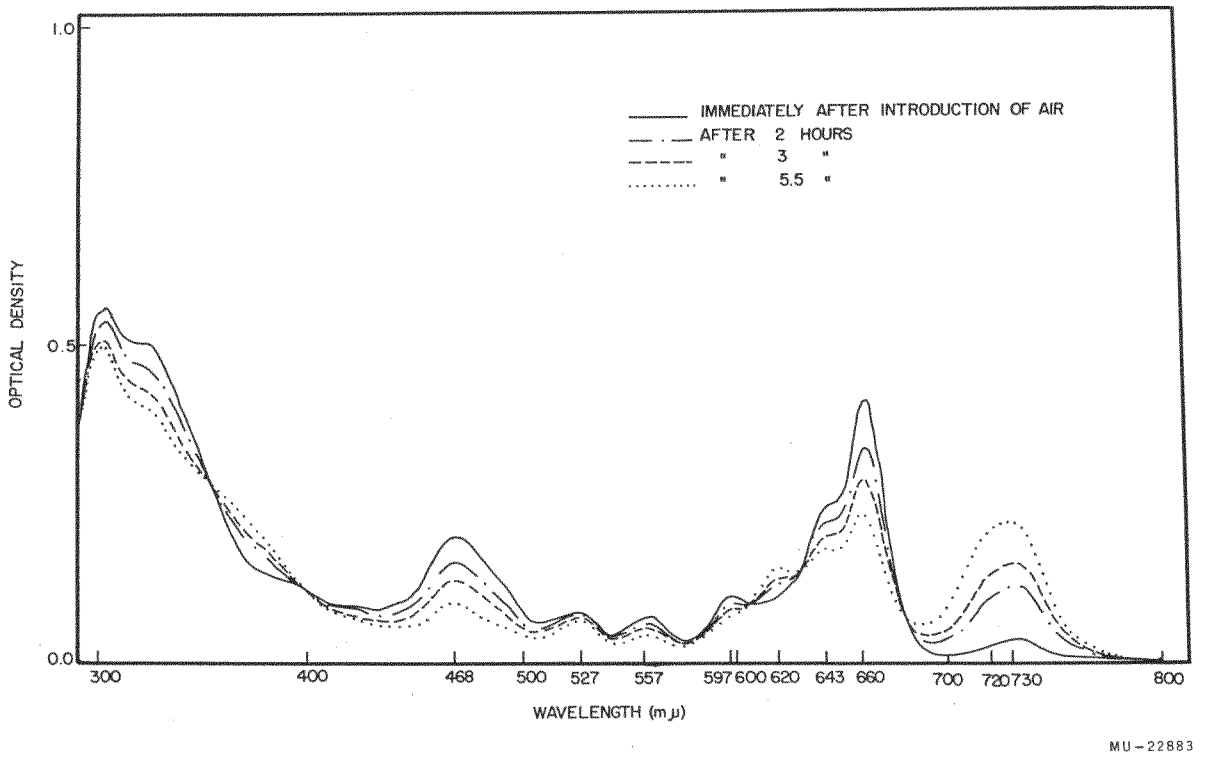

Fig. 28. Oxidation of manganese (II) phthalocyanine.

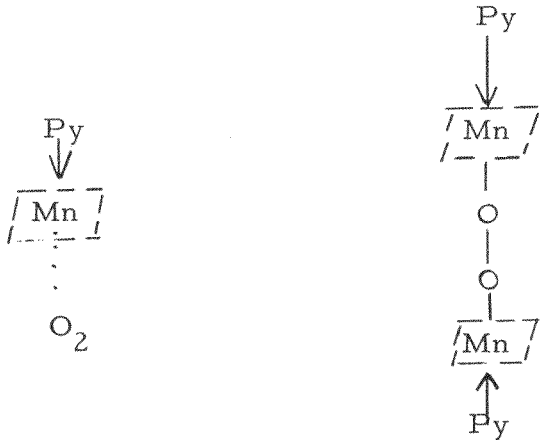

(1) (2)

Oxidation and Reduction in Other Solvents

The experiments described above and those by Markham had been carried out with only pyridine as a solvent. Now other solvents than pyridine were tried, and manganese phthalocyanines were found to be soluble in 1-chloronaphthalene, although only slightly, and somewhat less soluble in chlorobenzene, ethanol, and methanol. When manganese (II) phthalocyanine was dissolved in 1-chloronaphthalene, in the presence of air, a brown solution was obtained. The position of the main absorption peak at 726 mμ (Fig. 29) is close to the peak for the intermediate oxidation compound observed in pyridine solution (Fig. 22). The spectra of chlorobenzene and alcohol solutions were similar, with the maximum at 716 mμ. When crystals of pyridine-manganese (IV) phthalocyanine oxide were dissolved in these solvents, the band at 620 mμ was observed first, but soon disappeared, and exactly the same spectra as those obtained by dissolving Manganese (II) phthalocyanine in the presence of air were obtained. This may be explained by association of Manganese (IV) phthalocyanine monoxide into the dimer Manganese (III) phthalocyanine peroxide due to the solvent effect:

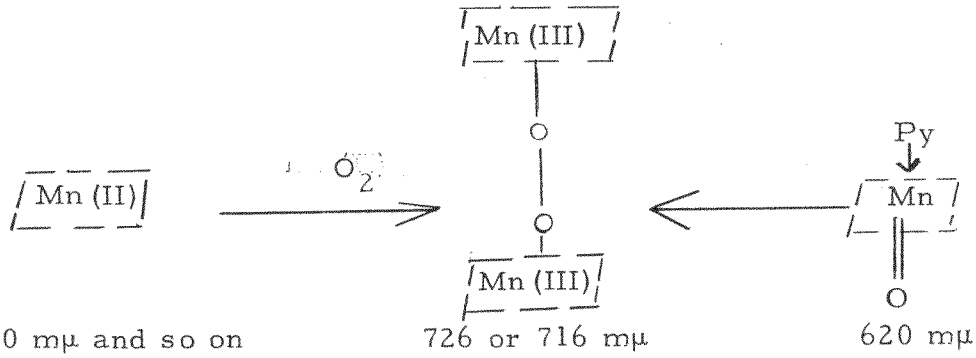

880 mμ and so on 726 or 716 mμ 620 mμ

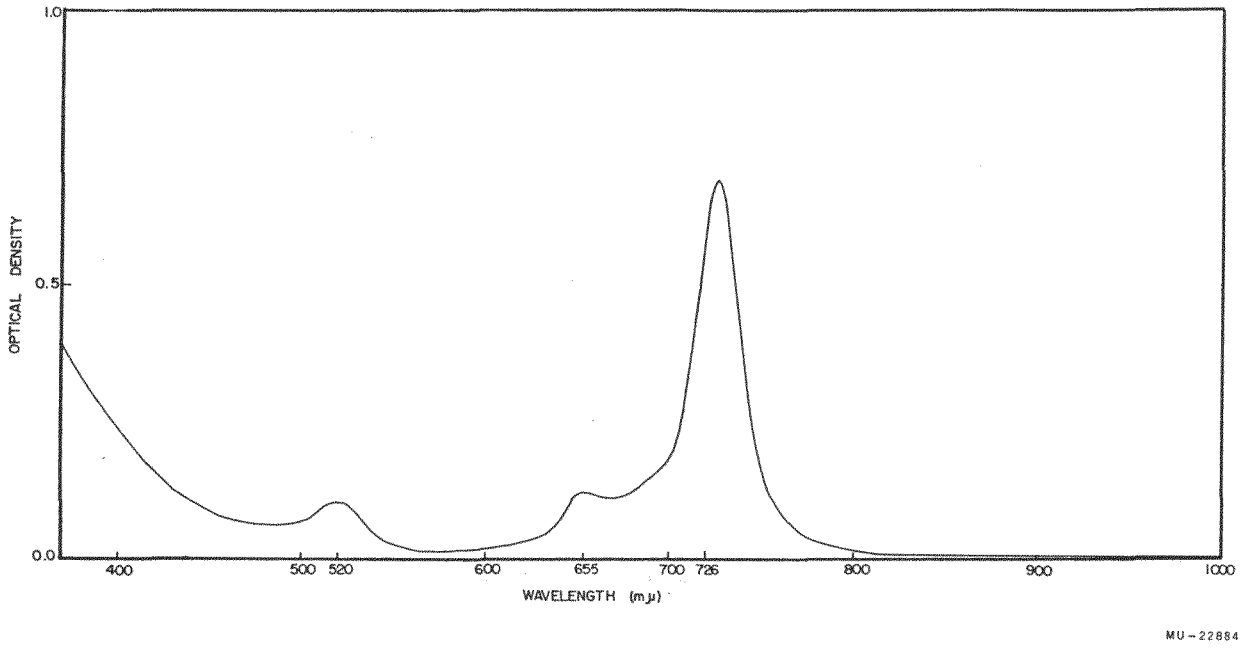

Fig. 29. Spectrum of manganese (III) phthalocyanine oxide in the 1-chloronapthalene solution.

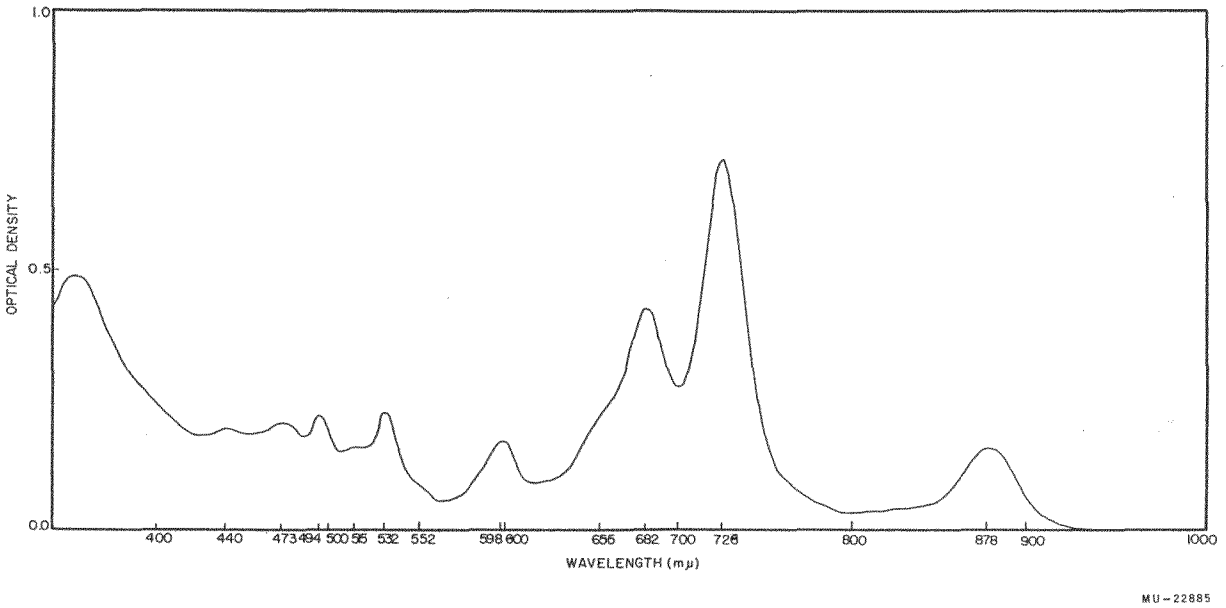

Fig. 30. Spectrum of manganese(II) phthalocyanine in 1-chloronaphthalene solution in the absence of air.

I could prove that the band at 726 mμ is due to the intermediate oxidation compound as follows. Manganese (II) phthalocyanine was dissolved in 1-chloronaphthalene in the absence of air, and the spectrum shown in Fig. 30 was obtained. This spectrum was similar to the spectrum of mangnaese (ii) phthalocyanine in pyridine except for the peak at 726 mμ, which is considered to be an oxidized manganese (iii) phthalocyanine peak.[13] When air was introduced into the solution, the peak at 726 mμ increased in intensity with the decrease of the peaks at 878, 682, 655, 598, 532, 494, 473, and 449 mμ, and eventually the spectrum identical with that in Fig. 29 was obtained. These bands decreased are attributed to Manganese (II) phthalocyanine (or its π complex with 1-chloronaphthalene) in 1-chloronaphthalene solution. For comparison, the spectrum of solid Manganese (II) phthalocyanine prepared by vacuum sublimation on the wall of an optical cell is shown in Fig. 31.

Requirement of Pyridine and Light for Reduction to Manganese (II) Phthalocyanine

Pyridine appears to play essential roles in these reactions. I tried to reduce Manganese (III) phthalocyanine oxide to Manganese (II) phthalocyanine by using reducing agents such as hydroquinone, benzaldehyde, and ascorbic acid, without any success. Pumping out the solution alternately with heating to near the boiling temperature of the solvent, illumination in vacuo, or combinations of these methods were tried, but no sign of appearance of Manganese (II) bands was observed. Only in the presence of pyridine and under illumination in vacuo did the reduction of Manganese (III) phthalocyanine oxide to Manganese (II) phthalocyanine take place. The spectrum of Manganese (III) phthalocyanine oxide in 1-chloronaphthalene, as shown in Fig. 29, was transformed by illumination in vacuo in the presence of pyridine to the spectrum which is very similar to the spectrum of Manganese (II) phthalocyanine in pyridine solution (Fig. 27). The similar phenomenon was also observed in the case of methanol solution of Manganese (III) phthalocyanine oxide (Fig. 32), although in this case the photoreduction was very sluggish. The spectrum of Manganese (II) phthalocyanine obtained from the methanol solution of Manganese (III) phthalocyanine in the presence of pyridine (20% of methanol solution) in vacuo and under illumination is shown in Fig. 33. A slight difference from the spectrum of Manganese (II) phthalocyanine in 1-chloronaphthalene solution is observed, due to the solvent effect.

The Effect of Light on the Change from Manganese (III) Phthalocyanine Oxide to Py·Manganese (IV) Phthalocyanine Oxide

The change from Manganese (IV) phthalocyanine oxide to Manganese (III) phthalocyanine oxide takes place upon addition of alcohol to the pyridine solution of Manganese (IV) phthalocyanine oxide. However, the reverse reaction does not take place in the absence of oxygen. Addition of pyridine in vacuo to the 1-chloronaphthalene or the methanol solution of Manganese (III) phthalocyanine oxide did not cause any change in the spectrum with λ_{max} 726 mμ or 716 mμ. Only when air was introduced to the solution was the increase of the band at 620 mμ and decrease of the band near 720 mμ observed. Light was found to have a profound effect on the change of Manganese (III) phthalocyanine oxide to Manganese (IV) phthalocyanine oxide. Figures 34a and 34b show how the light accelerated the change of the bands

[13] The band at 716 mμ or 726 mμ was tentatively ascribed to Manganese (III) phthalocyanine oxide, although the valence state of manganese has not been established yet.

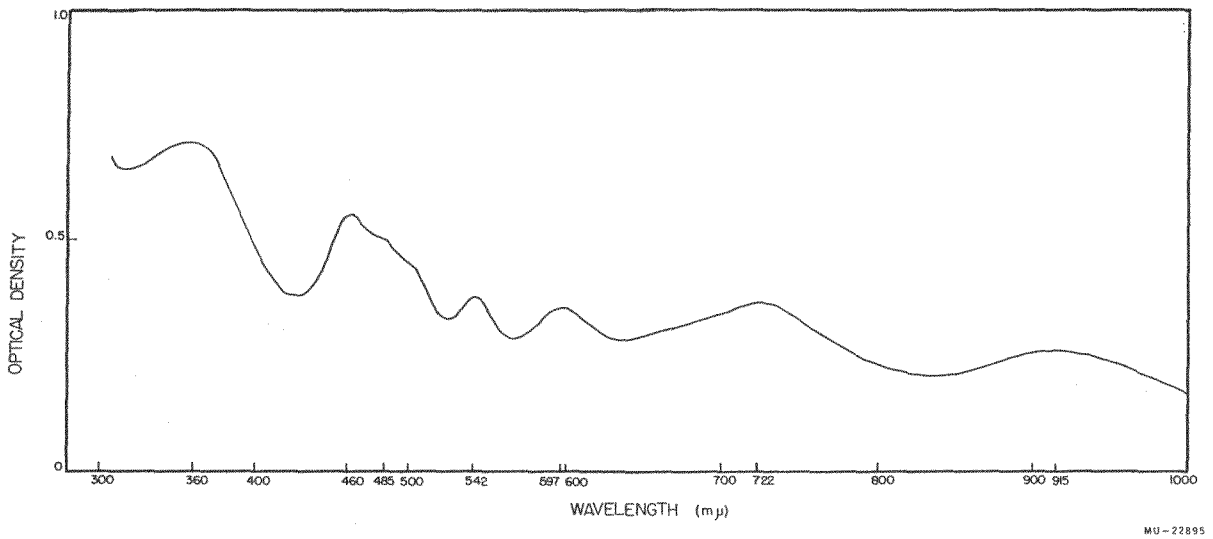

Fig. 31. Spectrum of solid manganese(II) phthalocyanine.

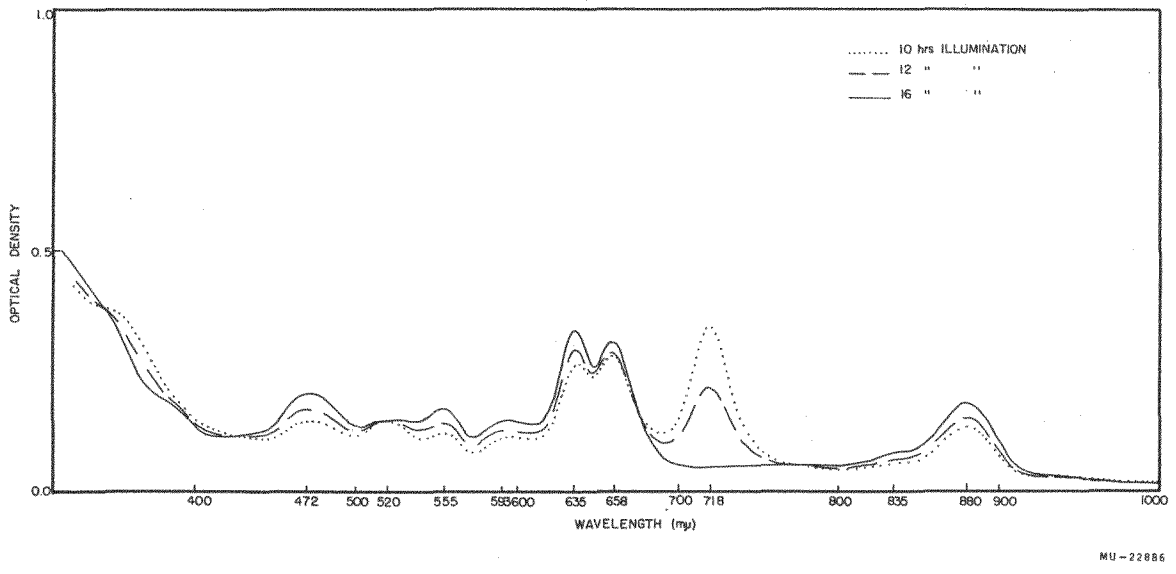

Fig. 32. Photoreduction of manganese (III) phthalocyanine to manganese (II) phthalocyanine in the methanol solution containing 20% pyridine.

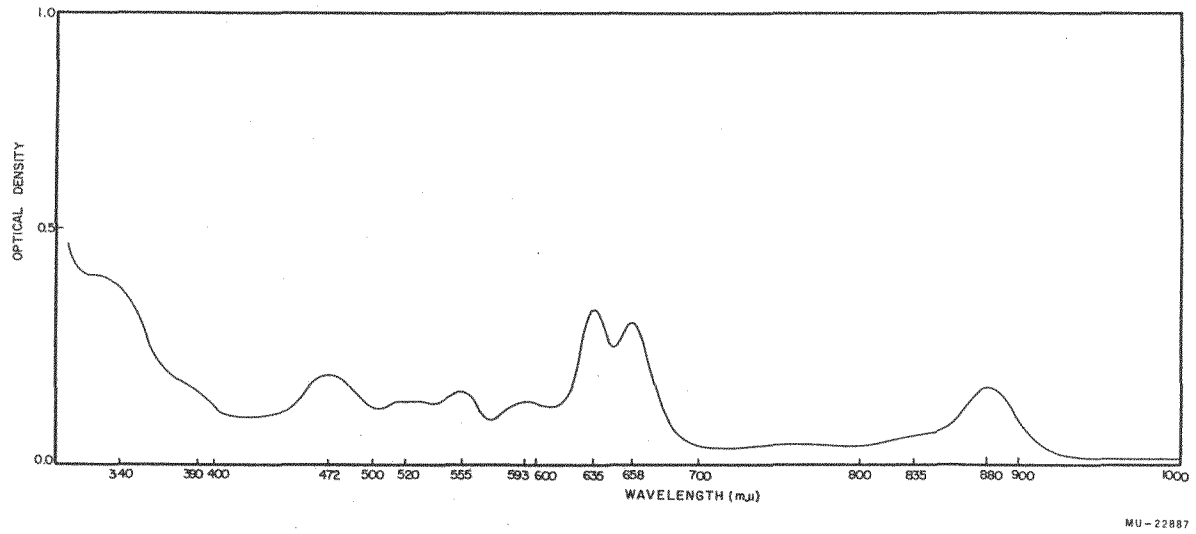

Fig. 33. Spectrum of photoreduced manganese (II) phthalocyanine in the methanol solution containing 20% pyridine.

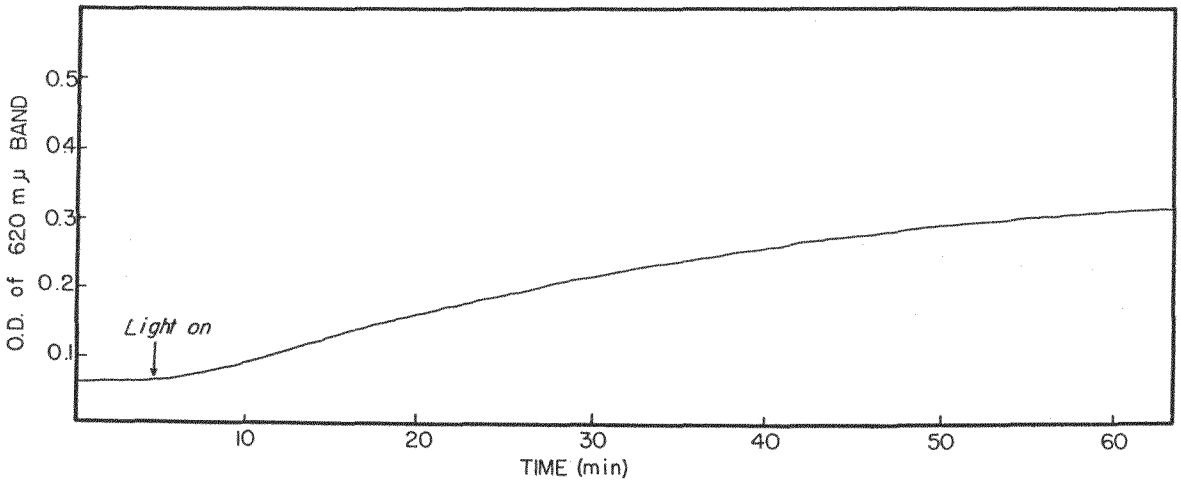

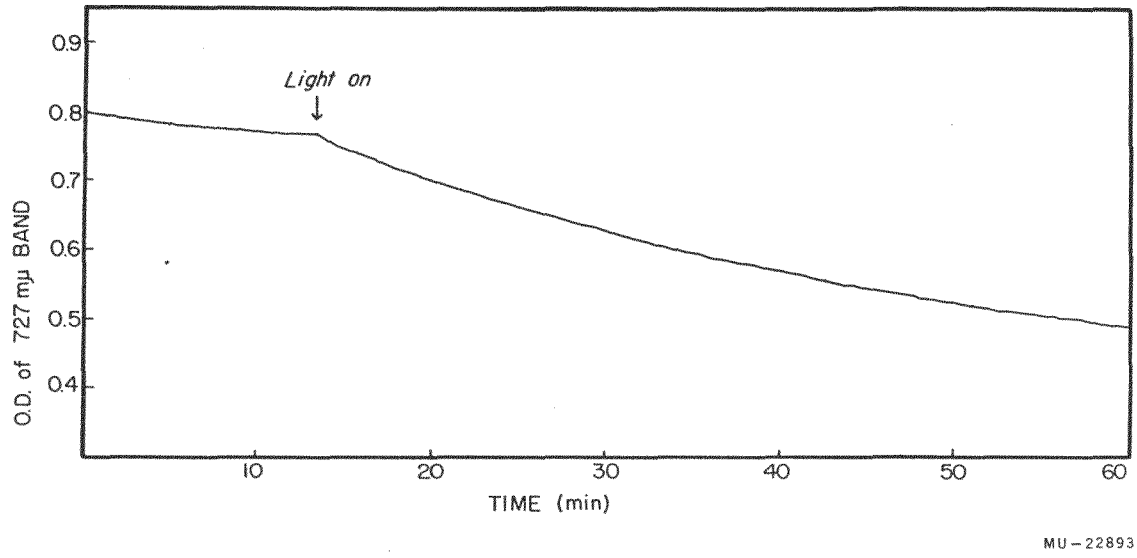

Fig. 34. Effect of light on the change of manganese (III) phthalocyanine oxide to manganese (IV) phthalocyanine oxide. a. Growth of the peak at 620 mμ. b. Disappearance of the peak at 727 mμ.

at 620 mμ and 720 mμ when 1 ml of pyridine was added to 2 ml of 1-chloronaphthalene solution of Manganese (III) phthalocyanine oxide. The ir lamp in the spectrophotometer was used as the light source.

The effect of the specific wave length of light was next investigated. The solution in the compartment of the spectrometer was illuminated from outside through appropriate filters. Pyridine (2.0 ml) was added to 1-chloronaphthalene solution (1.0 ml) of Manganese (III) phthalocyanine oxide and the increase of the band at 620 mμ was observed at atmospheric pressure under illumination with light of 720 mμ (Fig. 35). The rate of growth of the band at 620 mμ in the dark was very slow. When the light was turned on, the band at 620 mμ grew at a considerable rate after a short induction period. When the light was turned off, the rate of growth was unchanged for a short interval and then decreased. Illumination with light of 620 mμ had no effect on the rate of disappearance of the 723-mμ band of Manganese (III) phthalocyanine oxide.

Similar experiments were carried out with the rate of disappearance of Manganese (IV) phthalocyanine oxide. To a pyridine solution of Manganese (IV) phthalocyanine oxide, methanol was added, and the rate of disappearance of the band at 620 mμ and the rate of growth of the band at 723 mμ were observed. The reaction appears to be composed of rapid and slow steps. When the solution was illuminated with the ir lamp in the spectrometer, the rate of disappearance of the band at 620 mμ stopped, and after a slight growth the band diminished again (Fig. 36a). No effect of light was observed on the growth rate of the band at 723 mμ (Fig. 36b). Illumination with light of specific wave length (620 mμ and 730 mμ) did not show any effect.

The effect of light appears to be in breaking up the bridged structure of Manganese (III) phthalocyanine peroxide to Manganese (II) phthalocyanine or Manganese (IV) phthalocyanine oxide. In the absence of oxygen, the photoreduction of Manganese (III) phthalocyanine oxide to Manganese (II) phthalocyanine is predominant. In the presence of enough oxygen the change from Manganese (III) phthalocyanine oxide to Manganese (IV) phthalocyanine oxide is observed, since the reduced Manganese (II) phthalocyanine, if formed, would be reoxidized.

A Possibility of Polymer Formation for Manganese (IV) Phthalocyanine Oxide

Markham noted a peculiar phenomenon when he observed the spectra of the pyridine solution with different concentrations of Manganese (IV) phthalocyanine and diluted this stock solution to make solutions with concentrations of 1/10, 1/100, and 1/200, and kept these solutions in the dark for 3 days. They were examined spectroscopically, immediately after removal from the dark. It was found that bands at 716 mμ had developed in these solutions. The development of the band was most pronounced in the solution of 1/100 concentration, and became less pronounced in the solution of 1/200 concentration. This phenomenon is rather difficult to explain as an association (dimerization) of Manganese (IV) phthalocyanine monoxide to give Manganese (III) phthalocyanine oxide, because if it were that, the peak at 716 mμ should be the most pronounced in the most concentrated solution. A conceivable but less plausible explanation would be as follows: Manganese (IV) phthalocyanine oxide may form a polymer in concentrated solutions, as shown.

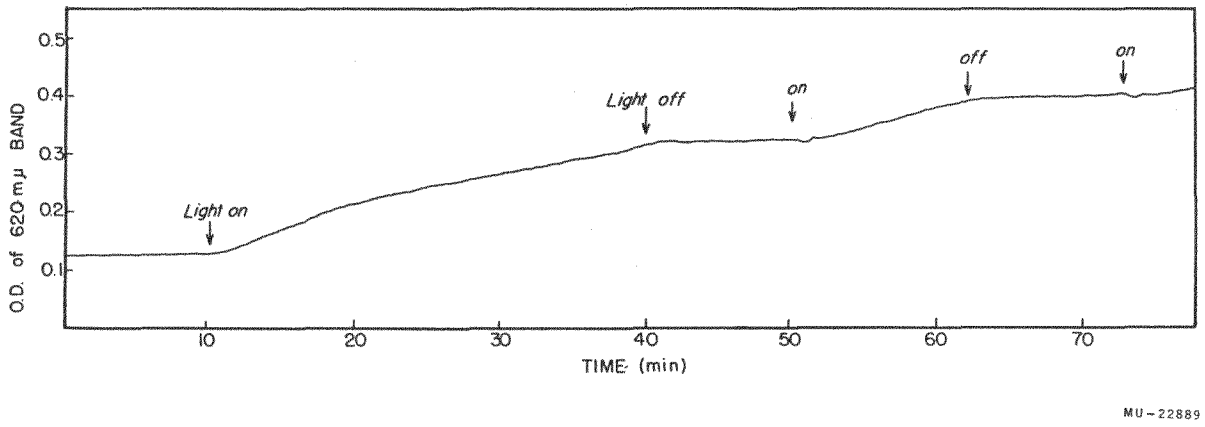

Fig. 35. Effect of light of specific wave length on the change of manganese (III) phthalocyanine oxide to manganese (IV) phthalocyanine oxide. Growth of the band at 620 mμ under illumination with light of 720 mμ.

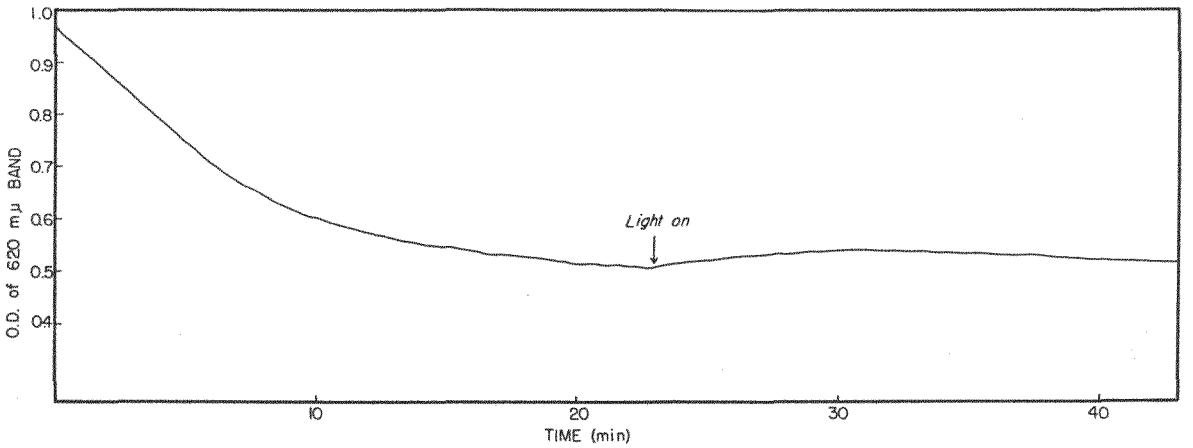

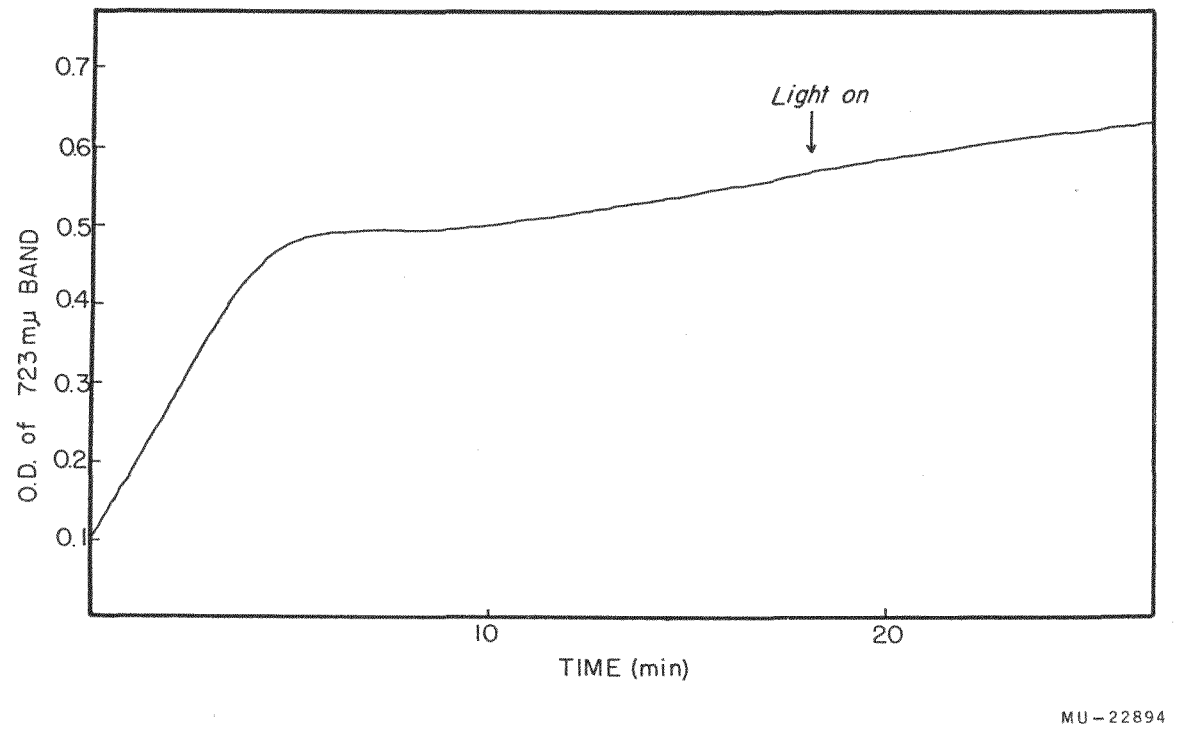

Fig. 36. Effect of light on the change of manganese (IV) phthalocyanine to manganese (III) phthalocyanine oxide. a. Decrease of the band at 620 mμ. b. Growth of the band at 723 mμ.

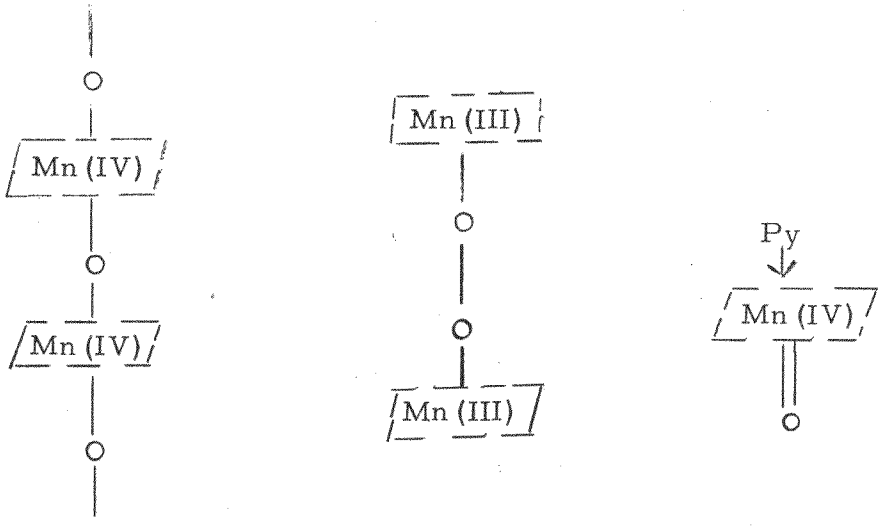

620 mμ 716 mμ 620 mμ

be broken up by dilution to dimer, i.e., Manganese (III) phthalocyanine peroxide, which is then broken up to monomer by further dilution. If the absorption bands of both Manganese (IV) compounds (polymer and monomer) should coincide, the band at 716 mμ would appear by dilution and then disappear by further dilution. The band at 716 mμ was photosensitive and was suppressed by light, while the band at 620 mμ grew.

The Effect of OH^- Ion

Markham has observed further strange behavior of manganese phthalocyanine compounds. He dissolved Manganese (II) phthalocyanine in a concentrated methanolic solution of sodium hydroxide and obtained a green solution with an absorption band at 678 mμ. However, he observed no change of the band upon adding methanolic sodium hydroxide to a solution of Manganese (IV) phthalocyanine oxide in pyridine. When he dissolved Py · Mn (IV) phthalocyanine oxide in methanol, a green solution having absorption maxima at 718 mμ and 645 mμ was obtained. Upon addition of sodium hydroxide to the methanol solution, he obtained a solution having a maximum at 678 mμ.

The bands at 718 mμ and 645 mμ are considered to belong to the Manganese (III) phthalocyanine oxide as described before, and if we assume that this compound reacts more readily with OH^- ion than does Manganese (IV) phthalocyanine oxide, this experimental result is easily explained.

Adding aqueous sodium hydroxide solution to the methanol solution of Manganese (III) phthalocyanine oxide (λ_{max} 716 mμ) dropwise, one can observe a very pronounced spectral change of the solution. Upon addition of a small amount of sodium hydroxide solution, a band is observed at 628 mμ which changes with time to a band at 702 mμ. By further addition of a small amount of sodium hydroxide solution, this peak at 702 mμ disappears and changes to a new band at 678 mμ. At least three species are considered to be involved in the reaction.

Titration of the aqueous methanol solution of Manganese (III) phthalocyanine oxide with dilute sodium hydroxide solution showed that this change is dependent on pH (Fig. 37). The band at 716 mμ disappeared at pH 10.0 and the band at 702 mμ was predominant between pH 10.0 and 11.0 but was displaced by the band at 678 mμ above pH 11.3. When this solution was titrated back with dilute solution of HCl, the change of the spectrum with pH occurred in reverse order and the original spectrum of Manganese (III) phthalocyanine was reproduced. When the solution stood in air, a white gel-like substance was precipitated, probably Manganese (IV) phthalocyanine hydroxide or its polymer.

From these results the reaction scheme in Fig. 38 is proposed tentatively.

At present the isolation of Manganese (III) phthalocyanine oxide is under way. Extraction of Py · Mn (IV) phthalocyanine oxide with methanol and evaporation of the extract gave a bluish-black powder. The ESR spectrum of this powder was different from that of Manganese (II) phthalocyanine or Py · Mn (IV) phthalocyanine oxide. The infrared spectrum was almost identical with that of Manganese (II) phthalocyanine. The amount of the sample was not enough for elementary analysis.

In photoreduction from Manganese (III) phthalocyanine to Manganese (II) phthalocyanine it has not yet been determined whether oxygen is evolved or pyridine-N-oxide is formed. Future work will be focused on this line of investigation.

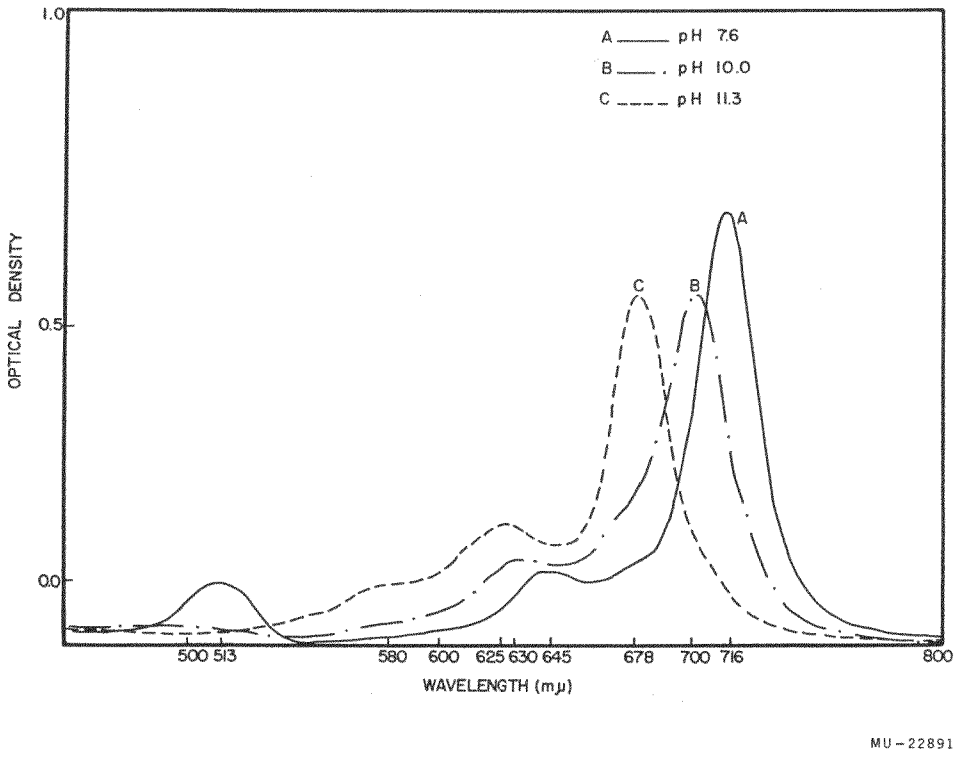

Fig. 37. Chance of the spectra of manganese (III) phthalocyanine oxide according to the change of pH.
A. pH 7.6 B. pH 10.0 C. pH 11.3

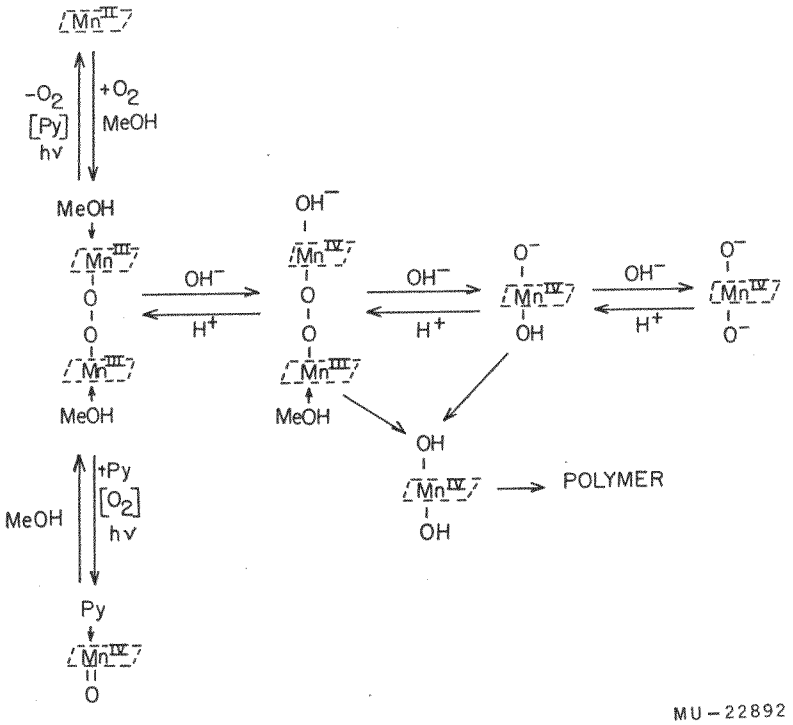

Fig. 38. Reaction scheme.

D. PLANT BIOCHEMISTRY

1. ESR IN CHLOROPLASTS IN WHICH HILL REACTIVITY IS INHIBITED

Gaylord M. Androes, Mary F. Singleton, and Gunter Schweig

In the preceding quarterly report[1] we told of an experiment which attempted to correlate Hill reactivity with the concentration of photoinduced unpaired electrons in spinach chloroplasts. The Hill reactivity was inhibited by the extraction of important pigments. The resulting correlation was uncertain. We now report on an experiment which attempts another such correlation. This time the Hill reactivity is stopped by the use of inhibitors. Application of these inhibitors immediately and completely blocks O_2 evolution while the remaining functions of the chloroplast continue unimpaired.

The experiment was performed in the following manner. Spinach chloroplasts were prepared in the usual way[2] at the Davis Campus, and immediately frozen in dry ice. In our laboratory a small amount of an inhibitor, atrazine or CMU (monuron) in buffer solution, was added to the chloroplasts, the inhibitors being present in sufficient concentration to completely block Hill reactivity. The mixture was then centrifuged at 600X g for 15 minutes. A control and samples containing each inhibitor were prepared. These were placed in the ESR microwave cavity in two forms: (a) painted on a quartz rod and dried in air, and (b) in the aqueous suspension cell.*

The experiment was performed at room temperature and with white light which passed through pyrex and water.

There were no differences between the ESR signals observed in the control and in the inhibited chloroplasts; the line position, line width, dark signal, photosignal rise time, ratio of light signal to dark signal, and photosignal decay times were all essentially constant among the three samples. The photosignal rise times were on the order of seconds in both the rod and cell samples. Decay times were on the order of minutes for the rod, on the order of seconds in the aqueous cell. New samples prepared from the frozen material on its second day in Berkeley behaved in the same way. More subtle differences, such as in ESR action spectra, were not investigated.

---

[1] G. Androes and M. Singleton, in Bio-Organic Chemistry Quarterly, UCRL-9519, Jan. 1961, p. 42.

[2] P. B. Sogo, N. G. Pon, and M. Calvin, Proc. Natl. Acad. Sci. U. S. 43, 387 (1957).

* This cell, because of its geometrical shape in relation to the distribution of electric field in the microwave cavity, allows the introduction of a certain amount of water into the cavity. Thus, while other considerations dictate the use of rather thick suspensions, the conditions of the experiment are much more normal than employed previously. The cell is made of quartz and is approximately 1X2X0.025 cm.

The six-line spectrum due to the Mn^{++} ion was observed in all samples in the aqueous cell, and in none of the samples painted on the rod. Again, the behavior of this signal was the same for all three samples. The behavior of the free radical and the Mn^{++} signals is shown in Fig. 39 as a function of light intensity and time.

This experiment could indicate that (a) if the unpaired electrons are in a direct line with O_2 evolution, then they must be separated from the point of O_2 inhibition (which is unknown) by many intermediates, or (b) the unpaired electrons are on the carbon-cycle side of the splitting of H_2O. In both cases the equilibrium concentration of unpaired electrons could be unaffected by the loss of Hill reactivity. The experiment could equally well indicate that the electrons are not in the photosynthetic pathway, and that any block imposed would not be reflected in the spin concentration or resonance characteristics. There are insufficient data for choice between these alternatives.

The Mn^{++} aspect of the results indicate that Mn^{++} is being irreversibly produced in the light (there is a small amount of light in the "dark" cavity before the illuminating lamp is turned on), and when a certain material is used up then Mn^{++} production ceases. The investigation of the Mn^{++} signal with reference to free-radical signals and other sample parameters is continuing.

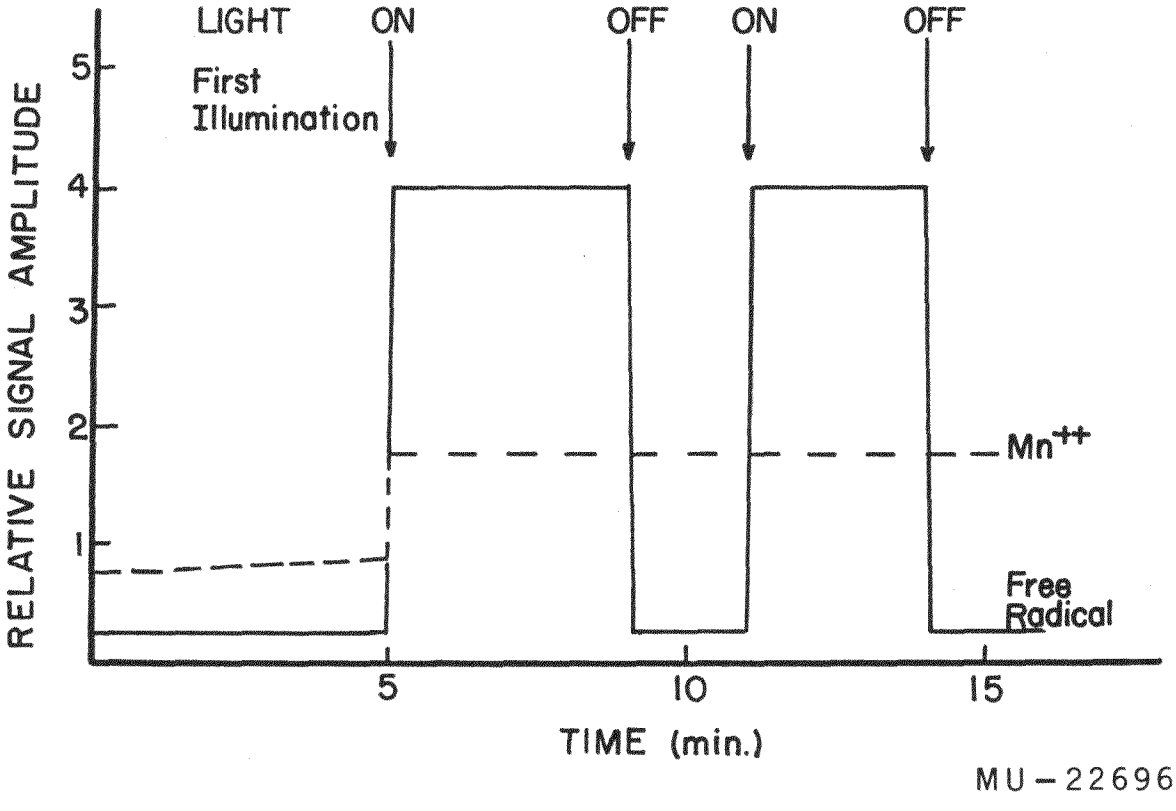

Fig. 39. Behavior of Mn^{++} and free radical ESR in aqueous cell as a function of light conditions and time.

2. SEPARATION OF PLANT PIGMENTS

Alexander Anderson and Melvin Calvin

Separation of the pigments into the broad classes of xanthophylls, carotenoids, and chlorophylls would be the first stage in the analysis of the extracts of plant material discussed in an earlier report.[1] The extraction of the pigments from the cellular material is carried out with a polar solvent (acetone or methanol), and the polar compounds xanthophylls can be partitioned into the methanol-water phase on the addition of petroleum ether, which then contains the larger part of the carotenoids and chlorophyll. The chlorophylls are separated from the carotenoids by adsorbing the chlorophyll on Celite or a diatomaceous earth. The carotenoids are washed through and the chlorophyll is later desorbed with a polar solvent. The broad classes of pigments obtained with these partition and adsorption-type experiments can then be separated into their particular members by column chromatography. Quinones are probably present in the original extract, and, because of the findings in experiments with phthalocyanine systems and quinones,[2] their presence in the extracts should be investigated. Plastoquinone had been reported[3] as being associated with the carotenoids, and can be separated from them with silicic acid chromatography.

This report gives the experimental details for the above type of separation, noting that the use of Celite as the agent for the separation of carotenoids and chlorophylls is awkward and leads to a possible conversion of the chlorophylls to pheophytins. The majority of the separated parts are tested for the presence of plastoquinone by means of the sodium borohydride test.[3] The ultraviolet absorption spectra of chlorophyll a and b were measured to see if there was a band at 255 mμ and what happened to it under reduction with sodium borohydride. Extracts from freeze-dried chloroplasts and Chlorella were analyzed. The separation of the methanol extract of Chlorella into a large number of pigments has been worked out without using Celite for the separation of the chlorophylls from the carotenoids.

I. Isolation of Plant Pigments from Spinach

Spinach was used rather than Chlorella, as it could be obtained in larger quantities and the principles worked out for spinach could be used for an analysis of methanol extracts of Chlorella. The procedure is outlined in Fig. 40.

---

[1] A. F. H. Anderson and M. Calvin, in Bio-Organic Chemistry Quarterly Report, UCRL-9408, Sept. 1960, p. 34.

[2] David Kearns, Electrical Properties of Organic Solids. I. Kinetics and Mechanism of Photoconductivity of Metal-Free Phthalocyanine. II. Effects of Added Electron Acceptors and Donors (Thesis), UCRL-9120, March 1960.

[3] N. I. Bishop, Proc. Natl. Acad. Sci. U. S., 45, 1696 (1959).

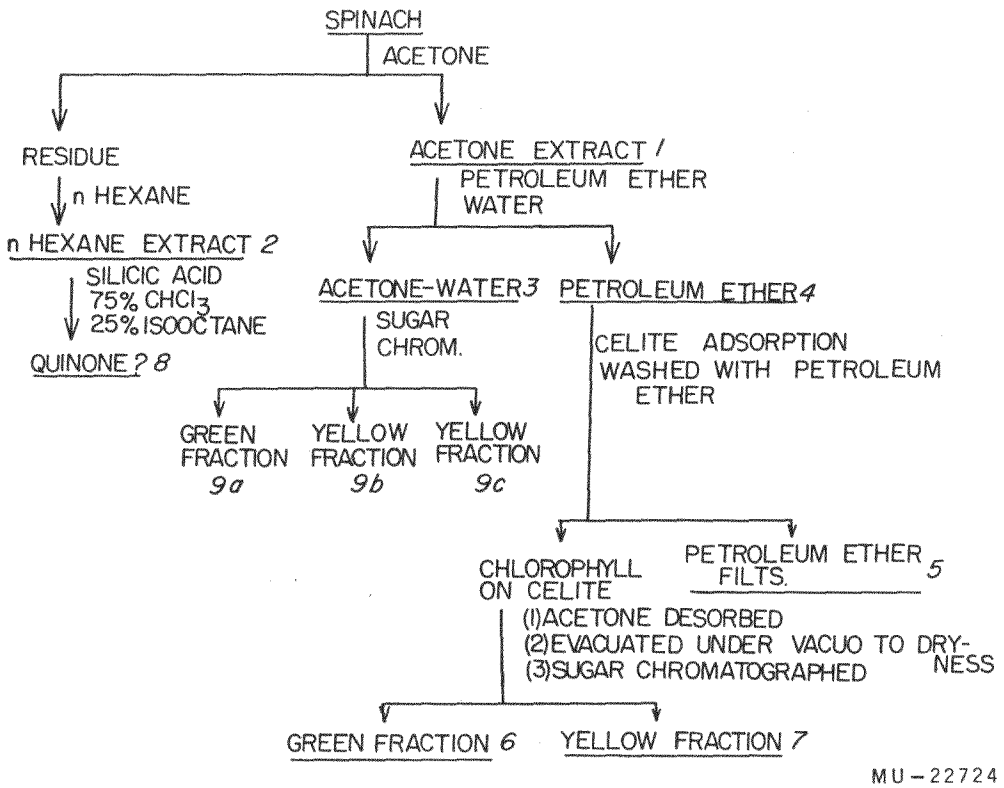

Fig. 40. Isolation of plant pigments from acetone.

Preparation of Acetone Extract

After the large veins were cut out of the spinach, it was washed and dried on blotting paper; 180 g of the spinach was ground with 500 ml of reagent-grade acetone in a Waring blender. The mixture was filtered through a 5-in. Buechner funnel and the cake washed with 50 ml of acetone to remove any traces of the remaining pigment, giving the acetone extract (marked "1" in Fig. 40). After the cake was sucked dry, it was washed with five lots of 40 ml of n-hexane to give the n-hexane extract (2 in Fig. 40).

Partitioning the Xanthophylls into the Polar Phase

One hundred ml of the acetone extract was placed in a separatory funnel and 30 ml of petroleum ether was added; 50 ml of 0.5% sodium chloride solution was carefully added down a filter funnel until two phases were obtained. We then had two phases, one an acetone-water phase (3 in Fig. 40) containing the xanthophylls, and the other a petroleum ether phase (4 in Fig. 40) containing the chlorophylls and carotenoids.

Adsorption of the Chlorophylls on Celite and the Elution of Carotenoids

The petroleum ether phase after several washings with 0.5% sodium chloride solution was poured onto a 3-in.-diameter Buechner funnel packed to 1/2 in. from the top with Celite and washed with 200 ml of petroleum ether (bp, 30-60°) until the petroleum ether filtrates (5 in Fig. 40) were colorless. This method was unsatisfactory because of channeling of the Celite, which allowed some of the chlorophyll to pass through, contaminating the carotenoids.

A more successful approach was to pack a column 20 cm long and 5.5 cm in diameter with Celite, either by dry packing or as a slurry with petroleum ether. However, this procedure is also quite difficult to reproduce, and seems to bring about some alteration of the chlorophylls to pheophytins, especially in the presence of light.

Chromatography with Silicic Acid

Chromatographic columns (0.5 cm in diameter), inserted in a Buechner funnel so that gentle suction could be applied, were packed to a depth of 18 cm with silicic acid (Mallinckrodt 100 mesh), with slight tapping of the added portions. The column was washed with iso-octane (Philips spectroscopic grade) and the sample, dissolved in 10 ml of iso-octane, was added to the column. The column was developed with 25% chloroform:75% iso-octane to elute the carotenoids and then with 75% chloroform:25% iso-octane to carry the quinone away from the material at the top of the column. The band that travels with the 75% chloroform:25% iso-octane (8 in Fig. 40) is cut out of the column to prevent decomposition and tested for quinone.

Chromatography with Sugar

Columns (2-cm diam) inserted in a Buechner funnel so that gentle suction could be applied were dry packed with sugar (California and Hawaiian powdered cane sugar) to a depth of 20 cm. The chlorophyll mixture, desorbed with acetone and evaporated down, was applied to the column in a solution of 1 ml of pyridine and 10 ml of petroleum ether, and the column was developed

Fig. 41 (on facing page). Spectra of various fractions from extraction scheme shown in Fig. 40.

Solvent: 95% Alcohol.

1. Acetone extract -------
   Acetone extract reduced with $NaBH_4$ ————
2. n-Hexane extract -------
   n-Hexane extract reduced with $NaBH_4$ ————
3. Acetone-water phase ------
   Acetone-water phase reduced with $NaBH_4$ ————
4. Petroleum-ether phase -------
   Petroleum-ether phase reduced with $NaBH_4$ ————
5. Petroleum ether filtrates -------
   Petroleum ether filtrates reduced with $NaBH_4$ ————
6. Green fraction from sugar column ------
   Green fraction from sugar column reduced with $NaBH_4$ ————
7. Yellow fraction from sugar column ------
   Yellow fraction from sugar column reduced with $NaBH_4$ ————
8. Possible quinone ------
   Possible quinone reduced with reduced $NaBH_4$ ————
9. Fractions a, b, and c from sugar chromatograph of acetone-water extraction.

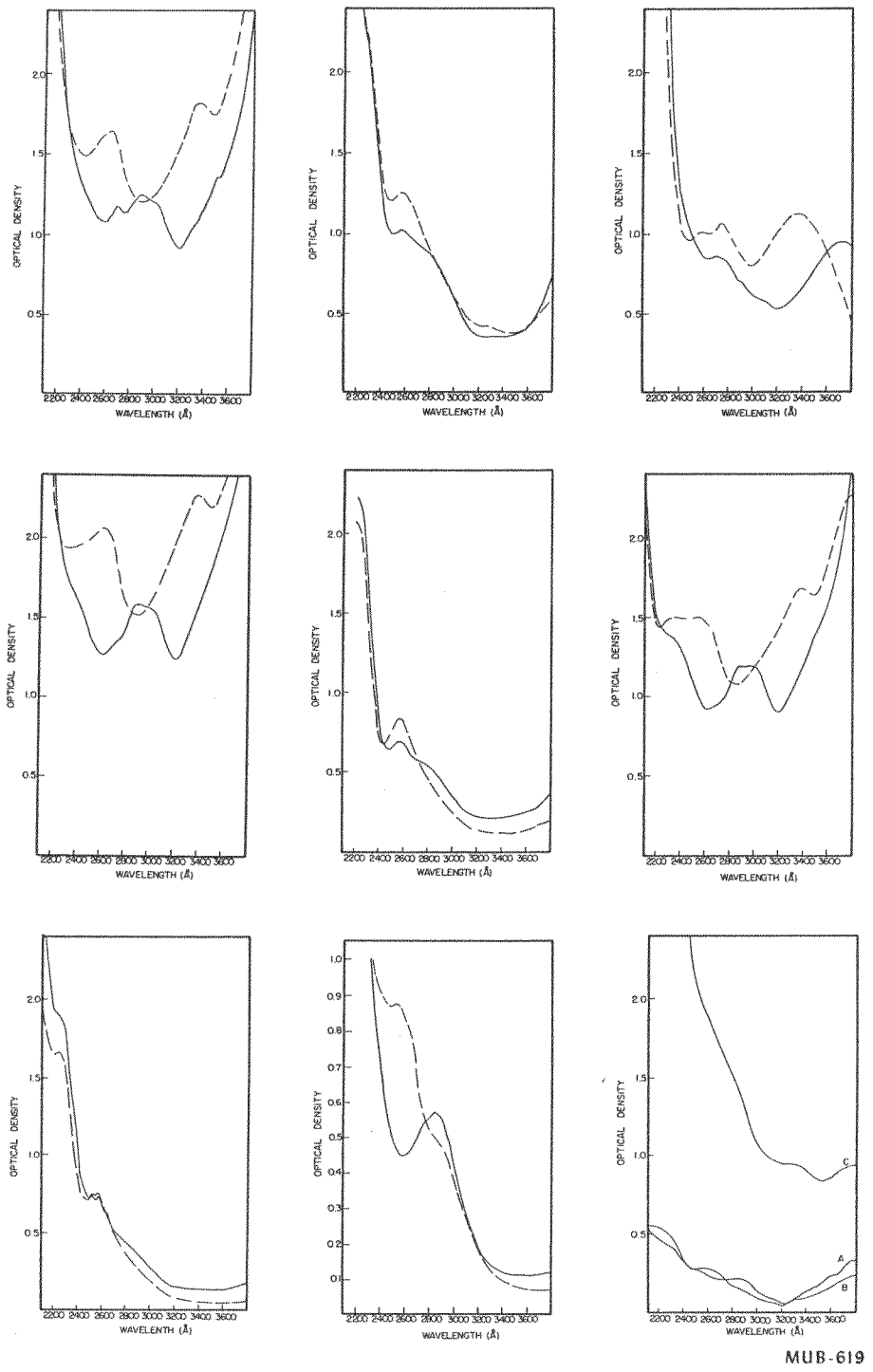
OPTICAL DENSITY
WAVELENGTH (Å)
2200 2400 2600 2800 3000 3200 3400 3600
C
A
B
MUB-619

Fig. 41.

with a mixture of benzene (4 parts), hexane (95 parts), and pyridine (1 part) to give one green zone (6 in Fig. 40) and one yellow zone (7 in Fig. 40). When the technique was applied to the evaporated acetone-water phase, it gave two yellow zones (9b and 9c in Fig. 40) and one green zone (9a in Fig. 40); the bands were cut out and eluted with ether.

Preparation of Solutions for Spectral Analysis

In searching for the quinone or characterizing the compound eluted from a column, it is necessary to measure the spectrum in a particular solvent. For testing the quinone the best solvent for the ultraviolet spectral analysis is 95% ethanol, in which the borohydride reduction is best carried out. In most cases it is best to evaporate down the extract or solution of the substance eluted from a column under vacuum with rotary evaporator to remove the uv-contaminating benzene or acetone. The sample is divided into two parts; one part is treated for 15 min with several milligrams of sodium borohydride, which is then removed by centrifugation.

Discussion of Spinach Pigment Separation

The separation of the pigments by the above procedure was too irreproducible for our projected ESR work, and because of the complex changes in the uv on sodium borohydride reduction, we were still uncertain about the location of the quinone in the various parts of the extraction procedure. The spectra of the various fractions (before and after reduction with sodium borohydride) are shown in Fig. 41. The changes in the uv spectrum of the chlorophylls due to sodium borohydride reduction were unknown, and investigation of their spectra in the region between 220 mμ and 280 mμ showed nothing of interest either before or after reduction with sodium borohydride. The changes in their visible spectrum on sodium borohydride reduction do show remarkable changes (Figs. 42 and 43), and these substances are similar in form to protochlorophyll or protopheophytin.

To cut down the extraction of a large number of pigments, Bishop's method of extracting freeze-dried chloroplasts and Chlorella with petroleum ether was tried as a means of isolating the quinone--without success. Perhaps the plastoquinone was in insufficient quantity, the silicic acid chromatography was not suitable, or -- like the chlorophyll-- it was altered when the green pigments were separated from yellow pigments on Celite. Chlorophylls were seen to change to an olive-green color on the Celite column. Whether this was a photochemical reaction or due to the acidity of the surface of the Celite has not been ascertained, but the product was pheophytin (Fig.44) which was the main product separated on a sugar column.

Because of the inconsistency of the spinach (winter caused the formation of large amounts of carotenoids in the plants) and the questionable value of the Celite adsorption technique, it was decided to tackle again the separation of methanol extracts of Chlorella. In the "acetone-spinach separation," the acetone-water phase on evaporation under vacuum produced a sticky mess which was hard to chromatograph, and a similar problem would present itself with the methanol-water phase separation. Joan Anderson[4] separated the photosynthetic pigments from methanol-water solutions on polyethylene columns, and this could be tried on our water-methanol phase.

[4] Joan M. Anderson, Research in Photosynthesis (Thesis), UCRL-8870, Sept. 1959.

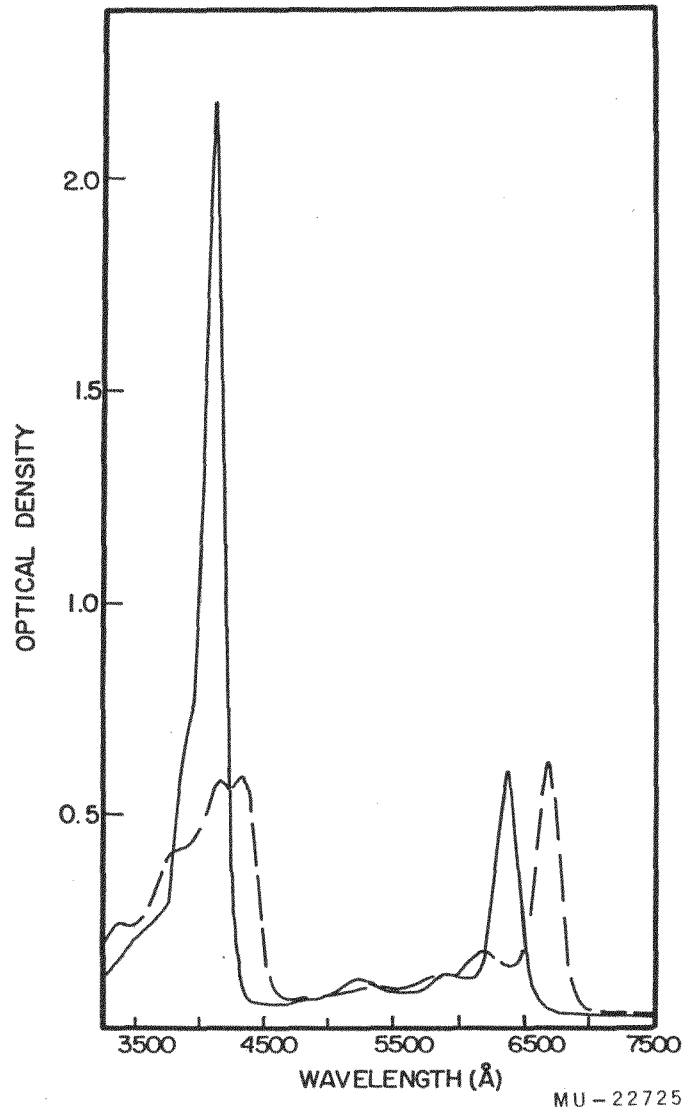

Fig. 42. Reduction of Chlorophyll a.

----- Chlorophyll a

——— Chlorophyll a reduced with $NaBH_4$

Solvent: ethanol.

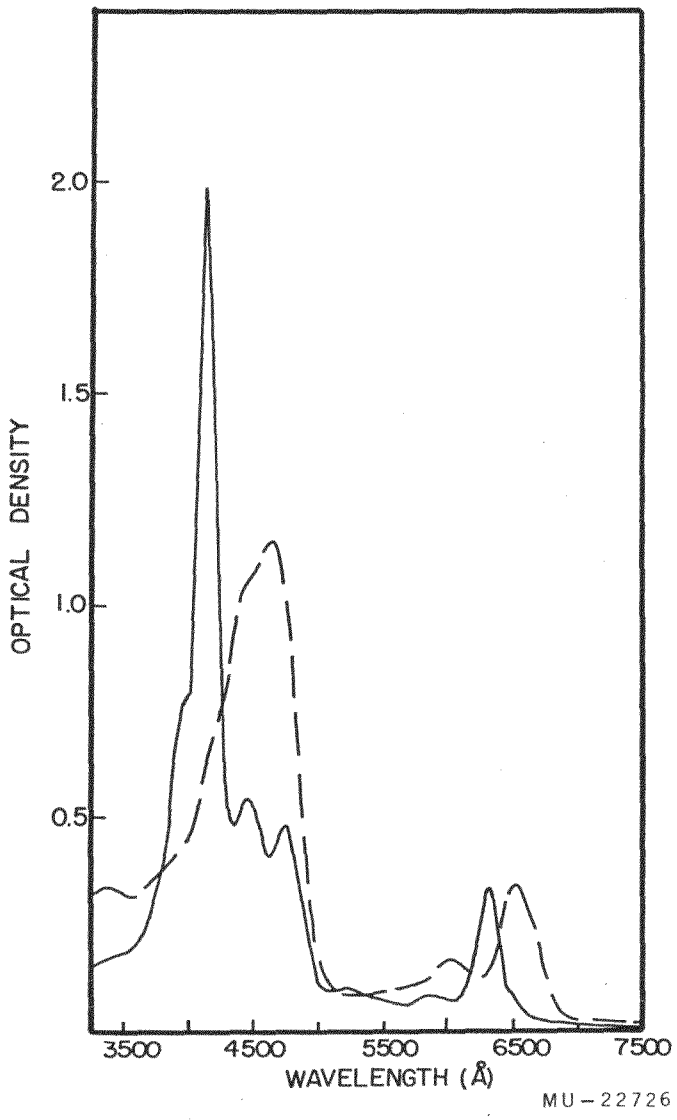

Fig. 43. Reduction of Chlorophyll b.

----- Chlorophyll b

——— Chlorophyll b reduced with $NaBH_4$

Solvent: ethanol.

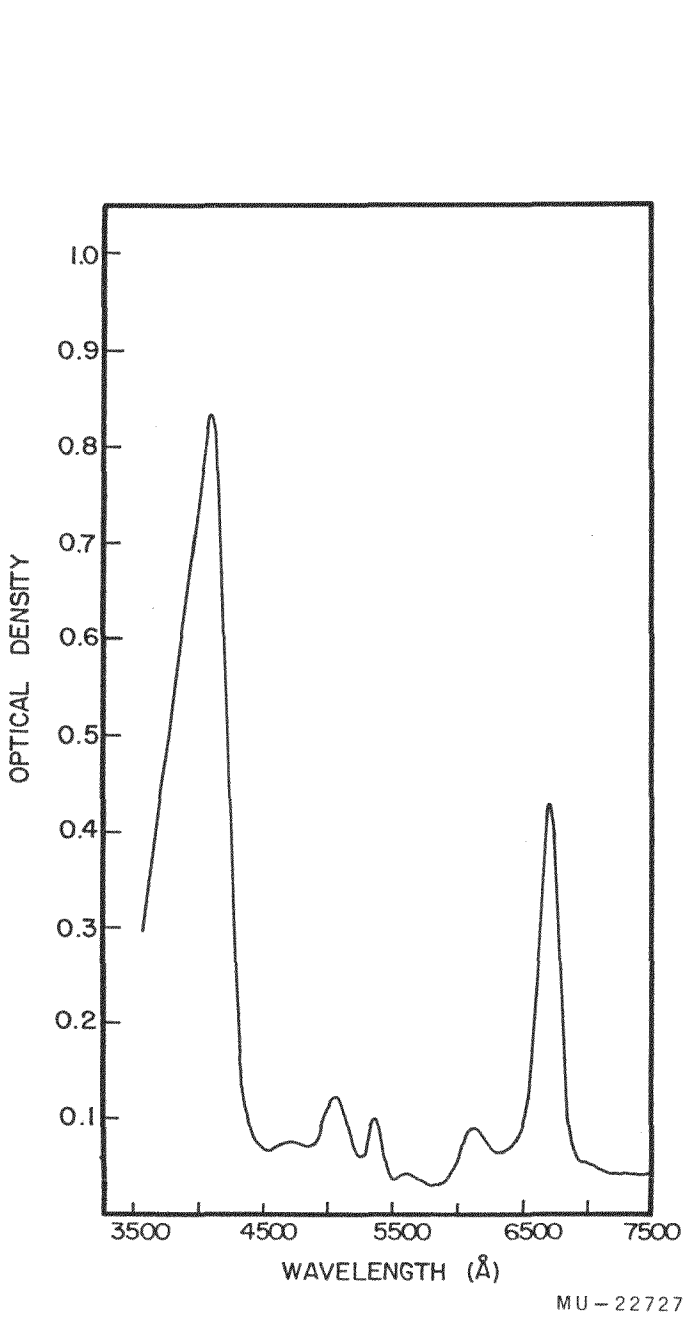

Fig. 44. Absorption spectrum of pheophytin. Solvent: ether.

The partitioning of the xanthophylls into the methanol-water phase and the chlorophylls into the petroleum ether phase would still be continued, as the ESR properties of the films prepared from these two phases were different;[1] however, the Celite adsorption would be dropped.

II. Separation of Methanol Extracts from Chlorella

The general outline of the separation is as shown in Fig. 45. Samples were taken as indicated and their pigments transferred to ether that had been washed with sodium carbonate and then redistilled from sodium.

Polyethylene Chromatography

Columns (2-cm diam) inserted in a Buechner funnel so that gentle suction could be applied were packed in small lots (30-ml beakers) to a depth of 20 cm, with a piece of filter paper placed on top. The methanol-water phase was applied directly to the column, which was then developed with 80% aqueous methanol. The various zones were eluted out of the column; after the first zone had been eluted, the column was developed with 95% methanol to give a complete elution of all material on the column. The eluted pigments were transferred to purified ether by the technique described in Part I and their spectra measured.

Sugar Chromatography

A column (1.9-cm diam) was packed to a depth of 18 cm with C&H confectioner's sugar and inserted in a Buechner funnel so that slight suction could be applied. The petroleum ether fraction, after being dried for a short time with sodium sulfate, was applied to the sugar column and then developed with 1.5% isopropanol in iso-octane. The yellow fraction of the carotenoids was washed through and then the chlorophylls. The compounds were evaporated under vacuum and redissolved in ether to determine their spectrum.

Discussion Part II

The use of polyethylene as a chromatographic adsorbent for the separation of the pigments in the methanol-water phase was successful. The pigments separated are listed in Fig. 45 in order of elution from the polyethylene column, and their spectra are shown in Figs. 46, 47, and 48.

The appearance of pigments (Fig. 47), one with absorption bands at 638 mμ and 448 mμ and the other at 645 mμ and 455 mμ, is of interest, and although they resemble protochlorophyll and chlorophyll b, they do not fit the recognized values for the spectra of these molecules. Further purification and characterization is in progress.

The pigments separated on sugar are shown in Fig. 49 and the larger-than-normal intensity of the uv absorption of the carotenoids should be noted.

With several modifications, the procedure given in Part II allows an excellent mapping of the pigments extracted from Chlorella with methanol,

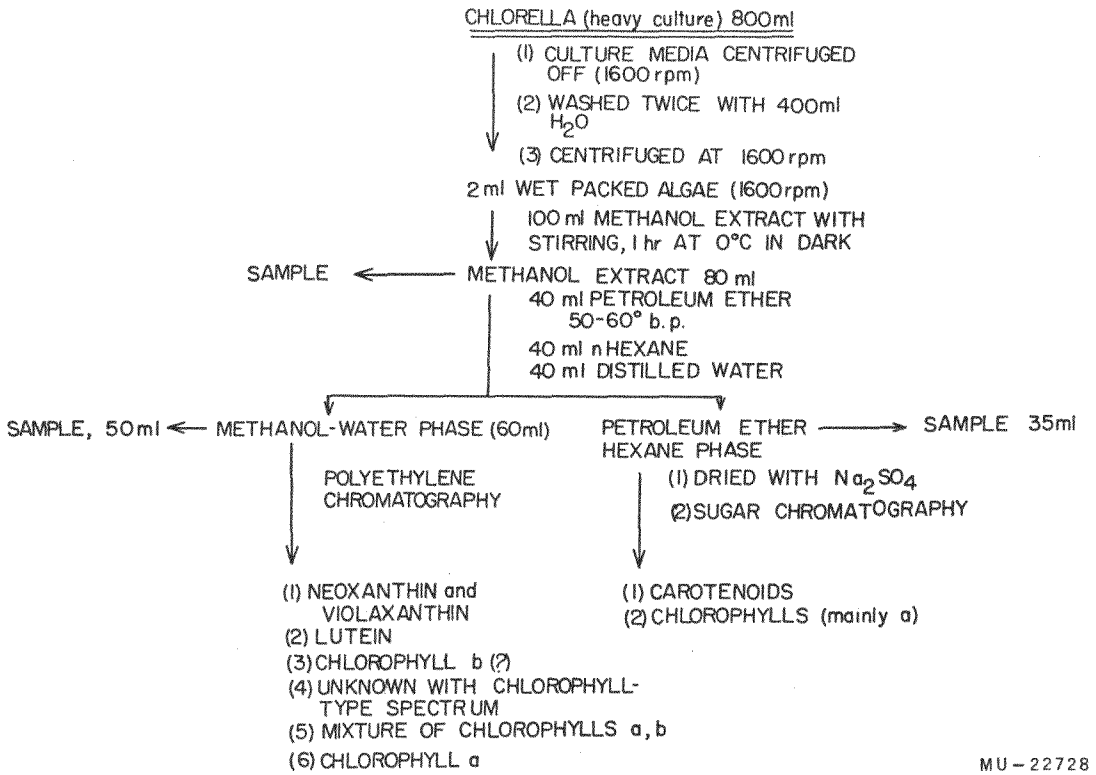

Fig. 45. Isolation of plant pigments from Chlorella.

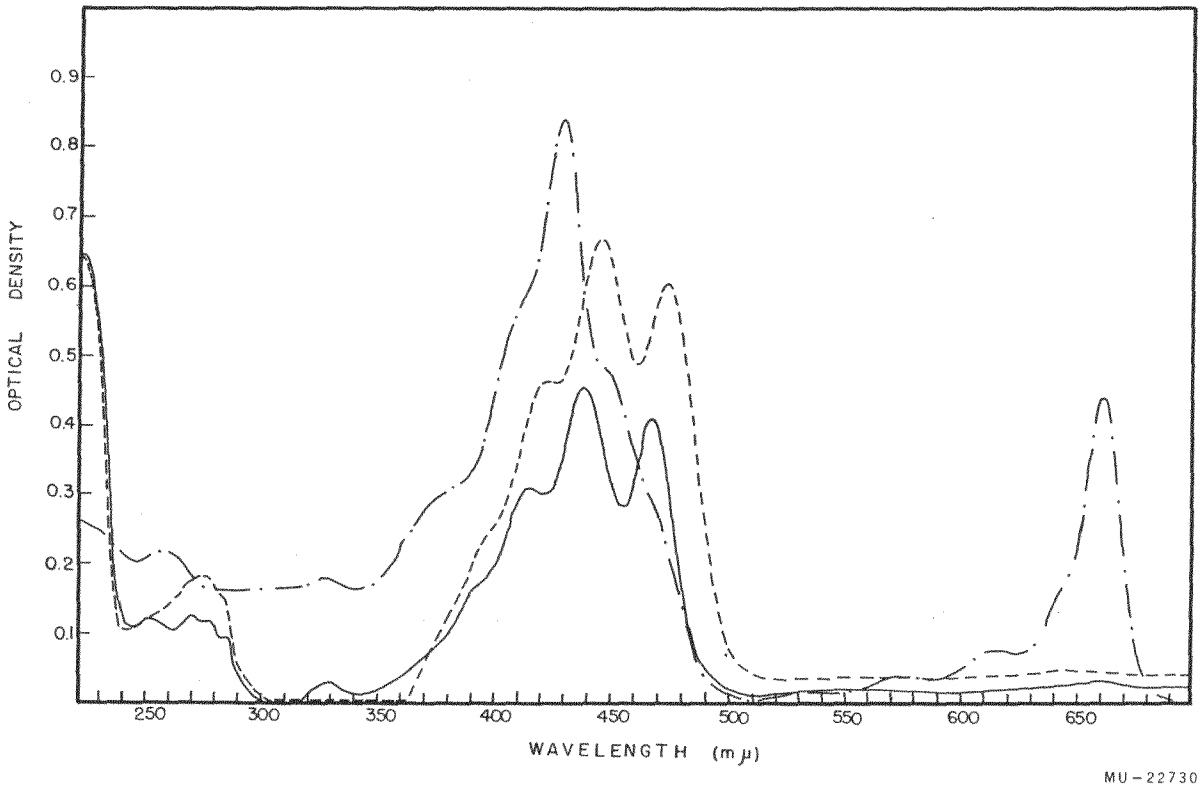

Fig. 46. Polyethylene chromatography. Fractions 1 and 2.

. - . - . - . - MeOH - H_2O phase

———————— Neoxanthin, Fraction 1.

---------- Lutein, Fraction 2.

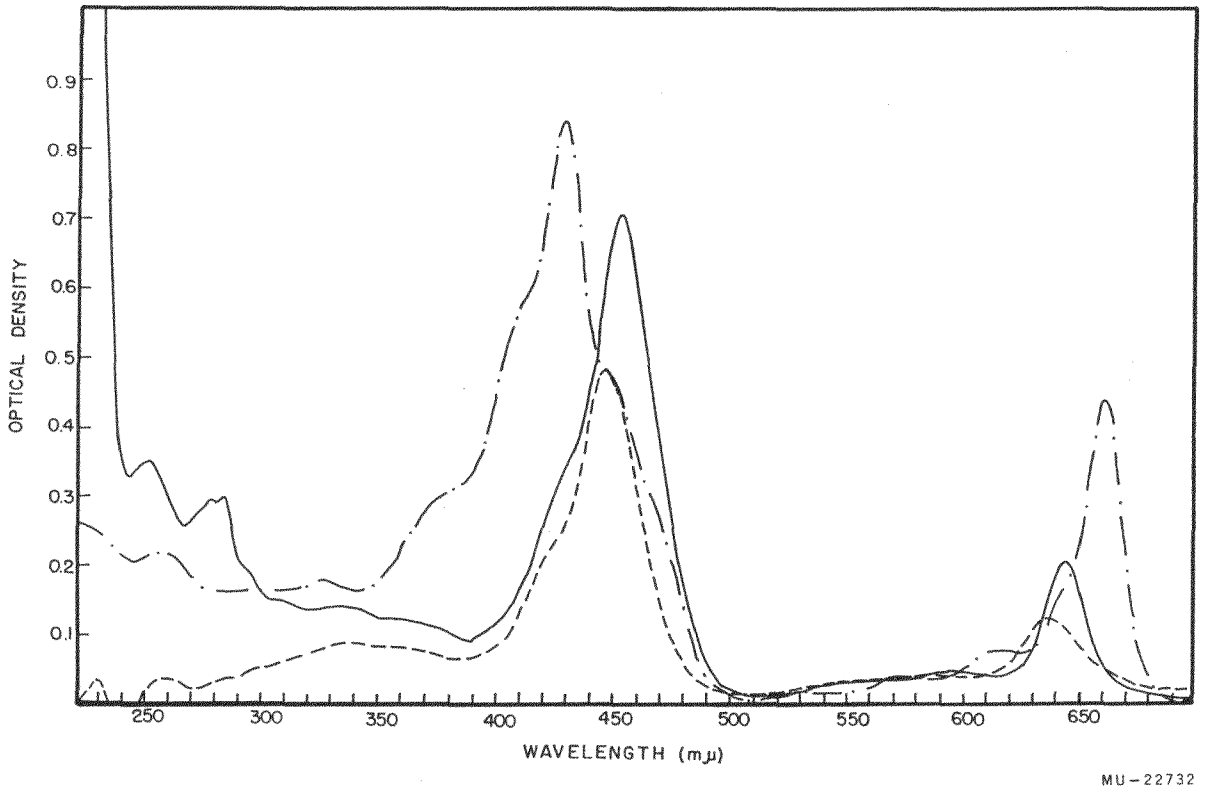

Fig. 47. Polyethylene chromatography, Fractions 3 and 4.

-.-.-.-.- MeOH - H_2O Phase

---------- Protochlorophyll (?), Fraction 3.

———————— Chlorophyll b (?), Fraction 4.

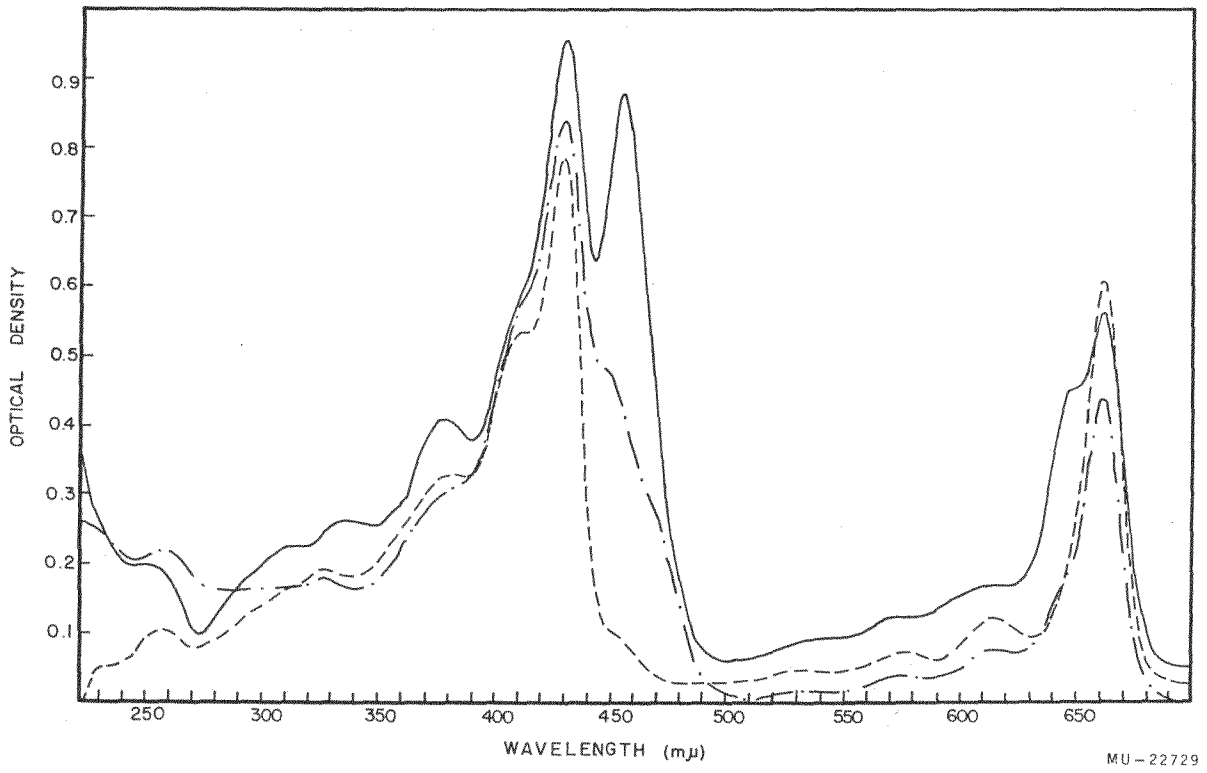

Fig. 48. Polyethylene chromatography, Fractions 5 and 6.

-.-.-. MeOH - H_2O phase

———— Chlorophyll a and b, Fraction 5.

---------- Chlorophyll, Fraction 6

Solvent: ether.

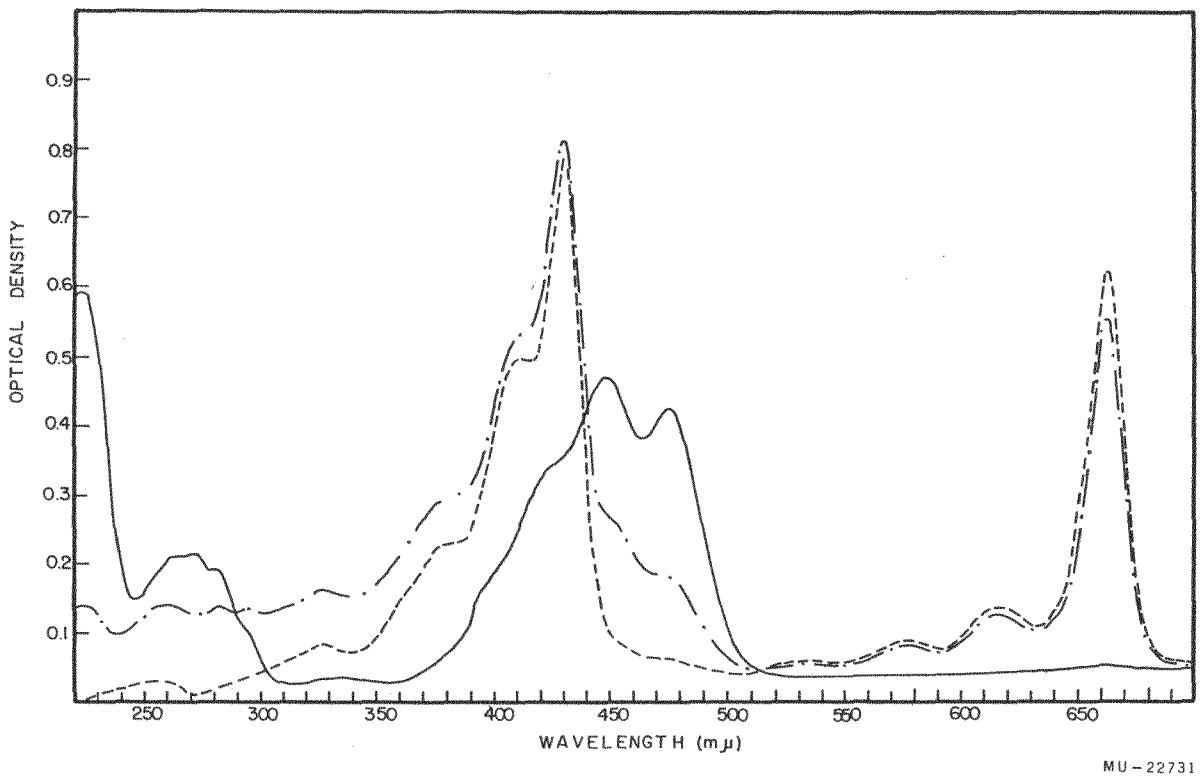

Fig. 49. Sugar chromatography of petroleum ether fraction.
-.-.-.- Petroleum ether phase.
———— Carotenoids.
---------- Chlorophyll a.
Solvent: ether.

opens up the extract for detailed testing of the constituent pigments for photoinduced paramagnetism.

3. A STUDY OF LIGHT-CATALYZED HYDROGEN TRANSPORT UNDER PHOTOSYNTHETIC CONDITIONS

Part I: HYDROCARBON CAROTENOIDS

Elie A. Shneour

The unique ability of higher plants and algae to absorb light energy and to use it to drive a series of chemical reactions has often been expressed by the general equation

$$2\,H_2O + CO_2 \xrightarrow[\text{light}]{\text{Chlorophyll}} (CH_2O) + H_2O + O_2 \cdot$$

This over-all reaction might occur in stages:

$$2H_2O + 2X \longrightarrow 2XH_2 + O_2 , \qquad (1)$$

$$2XH_2 + CO_2 \longrightarrow (CH_2O) + 2X + H_2O . \qquad (2)$$

Here X is one or more substances in a series of reactions that eventually lead to the reduction of CO_2 to carbohydrates.

Carotenoids are intimately associated with chlorophyll in the photosynthetic apparatus of green plants. For this reason we thought that α-carotene or β-carotene (or both) might be an integral part of the hydrogen transport system represented by X. A future report will consider the hydroxylated carotenoid, lutein, in this role.

Although the exact nature of the hydrogen transport mechanism that might involve α- and (or) β- carotene need not concern us here, we can propose two broad possibilities: First, a reversible reduction at one or more of the eleven double bonds, or, second, one or more hydrogen-exchange reactions. In this latter case, the most likely site of such an exchange would be at positions 3, 4, and 3', 4' of the molecule of β-carotene (Fig. 50)

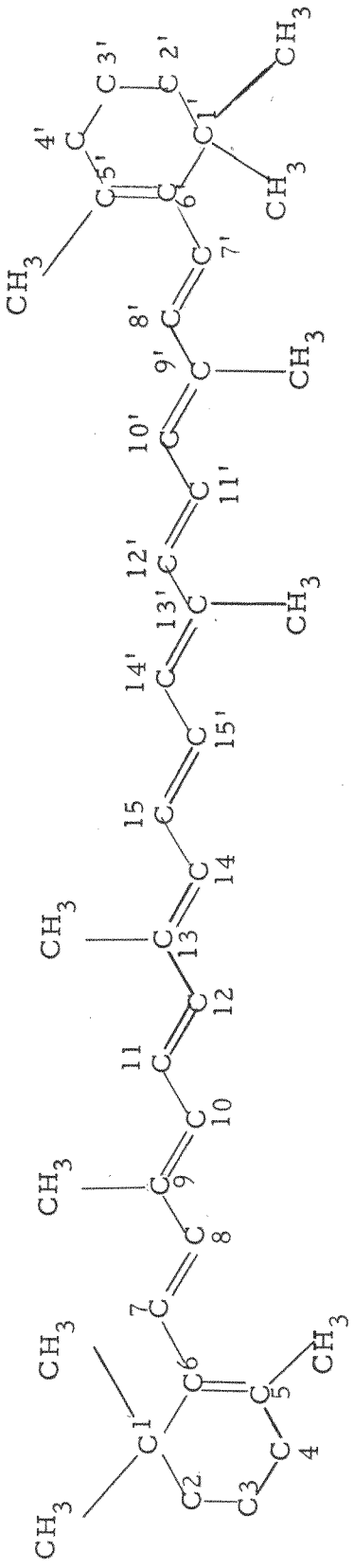

β carotene

In order to test this hypothesis, tritium oxide could presumably be substituted for water. If the steady-state concentration of the tritium-labeled carotenoid resulting from the photolysis of tritium oxide is sufficiently high for detection, it should be possible to isolate and to measure light-induced incorporation of tritium into carotenoids. This was the object of the study described below.

Experimental Procedure

Two systems were used to test the hypothesis:

(a) A nonbiological-model system. This consisted of a solution of both β-carotene and a chlorophyll mixture in either pyridine or paradioxane, according to the procedures of Brody et al.[1] To these solutions, some tritiated water could be added without causing a separation of phases. The light-induced incorporation of tritium into β-carotene in the presence of chlorophyll was determined.

(b) A spinach chloroplast system. Experiments were carried out both with whole spinach chloroplasts and with fragmented chloroplast fractions prepared according to Park et al.[2] Experiments with chloroplast fractions were done in the presence and in the absence of a Hill reaction oxidant. In all these experiments, no carrier carotenoids were added. All of the α- and β- carotenes isolated were extracted from the natural material used.

Nonbiological-Model System

Two experiments were carried out with this system. These were identical except for the solvent used: pyridine in the first and paradioxane in the second. The components added to sealed 3.0-ml glass flasks are shown in Table VI.

---

[1] S.S. Brody, G. Newell, and T. Castner, J. Phys. Chem. 64, 554 (1960).

[2] R.B. Park, N.G. Pon, K.P. Louwrier, and M. Calvin, Biochim, et Biophys. Acta 42, 27 (1960).

Table VI. Reaction Components

	First experiment		Second experiment	
	Tube 1	Tube 2	Tube 3	Tube 4
Chlorophylls solution[a]		0.2 ml		0.2 ml
Carotenoids solution[b]	0.9 ml	0.9 ml	0.9 ml	0.9 ml
Solvent added:				
Pyridine	0.2 ml			
p-dioxone			0.2 ml	
Experimental condition	Dark	Light	Dark	Light

[a] α - and β- carotenes, mixture 15:85, concentration 50 mg/liter.

[b] Commercial chlorophylls suspension, concentration 10 mg/liter.

The following procedure was used with each tube: At time = 0, 0.1 ml of tritiated water (20 mC) was added to the tube and shaken in the dark. At time=2 min. the tube was exposed for 10 min. to an incandescent source of 10,000 foot-candles at 25°C with continuous shaking. At time=15 min, the contents of the tube were dumped into 10 ml of NaCl-saturated water. One ml of petroleum ether was then added to extract the lipoids, including the hydrocarbon carotenoids, from the reaction mixture. The petroleum ether extract (epiphase) was then washed free of tritium oxide by shaking the epiphase with several successive fractions of NaCl-saturated water until no radioactivity remained in the aqueous phase (hypophase). Control tubes were handled in the same manner--the reaction medium was treated with tritiated water for 15 min, but without illumination. The washed epiphase of each tube was then distilled off in vacuum at 30°C. The residue was redissolved in a small amount of benzene and chromatographed on Schleicher and Schuell Paper #287 according to the procedure described by Jensen and Jensen.[3] The α- and β- carotene bands were cut out and eluted directly into scintillation solution No. 2 (toluene, p-dioxane, ethanol, naphthalene, PPO, and POPOP). An aliquot of the solution was examined with the Cary Recording Spectrophotometer and the absorption spectrum compared with a standard in order to determine purity and concentration. The radioactivity of the carotenoid solution was then measured (after chlorine water bleaching; see special note) with the Packard Automatic Tri-Carb scintillation counter. The chlorophyll band from the paper chromatograms was also eluted and its radioactivity measured in the same manner.

[3] A. Jensen and S. L. Jensen, Acta Chim. Scand. 13, 1863 (1959).

In all these experiments, no significant radioactivity could be detected in either the dark or the illuminated samples. Thus, no transfer of tritium to the hydrocarbon carotenoids occurred under the conditions of our experiments.

Spinach Chloroplast System

Experiments were conducted with

(a) whole spinach chloroplasts;
(b) protein-free fraction of spinach chloroplasts, prepared according to Park et al.[2] (excess reduced trichlorophenol indophenol/added as the Hill-reaction oxidant);
(c) protein-free fraction of spinach chloroplasts, as in (b) above, but with no Hill-reaction oxidant.

The active biological material was suspended in 0.01 M pH 7.2 buffer and tritiated water was added at time=0. At time=3 min, the suspension was exposed to an incandescent light source of 10,000 foot-candles at 25° C for 2 min. (Experiment (b) was exposed only 1 min.) At time=5 min the contents of each sample tube were dumped into 10 ml of a NaCl-saturated solution. The dark control tubes were treated with tritiated water for the same total length of time as for the illuminated samples. Extraction with petroleum ether, chromatographic treatment, and radioactivity measurement followed the same procedure as used for the experiments with the nonbiological-model system.

Conditions and results of Experiments (a) and (c) are summarized in Table VII.

Table VII. Experimental results

	Experiment (a)		Experiment (c)	
	Tube 1	Tube 2	Tube 3	Tube 4
Whole chloroplasts[a]	0.20 ml	0.20 ml		
Chloroplast fraction[b]			0.20 ml	0.20 ml
Tritium oxide[c]	0.30 ml	0.30 ml	0.30 ml	0.30 ml
Illumination	Dark	Light	Dark	Light
μC/μM activity found in:				
Hydrocarbon carotenoids	7.34×10^{-2}	5.18×10^{-2}	4.95×10^{-2}	6.60×10^{-2}
Chlorophyll fraction	4.75×10^{-1}	12.4×10^{-1}	5.05×10^{-1}	3.54×10^{-1}

[a] Chlorophyll concentration 24 mg/liter.
[b] Chlorophyll concentration 21 mg/liter. Hill activity: 188 μM/hr/mg chlorophyll.
[c] Final specific activity of each sample: 2.95 μC/μM. Diluent buffer: 0.01 M pH 7.3.

Conditions and Results of Experiment (b)

Chlorophyll concentration: 18.0 mg/liter. Hill activity: 105 μM/hr/mg chlorophyll. Final specific activity of tritium oxide in sample: 1.48 μC/μM. Hill reaction oxidant: excess reduced trichlorophenol indophenol added. Results: No significant radioactivity found in either hydrocarbon carotenoids or chlorophyll band.

Discussion

In the past, a number of investigators have attempted to demonstrate transfer of hydrogen under photosynthetic conditions. Norris, Ruben, and Allen used deuterium oxide and tritium oxide with Chlorella.[4] Weigl and Livingston[5] tried a model system in neutral organic solvent. Some experiments with Chlorella were carried out in this Laboratory. In no case could hydrogen transfer to chlorophyll be demonstrated. More recently, Vishniac[6] reported incorporation of tritium into the carotenoids and chlorophylls of Chlorella. Significantly higher incorporations were reported from illuminated samples. The latest unpublished evidence, however, suggests that these results may not be allowed to stand.

In short, the data presented in this report confirm and strengthen the view that the hydrocarbon carotenoids and the chlorophylls do not act as hydrogen carriers in green plant photosynthesis. They may function as semiconductors for electrons and holes resulting from absorption and from the primary conversion of light energy.

Special Note

In the course of the investigations described in this report, a problem arose in connection with the liquid-scintillation counting of the carotenoids. Nearly total quenching of the scintillations occurred with as little as 1.5 mg β-carotene per liter of scintillation solution No. 2. A number of procedures exist for the counting of highly colored solutions.[7] These proved far too cumbersome for our purpose. We decided to try direct bleaching of the carotenoid solution, taking advantage of the instability of carotenoids to acids, to oxidizing media, and to light. The agents used were perchloric acid, fuming nitric acid, sodium hypochlorite solution, hydrogen peroxide solution, acetic acid in the presence of illumination from a GE uv germicidal lamp, bromine water, and chlorine water. Freshly prepared saturated chlorine water was the most effective. Immediate and complete bleaching could be

[4] T. H. Norris, S. Ruben, and M. B. Allen, J. Am. Chem. Soc. 64, 3037 (1942).

[5] J. W. Weigl and R. Livingston, J. Am. Chem. Soc. 74, 4160 (1952).

[6] W. Vishniac, Brookhaven Symposia in Biology 11, 54 (1958).

[7] R. J. Herberg, Anal. Chem. 32, 1468 (1960).

achieved with a counting efficiency of 5.3%, with as little as 0.05 μM of Cl_2 (contained in 0.100 ml water) for 0.05 μM of carotenoid.

Upon standing, the solutions underwent gradual discoloration over 24 hr, with a concomitant drop in counting efficiency. The counting efficiency could then be brought back to 5.3% upon addition of a small amount of bleaching solution. An example of the results obtained with the direct bleaching technique is as follows.

Scintillation solution No. 2 with internal tritium standard containing 96,500 disintegrations/min yielded 7,000 counts/min for an efficiency of 7.2%. Addition of β-carotene to give a concentration of 2.0 mg/liter resulted in nearly total quenching: 12 counts/min. Then 0.100 ml bleaching solution was added, yielding 5,021 counts/min for an efficiency of 5.2%. After 24 hr, the count was down to 3,635. Addition of 0.050 ml bleaching solution brought it back to 7,118 counts/min. The gradual discoloration is probably due to the slow transfer and absorption of chlorine by a scintillation-solution component. Mr. Fritz H. Woeller of this Laboratory has investigated the nature of the quenching and has concluded that it is due to the color of the carotenoid. "POPOP" is usually added as a secondary fluor to shift the fluorescence spectrum to match the sensitivity of the photomultiplier. The carotenoid absorption spectrum overlaps the POPOP-shifted fluorescence spectrum. This drastically reduces rather than enhances the efficiency of counting. Counting efficiency with tritium (β-carotene, 6 mg/liter) is

with POPOP secondary fluor	1.7%
without POPOP " "	8.9% .

(This experiment was done with the manual counter in Donner Laboratory, which is capable of higher efficiencies than the automatic unit.)

Another factor involved in these measurements is the pulse-height discriminator circuit of the Packard Tri-Carb counter, which blocked the very-low energy scintillations resulting from carotenoid color quenching.

All these problems are minimized with direct bleaching.

4. THE METABOLISM OF C^{14}-RIBULOSE DIPHOSPHATE BY SPINACH CHLOROPLASTS

Roderic B. Park and Ning G. Pon

In Chlorella pyrenoidosa about 90% of the carbon dioxide fixed during photosynthesis flows through phosphoglyceric acid (PGA). PGA is the first stable product in photosynthetic CO_2 fixation, and is formed from the reaction of CO_2 and the 5-carbon sugar ribulose diphosphate (RuDP) in the presence of the enzyme carboxydismutase. The products of this reaction in the presence of purified carboxydismutase are two molecules of PGA. One of the PGA's contains the fixed CO_2 as a carboxyl carbon, the other is derived entirely from the carbon of RuDP. Calvin and Massini suggested that the products of the CO_2 fixation reaction in intact cells, on the other hand, may be 1 PGA (containing the fixed CO_2) and 1 triose phosphate.[1] In this case, the triose phosphate would result from a reductive cleavage of the unstable 6-carbon intermediate formed from CO_2 and ribulose diphosphate. Recently Bassham and Kirk have obtained evidence for this proposed pathway by kinetically analyzing $C^{14}O_2$ fixation by intact Chlorella cells.[2] We wished to test whether this pathway was also operative in a sonically ruptured spinach chloroplast system. The chloroplast system presents no permeability barriers to entrance of phosphorylated compounds such as exist in Chlorella cells. We could feed C^{14}-RuDP directly to the system in light and in dark and then observe whether the first products of photosynthesis were two PGAs or 1 PGA and 1 triose phosphate. We sampled the reaction mixture at various times after addition of C^{14}-RuDP and plotted the monophosphate/PGA ratio of the various samples as a function of the time of incubation. Extrapolation of this curve to zero time should tell us whether the products of the main CO_2 fixation reaction in the illuminated enzyme system are 2 PGAs or 1 PGA and 1 triose phosphate.

Methods

Preparation of RuDP-C^{14}

RuDP-C^{14} was prepared from Chlorella pyrenoidosa according to Mayaudon et al.[3] In this procedure 85 ml of a 1.5% suspension of the algae was allowed to photosynthesize with $HC^{14}O^-_3$ (0.025 millimole per ml algae per min) in saturating light for 5 min. Nitrogen gas was then bubbled through the algal suspension for exactly 30 sec and the algae were extracted with 80% ethanol at room temperature. The 20% extract of the resultant precipitate was chromatographed for 2 days in phenol-water followed by washing of the paper chromatogram with 95% ethanol. The radioactive diphosphate compound, found in a very active band with the lowest R_f, was located by radioautography and eluted from the paper. The following tests showed that this compound was RuDP;

(a) the radioactive compound had an R_f corresponding to that of a diphosphate and definitely less than that of authentic 3-PGA, and

---

[1] M. Calvin and P. Massini, Experientia 8, 445 (1952).

[2] J. A. Bassham and M. Kirk, Biochim. et Biophys. Acta 44, 447 (1960).

[3] J. Mayaudon, A. A. Benson, and M. Calvin, Biochim. et Biophys. Acta 23, 342 (1957).

(b) Treatment of the compound with partially purified acid phosphatase (Polidase-S from Schwartz, Inc.) produced another compound which co-chromatographed exactly with ribulose in two different solvent systems. The eluate was taken to dryness and redissolved in 0.7 ml of water.

Preparation of the Incubation Mixture

The incubations were run in 50-ml flasks 3 cm in diameter. Each flask was capped with a standard tapered 24/25 ground glass joint which had two openings plugged with rubber serum caps. Three needles were inserted into each flask; one to inject RuDP, one for withdrawal of samples, and one short needle to provide pressure equalization.

Each reaction mixture in a final volume of 1.42 ml contained, in micromoles: $MgCl_2$, 4.0; $MnSO_4$, 1.6; adenosine diphosphate, 1.0; triphosphopyridine nucleotide, 0.2; thiamine pyrophosphate, 1.4; ascorbate, 2.5; and glutathione 1.3. One ml of fragmented chloroplasts with 1.2 mg of chlorophyll was added to the reaction mixture and 8.0 μM of $NaHC^{12}O_3$ was preincubated, in the light and dark at 24°C, with the chloroplasts for 10 min. RuDP-C^{14} (200 microliters) was added and 0.1-ml samples were withdrawn at 20 sec, 2 min, 4 min, 8 min, and 16 min. Each sample was injected into 0.5 ml of 95% ethanol at room temperature. The precipitate was extracted with 20% ethanol, 95% ethanol, and water successively. The extracts were pooled, concentrated under reduced pressure, and applied on paper for chromatography according to Bassham and Calvin.[4] The following controls were also performed: (a) same conditions as above except that the chloroplasts were replaced by the suspending buffer; and (b) same conditions as above except that no RuDP-C^{14} was added and the $NaHC^{12}O_3$ was replaced with 8.0 μM of $NaHC^{14}O_3$, 200 μC. The latter was incubated for 30 min and was treated according to Park et al.[5]

Results

The ratios of sugar monophosphate to PGA are plotted as a function of the time of C^{14}-RuDP incubation in Fig. 51. These data, when extrapolated to zero time, give a monophosphate/PGA ratio of about 0. This is the result that would be expected if the main CO_2 fixation reaction in the broken spinach system yielded two PGA's rather than 1 PGA and 1 triose phosphate. The PGA count was not corrected for dilution by $C^{12}O_2$ fixed during the incubation. This is unnecessary, since this correction would give an even lower ratio of triose monophosphate to PGA. Although this result disagrees with the findings of Bassham and Kirk,[2] it may merely be indicative of the differences between the two photosynthetic systems in which the studies were made. All reported spinach chloroplast systems have not more than 5% of the CO_2 fixation capacity of the spinach leaf on a unit chlorophyll basis. Thus, the fact that we see 2 PGA's as the product of the carboxydismutase reaction in our spinach chloroplast system does not mean that the products in the intact

[4] J.A. Bassham and M. Calvin, The Path of Carbon in Photosynthesis (Prentice-Hall, Englewood Cliffs, New Jersey, 1957).

[5] R.B. Park, N.G. Pon, K.P. Louwrier, and M. Calvin, Biochim. et Biophys. Acta 42, 27 (1960).

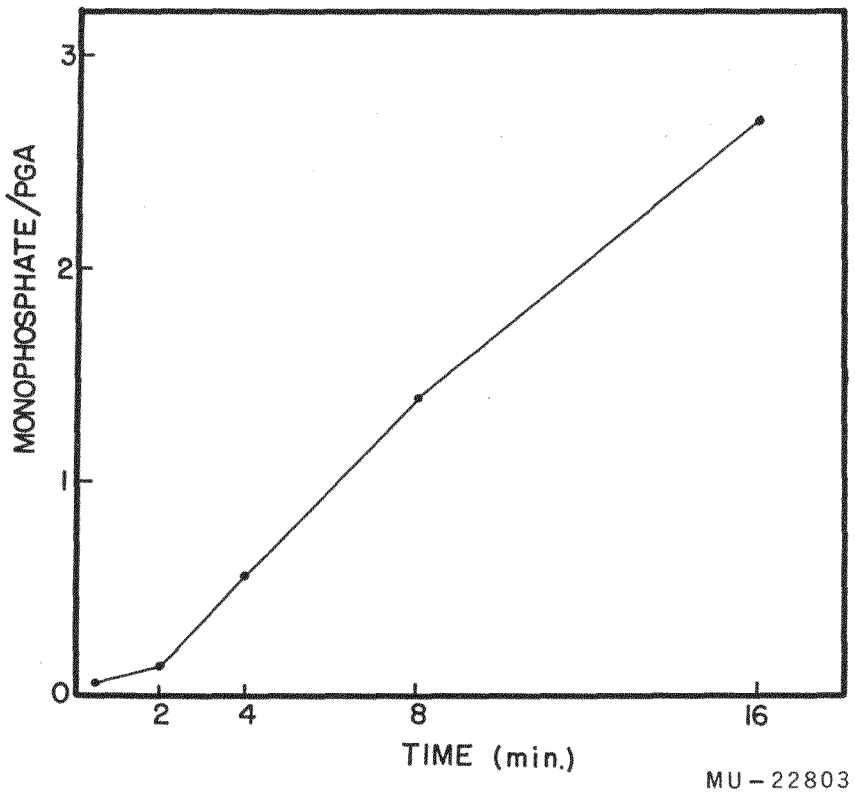

Fig. 51. Plot of ratio of sugar monophosphate to PGA as a function of time of C^{14}-RuDP incubation.

leaf were also two PGA's. The preparation of photosynthetically more active chloroplast systems may show 1 PGA and 1 triose as a product of the carboxydismutase reaction and thus resolve the discrepancy between our present results and those of Bassham and Kirk.[2] (The chloroplasts used in our experiments fixed approx 1 μM of carbon per mg chlorophyll per hr in the light, with a light-to-dark fixation ratio of 50 to 1. This fixation represents 0.5% that of the intact leaf.)

The discrepancy we have found provides an additional limitation which must be considered when chloroplasts are used as a model for studying the photosynthetic path of carbon.

5. THE LOCATION OF CARBOXYDISMUTASE IN LEAVES OF HIGHER PLANTS

Ulrich Heber

Recently the question has been disputed whether the well-known dark reactions of photosynthesis are specifically photosynthetic or common to all cells, regardless of whether or not the cells are photosynthetically active. The key enzyme of the dark reactions is the carboxydismutase, which catalyzes the uptake of the major part of photosynthetically bound CO_2. This enzyme has been found repeatedly in nonphotosynthetic organisms or nonphotosynthetic parts of plants, indicating a nonspecific function in respect to photosynthesis. The objection remains that nonphotosynthetic organisms or parts of plants are derived phylogenetically from the respective photosynthetic forms.

Photosynthesis always occurs in particular parts of the cell possessing a specific structure. If carboxydismutase is linked specifically to photosynthesis, it is likely to occur in the photosynthetic units--in the higher plants, in the chloroplasts. Otherwise it might be distributed in the whole cell. Smillie and Fuller[1] were able to show that the activity of carboxydismutase is parallel with the chlorophyll content of preparations obtained from the fractionation of frozen dried leaves.[2] On the other hand, it has been found that only a minor part of the total carboxydismutase content of the leaf is present in the chloroplasts after isolation following grinding in sucrose buffer. This, however, might be due to leaching during the isolation procedure. In our experiments we tried to obtain chloroplasts of high purity in a "nonaqueous" method that does not allow perturbance of the original location of carboxydismutase in the living cell, and compared their activity with that of the whole cell and of chloroplast-depleted tissue.

Material

Leaves of Tetragonia expansa and Nicotiana tobaccum were obtained directly from the field. Spinacea oleracea was purchased at a local market.

Methods

Chloroplasts were isolated in nonaqueous medium consisting of petroleum ether and carbon tetrachloride.[3] In brief, the isolation is carried out as follows: Leaves are quickly frozen in petroleum ether at approx -70°C and then frozen dried at -20°C. After grinding in a mixture of petroleum ether and carbon tetrachloride, the material is subjected to centrifugation steps at different densities of the suspending medium starting with a density of approx 1.4. Different constituents of the cell successively sediment according to their densities. The fractions containing the chloroplasts are collected and the same procedure is repeated at least twice to remove impurities of the chloroplast fraction. As described elsewhere,[4] it was important to apply further purification steps in addition to the normal

[1] R.M. Smillie and R.C. Fuller, Plant Physiol 34, 651 (1959).

[2] C.R. Stocking, Plant Physiol 34, 56 (1959).

[3] M. Behrens, in Handbuch Physiol. Chem. Arbeitsmethoden, Abderhalden, Ed. (1938); U. Heber, Berdeut. botan. Ges. 70, 371 (1957).

[4] U. Heber, E. Tyszkiewicz, R. Park, and M. Calvin, in preparation.

procedure to obtain preparations of maximum purity. These steps remove mainly stomata and particles smaller than chloroplasts. For the carboxydismutase determinations, we used three fractions: chloroplasts, unfractionated tissue, and chloroplast-depleted tissue. In order to maintain comparable conditions, all fractions were treated in a comparable manner. Exposure to organic solvents in all cases was the same, as well as temperature environments and drying conditions. The fractions were characterized by chlorophyll and protein determinations in addition to the carboxydismutase determinations. Chlorophyll was determined according to Arnon[5] and protein according to Lowry,[6] after appropriate checks with the Kjeldahl procedure. Carboxydismutase was determined as follows:[7] small test tubes contained in a volume of 100 µl the following compounds, expressed in micromoles: TRIS, 15.0; $MgCl_2$, 2.0; cysteine, 0.5; RuDP, 0.4; and $NaHC^{14}O_3$, 0.5. pH was 8.0. The reaction was started by addition of 100 µl of solution containing approx 30 µg of protein, and terminated by addition of 50 µl 50% CH_3COOH after 10 min. C^{14}-PGA that was formed was counted after an aliquot sample of the reaction mixture had been spread on aluminum planchets.[8] From the available chlorophyll and protein data, one can easily calculate the ratio of chloroplast protein to total protein as well as the yield of chloroplasts obtained from the dried leaves.

The percentage of chloroplast protein present, compared with the total protein originally present (=100z), is obtained by application of the equation $\frac{x}{y} = z$, when x is the average ratio of chlorophyll to the total protein and y the ratio of chlorophyll to protein in the isolated chloroplasts. (The chlorophyll content of the isolated chloroplasts has to be corrected for loss of chlorophyll.[9]) In the same way, the yield of the isolated chloroplasts is calculated: When u is the total amount of chlorophyll in the isolated chloroplasts and v is that in the tissue prior to the isolation procedure, the ratio $\frac{u}{v} \times 100 = w$ is the percentage of chloroplasts isolated from the total chloroplasts originally present in the leaf material.

The location or distribution of carboxydismutase is calculated in two different ways. Method I: by comparison of the specific activity (in counts/min of labeled PGA formed per mg protein) of chloroplast protein with that of intact tissue. Method II: by comparison of the specific activity of intact tissue with that of chloroplast-depleted tissue.

I. The value $\frac{\text{sp act. in chloroplasts} \cdot z \cdot 100}{\text{sp act. in intact tissue}}$ represents directly the percentage of the total carboxydismutase content of the cell located in the chloroplast.

II. The equations $z \cdot a + (1 - z)\, b = \text{sp act. of intact tissue}$, and

[5] D.I. Arnon, Plant Physiol. 24, 1 (1949).
[6] O.H. Lowry, N.J. Rosebrough, A.L. Farr, and R.J. Randall, J. Biol Chem. 193, 265 (1951).
[7] Ning G. Pon, Studies on the Carboxydismutase System and Related Materials (Thesis), UCRL-9373, Aug. 1960.
[8] M. Calvin, C. Heidelberger, J.C. Reid, B.M. Tolbert, P.E. Yankwich, Isotopic Carbon, New York, 1949, 476 pp.
[9] U. Heber, Z. Naturforsch. 15b, 95-109 (1960).

$$\frac{(z - z\,\frac{w}{100})\,a + (1 - z)\,b}{1 - z\,\frac{w}{100}} = \text{sp act. of chloroplast-depleted tissue permit}$$

calculations of the specific activity of protein in chloroplasts (=a) and in the cytoplasm (=b), since z, w, and the specific activity in intact and depleted tissue are known. From a, b, and z, the percentage of the total amount of carboxydismutase present in the chloroplasts can easily be obtained. It was found, however, that calculated values for b were mostly negative, an obviously senseless result meaning that more than 100% of the carboxydismutase is present in the chloroplasts. Reasons for this phenomenon are discussed later. To avoid this difficulty, we compared the decrease of the specific activity of tissue after removal of chloroplasts with the amount of chloroplasts removed. The differences between Methods I and II are discussed later.

Results

Results obtained according to Method I are listed in Table VIII. As can be seen, especially from comparison of Experiments 7 and 8, results depend greatly on the purity of the chloroplasts. Generally speaking, when more than 60% of the total protein is obtained in the chloroplast fraction, this is an indication of impurity.[9] As a rule, we obtained relatively low specific activities in chloroplasts when the ratio of chloroplast protein to total protein was high, indicating contamination by cytoplasmic material (part of the results are not listed in Table VIII). In some cases (Expts 1, 2, 7), approx 100% of the activity of carboxydismutase, and in all cases the major part, was calculated to be in the chloroplasts. Sometimes, however, the calculated specific activity of the cytoplasm was distinctly above the possible limits of error (for instance, Expts 3 and 7). This seemed to show that in fact not all the carboxydismutase is located in the chloroplasts, and that a relatively low level is maintained in the cytoplasm.

There are, however, other possible explanations. One of them would be that carboxydismutase needs the cooperation of activators located in the cytoplasm or in the vacuole to display full activity. Therefore, the activity of isolated pure chloroplasts might be lower than that of the mixed preparations. In consequence, the calculation would reveal a distribution of carboxydismutase that is not reflected by the real situation in the cell.

We therefore employed another method (Method II, Table IX) to determine the distribution of carboxydismutase without measuring the activity of isolated chloroplasts. The specific activity of chloroplast-depleted tissue is compared with that of intact tissue. This method is quite insensitive to contamination of the isolated chloroplasts with cytoplasmic protein, and gives direct qualitative and -- under given circumstances (as mentioned above)-- quantitative evidence about the location of substances in chloroplasts or cytoplasm. When the specific activity of an enzyme in the tissue increases after removal of chloroplasts, this particular enzyme is located preferentially in the cytoplasm. When the specific activity decreases, the enxyme may be

Table VIII. Distribution of carboxydismutase in the cell, as determined by Method I

Experiment number; material	Chloroplast protein (% of total protein, 100 z)	Sp Act.[a] of carboxydismutase			Sp Act. ratio, B:A	Carboxy-dismutase in chloro-plasts (%)
		total protein	chloroplast protein	cytoplasm[b]		
1 Nicotiana	56	1.05×10^{6}	2.03×10^{6}	.00	1.93	110
2 Nicotiana	60.7	5.95×10^{4}	9.25×10^{4}	0.84×10^{4}	1.56	95
3 Tetragonia	61.2	0.8×10^{6}	1.0×10^{6}	0.44×10^{6}	1.25	77
4 Tetragonia	54.0	1.41×10^{6}	2.32×10^{6}	0.35×10^{6}	1.65	89
5 Spinacea	57.0	0.57×10^{6}	0.90×10^{6}	0.13×10^{6}	1.58	90
6 Spinacea	58.0	1.47×10^{6}	2.02×10^{6}	0.71×10^{6}	1.38	80
7 Spinacea	64.0	0.75×10^{6}	1.12×10^{6}	0.12×10^{6}	1.49	96
8 Spinacea	73.0	0.85×10^{6}	0.84×10^{6}	0.88×10^{6}	0.99	73

[a] Specific activity (as PGA-C^{14}) in counts/min per mg protein (for 10 min incubation).

[b] Calculated according to $\frac{\text{sp act. of the total protein} - az}{1z}$.

Table IX. Distribution of carboxydismutase in the cell as determined by Method II

Experiment number; material	Chloroplast protein (% of total protein, 100z)	Sp Act.[a] of carboxydismutase in		Decrease in activity after chloroplast removal (%)	W, yield of chloroplasts (% total chloroplasts)	Carboxydismutase in chloroplasts (%)
		total protein	Chloroplast-depleted protein			
4 Tetragonia	54.0	1.41×10^{6}	1.17×10^{6}	17	14	>100
6 Spinacea	58.0	1.47×10^{6}	1.18×10^{6}	20	16	>100
7 Spinacea	64.0	0.75×10^{6}	0.67×10^{6}	11	22	>100
8 Spinacea	73.0	0.85×10^{6}	0.58×10^{6}	32	33	>100
9 Spinacea	67.1	1.92×10^{6}	1.46×10^{6}	24	24	>100

[a]Specific activity (as PGA-C^{14}) in counts/min per mg protein (for 10 min incubation).

located mainly in the chloroplasts. No change in the specific activity suggests an equal distribution within the cell. We observed, after removal of the indicated amount of chloroplasts (Table IX), an appreciable decrease in the specific activity of carboxydismutase in the tissue. This decrease amounted in all cases except in Expt. 7 to even more than should be expected if all the carboxydismutase were located entirely in the chloroplasts. This can be seen from the comparison of the loss of activity in the tissue after removal of part of the chloroplasts with the amount of chloroplasts removed. It has already been mentioned in the experimental section that the calculation according to the equations given for Method II leads to negative values for the specific activity of carboxydismutase in the cytoplasm. In contrast to the experiments listed in Table VIII, which seemed to show small amounts of carboxydismutase in the cytoplasm, the experiments of Table IX indicate thus that carboxydismutase is located entirely in the chloroplasts. The result of Expt. 7 (Table IX) cannot be fully understood, since in the same experiment, calculated according the Method I, nearly 100% of the carboxydismutase was found in the chloroplasts.

The question remains which of the two methods of calculation gives the true picture. This is considered now in brief.

Discussion

It has been shown that calculation according to Method I indicate a certain distribution of carboxydismutase between cytoplasm and chloroplasts (although the main part is located in the chloroplast), while according to Method II carboxydismutase is located entirely in the chloroplasts.

The disadvantages of Method I are that:

a. Chloroplasts are exposed to a more frequent change of the organic solvent during the isolation procedure than is the tissue, because of repeated purification steps. This may result in a greater loss of activity in chloroplasts than in tissue.

b. Possible stimulating interactions between an enzyme located in the chloroplasts and activators in the remainder of the cell are excluded when chloroplasts are assayed in a more or less pure state.

c. Contamination of chloroplasts by cytoplasm influences results markedly.

An advantage of Method I is that it is possible to compare chloroplasts directly with the unfractionated tissue.

Method II avoids some disadvantages of Method I, since:

a. Chloroplast-depleted tissue is exposed to the organic solvent in the same way as intact tissue without changing solvent.

b. Interactions between substances in chloroplast and in cytoplasm are possible.

c. Contamination of the removed chloroplast by smaller amounts of cytoplasm does not markedly affect the result.

Disadvantages of Method II are that differences in enzyme content between intact tissue and chloroplast-depleted tissue are not very high, since it is difficult to remove more than 30% of the chloroplasts, and that indirect methods of calculating the specific activity of chloroplast protein must be used. Therefore the accuracy of the assay method employed is of particular importance. The carboxydismutase assay seems to fulfill this requirement; the deviations of the results are within 5%.

We conclude that results obtained by application of Method II are probably more reliable than results obtained by Method I. Still it is not explained why in most cases the activity of chloroplast-depleted tissue is even lower than should be expected when carboxydismutase is located entirely in the chloroplasts. Further experiments must reveal the reason for this phenomenon.

Our results regarding the location of carboxydismutase in the chloroplast suggest that when carboxydismutase has been found in nonphotosynthetic plants or organisms, the location may be in cell organelles related to the chloroplasts of higher plants rather than in the cytoplasm.

Summary

The location of carboxydismutase in the leaf cells of Nicotiana tobaccum, Tetragonia expansa, and Spinacea oleracea was examined. The enzyme was found to be located entirely or nearly entirely in the chloroplasts. We cannot, however, absolutely exclude the possibility that a low carboxydismutase level is maintained in the cytoplasm of leaf cells.

6. FORMATION OF MONOMETHYL PHOSPHATE IN THE CHLOROPLASTS BY "METHANOL KILLING"

Edwige Tyszkiewicz

In a previous paper[1] it was pointed out that methanol could be responsible for the formation, in the chloroplasts, of a heretofore unidentified phosphorylated compound. This unknown compound arose only when chloroplasts were fed with $P^{32}O_4^{---}$ and then killed with methanol. Other killing agents such as trichloracetic acid, liquid nitrogen in the presence of some inhibitors, ethanol, n-propanol, or n-butanol did not produce it. Chloroplasts killed with ethanol, however, formed another compound identified by cochromatography as monoethyl phosphate. Subsequently it was found that monomethyl phosphoric acid (K and K Laboratories) cochromatographed exactly with the unknown P^{32}-labeled spot obtained after "methanol killing." The agent donating the phosphoryl group to the methanol remains unknown.

Because adenosine triphosphate* is almost instantly formed in chloroplasts in the presence of adenosine diphosphate and orthophosphate, it is possible that ATP can phosphorylate those alcohols. To test this possibility, P^{32}-labeled ATP, obtained from paper chromatograms of P^{32}-labeled plant extracts, was treated with four volumes of methanol in the presence of a pH 8.1 tris buffer for 1 hour. This is the same buffer conditions as used in the chloroplast experiments. A little decomposition of ATP was observed (6.5%), giving P^{32}-labeled inorganic phosphate, but no monomethyl phosphate. This result, therefore, excludes a nonenzymatic reaction of ATP on methanol. It is noteworthy that in some cases, when chloroplasts did not form ATP (e.g., when they were fed with $P^{32}O_4^{---}$ in the absence of ADP, and in the dark), monomethyl phosphate was still formed.

In order to determine the fraction of the chloroplasts responsible for the formation of this compound, sonically ruptured chloroplasts were subjected to ultracentrifugation at 145,000×g for 45 minutes. The supernatant and green precipitate were fed separately with $P^{32}O_4^{---}$ for 5 min and then killed with four volumes of methanol. The difference between the amounts of monomethyl phosphate formed in these two fractions is seen in Table X. These results show that the supernatant forms much more monomethyl phosphate than does the green precipitate fraction. The difference is more conspicious if one compares the ratios of μM of monomethyl phosphate to μg of chlorophyll present.

---

[1] E. Tyszkiewicz, in Bio-Organic Chemistry Quarterly Report, UCRL-9519, Dec. 1960.

*The following abbreviations are used in the text: ADP, adenosine diphosphate; ATP, adenosine triphosphate; Pi, orthophosphate; TPN, triphosphopyridine nucleotide; TPP, thiamine pyrophosphate; and GSH, glutathione.

Table X. Percentage of monomethyl phosphate formed in the presence and in the absence of 1.0 μM ADP in a reaction performed under nitrogen or under air

	In presence of 1.0 μM ADP				In absence of ADP			
	Supernatant		Green fraction		Supernatant		Green fraction	
	Dark	Light	Dark	Light	Dark	Light	Dark	Light
Nitrogen								
% of the total P^{32} present in the reaction mixture	0.33	0.39	0.01	0.023	0.47	0.14	0.02	0.01
% of the esterified PO_4^{-3}	23.9	17.2	8.3	0.15	59.	41.	22.6	25.4
μM of monomethylphosphate / μg of cholorphyll	93.	110.	0.12	0.28	132.	39.5	0.24	0.12
Air								
% of the total P^{32} present in the reaction mixture	0.08	0.19	traces	0.04	0.1	0.16	traces	0.04
% of the esterified PO_4^{-3}	7.1	14.5	--	0.13	17.5	27.4	--	22.1
μM of monomethylphosphate / μg of chlorophyll	41	97	--	0.86	51.5	82.4	--	0.86

Each reaction mixture contained (amount in μM): $MgCl_2$, 4.0; $MnSO_4$, 1.6; TPN, 0.02; TPP, 1.4; ascorbate, 2.5; GSH, 1.3; $K_2HP^{32}O_4$, 1.0; tris buffer, approx 15 μM. Supernatant or green fraction, 1 ml; total volume, 1.2 ml. Incubation time, 5 min followed by methanol killing (final volume: 5 ml). Supernatant and green fraction came from the same chloroplast preparation, and for each reaction mixture, supernatant and green fraction were taken from the same amount of initial chloroplasts.

The agent donating its phosphate group to methanol is not entirely destroyed after 1 min boiling. Thus chloroplast supernatant incubated with $P^{32}O_4^{---}$ for 5 min was boiled for 1 min, and then 4 volumes of methanol were added. Monomethyl phosphate was still formed, but only about 44% of the amount present when chloroplasts were killed directly by methanol; namely, 48 and 110 μM of monomethyl phosphate per μg chlorophyll were formed, respectively.

7. A POSSIBLE MECHANISM FOR THE 2, 4-DINITROPHENOL UNCOUPLING OF PHOSPHORYLATION: ITS DISPROOF

Gabriel Gingras and Edwige Tyszkiewicz

It was reported in a previous paper[1] that isolated chloroplasts in the presence of inorganic phosphate formed phosphate esters of methanol and of ethanol when killed with four volumes of these alcohols. We thought that there might be a correlation between this reaction and the effects of these alcohols at low concentrations (1 to 10%) on the CO_2 fixation in Scenedesmus.[2, 3] Another possibility we sought to test was that 2, 4-dinitrophenol might owe its effect as an "uncoupler" of oxidative and photosynthetic phosphorylations to an analogous reaction. A phosphate carrier such as ATP (or one of its precursors) might pass its phosphate group on to alcohols or 2, 4-dinitrophenol. This would cause an apparent uncoupling.

Methods

Spinach chloroplasts isolated as described previously[1] were incubated for 20 min in Tris buffer pH 8.1 in the light in the presence of $K_2HP^{32}O_4$, with various concentrations of the compounds indicated in Table XI. The reaction was terminated by a 5-min boiling. The precipitate was homogenized and an aliquot chromatographed on paper in two dimensions. The solvent systems used, described elsewhere in this quarterly report,[4] consist of isobutyric acid:NH_4OH:EDTA and butanol:propionic acid: water. Whatman No. 4 paper was used. Authentic samples of the phosphate esters were applied at the origin of the chromatograms at the same time as the chloroplast extract. After radioautography, the phosphate spots were revealed by the ammonium molybdate reagent.[5] The results are presented in Table XI.

Table XI. Results from phosphorylation experiment

Substrate	Concentration	Presence of Phosphate ester
Methanol	1%	+
Ethanol	1%	+
Ethanol	5%	+
Phenol	10^{-2} molar	-
p-nitrophenol	2×10^{-3} molar	-
2, 4-dinitrophenol	2×10^{-3} molar	-

[1] E. Tyszkiewicz, in Bio-Organic Chemistry Quarterly Report, UCRL-9519, Dec. 1960.
[2] M. Lefrançois and C. Ouellet, Can. J. Bot. 36, 457 (1958).
[3] M. Lefrançois and C. Ouellet, Can. J. Bot. 37, 499 (1959).
[4] E. Tyszkiewicz, this report, Paper D.8.
[5] C.S. Hanes and F.A. Isherwood, Nature 164, 1107 (1949).

Conclusion

The data do not support the mechanism of dinitrophenol-"uncoupling" presented above. However, it appears that simpler alcohols can be phosphorylated at low concentrations.

8. PAPER CHROMATOGRAPHY OF PHOSPHATE COMPOUNDS FROM PLANTS

Edwige Tyszkiewicz

The separation of phosphorus compounds becomes very important if one wants to follow phosphorous metabolism. The best separation of phosphate compounds in an aqueous-alcoholic plant extract was obtained by using the following solvent system on washed[1] Whatman No. 4 paper (values in parts by volume):

First dimension		Second dimension	
isobutyric acid	100	butanol	375
NH_4OH, 1 N	60	propionic acid	180
ethylene diamene tetraacetic acid, 0.1 M	1.6	water	245

The first solvent is usually used for separation of nucleotides. It also gives a very good separation of phosphorylated three-carbon compounds. See P values* given in Table XII. The second solvent system separates further the two groups of phosphates, and it is also satisfactory for hexose and mono- and diphosphate separation.

Figure 52 shows a radioautograph of a chromatogram of phosphate compounds formed after 5 min exposure to $P^{32}O_4^{---}$ in light.

[1] H. A. Krebs and R. Hems, Biochim. et Biophys. Acta 12, 172 (1953).

*The P value is defined as the ratio of the distance traveled by the phosphate ester to that by inorganic orthophosphate.

Table XII. P Values[a] of various phosphate esters

	First dimension[b]	Second dimension[c]
phosphoglyceric acid	0.72	0.7
glyceraldehyde phosphate	0.56	1.0
phosphoenolpyruvic acid	0.87	1.2
phosphohydroxypyruvic acid	1.14	1.4
dihydroxyacetone phosphate	1.6	1.9
monomethyl phosphate	1.3	1.5
monoethyl phosphate	1.7	2.4
phosphoethanol amine	1.2	0.75
adenosine-5-monophosphate	1.4	1.1
adenosine diphosphate	1.07	0.5
adenosine triphosphate	0.9	0.3
uridine diphosphoglucose	0.38	0.27
fructose-6-phosphate	0.60	0.50
glucose-6-phosphate	0.53	0.35
fructose-1, 6-diphosphate	0.3	0.15
inorganic orthophosphate	1.0	1.0

[a] The P value is defined as the ratio of the distance traveled by the phosphate ester to that by inorganic orthophosphate.

[b] In isobutyric acid: NH_4OH: versene.

[c] In butanol: propionic acid: water.

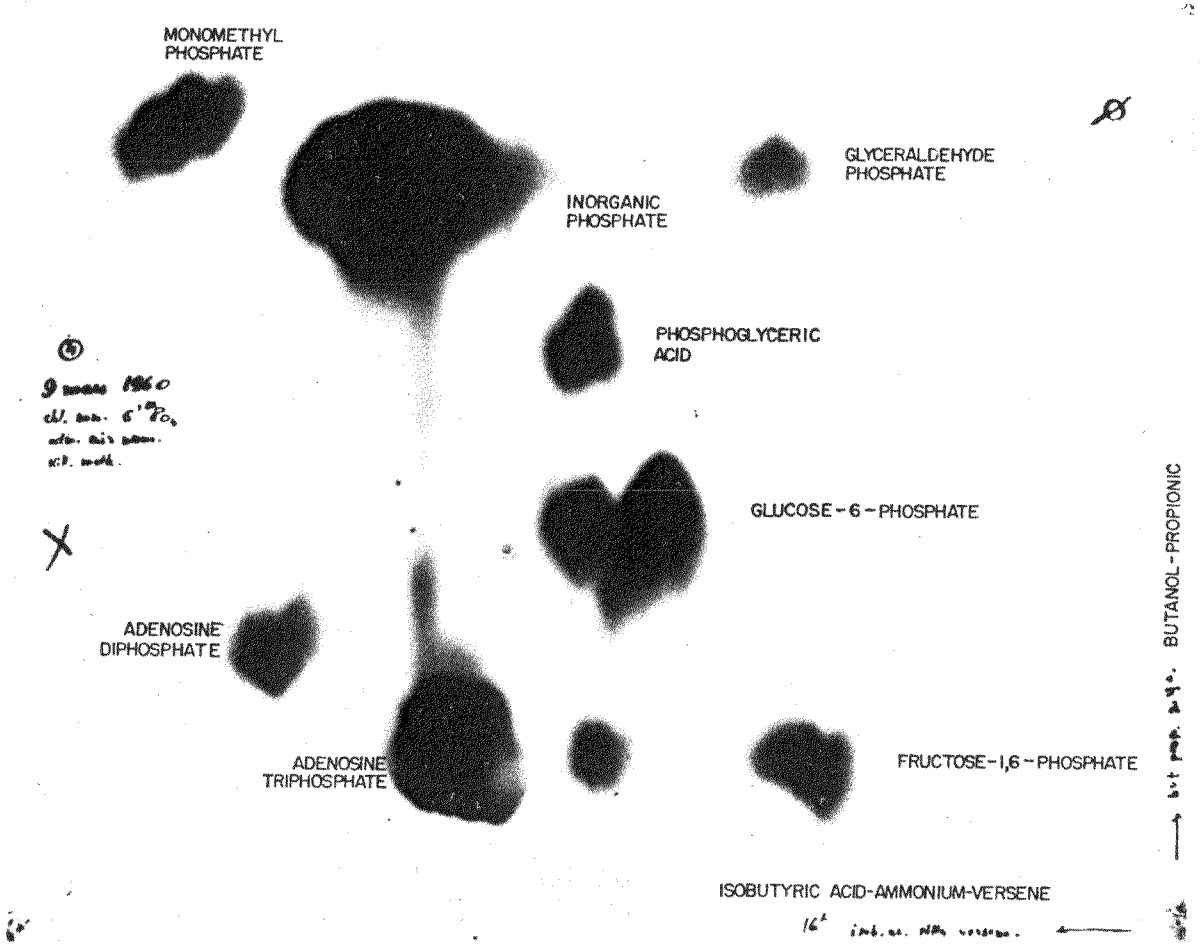

Fig. 52. Radioautograph of a chromatogram of phosphate compounds formed after 5 min exposure to $P^{32}O_4$ and light.

9. TRACER STUDIES WITH TRITIUM IN HYDROGEN-ADAPTED SCENEDESMUS

Richard A. Goldsby and Melvin Calvin

After a period of anerobic incubation in the dark, the green alga Scenedesmus develops hydrogenase activity. Hydrogenase makes it possible for Scenedesmus to use molecular hydrogen to reduce carbon dioxide, according to Eq. (1) and (2).

$$2n\ H_2 + n\ CO_2 \xrightarrow{\text{light}} (CH_2O)_n + n\ H_2O \quad \text{(Photoreduction)} \quad (1)$$

$$H_n + 1/2\ O_2 \longrightarrow H_2O + \text{energy} \quad \text{(Ox-hydrogen reaction)} \quad (2a)$$

$$\text{Energy} + 2\ H_2 + CO_2 \longrightarrow CH_2O + H_2O \quad (2b)$$

In a detailed manometric study, Gaffron established the stoichiometry and rates of Reactions (1) and (2).[1,2] He was able to show that the adapted state was destroyed by too high a partial pressure of molecular oxygen or exposure to light intensities above 200 foot-candles. Much useful information about hydrogen-adapted Scenedesmus has been gleaned from manometric observations. However, measurements of gas uptake do not elucidate the intermediary metabolism of the hydrogen and carbon assimilated by adapted Scenedesmus. Furthermore, manometric methods do not allow direct study of the hydrogenase enzyme.

The path of carbon in hydrogen-adapted Scenedesmus has been investigated by using C^{14}-labeled carbon dioxide.[3] Tritium has been used to study the generation, properties, and mechanism of the hydrogenase formed in Scenedesmus. Use of this tracer has also allowed determination of the fate of the hydrogen assimilated in Reaction (1). In order to make a direct study of hydrogenase, use has been made of the following exchange reaction catalyzed by hydrogenase:[4]

$$H_2 + H_2O \rightleftharpoons H_2O + H_2 \quad (3)$$

---

[1] H. Gaffron, Am. J. Bot. 27, 273 (1940).

[2] H. Gaffron, J. Gen. Physiol. 26, 195 (1942).

[3] Gabriel Gingras and Richard A. Goldsby (Lawrence Radiation Laboratory), unpublished work.

[4] A. Farkas, L. Farkas, and Yudkin, Proc. Roy. Soc. B 155, 373 (1934).

The Rittenburg group[5] has devised hydrogenase assays involving the ortho-parahydrogen conversion and deuterium exchange based on Reaction (3). However, both these techniques require complex and expensive instrumentation. We have devised an assay based on tritium exchange,

$$T_2 + H_2O \rightleftharpoons HOT + TH , \qquad (4)$$

which depends on the radioactivity of tritium. We have used this assay to study the generation and properties of the hydrogenase formed by Scenedesmus.

Methods

1. Plant Material

Scenedesmus obliquus was grown under sterile conditions as a photosynthetic autotroph in Myer's medium.[6] The temperature was 20° C and the pH was 7. Immediately before use the cells were harvested and centrifuged for 10 min at 5°C and 600×g in an International Refrigerated Centrifuge. The centrifuge tube was calibrated, and permitted a determination of the volume of wet-packed cells in a given volume of suspension. The packed cells were then resuspended in enough supernatant growth medium to yield the desired concentration $\frac{\text{(volume wet-packed cells)}}{\text{volume suspension}}$. The suspension at pH 7 was placed in a vessel of the type shown in Fig. 53. The reaction was then shaken in a constant-temperature bath.

2. Kinetic Measurements of Hydrogenase Formation

An empty vessel was flushed with hydrogen for 2 min. The system (see Fig. 54) was then closed and the tritium-hydrogen mixture in the reservoir was circulated through the system for 10 min. Then the algae suspension was injected into the vessel and the gas was allowed to recirculate for an additional 10 min. At various intervals after the algae were introduced, samples were withdrawn with a hypodermic syringe and killed in methanol. The methanolic solutions were immediately flushed with hydrogen gas to remove any dissolved tritium gas. Aliquots of the methanolic solutions were counted in the Packard Tri-Carb Liquid Scintillation Spectrometer.

3. Tritium Studies of the Adapted State

A Scenedesmus suspension was pipetted into a vessel and shaken in the dark under a stream of hydrogen (96% H_2 , 4% CO_2) for 4 hr. Two samples were than preilluminated for 5 min. After preillumination, a tritium-hydrogen mixture was circulated through one of the light samples and one of the dark samples. The second light-dark pair of samples received no tritium gas, but 0.5 cc of 58-mC/ml tritiated water was added. After 27 min of photoreduction, 15 ml of methanol was added to each of the four vessels to stop the reaction. The methanol solutions of samples which had been exposed to tritium gas were flushed with H_2 and counted for tritium by liquid scintillation. The methanol solutions of all four samples were centrifuged

[5] A. I. Krasna and D. Rittenburg, J. Am. Chem. Soc. 76, 3015 (1954).
[6] Jack Myers, Plant Physiol. 22, 590 (1947).

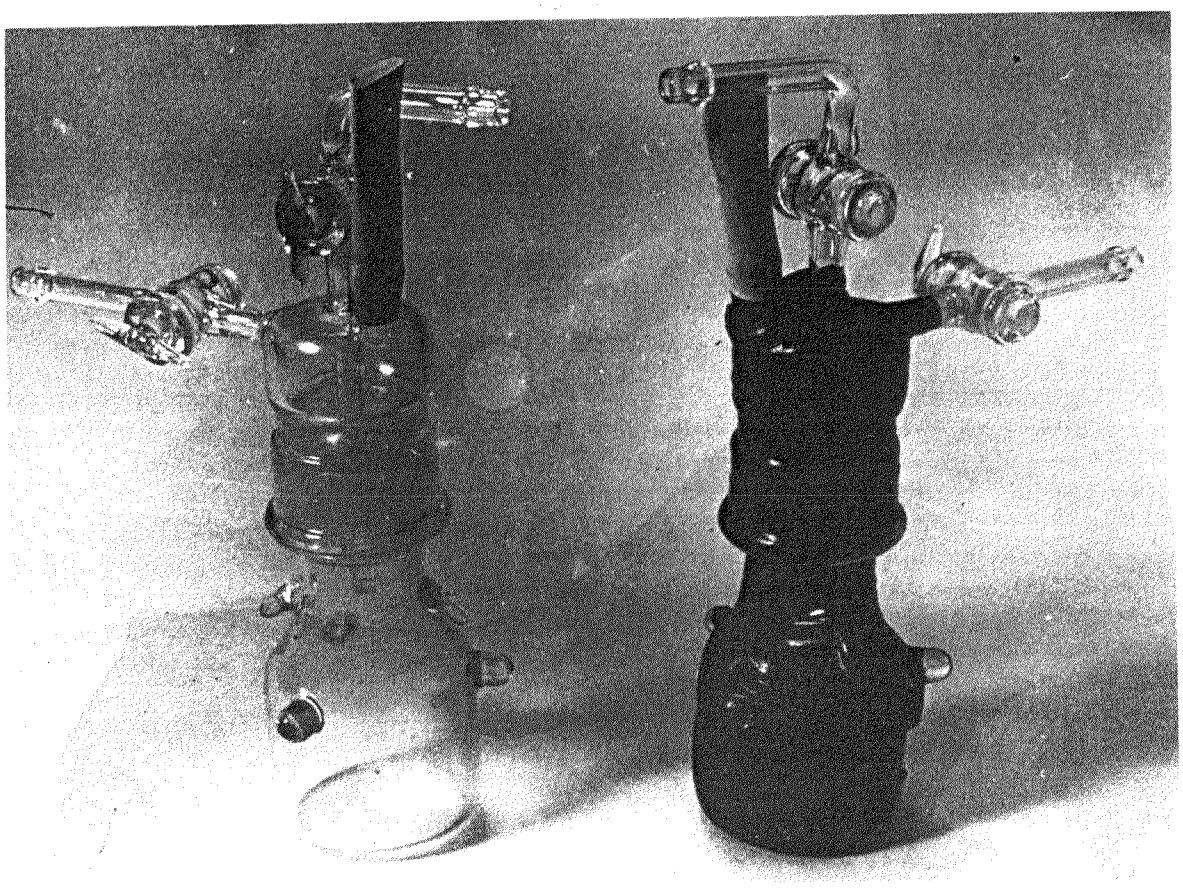

ZN-2783

Fig. 53. Incubation vessel. These vessels are made of pyrex glass and have a volume of approximately 50 ml. When necessary, the vessels are wrapped with Scotch brand plastic electrical tape to exclude light. In some of the experiments described in this paper 500-ml versions of this design were used.

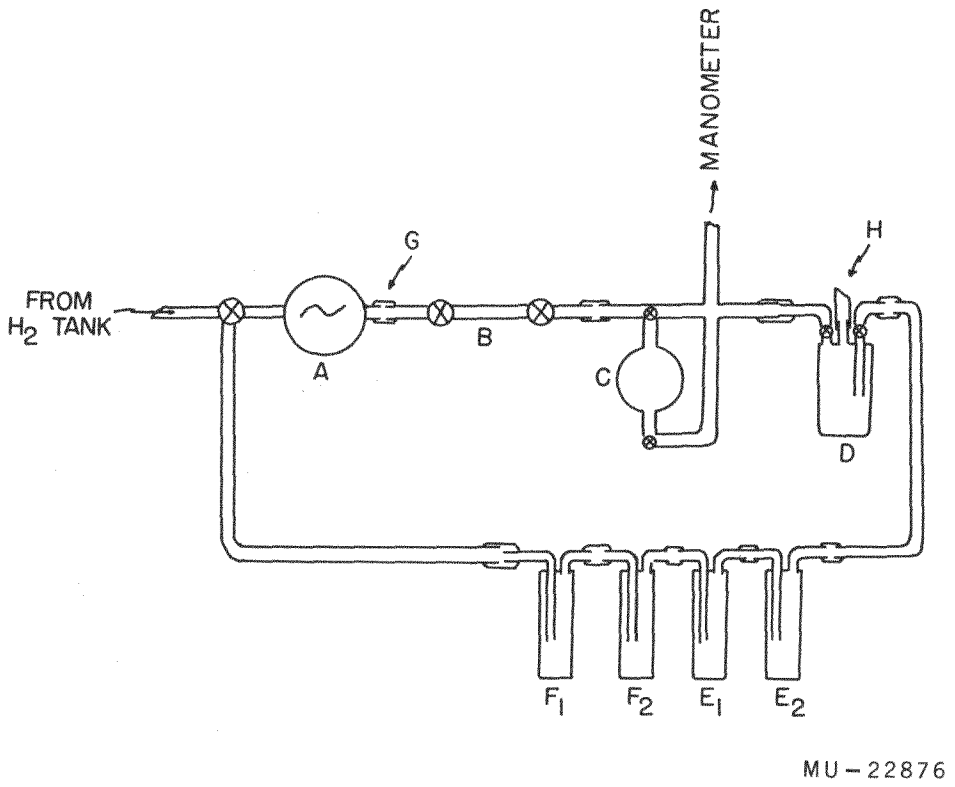

Fig. 54. Schematic outline of experimental setup. A, Scharr dynapump; B, gas-sampling tube; C, tritium reservoir; D, vessel or vessels in series containing algae; E_1 and E_2, traps containing distilled water; F_1 and F_2, traps containing chromous chloride (oxosorbent); G, rubber sleeve; H, rubber policeman.

and the supernatants decanted. The residues were extracted again with 5 ml of 20% methanol and finally with 5 ml of water. The extracts of each of the four samples were evaporated to dryness under vacuum at room temperature. The residues were redissolved in 5 ml of 20% methanol and re-evaporated to dryness. The residues then contained tritium only in nonexchangeable positions. The distillates from the samples that were under tritium gas were collected and counted by liquid scintillation. The residues from all four samples were dissolved in 5 ml of 80% methanol and counted for tritium.

4. General

In all experiments trituim counts were determined as disintegrations per minute by use of an internal standard.[7] A sample of the tritium-hydrogen gas in the system was taken for a measurement of specific activity. The specific activity was determined by converting a known volume of this gas to water over hot copper oxide. The water was collected and counted by liquid scintillation.

Results and Discussion

Figure 55a and 55b show plots of the accumulation of tritium vs time during the adaptation of Scenedesmus under a tritium hydrogen atmosphere. The semilogarithmic plot shows that the increase in tritium is strongly exponential over the first 120 min of adaptation. The linear plot shows that during the next 120 min the exponential component grows weaker and a linear component grows stronger. After about 275 min the rate of accumulation is quite constant, and the accumulation of tritium is linear. These curves show that hydrogenase is formed in an exponential fashion. Once formed, the hydrogenase continues to exchange tritium out of the gas phase into the water phase at a constant rate. Inspection of Figs. 55a and 55b shows that some hydrogenase is present in Scenedesmus after only 5 min of adaptation. It is also apparent that after about 3 hr the formation of hydrogenase is essentially complete. The exponential rise in hydrogenase activity suggests that the enzyme is formed in an autocatalytic fashion. Each unit of hydrogenase formed seems to catalyze the formation of additional units of enzyme until the full complement of hydrogenase is formed.

The hydrogenase may be formed by modification of a pre-existing protein or by induction of new enzyme synthesis. We have found that adding glucose--an energy source--or chloromycetin--an inhibitor of protein synthesis--does not accelerate or retard the rate of hydrogenase appearance during adaptation. However, dithionite--a reducing agent--accelerates the formation of hydrogenase (see Fig. 56) in Scenedesmus. This finding leads to the conclusion that hydrogenase is activated in Scenedesmus by reductive modification of a pre-existing protein. It is possible that under the normal conditions of adaptation to hydrogen the first units of hydrogenase formed supply electrons for the reduction required to produce additional units of

[7] Operation manual for Tri-carb liquid scintillation spectrometer, 1959. Packard Instrument Co.

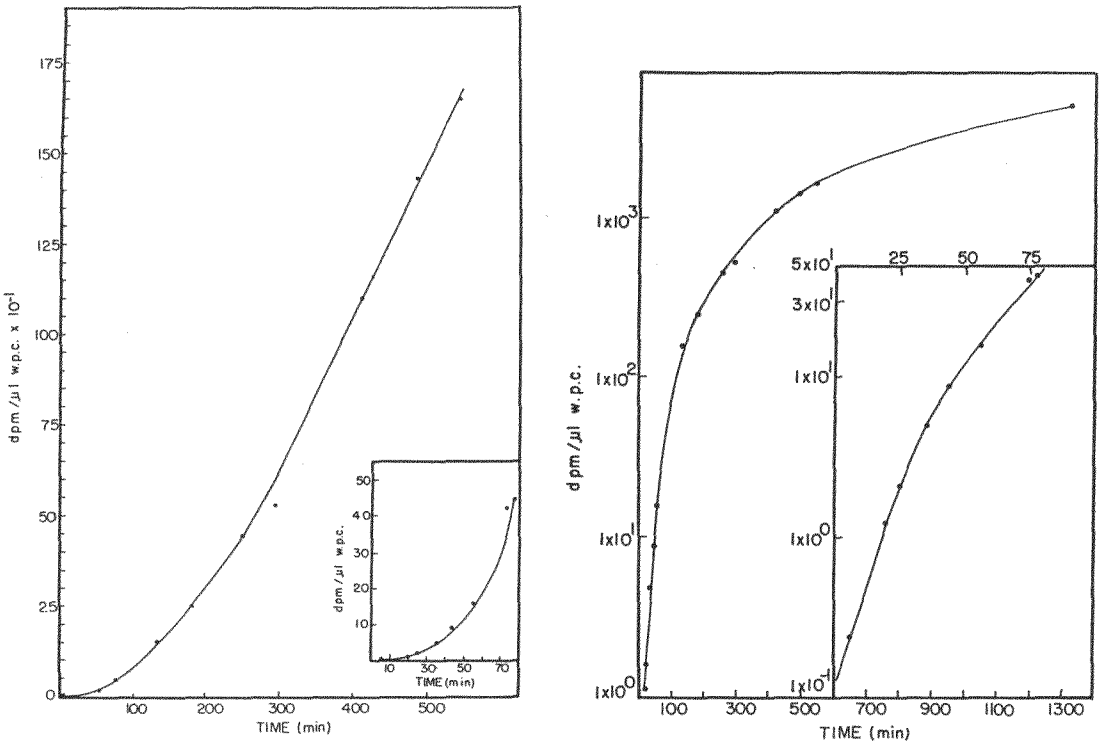

Fig. 55. Time course of Scenedesmus adaptation. 26 ml of Myer's medium containing 170 µl of wet packed Scenedesmus under 500 ml of tritiated hydrogen gas. The temperature was 25°C and the pH 7.

a. Semilog plot b. Linear plot

hydrogenase. This would account for the exponential appearance of hydrogenase during the adaptation of Scenedesmus.

Under normal circumstances, Scenedesmus will not adapt to hydrogen in the presence of light.[8] Gaffron has suggested that the hydrogenase is oxidized by products of the Hill reaction when the light intensity exceeds about 200 foot-candles. We felt that in the presence of CMU, a compound known to block the Hill reaction, it might be possible to adapt Scenedesmus in the presence of light. If CMU (mono-chloro-p-phenyl dimethyl urea) is added, Scenedesmus may be adapted even in the presence of light (see Fig. 56). Figure 56 also shows that the presence or absence of carbon dioxide has no significant effect on hydrogenase appearance.

Once the hydrogenase is formed, factors such as light, oxygen, cyanide, carbon monoxide, and temperature affect its activity. Most of these factors have been studied by manometric methods.[9] But manometry does not measure the hydrogenase directly. Manometric methods measure the rates of reduction of some electron acceptor by an enzyme system that may contain several members. As a result, the effect that one sees during manometric studies of hydrogen-adapted Scenedesmus may be due to changes in hydrogenase activity or merely to changes in the activity of some intermediate electron carrier. However, catalysis of the exchange reaction (Eq. (4)) is a fundamental property of hydrogenase. The tritium-exchange studies described below have given a quantitative measure of the effect of various environmental conditions on the hydrogenase itself.

The activity of the hydrogenase varies with temperature. Figure 57 shows a plot of the log of hydrogenase activity vs the reciprocal of the absolute temperature. The slope of this Arrhenius plot has been used to calculate an activation energy of 7.65 kcal for Scenedesmus hydrogenase. The hydrogenase of Proteus vulgaris, a bacterium, has been found to be 7.7 kcal.[10]

Earlier in vivo assays of hydrogenase activity in Scenedesmus depended on measurements of gas uptake during either photoreduction (Eq. (1)) or the ox-hydrogen reaction (Eq. (2)). The results given in Table XIII show that hydrogenase is significantly inhibited by the low light intensities used to carry on photoreduction or the small amounts of molecular oxygen commonly used in the ox-hydrogen reaction. Table XIV shows the effect of PMS (phenazine methosulfate), a dye that initiates a form of cyclic photophosphorylation and blocks the Hill reaction.[11] Even at the high light intensity of 2,000 foot-candles, PMS prevents extensive deactivation of the hydrogenase,[12] presumably by preventing the formation of oxygen by the Hill reaction.

---

[8] H. Gaffron, Biol. Rev. Cambridge Phil. Soc. 19, 1 (1944).

[9] H. Gaffron, J. Gen. Physiol. 26, 195 (1942).

[10] H. D. Hoberman and D. Rittenburg, J. Biol. Chem. 147, 211 (1943).

[11] A. T. Jagendorf and M. Avron, J. Biol. Chem. 231, 277 (1958).

[12] Richard A. Goldsby, unpublished manometric data.

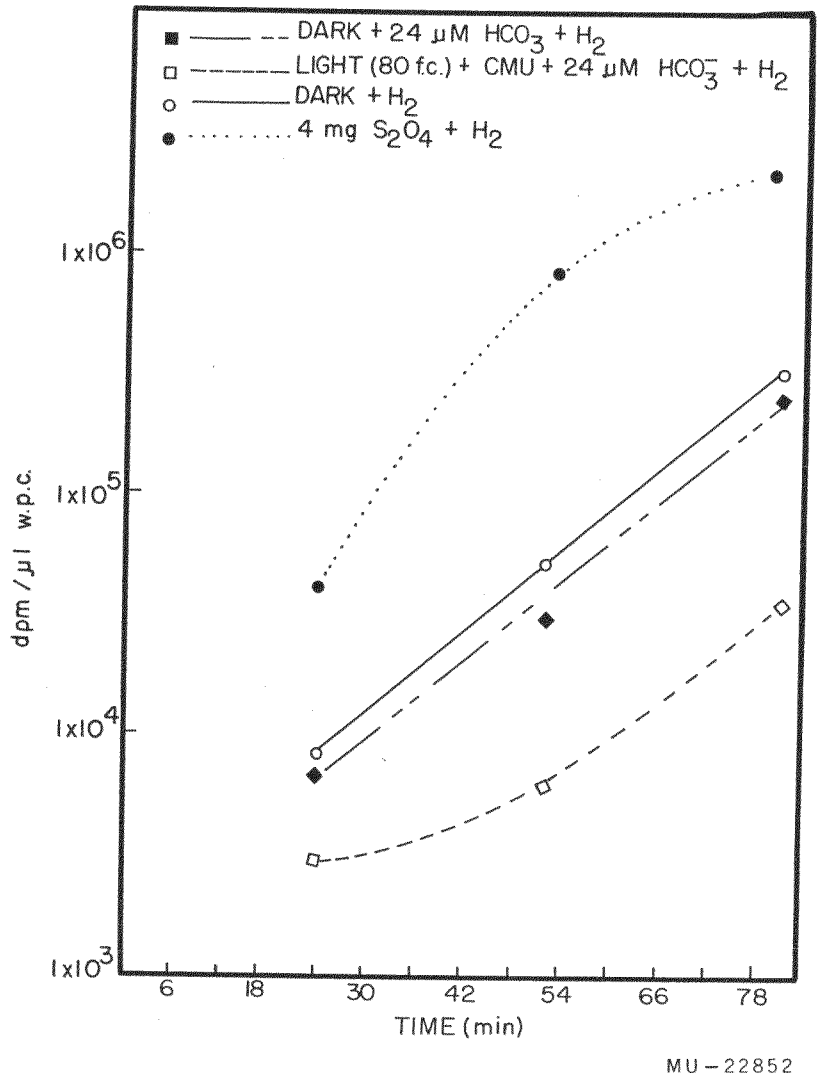

Fig. 56. Effect of light, CO_2, and S_2O_4 on the rate of Scenedesmus adaptation. Each vessel contained 3 ml of Myer's medium and 36 μl of wet packed Scenedesmus cells under 50 ml of tritiated hydrogen gas. Vessel 2 contained sufficient CMU to maintain a saturated solution (about 2 mg). Vessel 4 contained 4 mg of $Na_2S_2)_4$. Vessels 2 and 1 contained 24 μm of $NaHCO_3$.

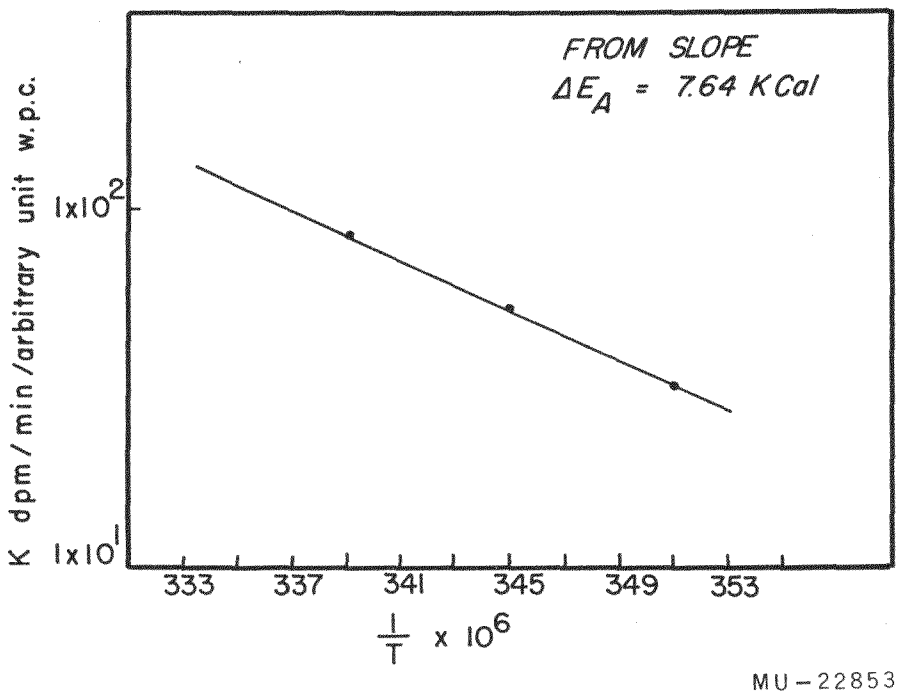

Fig. 57. Effect of temperature on Scenedesmus hydrogenase activity: 45 µl of wet packed Scenedesmus cells in 30 ml of Myer's medium were adapted under hydrogen for 18 hr at 25°C and pH 7. Rates were determined under tritiated hydrogen at 12.0, 17.1, and 23.3°C.

Table XIII. Effect of oxygen and light on Scenedesmus hydrogenase

Condition	"µl" H_2 exchanged per hour per µl w.p.c.	Inactivation (%)
Light (80 ft-c)	1.54	26
Dark ft-c	2.04	0
Dark + 0.4% oxygen added 1 hr prior to introduction of T_2	1.74	15
Dark + 0.4% oxygen added 10 min prior to introduction of T_2	0.885	56

Each vessel contained 4 cc of Myer's medium and 84 µl of wet packed cells (w.p.c.) of Scenedesmus. The samples were adapted for 8 hr under 96% H_2 - 4% CO_2. The temperature was 24° C and the pH was 7. The specific activity of the gas phase after addition of tracer was 171 µC/cc.

Table XIV. Protection of hydrogenase at high light intensities

Condition	Activity (µC/µl w.p.c./hr)	Inactivation (%)
Bright light (2,000 ft-c)	3.14×10^3	98.6
Dark	218×10^3	0
Bright light (2,000 ft-c) + 1.56 µM PMS	182×10^3	19.6
Dark + 1.56 µM PMS	227×10^3	0

Each vessel contained 4 cc of Myer's medium and 180 µl of wet packed cells (w.p.c.) of Scenedesmus. The samples were adapted for 11.5 hr under 98.5% H_2 - 1.5% CO_2. The temperature was 23° C and the pH was 7.1; 1.56 µM of PMS (phenazine methosulfate) was added 15 min prior to addition of the tracer.

The inhibitory effects of cyanide and carbon monoxide on Scenedesmus hydrogenase are shown in Table XV and Fig. 58, respectively. Visible light partially reverses the inhibition of carbon monoxide. The inhibition of Scenedesmus hydrogenase by cyanide and carbon monoxide shows that a heavy metal is a vital constituent of this enzyme. Mineral nutrition experiments have shown that Scenedesmus that are deficient in iron are unable to carry out photoreduction (Eq. (1)). This result has been interpreted as showing that the Scenedesmus hydrogenase has a structural requirement for iron. However, the assay (reduction of CO_2 by molecular H_2) did not measure the hydrogenase activity directly. The iron-deficiency experiment may mean that iron is required for some intermediate electron carrier between hydrogenase and the site of CO_2 reduction. A positive identification of the heavy metal involved in Scenedesmus hydrogenase awaits purification of the enzyme itself.

The chemical nature of Scenedesmus hydrogenase, like that of all other hydrogenases described to date, is only vaguely known. Scenedesmus hydrogenase contains a heavy metal bound to some sort of prosthetic group. It is capable of using molecular hydrogen as an ultimate source of electrons for cellular reductions. We do have some evidence for the form in which the electrons are supplied by the hydrogenase. Our studies with tritium show that when the tracer is supplied to hydrogen-adapted Scenedesmus as tritiated hydrogen gas, no appreciable tritium label appears in organic compounds. This is true in the light or in the dark. On the other hand, if the tracer is supplied to the system as tritiated water, there is a light-dependent fixation of tritium into organic compounds during photoreduction. These results, summarized in Table XVI, show that molecular hydrogen is used only as a source of electrons for cellular reductions. Whatever protons are incorporated during reduction come from the aqueous phase.

Table XV. Effect of CN on hydrogenase activity

Vessel No.	Experimental condition	Activity (dpm/μl w.p.c.)	Inactivation (%)
1	Scenedesmus + No CN^-	385,000	0
2	Scenedesmus + 10^{-3} M CN^-	92,400	79
3	Scenedesmus + 10^{-2} M CN^-	26,200	94

Each vessel contained 4 cc of Myer's medium containing 80 μl of wet packed Scenedesmus cells. All samples were adapted for 5 hours under 98.5% H_2 - 1.5% CO_2. KCN was added to vessels 2 and 3 one hour prior to introduction of the tracer. The temperature was 23° C and the pH was 7.

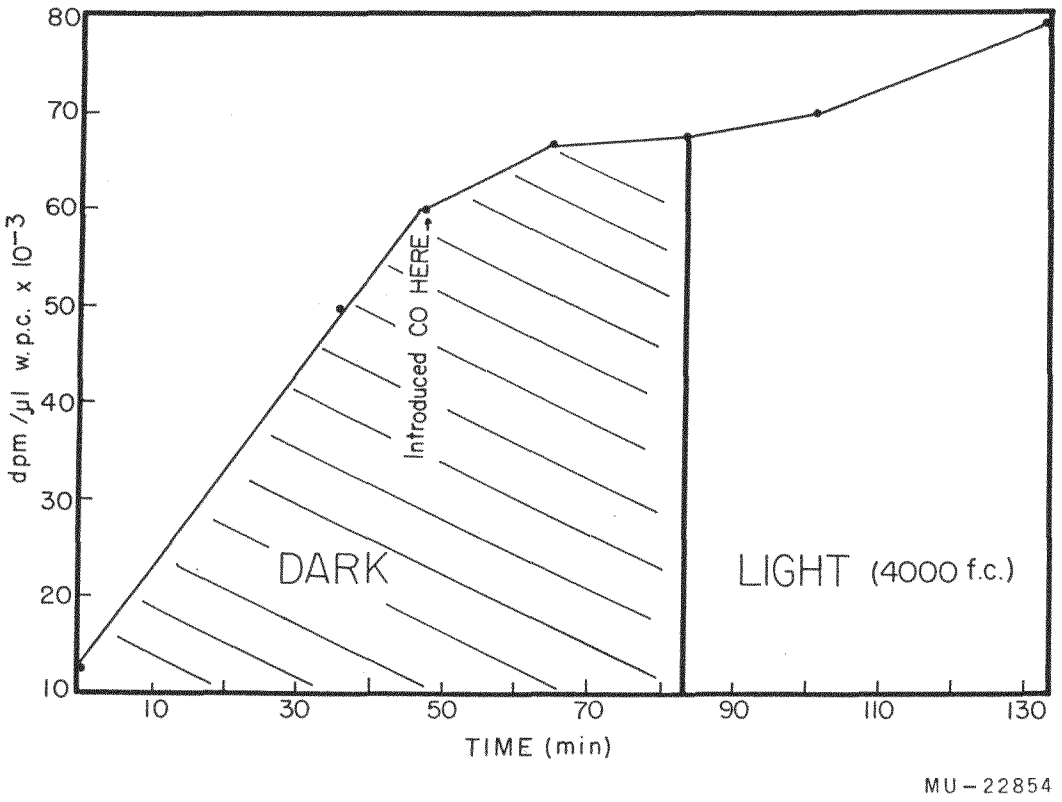

Fig. 58. Effect of light on CO inhibition of Scenedesmus hydrogenase: 175 µl of wet packed Scenedesmus cells in 35 ml of Myer's medium were adapted for 16 hr under hydrogen; 7.8 µM of PMS was added at the close of adaptation. After 47 min exposure to tritiated hydrogen, sufficient carbon monoxide was added to make the system 33% CO - 67% H_2 . The temperature was 22°C and the pH 7.

Table XVI. Variation of tritium labeling with source of tritium

Vessel No.	Experimental condition	Tritium supplied in	Activity fixed ($\mu C/hr/\mu l$ w.p.c. $\times 10^3$) Exchangeable	Nonexchangeable
1	Light	gas phase	39.8	.52
2	Dark	gas phase	79.4	1.1
3	Light	aqueous phase	-	14.7
4	Dark	aqueous phase	-	8.4

Each vessel contained 81 µl of wet packed Scenedesmus cells (wpc) in 4 ml of Myer's medium. All samples were adapted 4 hr under 96% H_2 - 4% CO_2. After adaptation, the light samples were preilluminated 5 min. Tritium gas was added to Vessels 1 and 2 (final sp. act. 79.5 µC/ml), and tritiated water was added to Vessels 3 and 4 (final sp. act. 3 mC/ml). The temperature was 23°C and the pH was 7.

Summary

We have developed an assay for hydrogenase that depends upon the exchange reaction

$$T_2 + HOH \rightleftharpoons HOT + TH.$$

The rate of this exchange is proportional to the amount of active hydrogenase present. This assay has been used to make an in vivo study of the generation and properties of Scenedesmus hydrogenase. Our study has shown that the hydrogenase of Scenedesmus is formed by modification, probably reduction, of a pre-existing protein. The formation of hydrogenase is essentially complete after about 2 hours. The kinetics of hydrogenase formation suggest that its formation is an autocatalytic process. Each unit of hyrogenase formed appears to facilitate the formation of more units, perhaps by providing additional reducing power for the reduction of the inactive form of the enzyme. Scenedesmus hydrogenase is quite sensitive to small amounts of molecular oxygen. Cyanide and carbon monoxide are powerful inhibitors of the active hydrogenase. The carbon monoxide inhibition is partially reversed by visible light. Such behavior indicates that a heavy-metal prosthetic group is a critical component of the enzyme's structure. Scenedesmus hydrogenase uses molecular hydrogen as a source of electrons, but not protons. This suggests that the hydrogenase operates in the following fashion:

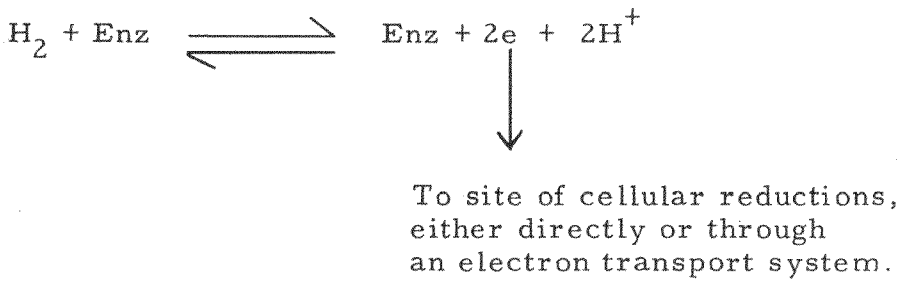
H_2 + Enz
Enz + 2e + $2H^+$
To site of cellular reductions,
either directly or through
an electron transport system.

10. COMPARISON OF TRITIUM AND CARBON-14 LABELING OF THREE COMPOUNDS DURING PHOTOSYNTHESIS IN CHLORELLA

Richard A. Goldsby and J. A. Bassham

Glycolic acid seems to play an important, though presently obscure, role in the intermediary metabolism of photosynthesis. The incorporation of C^{14} into glycolic acid during photosynthesis is increased strikingly when the level of carbon dioxide becomes low.[1] Tolbert has suggested that glycolic acid acts as a hydrogen carrier ferrying electrons from the chloroplast to the cytoplasm.[2] Tanner has suggested that glycolic acid is a primary product of carbon fixation during photosynthesis.[3] Some experimental support for these proposals by Tolbert and Tanner have been provided by the tritium labeling experiments of Moses and Calvin.[4] These workers found that glycolic acid appeared to be the most heavily labeled compound formed when Chlorella were allowed to photosynthesize in tritiated water. In these experiments, the amount of tritium in glycolic acid was estimated by film densitometry rather than by actual counting. Because of the uncertainty involved in equating film blackening to the absolute activity contained in a spot on a paper chromatogram, we have repeated the tritium-labeling experiments described above in all essential details save one. Instead of estimating the activity of glycolic acid by densitometry, we have made an absolute determination of the radioactivity in glycolic acid by liquid scintillation counting. We have also compared the H^3 and C^{14} labeling of glycolic, 3-phosphoglyceric, and malic acids during photosynthesis.

Experimental Procedure

Samples consisting of 0.3 ml of a 30% Chlorella suspension were placed in each of two vessels, one illuminated and one dark. The light vessel was preilluminated for 5 min in the absence of CO_2. After preillumination, 1 ml of tracer solution (3.72 μm HCO_3 containing 75 μC C^{14} in H_2O containing 37.2 mC H^3) was added to each vessel, producing a 6.9% suspension; 0.5-ml samples were taken and killed in 3 ml of methanol according to the following schedule:

Light	Time(min)	Dark	Time (min)
Sample 1	2.25	Sample 1	2
Sample 2	8	Sample 2	7.5

The samples were extracted with 4 ml of 80% methanol, 4 ml of 20% methanol, and 4 ml of water. A known amount of C^{14}-labeled glycolic acid was added to each of the dark samples. The total soluble extract of each

[1] A. T. Wilson and M. Calvin, J. Am. Chem. Soc. 77, 5948 (1955).

[2] N. E. Tolbert, Brookhaven Symposia in Biology No. 11, 271 (1958).

[3] H. A. Tanner, T. E. Brown, C. Eyster, and R. W. Treharne, Ohio 60, 231 (1960).

[4] V. Moses and M. Calvin, Biochim. et Biophys. Acta 33, 297 (1959).

sample was evaporated to dryness. The residues were redissolved in 5 ml 80% methanol, allowed to stand 20 minutes, and evaporated to dryness. This process was repeated until a total of 20 ml 80% methanol was evaporated. The residue, now free of exchangeable tritium, was redissolved in 80% methanol. A portion of the methanolic extract was counted for tritium and C^{14} activity and a portion was applied to paper chromatograms. The chromatograms were developed with phenol-water in the first dimension and butanol—propionic acid in the second dimension. The paper chromatograms were than placed on x-ray film for autoradiography. Those compounds having the R_f's expected for PGA, malic acid, and glycolic acid were eluted from the paper and counted for C^{14} and H^3 in the Tri-carb Liquid Scintillation Counter.

In these experiments, all the radioactivity measurements were made by using the methods of liquid scintillation counting. The liquid scintillation counter counts C^{14} in the presence of tritium under all circumstances. However, unless there is much more tritium than C^{14} (at least 10 to 100 times as much), tritium may not be counted accurately in the presence of C^{14}. Therefore, the sample was counted for C^{14} and then oxidized with chromic acid, flushed with cold CO_2, and re-counted for tritium (see Table XVII).

Results and Discussion

Table XVII shows the absolute fixation of tritium and C^{14} in the light and in the dark. Of the three compounds analyzed, PGA contains the most tritium. From other work, we know that the PGA is essentially "saturated" with C^{14} after 2 to 3 min photosynthesis with bright light in the presence of C^{14}.[5] Apparently PGA is also saturated with T by that time, since the ratio of T to C^{14} in the PGA does not change significantly during the time between the first sample at 2.25 min and the second sample at 8 min in the light. Both T and C^{14} labeling of the PGA pool are thus measures of its concentration, which declines about 60% from 2.25 min to 8 min. This decrease in PGA no doubt occurs because the cells exhaust the supply before 8 min and the carboxylation reaction leading to PGA ceases, while at the same time PGA reduction, requiring only light, continues.

In contrast to PGA, malic acid, at 2.25 min, is far from saturated. Its C^{14} label, coming from carboxylation of three-carbon compounds derived from PGA followed by reduction, is appreciable, but its T label is still

[5] J. A. Bassham and M. Kirk, Biochim. et Biophys. Acta 43, 447 (1960).

Table XVII. Fixation of tritium and C^{14}

	Time (min)	Total soluble C^{14} (dpm/.09 cc wpc)[b]	Total soluble H^3 (dpm/.09 cc wpc)	% Total H^3 and C^{14}						Ratio dpm H^3 to dpm C^{14}		
				Glycolic acid[a]		PGA		Malic acid				
				H^3	C^{14}	H^3	C^{14}	H^3	C^{14}	Glycolic acid	PGA	Malic acid
Light	2.25	5.64×10^6	7.32×10^7	0.78	1.2	10.5	7.3	.08	2.9	8.45	21.4	0.357
Light	8	5.85×10^6	1.03×10^8	1.5	29.4	4.2	3.7	.11	.18	.89	20.0	10.7
Dark	2	1.22×10^5	5.35×10^6	18.6	--	--	--	--	--	--	--	--
Dark	7.5	1.27×10^5	5.25×10^6	--	--	--	--	--	--	--	--	--

[a] Corrected for volatility losses. Two-thirds of the total glycolic acid is lost during the evaporation procedure and 1/6 of the total is lost by evaporation from the paper chromatogram during development and autoradiography.

[b] cc wpc = cm^3 of wet-packed Chlorella (suspended in medium as specified in experimental procedure).

very small. If we compare the ratio of nonexchangeable hydrogen atoms to carbon atoms in these molecules,

PGA

H/C = 1

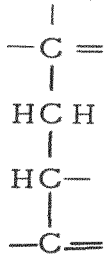

Malic acid
H/C = 3/4

Glycolic acid
H/C = 1

We see that it is 1 for PGA and 3/4 for malic acid. Thus, from the dpm ratio of T/C^{14} in PGA (about 20), we might expect the dpm ratio for malic acid to be 15 when the molecules of malic acid are saturated with respect to both T and C^{14}. In fact the ratio at 8 min is about 10, the saturation value to be expected if two nonexchangeable hydrogen atoms come from PGA or water while the third comes from some unlabeled organic compound, directly via nonphotosynthetically formed unlabeled PNH. This third hydrogen atom would then become bonded to a carbon atom of malic acid during reduction of the carboxylation product. This would explain the low tritium labeling of malic acid at the shorter times also:

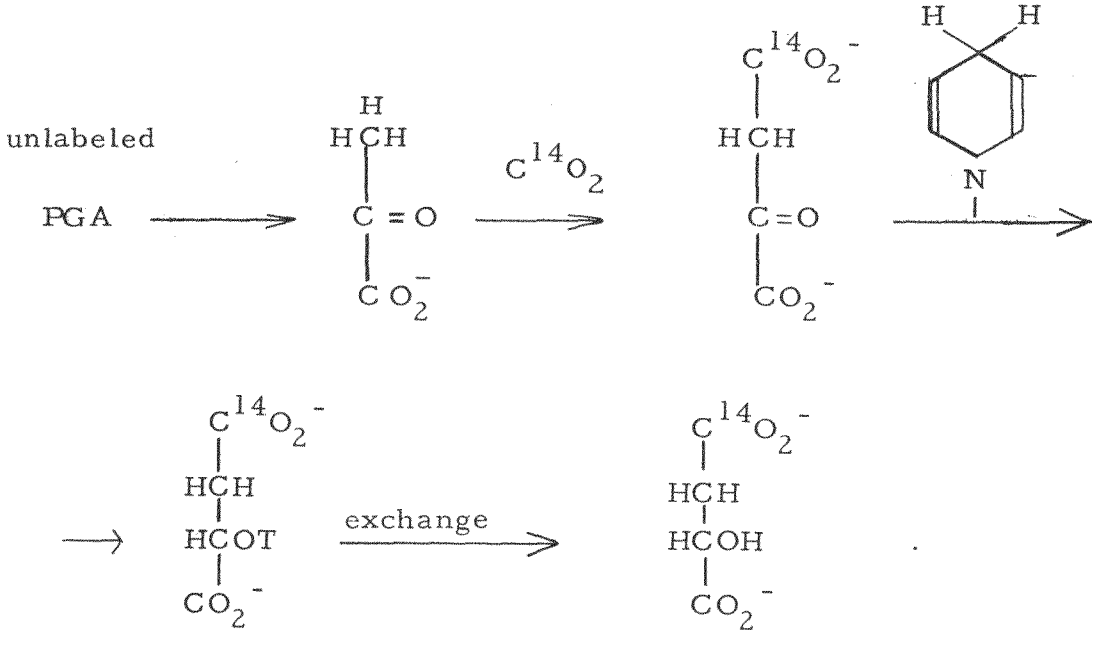

As has been reported in many previous experiments,[6,7] the C^{14} labeling of the glycolic acid increased very markedly when the carbon dioxide pressure dropped (between 2.25 and 8 min in this experiment). However, the T label in glycolic acid increased much less than the carbon labeling, the result being that the ratio of T/C^{14} dpm dropped markedly. In other words, glycolic acid was being synthesized from C^{14} by some nontritiated source. The T/C^{14} was so low, in fact, that the glycolic acid formed after the CO_2 pressure dropped must have derived both of its nonexchangeable hydrogen atoms from an unlabeled source. Conceivably, a major part of the C^{14}-labeled glycolic acid at 8 min came from some unstable biochemical compound which was converted to glycolic acid during killing or the subsequent workup, with tritium label being lost in the process. This possibility requires further investigation.

If the observed labeling of the glycolic acid at 8 min is indicative of the labeling of glycolic acid in the biological system, it is difficult to interpret in terms of known reactions. Such labeling would seem to be not explainable either on the basis of Tanner's hypothesis of a direct photochemical reduction of CO_2[8] or on the basis of direct derivation from the two terminal carbon atoms of the carbon-reduction cycle of photosynthesis,[9] since either pathway should introduce both carbon and nonexchangeable tritium into the molecule. Some transfer of protons from an unlabeled source to a C^{14}-labeled skeleton would seem to be indicated, but the details of such a reaction cannot be pictured without some further experiments.

When the above experiment was repeated in the absence of oxygen under an argon atmosphere, glycolic acid did not accumulate as the supply of CO_2 was used up. Indications of an oxygen requirement for glycolic acid accumulation have been observed by Park and Pon[10] and also by Bassham and Kirk.[11] The failure to find glycolic acid under anaerobic conditions is difficult to understand.

---

[6] A. T. Wilson and M. Calvin, J. Am. Chem. Soc. 77, 5948 (1955).

[7] N. E. Tolbert, in The Photochemical Apparatus: Its Structure and Function. Brookhaven symposium on Biology 11, 271 (1958) (Office of Technical Services, Dept. of Commerce, Washington, D.C.).

[8] H. A. Tanner, T. E. Brown, and C. Eyster, and R. W. Treharne, Biochem. Biophys. Research Communs. 3, 205 (1960).

[9] J. A. Bassham and M. Calvin, in Biogenesis of Natural Substances, Marshall Gates, Ed. (Interscience publishers, in press).

[10] Roderic B. Park and Ning Pon, unpublished observations on CO_2 fixation in chloroplasts.

[11] J. A. Bassham and Martha R. Kirk, unpublished observations on CO_2 fixation in Chlorella.

It should be mentioned that on the autoradiograph of the 2.25-min-light sample, glycolic acid caused as much film darkening as PGA. However, determination of the radioactivity in these two compounds shows that there is ten times as much C^{14} in PGA. This is probably accounted for by condensation of glycolic acid evaporated from the chromatogram directly onto the film surface. In this experiment, estimation of the relative label by densitometry would have given too high a value for glycolic acid.

11. CARBON DIOXIDE METABOLISM IN HYDROGEN-ADAPTED *SCENEDESMUS*

Gabriel Gingras, Richard A. Goldsby, and Melvin Calvin

A few organisms dispersed among three phyla have the ability to use molecular hydrogen for their metabolism. This is a very strange faculty, for in nature hydrogen gas is certainly uncommon. Even more surprising, perhaps, is that green algae such as *Scenedesmus* or *Chlamydomonas* have hydrogenase as a constitutive enzyme. *Scenedesmus*, for example, shows hydrogenase activity (as measured by the isotope-exchange reaction) after a few minutes of incubation under hydrogen.[1] The enzyme, moreover, is inhibited by very small concentrations of oxygen.[2] The obvious question, then, is what is the role of hydrogenase in an aerobic organism such as *Scenedesmus*?

More easily answered questions are (a) what is the path of carbon in photoreduction (CO_2 fixation in the light under hydrogen) and the oxhydrogen reaction (CO_2 fixation in the dark under a mixture of hydrogen and oxygen); and (b) what are the sources of energy for the CO_2 fixation?

The carbon-reduction cycle is so often seen among autotrophs that it seems to be the rule among these organisms. It has been found to occur in hydrogen bacteria,[3,4] for example. However, there is evidence that in hydrogen-adapted *Scenedesmus*, CO_2 enters mostly through malic acid.[5] Since this evidence is not unequivocal, we decided to reinvestigate the problem.

Methods

Scenedesmus obliquus grown under constant temperature, pH, illumination, etc.[6] was used throughout the work. After harvest, the cells were centrifuged and resuspended in growth medium,[7] diluted fivefold. The suspension contained 2.5 ml of packed cells (centrifugation for 15 min at 600 x g) per 100 ml. The experiments were carried out in special airtight vessels(refer again to 53)whose tops were fitted with gas inlet and outlet closed by stopcocks, and another inlet closed by a rubber policeman through which liquids or gases could be injected. Each vessel contained 4.0 ml (i.e., 0.1 ml packed cells) of algal suspension at pH 7.0.

---

[1] Richard A. Goldsby, Thesis, University of California, 1961.

[2] H.F. Fisher, A.E. Krasna, and D. Rittenberg, J. Biol. Chem. 209, 569 (1954).

[3] A.O.M. Stoppani, R.C. Fuller, and M. Calvin, J. Bacteriol. 69, 491 (1955).

[4] G. Milhaud, J.P. Aubert, and J. Millet, Compt. rend. 243, 102 (1956).

[5] E. Badin and M. Calvin, J. Am. Chem. Soc. 72, 5266 (1950).

[6] J.A. Bassham, and M. Calvin, The Path of Carbon in Photosynthesis, Prentice Hall (1957) pp 28-33.

[7] J. Myers, Plant Physiol. 22, 590 (1947).

The cells were hydrogen-adapted in complete darkness for 7 hr with constant shaking under a flow mixture of 99% H_2 and 1% CO_2 . Before reaching the algae, this gas mixture was passed through three $CrCl_2$ (Oxsorbent) traps followed by two water traps to remove the traces of O_2 it contained. At the completion of the adaption period, the vessels were swept with either 99% air and 1% CO_2 , or 99% H_2 and 1% CO_2. Depending on the experiment, the cells were then subjected to various treatments (preillumination, preincubation with inhibitors, etc.) prior to the injection of 200 μC (7.8 μM) of $NaHC^{14}O_3$. Incubation in the presence of $NaHC^{14}O_3$ was conducted at 21 to 23° C with constant shaking. The reaction was stopped by removing the top of the vessel and rapidly adding 16 ml of methanol. This operation can easily be carried out within 5 sec. An aliquot of the alcoholic suspension was counted and the rest of the cells extracted twice in 80% methanol at 60° C and twice in 20% methanol at room temperature.

Aliquots of the combined extracts were chromatographed on paper in two dimensions (phenol:water and butanol: propionic acid:water), and the resulting spots mapped by radioautography and identified by cochromatography with authentic samples. The radioactivities were determined by direct counting on the paper with the help of a Geiger-Mueller tube. The figures are reported as percent of the soluble radioactivity and were calculated by taking the ratio of the radioactivity in one compound to the total radioactivity found on the chromatogram and multiplying by 100.

Results

1. $C^{14}O_2$ Fixation Pattern in the Light

The algae were treated as described before, then preilluminated for 5 min prior to the addition of $NaHC^{14}O_3$. Toward the end of the preillumination period various volumes of air were injected into the vessels so as to give the O_2 concentrations shown in Table XVIII. Incubation period in the presence of $NaHC^{14}O_3$: 30 min; light intensity at the surface of the vessels: 1250 lux.

Table XVIII shows that the total carbon fixation under hydrogen is about 2.5 times that under air. In contrast to the dark fixation (see Table XIX), the light fixation under hydrogen is unaffected by oxygen except at the 5% level, where there is inhibition. This inhibition can best be explained by an oxygen inactivation of the hydrogenase.[2] Table XVIII also shows that under air, the percentage of C^{14} in the mono- and diphospho-sugars is higher than under hydrogen. The reverse is true for PGA and alanine which contain a greater share of the C^{14} under hydrogen. Only alanine, malic, aspartic, and glutamic acids are affected by increasing the oxygen concentration under hydrogen. This might be explained as follows: If the formation of malic acid depends on a reductive carboxylation reaction, a decrease in the ratio of reduced coenzyme to oxidized coenzyme by respiration will have the effect observed, a decrease in the labeling of malic acid. A similar argument can be used to explain the stimulating effect of oxygen on the labeling of glutamic acid. Let us assume that, as appears likely, the rate-limiting step in the over-all synthesis of glutamate is the formation of α-ketoglutarate by the Krebs cycle; then an increase in the ratio

Table XVIII. CO_2 fixation pattern in the light

Total fixation given in counts/min; the rest of the data in percentage of the soluble activity.

Gas	H_2	H_2, 0.1%O_2	H_2, 0.5%O_2	H_2, 1.5%O_2	H_2, 5%O_2	Air
Total fixation (10^6 cpm)	21.6	23.2	21.7	24.6	14.8	8.8
Sugars Mono P (%)	15.6	20.2	16.7	17.8	23.6	29.2
Sugars Di P (%)	0.8	1.1	0.7	0.5	0.3	3.0
PGA (%)	32.9	32.0	32.5	27.8	30.6	20.3
PEPA (%)	2.6	1.9	1.8	1.6	3.6	3.5
Citric acid (%)	0.4	0.6	0.4	0.7	1.7	1.0
Malic acid (%)	6.3	3.3	4.1	4.0	1.6	2.5
Aspartic acid (%)	7.3	12.2	14.4	12.5	13.0	14.2
Glutamic acid (%)	1.2	2.3	3.2	3.0	6.2	4.5
Serine (%)	4.3	4.3	4.3	4.2	3.6	2.2
Glycine (%)	0.5	0.5	0.4	0.8	0.8	0.3
Alanine (%)	26.2	18.8	19.3	17.0	9.3	11.8
Unaccounted for (%)	1.7	2.5	3.5	7.8	5.4	7.2

Table XIX. CO_2 fixation pattern in the dark

Total fixation given in counts/min; the rest of the data given in percentage of the soluble activity.

Gas	H_2	H_2, 0.1% O_2	H_2, 0.5% O_2	H_2, 1.5% O_2	H_2, 5% O_2	Air
Total fixation (10^6 cpm)	1.1	1.5	2.9	6.6	16	0.38
Mono P Sugars (%)	16.3	16.1	13.6	18.6	19.5	3.5
DiP Sugars (%)	7.1	9.7	6.2	2.6	1.8	0
PGA (%)	6.6	7.4	18.5	23.3	25.7	17.4
PEPA (%)	1.0	0.3	1.8	2.7	1.6	1.0
Citric acid (%)	1.9	0.3	0.1	0.8	0.8	9.2
Malic acid (%)	11.2	10.3	8.2	8.0	5.0	9.5
Aspartic acid (%)	1.3	0.6	1.6	3.1	8.7	37.9
Glutamic acid (%)	0	0	0	0.9	2.2	20.5
Serine (%)	0.5	0.2	1.5	2.6	4.7	0
Glycine (%)	0.6	0.2	0.4	0.9	0.9	0
Alanine (%)	50.3	54.5	47.0	28.2	25.8	0.8
Unaccounted for (%)	0	0	0.9	6.6	3.2	0

of reduced to oxidized coenzyme will favor glutamate formation. We have observed relatively large amounts of α-ketoglutaric acid under similar conditions when an oxidant such as methylene blue is added to the cells in the dark; α-ketoglutaric acid is usually not seen under our experimental conditions. The effect of added oxygen on the labeling of alanine is rather striking, but it is even more so in the dark fixation pattern; it is discussed in the next section.

2. $C^{14}O_2$ Fixation Pattern in the Dark

This experiment was carried out at the same time and with the same population of cells as the light CO_2 fixation experiment. Conditions were the same in both cases, except that here the vessels were wrapped with masking tape so as to keep their contents in complete darkness.

Table XIX shows that under hydrogen, $C^{14}O_2$ fixation is again about three times as high as under air. When oxygen is added to the hydrogen, a remarkable phenomenon occurs: the $C^{14}O_2$ fixation increases with oxygen concentration until, at 5% O_2, it reaches a level comparable to that obtained by photoreduction (Table XVIII). This is the oxhydrogen reaction studied by Gaffron.[8] Photoreduction and oxhydrogen reactions are comparable not only in the rates, but also in the patterns of CO_2 fixation. Compare, for example, the 5% O_2 dark fixation pattern with the 0.5% O_2 light fixation pattern. So far as carbon dioxide fixation is concerned, we have achieved photosynthesis in the dark!

We think these results clearly indicate that molecular hydrogen is utilized for the reduction of a coenzyme which can either directly reduce carbon compounds or reduce oxygen via the electron transport chain with the production of high-energy phosphates.

Table XIX and Fig. 59 show that as the concentration of oxygen is raised, the proportion of C^{14} in the sugar diphosphates and in alanine decreases and, instead, goes up in PGA and in aspartate. The high sensitivity of alanine to oxygen is especially interesting. It indicates that this amino acid is formed mostly by a reductive process. This process could be indirect like a reductive amination of α-ketoglutarate or of oxaloacetate, followed by transamination with pyruvate, or it could be direct, i.e., reductive amination of pyruvate. This last reaction has been found to occur in bacteria[9] but has not been reported in plants.

Although the second hypothesis might appear more attractive, the first is sufficient to explain our results. Reducing conditions might lead either to an accumulation of pyruvate or to an increased rate of reduction of α-ketoglutarate to glutamate which enters in the following equation:

---

[8] H. A. Gaffron, J. Gen. Physiol. 26, 241 (1942).

[9] J. M. Wiame and A. Piérard, Nature 176, 1073 (1955).

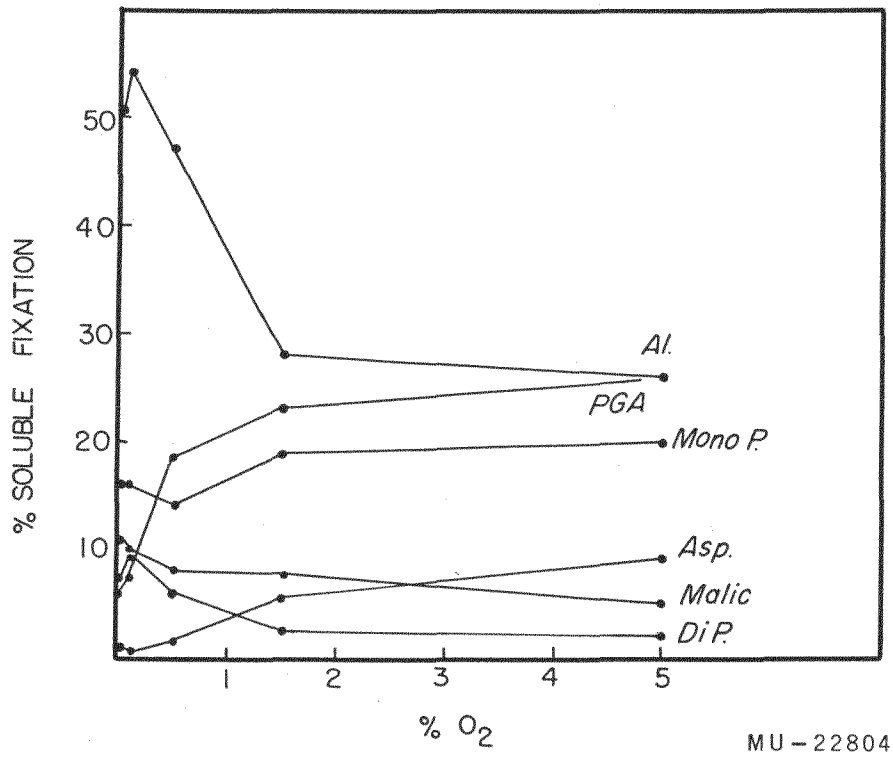

Fig. 59. $C^{14}O_2$ fixation pattern in the oxhydrogen reaction at different oxygen concentrations.
Incubation 30 min at 22°C with 200 μC $NaHC^{13}O_3$ in the dark.
Gas phase: hydrogen and various amounts of oxygen.

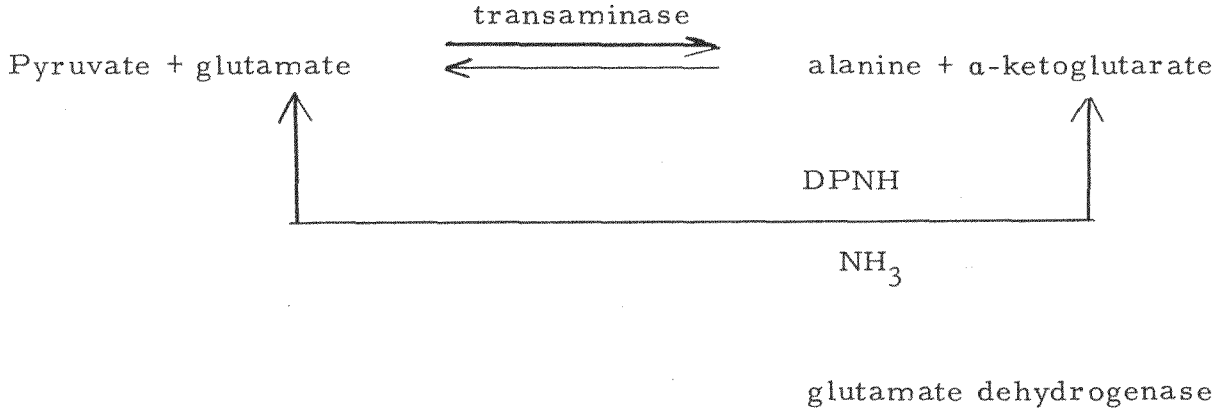

An accumulation of pyruvate will increase the rate of transamination if the reductive amination of α-ketoglutarate is fast enough to regenerate the glutamate consumed.

We have also to explain why addition of O_2 causes the percentage of C^{14} to decrease in the sugar diphosphates while remaining constant in the monophosphates and increasing in PGA. This problem is now under investigation.

3. Kinetic Experiment

Until now we have assumed that the oxhydrogen $C^{14}O_2$ fixation observed occurs via the carbon reduction cycle. Although this has generally been found to be true in chemosynthetic bacteria,[3,4] the evidence for such a mechanism in Scenedesmus is lacking. In fact it has been thought that under H_2 at low light intensity (490 lux) or in the dark with 0.5% O_2, most of the CO_2 fixation occurs via malic acid.[5] Since our fixation patterns in the dark were so similar to those obtained in the light, we decided to reinvestigate that problem kinetically.

The experimental procedure was the same as described before. The sampling technique was different, however. After the $NaHC^{14}O_3$ had been introduced in a tuberculin syringe through the policeman, the cells were rapidly shaken by hand and a 1.0-ml sample was taken in the syringe and rapidly injected in methanol. The first two points were 1.0-ml samples, the following were 0.5-ml samples. The cells were either preilluminated or preincubated with 1.5% O_2 for 5 min before addition of $NaHC^{14}O_3$.

a. Light CO_2 Fixation

Figure 60 shows that under air at 1250 lux CO_2 enters mainly through PGA and is reduced via the carbon reduction cycle.[10] At the same light intensity, but under hydrogen (Fig. 61), most of the CO_2 is fixed in PGA but an appreciable fraction is fixed in malic or oxaloacetic acids. Observe

[10] J.A. Bassham, A.A. Benson, L.D. Kay, A.Z. Harris, A.T. Wilson, and M. Calvin, J. Am. Chem. Soc. 76, 1760 (1954);

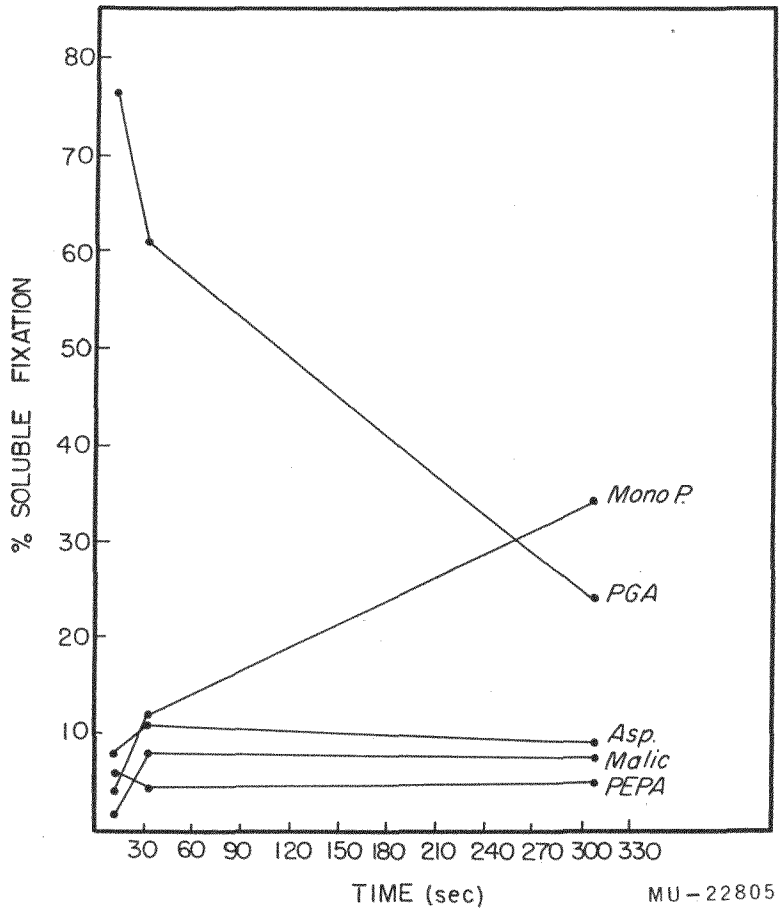

Fig. 60. Kinetics of CO_2 fixation in photosynthesis at low light intensity. Gas phase: air. Light intensity: 1250 lux.

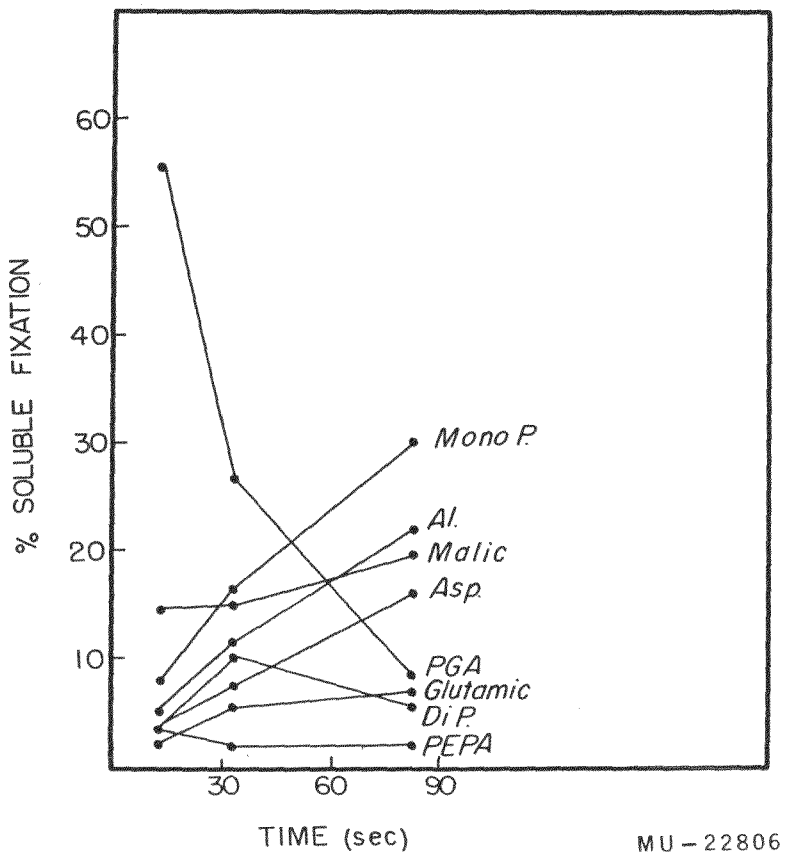

Fig. 61. Kinetics of CO_2 fixation in photoreduction at low light intensity. Gas phase: Hydrogen. Light intensity: 1250 lux.

(Fig. 61) the rapid rise in the activity of malic and aspartic acids, and compare with fixation rates in these compounds under air. It is of interest also that the decrease in the percent of C^{14} in PGA is more rapid under hydrogen than under air and is accompanied by a faster increase in alanine and the sugar monophosphates. This we take to agree with the conclusion reached in the previous experiment that hydrogen is used in the reduction of PGA and in the transamination or the reductive amination of pyruvate.

The same experiment was performed at high light intensity (32,000 lux) to show the effect of inactivation of hydrogenase on the kinetics of CO_2 fixation. At such light intensities the rate of photosynthetic oxygen evolution is too rapid to be compensated for by hydrogen uptake, and the oxygen accumulated inactivates the hydrogenase.[2] Figures 62, 63, and 64 show the kinetics of CO_2 fixation at 32,000 lux under conditions of photosynthesis (Fig. 62), of photoreduction (Fig. 63) and photoreduction in the presence of CMU (Fig. 64).

One interesting feature of these experiments is that in the presence of CMU, alanine takes up C^{14} much more rapidly than either under air or under H_2 alone. It is well known that CMU prevents inactivation of the hydrogenase by blocking photosynthetic oxygen evolution.[11]

b. Dark CO_2 fixation

In the dark under hydrogen (Fig. 65), CO_2 seems to enter mainly through aspartic and malic acids, although a small percentage probably enters through PGA. An unidentified spot was observed below aspartic acid on our radioautograms but showed no activity in the liquid scintillation counter. Since about three months elapsed between chromatography and counting, we think the compound probably decomposed and volatilized in that period. Such a behavior would be consistent with oxaloacetic acid.

Figure 66 shows that the oxhydrogen-driven CO_2 fixation occurs mainly via PGA, at least at 1.5% oxygen, the concentration we used in this experiment. Badin reported evidence suggestive of a predominance of malic acid over PGA as an entry of CO_2 in hydrogen adapted Scenedesmus at very low (490 lux) light intensity or in the oxhydrogen reaction (0.5% O_2).[5] An objection can be raised against those experiments, however; the algae were not killed anaerobically but were exposed to air for 3 to 4 min before killing. For the initial, critical points, exposure to air could cause a large difference.

4. CO_2 Fixation and Hydrogenase Activity

The rate of CO_2 fixation in the oxhydrogen reaction depends on two opposite factors: (a) the energy-yielding reaction and (b) the inactivation of hydrogenase by oxygen. Increasing the oxygen tension will accelerate the energy-yielding reaction up to a certain limit; on the other hand, it will also inhibit the hydrogenase and this will tend to decrease the oxhydrogen reaction.

[11] N.I. Bishop, Biochim. et Biophys. Acta. 27, 205 (1958).

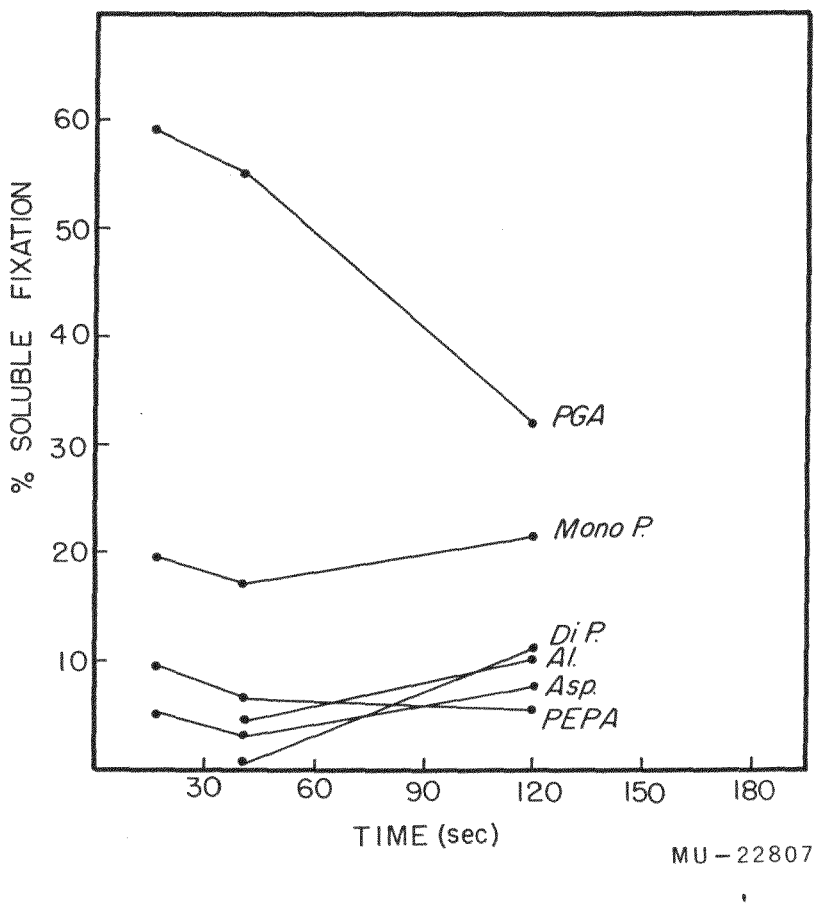

Fig. 62. Kinetics of CO_2 fixation in photosynthesis at high light intensity. Gas phase: Light intensity, 32,000 lux.

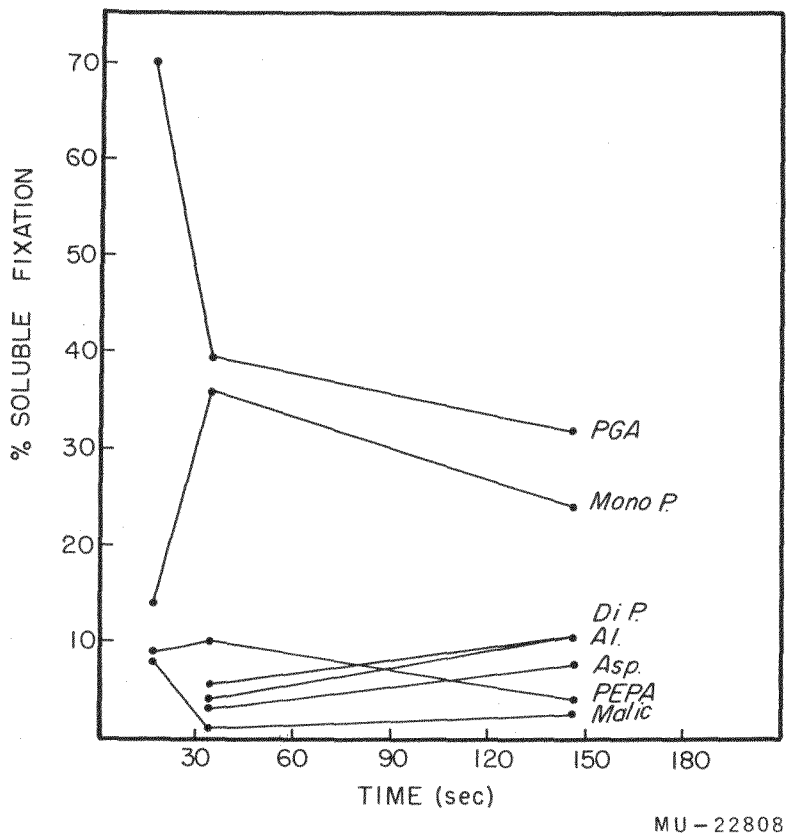

Fig. 63. Kinetics of CO_2 fixation in photoreduction at high light intensity. Gas phase: hydrogen. Light intensity: 32,000 lux.

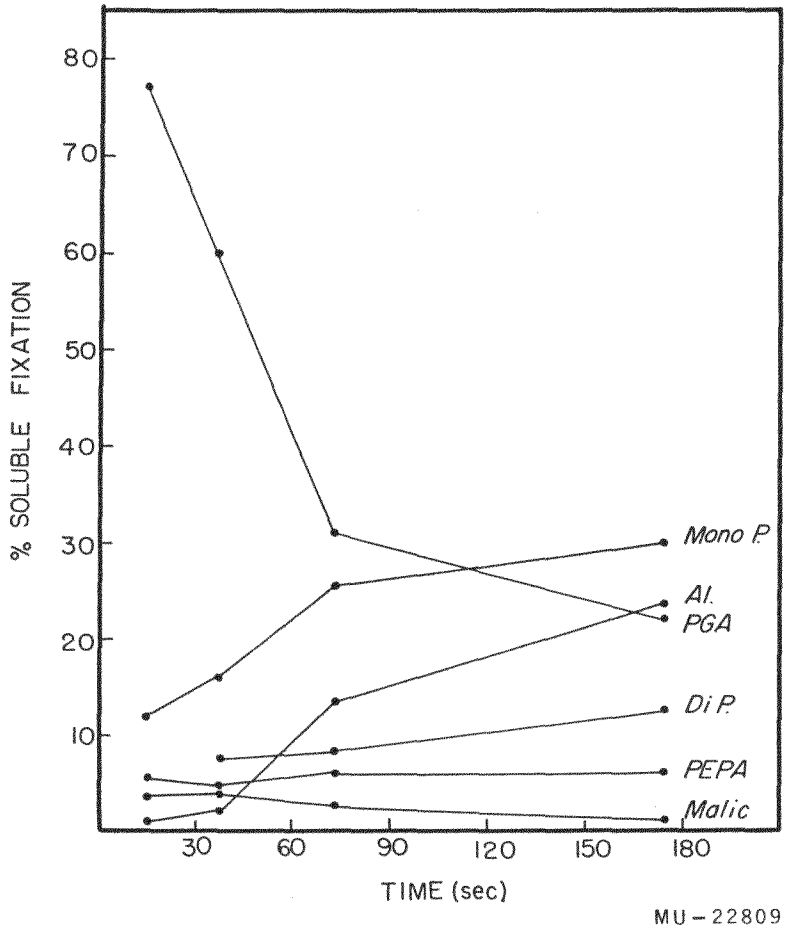

Fig. 64. Kinetics of CO_2 fixation in photoreduction at high light intensity Effect of CMU. Gas phase: Hydrogen. Light intensity: 32,000 lux. Final CMU concentration: saturated.

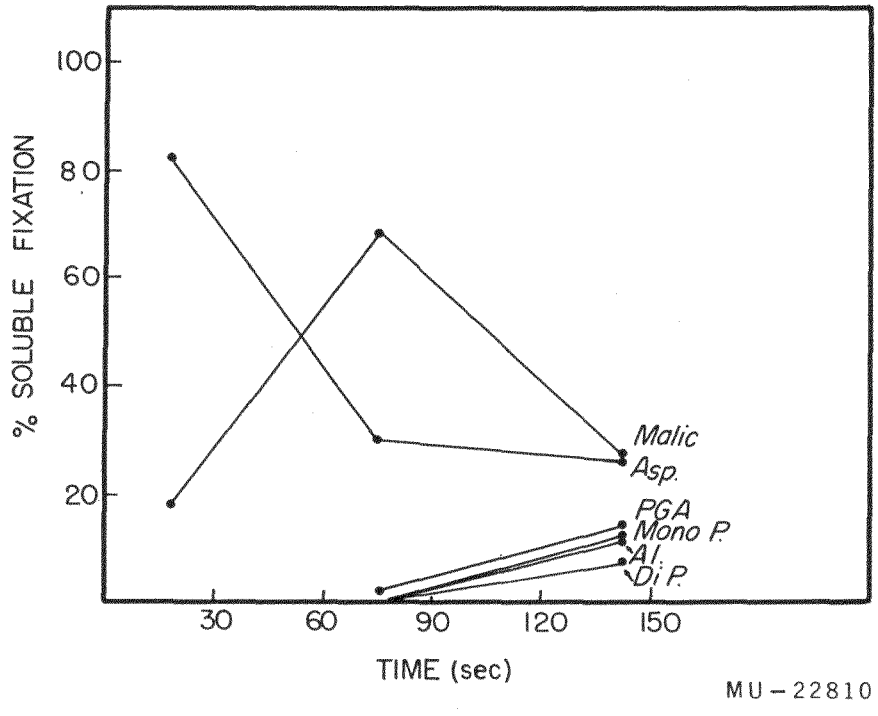

Fig. 65. Kinetics of CO_2 fixation in the dark under hydrogen.

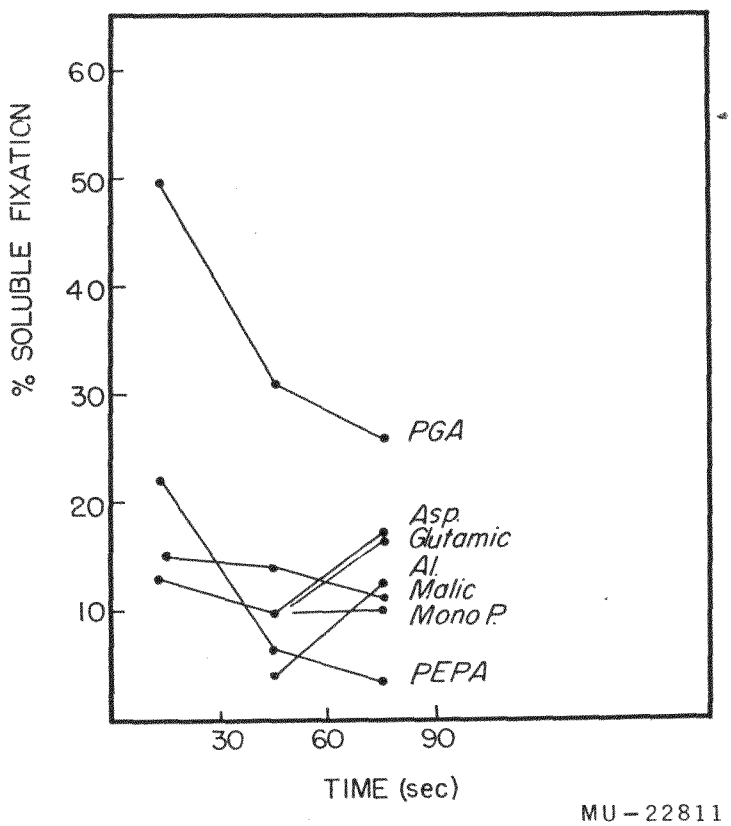

Fig. 66. Kinetics of CO_2 fixation in the oxhydrogen reaction. Gas phase: Hydrogen + 1.5% oxygen. Dark.

In order to measure hydrogenase activity under different oxygen tensions we had recourse to the isotope-exchange reactions discovered by Farkas et al.[12] and used by Hoberman and Rittenberg[13] as an assay method for hydrogenase:

$$D_2O + H_2 \xrightleftharpoons{\text{hydrogenase}} HD + DOH\ .$$

Instead of following the rate of exchange of D_2O with H_2, which requires rather specialized equipment, we followed the exchange of T_2 in the gas phase with H_2O in the medium:

$$H_2O + T_2 \xrightleftharpoons{\text{hydrogenase}} HT + HOT\ .$$

The algae are simply incubated in the dark in the presence of a tracer amount of T_2 in the hydrogen atmosphere. After a certain period of time, the reaction is stopped by methanol and the suspension swept with H_2 to remove dissolved tritium. A sample is counted in the scintillation counter. More detailed information on this assay method will be found in Ref. 1. (It should be noted that this assay method is valid in vivo only because tritium gas is not fixed in the organic compounds, but only in the water.[1])

A double labeling experiment was carried out as follows: The algae were hydrogen adapted for 7 hr as usual. Each vessel contained 80 µl of packed cells in a volume of 3.0 ml of 1:5 diluted growth medium. The atmosphere of the vessels was then replaced with a mixture of H_2 and T_2, the algae left in contact with this mixture for 35 min, then 30 µC (25 µmoles) of $NaHC^{14}O_3$ injected, followed by various volumes of air, and a 1.0 ml sample immediately taken. Ten minutes later the rest of the algae were killed.

The samples were counted in the scintillation counter where, because of the low C^{14} fixation, it was possible to count separately activity due to C^{14} and activity due to tritium. Figure 67 shows the fixation following injection of air.

Carbon dioxide fixation is shown to attain a maximum between 0 and 0.5% O_2 and to decline as oxygen tension is increased. This is in contrast to the experiment reported in Table XIX in which CO_2 fixation increased almost linearly with O_2 tension, up to 5% O_2. We think this apparent discrepancy is due to the smaller volume of the suspension and to the much faster rate of shaking in the present experiment. In the first experiment the rate of diffusion of oxygen was limiting and permitted the hydrogenase

[12] A. Farkas, L. Farkas, and Yudkin, Proc. Roy. Soc. (London) 155, 373 (1934).

[13] H. D. Hoberman and D. Rittenberg, J. Biol. Chem. 147, 211 (1943).

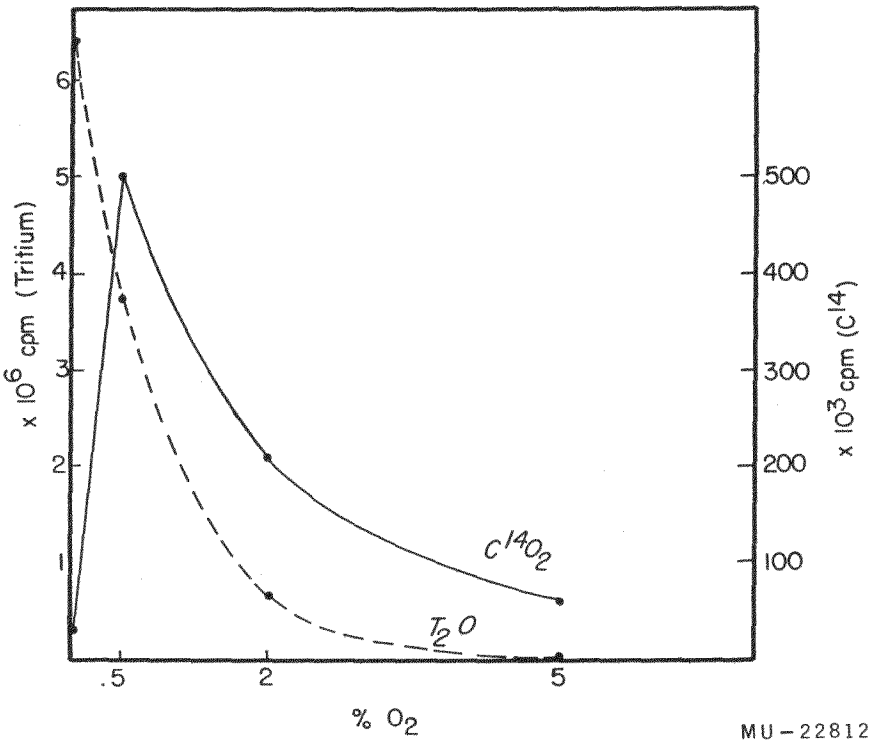

Fig. 67. The effect of oxygen on the rate of CO_2 fixation and on hydrogenase activity.

to go on working, even at 5% O_2, as witnessed by the almost linear relationship between CO_2 fixation and oxygen concentration. In the present experiment the rate of diffusion of O_2 is much faster, so that the enzyme is inactivated completely at 5% O_2 (Fig. 67).

This experiment shows the expected parallelism between CO_2 fixation and hydrogenase activity. There must be an optimal point where the enzyme is active enough and the oxygen pressure high enough to permit the oxhydrogen reaction to proceed at maximal rate. This point appears to be between 0 and 0.5% O_2 under the conditions of this experiment.

5. Inhibitor Studies

In the hope of learning more about the mechanism of the photoreduction and the oxhydrogen reactions, we studied next the effect of various inhibitors on the CO_2 fixation. The usual experimental procedure was followed with the exception that the cells were preincubated with the inhibitors for a period of 60 min before addition of $NaHC^{14}O_3$. Table XX shows the effect of high concentrations of Menadione (vitamin K_3), 2,4-dinitrophenol, and CMU (3-(4-chlorophenyl)-1,1-dimethylurea) on photosynthesis and on photoreduction. Photosynthesis appears to be the more sensitive to all three inhibitors. The effect of CMU, a Hill reaction inhibitor, is particularly striking: it inhibits photosynthesis twice as much as it inhibits photoreduction.

Table XXI shows the effect of the three inhibitors on $C^{14}O_2$ fixation under hydrogen, air, and a mixture of hydrogen and oxygen. Menadione inhibits the fixation under air and under hydrogen + oxygen; this is consistent with an inhibition of respiration as reported elsewhere.[14] Both the air and the oxhydrogen fixations are more sensitive to menadione than photoreduction. Likewise, the hydrogen and the oxhydrogen fixations are more sensitive to dinitrophenol than photoreduction. CMU does not appreciably affect any of the dark fixations.

Discussion

The data are consistent with the proposal that there is a reduction of a coenzyme by molecular hydrogen. When oxygen is added in the dark, some of the hydrogen is combined with oxygen to yield water and high-energy phosphates; the reduced coenzyme and the high-energy phosphate can be used to reduce CO_2 via the carbon reduction cycle. This oxhydrogen reaction exhibits respiration-like sensitivity to menadione and to 2,4-dinitrophenol.

Carbon dioxide fixation under hydrogen at the light intensity used here is from two to four times as fast as under air. It is clear from this that molecular hydrogen contributes electrons for the reduction of carbon compounds. At the concentrations used, the three inhibitors block photosynthetic fixation almost completely, but they affect photoreduction to a much smaller extent. It is interesting to note that photoreduction even in the presence of

[14] H. A. Gaffron, J. Gen. Physiol. 28, 259 (1944).

Table XX. Effect of inhibitors on $C^{14}O_2$ fixation in photosynthesis and photoreduction

Light intensity: 1250 lux
Final concentration of inhibitors indicated in parentheses.
Preincubation with the inhibitors: 60 min
Incubation with $NaHC^{14}O_3$: 30 min

Gas phase	Inhibitor	Total $C^{14}O_2$ fixation (cpm$\times 10^6$)	inhibition %
Hydrogen	none	18.1	--
Hydrogen	Menadione (saturated)	5.9	65
Hydrogen	CMU (saturated)	9.7	45
Hydrogen	2, 4-DNP(10^{-3} M)	7.2	60
Air	none	3.8	--
Air	Menadione (saturated)	0.08	98
Air	CMU (saturated)	0.3	92
Air	2, 4 DNP (10^{-3} M)	0.05	99

Table XXI. Effect of inhibitors on the dark $C^{14}O_2$ fixation

Preincubation with inhibitors: 60 min
Incubation with $NaHC^{14}O_3$: 30 min
Final concentration of inhibitor in parentheses

Gas Phase	Inhibitor	Inhibition (%)
Hydrogen	Menadione (saturated)	0
Hydrogen	CMU (saturated)	0
Hydrogen	2,4-DNP (10^{-3} M)	90
Air	Menadione (saturated)	97
Air	CMU (saturated)	0
Air	2,4-DNP (10^{-3} M)	70
Hydrogen + 1.5% O_2	Menadione (saturated)	80
Hydrogen	CMU (saturated)	0
Hydrogen	2,4-DNP (10^{-3} M)	98

these inhibitors still fixes more $C^{14}O_2$ than does photosynthesis at these low light intensities.

What can we conclude on the basis of this evidence about the mechanism of photoreduction? Many mechanisms can be imagined, but we will limit ourselves here to four possibilities.

1. Under hydrogen in the light, a noncyclic photophosphorylation of the type discovered by Arnon[15] in chloroplasts would normally be operating, but the oxygen, or a precursor, would be reduced by molecular hydrogen along the respiratory pathway. As long as the light intensity was low enough, very little oxygen would be evolved, but at high light intensities the hydrogenase could not keep up with oxygen production, and oxygen would appear in the gas phase, at the same time inactivating the hydrogenase, and the organism would revert to photosynthesis. This would account for the results of Horwitz[16] and of Horwitz and Allen[17] on oxygen evolution and oxygen exchange in hydrogen-adapted algae. When menadione, phenazine methosulfate (PMS has been found to prevent inactivation of the hydrogenase at high light intensities[1]), and perhaps CMU and o-phenanthroline were added the organism would switch to a cyclic type of photophosphorylation whereby no oxygen would be evolved:

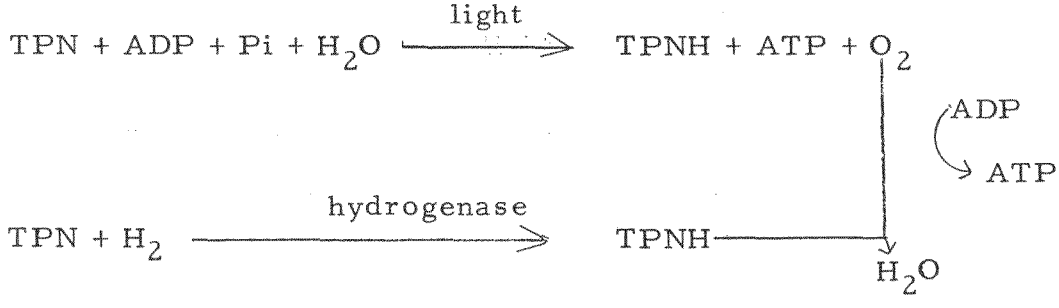

although menadione and phenazine methosulfate may induce "cyclic" photophosphorylation, this does not appear to be the case for CMU or for o-phenanthroline, so this hypothesis lacks generality. Another more serious objection is the relative insensitivity of CO_2 fixation under H_2 to high concentrations of 2,4-dinitrophenol. The mechanism proposed above does not predict a greater resistance to 2, 4-dinitrophenol under H_2 than under air.

---

[15] D.I. Arnon, Nature 184, 10 (1959).

[16] L. Horwitz, Arch. Biochem. Biophys. 66, 23 (1957).

[17] L. Horwitz, and F.L. Allen, Arch. Biochem Biophys. 66, 45 (1957).

2. This would involve exclusively a cyclic type of phosphorylation in in which the elements of water, separated by photolysis, would recombine, with the formation of high-energy phosphates. Molecular hydrogen would then be the only source of electrons to carbon compounds:

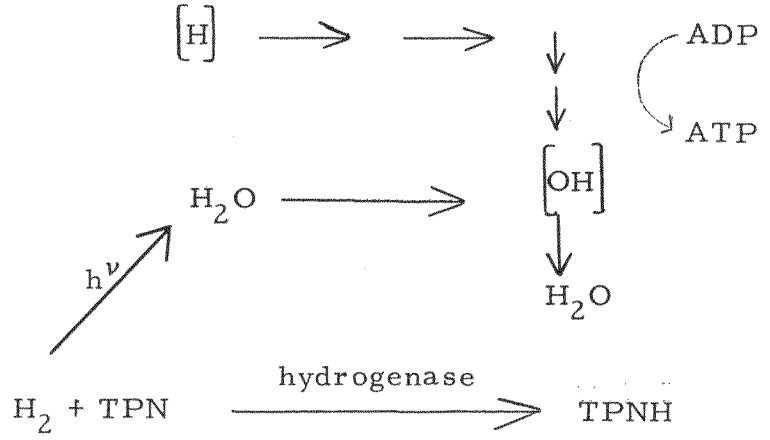

This scheme has the disadvantage that further assumptions are necessary to explain why bright light causes a reversal to photosynthesis. It fails also to explain why CMU, a powerful inhibitor of the Hill reaction, does not have more effect on photoreduction.

3. A combination of cylic and noncyclic photophosphorylation is subject to the same objections as the cyclic mechanism proposed above: CMU should inhibit it almost completely, since both processes depend on the Hill reaction.

4. The last possibility we consider is that photolysis of water is only facultative under hydrogen. In other words, there would be a competition between noncyclic photophosphorylation (Reaction 1) and a literal photo-reduction (Reaction 2):

$$TPN + H_2O + ADP + Pi \xrightarrow{h\nu} TPNH + ATP + O_2 \qquad (1)$$

$$TPN + H_2 + ADP + Pi \xrightarrow{h\nu} TPNH + ATP\ . \qquad (2)$$

At low light intensity, Reaction (2) would be predominant and the oxygen produced by Reaction (1) would be reduced by an oxhydrogen reaction which could produce even more ATP. At higher light intensities the rates of both reactions might increase in the same proportion, but as more oxygen was produced the hydrogenase would gradually be inhibited in an autocatalytic fashion until the alga would revert to photosynthesis.

Reaction (2) is nothing more than a photosensitized reduction. It is well known that certain dyes (chlorophyll in the Krasnovsky reaction, acridine dyes, tetrazolium salts)when they are in an excited state are easily reduced by such reducing agents as ascorbic acid or gluthathione. What we are proposing, then, is that perhaps such a reaction occurs with hydrogen, ATP being generated in the process. This type of mechanism could apply as well to hydrogen bacteria or to anaerobic photosynthetic organisms requiring organic compounds as a source of electrons.

The mechanisms presented above are nothing but speculation--as they are bound to be, given the scarcity of facts we now have. Nevertheless, some of them are subject to experimental test. According to the last mechanism, for instance, oxygen exchange between the water and the gas phase should be minimal under CMU inhibition of CO_2 photofixation in the presence of hydrogen.

12. THE SYNTHESIS OF VERY-HIGH-ACTIVITY C^{14} SUGARS

Karl K. Lonberg-Holm and V. Moses

A batch of very-high-activity C^{14} sugars has been made by the method discovered by Putman.[1] A similar (unreported) preparation was made in 1956. Sucrose was isolated from a young excised Canna indica leaf that has been exposed to $C^{14}O_2$ and light. The leaf is frozen and ground in liquid nitrogen and killed and extracted successively with hot 80% and 20% alcohol. The water-soluble substances are deionized with ion-exchange resins, and then the major product, sucrose, is isolated by repeated chromatography on Whatman 3 M filter paper with phenol-water and butanol—propionic acid—water solvents. Some free glucose and fructose can also be found. The sucrose is inverted enzymatically and the glucose and fructose products are purified by repeated chromatography. The specific activity of the sucrose can be calculated roughly from the weight of the yield, or the inverted products may be assayed by a microdetermination of the sugar.[2] In the recent synthesis the chemical determical determination has not been done yet, but the approximate lower limit of the specific activity determined by weight is high enough to be worth a special report. Details are given in Tables XXII and XXIII.

Since our starting CO_2 contained 43% of the total carbon as C^{14}, 29% of the carbon atoms in the products are C^{14}. The exceptionally high activity of the products must be due to the leaf's having had a very small pool of free sucrose. This may have been due to one of two factors; (a) the individual character of the plant used (it is being saved), or (b) abuse of the plant for a few months prior to the synthesis by frost, desiccation, sub-optimal light, and repeated removal of its youngest leaves.

---

[1] E. W. Putman and W. Z. Hassid, J. Biol. Chem. 196, 749 (1952).

[2] K. K. Lonberg-Holm, in Chemistry Division Quarterly Report, UCRL-3710, March 1957, p. 43.

Table XXII. The dilution of C^{14} during sucrose synthesis

	Experiment	
	1956	1961
Leaf weight (g)	3.9	4.0
Exposure (hr)	18	18.5
$BaCO_3$ used (mg)	377	369
$BaCO_3$ activity (mC)	34	49.3
Sp act. Ba CO_3 (C/mole carbon)	18	26.4
Sucrose yield (mg)	80	33
Sucrose activity (mC)	17.9	20.6
Sp act. sucrose (C/mole carbon)	6.3	17.8

Table XXIII. Starting activity in various fractions (in percent)

	Experiment	
	1956	1961
Total solubles	78	66
"Starch"[a]	7	14
"Amino acids" (Dowex-50 eluate)	6	4
"Organic acids" (Dowex-1 eluate)	2	5
Sucrose	53	42

[a]Soluble after 1 to 1.5 hr; 100°; 0.1 N HCl.

13. THE ISOLATION OF VITAMIN B_6 COMPOUNDS FROM ALGAE

John M. Turner

The name "vitamin B_6" was given by György[1] in 1934, to designate a factor that prevented acrodynia in rats. Since the recognition of this factor, a group of chemically related compounds has been shown to possess vitamin B_6 activity. These compounds are pyridoxine, pyridoxal, pyridoxamine, and their respective 5-phosphates.

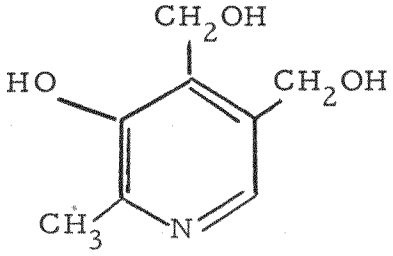

Pyridoxine

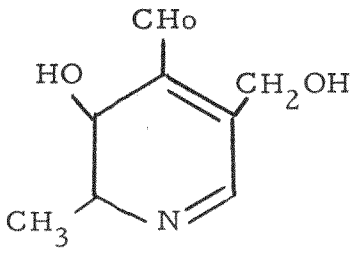

Pyridoxal

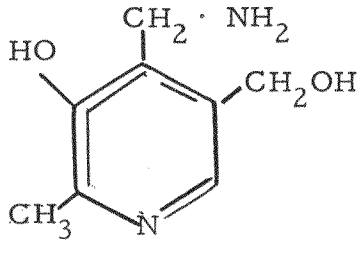

Pyridoxamine

The vitamin function of these compounds depends on their conversion to pyridoxal-5-phosphate, which is the coenzyme of a large number of enzymes involved in amino acid metabolism. The nature, function, and metabolism of vitamin B_6 have recently been reviewed by Snell[2] and Braunstein.[3]

Virtually no information on the biosynthesis of the pyridine ring moiety of vitamin B_6 is available, and it is with this lack in mind that the work reported below has been carried out. Although microbiological assay procedures have been developed for determining the vitamin B_6 content of biological materials, no convenient method exists for their quantitative isolation and assay. The following report describes the development of a chromatographic method for the isolation of pyridoxine, pyridoxal, and pyridoxamine, and a sensitive chemical method of assay.

Experimental Methods

Assay of vitamin B_6 Compounds

Stiller et al.[4] first reported that pyridoxine reacts with 2,6-dichloroquinonechloroimide (DCQCI), to form a blue dye. The reaction is of the

[1] P. György, Nature 133, 498 (1934).

[2] E. E. Snell, Vitamins and Hormones 16, 77 (1958).

[3] A. E. Braunstein, in The Enzymes, Ed. by Boyer, Lardy, and Myrbäck 2nd Ed., Vol. 2 (Academic Press, Inc., New York, 1959), p. 113.

[4] E. T. Stiller, J. C. Keresztesy, and J. R. Stevens, J. Am. Chem. Soc. 61, 1237 (1939).

Gibbs-indophenol type, and is general for vitamin B_6 compounds that are unsubstituted in the 6 position. After the discovery of pyridoxal and pyridoxamine, Melnick et al.[5] reported the use of DCQCI for their colorimetric assay, using pure compounds.

In the work presented here, the finally adopted reaction mixture composition was: vitamin B_6 soln, 1.0 ml; isopropanol, 2.5 ml; NH_4OH/NH_4Cl soln (160 g NH_4Cl in 700 ml H_2O, plus 40 ml conc. NH_4OH, dil. to 1 liter), 1.0 ml; and DCQCI reagent (0.4 g/L isopropanol), 0.5 ml. The course of color development was followed by continuous scanning of absorption in the visible range. Results are summarized in Table XXIV.

Table XXIV. Development, stability, and absorption characteristics of colors produced by vitamin B_6 compounds (50 mμmole) with DCQCI reagent

	Pyridoxine	Pyridoxal	Pyridoxamine
λ max (mμ)	648	640	643
Development time (min:sec)	4:00	10:00	5:00
Period of stability[a] (min:sec)	1:10	11:00	1:30
Max. O.D. @ λ_{max}	0.48	0.66	0.44
Max. O.D. @ 645 mμ	0.47	0.64	0.44

[a]The period of color stability is the time interval during which the absorbancy varies ±2% from the maximum observed.

Construction of calibration curves, using between 10 and 100 mμmole of each vitamin B_6 compound, showed a linear relationship with color density up to 50 mμmoles. If the conditions of color development are made more alkaline, rate of development increase but λ_{max} and absorbancy values remain the same. It is convenient to follow color development at 645 mμ with time in all cases.

Chromatography of vitamin B_6 Compounds

A number of solvent systems are available for the resolution of vitamin B_6 mixtures by paper chromatography. Results obtained are given in Table XXV.

[5]D. Melnick, M. Hochberg, H. W. Hines, and B. L. Oser, J. Biol. Chem., 160, 1 (1945).

Table XXV. Resolution of vitamin B_6 mixtures

Solvent System	Pyridoxine	Pyridoxal	Pyridoxamine	Ref.
1. n-propanol : 10% HCOOH (80:20)	0.70	0.66	0.30	6
2. water : acetone : tert. butanol: diethylamine (20 : 35 : 40 : 5)	0.31	0.64	0.70	7
3. phenol : water (72 : 28)	0.83	0.80	0.55	--
4. butanol : water : propionic acid (64 : 4 : 31 : 7)	0.71	0.90	0.84	--

The positions of spots on paper chromatograms were detected by fluorescence in uv light, and by spraying with DCQCI reagent (1% in benzene) followed by exposure to NH_3 vapor. The use of solvent systems Nos. 1 and 2 and Nos. 3 and 4 gives satisfactory resolution in two-dimensional chromatography.

A number of ion-exchange columns have been described for the isolation of vitamin B_6 compounds, but until recently several such columns were required for the effective resolution of mixtures. Such procedures are complex and time-consuming.[8] In 1959, MacArthur and Lehman described the use of Dowex AG 50W-X8 for the separation of pyridoxine, pyridoxal, and pyridoxamine in one operation.[9] This strongly acidic cation-exchange resin was used in the Na^+ form. Attempts to repeat their work were unsuccessful, even after further information was obtained in which the K^+ resin form was advocated.[10] By modification of the elution buffers, however, a fairly successful method has been developed. A mixture of pure vitamin B_6 compounds was absorbed on the resin at pH 4.5, the column was washed with KH_2PO_4 buffer mixtures, and pyridoxal, pyridoxine, and pyridoxamine successively eluted with buffers ranging from pH 7.0, 0.1 M to pH 8.0, 1.0 M. Eluate was collected in 10-ml fractions; B_6 content was detected by scanning in the uv between 230 and 410 mμ, and assayed by using the previously described DCQCI reagent (see Figs. 68 and 69).

[6] P. Fasella and C. Baglioni, Acta Vitaminol. 10, 27 (1956).

[7] V. W. Rodwell, B. E. Volcani, M. Ikawa, and E. E. Snell, J. Biol. Chem., 233, 1548 (1958).

[8] K. Fujino, Vitamins (Japan) 9, 100 (1955).

[9] M. J. MacArthur and J. Lehmann, J. Assoc. Offic. Agr. Chemists 42, 619 (1959).

[10] E. W. Toepfer (Food Composition Lab., U.S. Dept. of Agric. Washington 25, D.C.) personal communication.

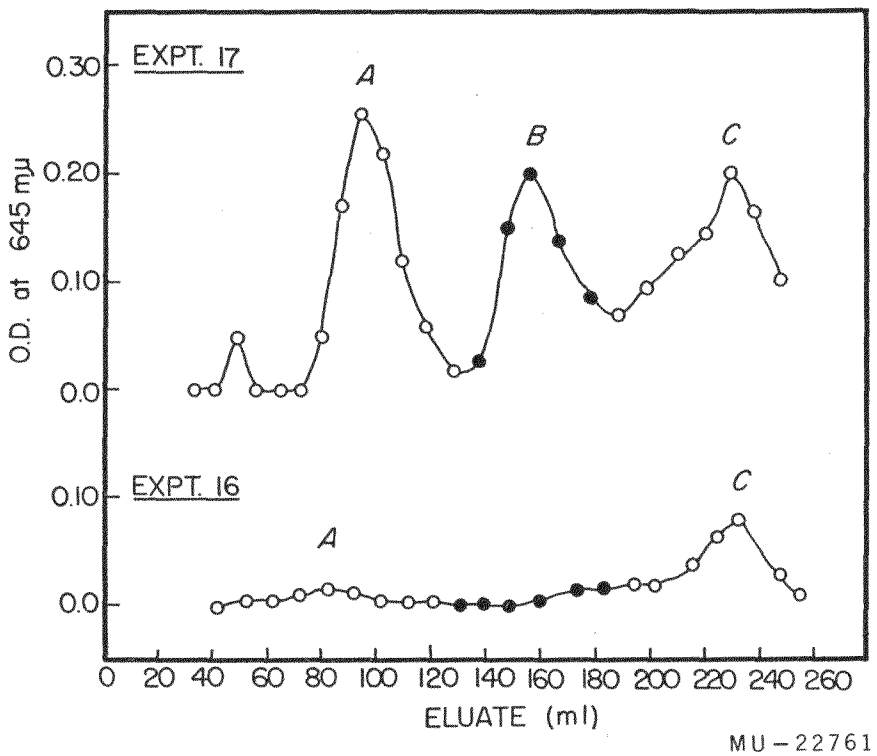

Fig. 68. Elution of vitamin B_6 compounds and algal extract from Dowex column. Algal extract was prepared as described in the text, adjusted to pH 4.5, and divided into two equal aliquots. To one aliquot was added approx 1 μM each of pyridoxal, pyridoxine, and pyridoxamine. After application to Dowex-K^+, each column was washed with 70 ml 0.02 M Kacetate, pH 5.5, and 100 ml 0.04 M Kacetate, pH 6.0. Washings were discarded. Elution was carried out stepwise, using 120 ml 0.10 M Kacetate, pH 7.0, and 130 ml KCl-K_2HPO_4 soln (1.10 M for K^+), pH 8.0. Eluate was collected in approx 10-ml samples.

In Experiment 16, the simple algal extract was used. The vitamin B_6 markers were added in Experiment 17.

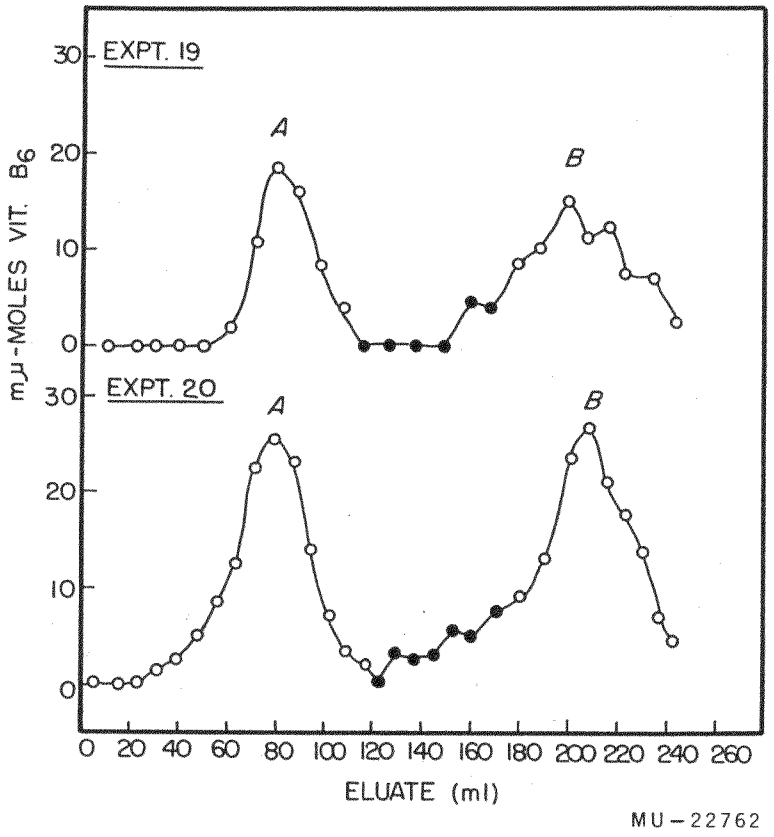

Fig. 69. Elution of algal vitamin B_6 from Dowex column. Procedure was the same as for Fig. 68. No vitamin B_6 markers were present. Experiment 20 involved the use of double the amount of algal extract used in Experiment 19. For further details, see text.

Extraction of Vitamin B_6 from Biological Material

The use of microbiological assay methods has shown that at least 50% of vitamin B_6 exists in bound forms, and that hydrolytic procedures are necessary for its release. The methods described in the literature have been reviewed.[11]

In this work, whole algae, accumulated in the overflow from the "algae farm," are harvested and autoclaved for 2 hr at 125° in 0.055 N H_2SO_4.[12] Enzymic methods for the release of bound vitamin B_6 compounds are now being investigated.

Before it was realized that pyridoxine was not the sole vitamin B_6 compound in nature, solvent extraction was employed for extraction. Thus Green, in 1939, used n-propanol or n-butanol for the continuous extraction of pyridoxine,[13] and Scudi used n-butanol.[14]

A study is now being made of the use of solvents for the concentration of vitamin B_6 compounds from biological materials. The distribution of pyridoxine, pyridoxal, and pyridoxamine between buffers and various solvents has been measured at various pH values. Results are given in Table XXVI.

Results

Paper Chromatography

Ethanolic extracts of Chlorella, heavily labeled with C^{14} from a "steady state" experiment, were chromatographed in the regular solvent systems, with and without added vitamin B_6 markers. Acid-hydrolized extracts were also chromatographed. In no case could endogenous vitamin B_6 compounds be detected by spraying with DCQCI reagent. Spots due to added marker compounds did not correspond to any C^{14} - labeled compound detected by autoradioradiography.

Column Chromatography

Acid hydrolysis of Chlorella cells, harvested by using a Sharples centrifuge, yielded a heavy suspension. After centrifugation to remove coagulated protein and other cell debris, the green supernatant was filtered and neutralized with KOH to pH 4.5. The clear solution was passed down a 53-cm column, containing 50 ml wet-packed 100-200 mesh Dowex AG50W-X8. After washing, elution for vitamin B_6 compounds was carried out as previously described. From each sample of eluate collected (approx 10 ml), 1.5 ml was taken for assay of vitamin B_6, using DCQCI. The formation of color, λ_{max} value, time for maximum color development, etc. were taken as criteria of identity. (With a Cary recording spectrophotometer, an increase in absorbancy of 0.005 unit is the smallest change that can be detected. This

[11] M. J. Woodring, and C. A. Storvick, J. Assoc. Offic. Agr. Chemists, 43, 63 (1960).
[12] J. G. Morris, D. T. D. Hughes, and C. Mulder, J. Gen. Microbiol. 20, 566 (1959).
[13] R. D. Green, J. Biol. Chem. 130, 513 (1939).
[14] J. V. Scudi, J. Biol. Chem. 139, 707 (1941).

Table XXVI. Distribution coefficients between buffer saturated with organic solvent, and solvent saturated with buffer. Buffers were 0.09 M with respect to salts. Final B_6 concentration was 10^{-4} M, and the ratio of organic to aqueous phases was 4 : 1. Equilibration was carried out at 30°.

	Solvent					
	n-butanol			Chloroform		
B_6 Compound	pH 4.0	6.0	10.0	4.0	6.0	10.0
Pyridoxine						
DCQCI method	0.70	0.61	0.19	---	--	--
uv absorption	0.81	0.46	0.23	0.16	0.06	0.03
Pyridoxal						
DCQCI	0.05	0.08	0.20	--	--	--
uv	0.04	0.03	0.25	0.01	0.04	0.04
Pyridoxamine						
DCQCI	0.33	0.42	0.22	--	--	--
uv	0.38	0.41	0.30	0.04	0.02	0.04

corresponds to approx 0.1 mμmole vitamin B_6). The results of the above procedure, using a pair of matched columns and equal amounts of algal hydrolysate to one of which were added vitamin B_6 markers, are shown in Fig. 68. In Expt. 17 the recovery of the markers pyridoxal, pyridoxine, and pyridoxamine is represented by peaks A, B, and C respectively. Peak materials were identified from DCQCI color development characteristics. Experiment 18 involved algal extract alone, equivalent to approx 3.8 (wet wt) Chlorella. Peak C corresponds to approx 36 mμmoles pyridoxamine, i.e., 54 mμ moles/g dry wt algae (dry wt measured as 17.7% wet wt).

The chromatographic isolation of vitamin B_6 from different amounts of algae, using a pair of identical columns, is shown in Fig. 69. In this case, 10.0 g and 20.0 g of freshly harvested algae were used, corresponding to 1.77 and 3.54 g dry weight respectively. Full points on the curves represent the expected position of pyridoxine. In Expt. 19, peak A corresponds to 60 mμmoles pyridoxal, peak B to 74 mμmoles pyridoxamine. In Expt. 20, with double the amount of algae, values of 127 and 317 mμ moles were obtained. These values correspond to 35 and 40 mμmoles/g dry wt Chlorella for pyridoxal and pyridoxamine respectively. The slight color formation in the pyridoxine region corresponds to 6 mμmoles/g dry wt, although this is approaching the limits of measurement. Samples contributing to peak A in Expt. 20 have been combined, concentrated to dryness at reduced pressure, and extracted with four 10-ml samples of n-butanol. After evaporation of the butanol extract to dryness, and taking up the residue in 10 ml water, a 1.5-ml sample was used for color development with DCQCI reagent. The absorption spectrum of the resulting color, after 10 min development, is compared with that of authentic pyridoxal in Fig. 70.

Further tests of the identity of peak materials are in progress. In experiments where a sample of C^{14}-labeled algal extract was chromatographed with added vit. B_6 markers, most of the labeled compounds were washed from the column before elution of pyridoxal with pH 7 buffer.

The use of longer resin columns for improved resolution of Vit. B_6 mixtures is being investigated.

Conclusions

The use of column chromatography for the isolation of vitamin B_6 compounds, and the development of a sensitive chemical assay, promise to be convenient tools for a study of vitamin biosynthesis. Refinements of the extraction procedures, column conditions etc., are being investigated.

Values for the total vitamin B_6 content obtained by using Chlorella are of the same order as those obtained by using other green plant materials and microbiological assay methods.[15] The differing ratios of pyridoxamine and pyridoxal observed in Expt. 16 and Expts. 19 and 20-- i.e., approx. 1.2 and 7.5-- may reflect different metabolic states at the time of harvesting. Thus relatively higher amounts of pyridoxal could result from oxidation of the amine form.

[15] J.C. Rabinowitz and E.E. Snell, J. Biol. Chem. 176, 1157 (1948).

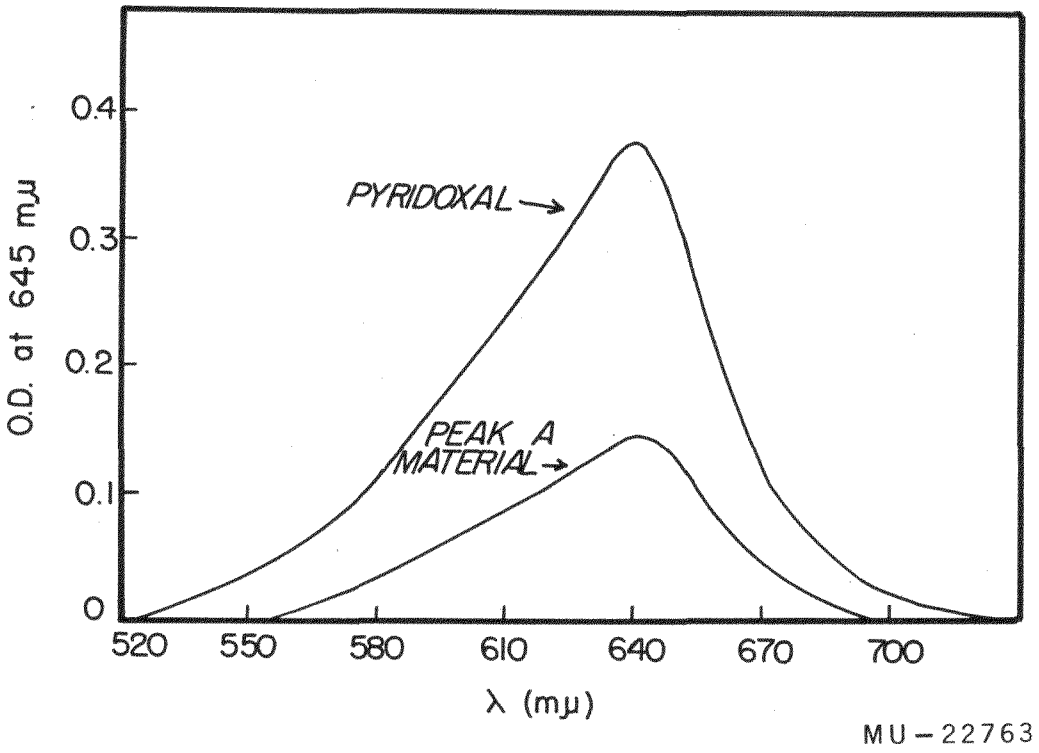

Fig. 70. Absorption spectra of peak A material and pyridoxal with 2, 6-dichloroquinonechloroimide.
The procedures for concentrating peak A material and for developing color with DCQCI reagent are described in the text. Approx 30 mμmole authentic pyridoxal was used.

E. BIOCHEMISTRY

1. PYRIDOXAL PHOSPHATE BREAKDOWN BY AN ALKALINE PHOSPHATASE PREPARATION

John M. Turner

Pogell has demonstrated the presence of phosphatase activities for pyridoxal and pyridoxamine phosphates in rabbit liver fractions.[1] Wada et al. have also demonstrated the breakdown of pyridoxal and pyridoxine phosphates in rabbit liver preparations.[2] Roberts, Rothstein, and Baxter have obtained results indicating the presence of pyridoxal phosphate phosphatase activity in brain tissue,[3] and these results have been confirmed by Begum and Bachhawat, who suggest that a nonspecific acid phosphatase is involved.[4] Evidence for pyridoxal phosphate destruction in Neurospora crassa extracts has been obtained by Wainwright,[5] and for pyridoxamine phosphate breakdown in the fungus Ophiostoma multiannulatum by Wikberg.[6] The latter author has suggested that an acid phosphatase is involved. Turner and Happold have demonstrated pyridoxal phosphate phosphatase activity in Escherichia coli extracts.[7] Using direct spectrophotometric methods for the assay of activity, they suggest that an alkaline phosphatase is involved.

The following report presents evidence that pyridoxal phosphate, also pyridoxamine phosphate, is readily hydrolized by purified alkaline phosphatase preparations.

Alakline phosphatase preparations may be of use for converting phosphorylated forms of vitamin B_6 (pyridoxal, pyridoxamine, and pyridoxine) to their free bases, prior to the isolation of the vitamin from biological material.

---

[1] B.M. Pogell, J. Biol. Chem. 232, 761 (1958).

[2] H. Wada, T. Morisue, Y. Nishimura, Y. Morino, Y. Sakamoto, and K. Ichihara, Proc. Japan Acad. 35, 229 (1959).

[3] E. Roberts, M. Rothstein, and C.F. Baxter, Proc. Soc. Exptl. Biol. Med. 97, 796 (1958).

[4] A. Begum and B.K. Bachhawat, Ann. Biochem. and Exptl. Med. (Calcutta) 20, 143 (1960).

[5] S.D. Wainwright and D.M. Bonner, Can. J. Biochem, 37, 741 (1959).

[6] E. Wikberg, Physiol. Plantarum 13, 616 (1960).

[7] J.M. Turner and Frank C. Happold, Biochem. J., 78, 364 (1961).

Experimental Procedure

Materials

Alkaline phosphatase

An "intestinal phosphatase" preparation, of bovine origin, was obtained from Armour Laboratories, Chicago, Illinois. A similar preparation was obtained for purposes of comparison, from Worthington Biochemical Corp., Freehold, New Jersey.

Chemical compounds

Pyridoxal and pyridoxamine phosphates, also pyridoxal and p-nitrophenyl phosphate, were obtained from California Corporation for Biochemical Research, Los Angeles, California. Versenol, i.e., n-hydroxyethyl-ethylene-trisodium acetate, was obtained from Bersworth Chemical Company, Framingham, Massachusetts.

Assay of Phosphatase Activities

Pyridoxal phosphate as substrate

The standard composition of reaction mixtures was: buffer, 0.04 M Veronal, pH 8.9, in 2.0 ml; enzyme preparation 0.1 mg protein in aqueous solution, 0.1 ml; pyridoxal phosphate, 0.4 μM in 0.4 ml; and water or additions to give a total volume of 4.0 ml. All reactions were carried out at 37° for 4 min unless otherwise stated. Reactions were stopped by the addition of 0.5 ml 2.5 N NaOH, and absorption values were read in uv light at 390 and 300 mμ, i.e., λ_{max} values for substrate and product against the appropriate blanks. A Cary Recording Spectrophotometer Model 14 was used. The amounts of pyridoxal phosphate and of the free base present were calculated as described by Turner and Happold.[7] At the pH of 0.28 N NaOH i.e., approx. pH 13-- $E^{300}_{\text{pyridodoxal}} = 7000$; $E^{390}_{\text{pyridoxal}} = 800$; $E^{300}_{\text{pyridoxal phosphate}} = 1200$; and $E^{390}_{\text{pyridoxal phosphate}} = 6300$. From these measured values, one can show

$$[\text{pyridoxal phosphate}] = (1.63\, E^{1\text{ cm}}_{390} - 0.19\, E^{1\text{ cm}}_{300}) \times 10^{-4}\ M,$$

$$[\text{pyridoxal}] = (1.48\, E^{1\text{ cm}}_{300} - 0.28\, E^{1\text{ cm}}_{390}) \times 10^{-4}\ M.$$

Thus, by use of controls in which water replaces substrate, the absolute amounts of pyridoxal and its phosphate also can be calculated. For example, with a standard solution containing pyridoxal phosphate and pyridoxal in 0.28 N NaOH, where each component was 0.50×10^{-4} M, the $E^{1\text{ cm}}$ values at 300 and 390 mμ were found to be 0.405 and 0.358 respectively. By substitution of these values in the above equations, the respective concentrations of pyridoxal phosphate and pyridoxal are calculated as $0.51 \times$ and 0.50×10^{-4} M.

In practice, it is convenient to use controls in which substrate or enzyme is added after the NaOH. If absorption values are read at 300 mμ with the control used as blank, and the control itself is read at 390 mμ, with the stopped reaction mixture used as blank, then the changes in both substrate and product concentrations can be calculated. A simple expression can be derived with which it is possible to calculate the mean amounts of substrate utilized and product formed. Thus, for a stopped reaction mixture having the composition above,

$$\text{Mean, } \Delta \text{ substrate and } \Delta \text{ product} = 0.304\ \Delta E^{1\text{ cm}}_{390} + 0.290\ \Delta E^{1\text{ cm}}_{300}\ \mu\text{mole.}$$

Pyridoxamine phosphate and p-nitrophenyl phosphate as substrates

Reaction-mixture composition was the same as with pyridoxal phosphate as substrate except that 2.0 μM substrate was used. The higher substrate concentration was necessary owing to greater reaction velocities with the above compounds. After incubation at 37°, reactions were stopped by the addition of NaOH. Phosphatase activity was measured by the assay of inorganic phosphate, according to the method of Gomori (1941-2).[8] A Beckman DU spectrophotometer was used for absorption measurements at 675 mμ. In a number of experiments with p-nitrophenyl phosphate, this compound was directly substituted for pyridoxal phosphate in the procedure previously described. The absorption of stopped reaction mixtures was read at 400 mμ, with use of the appropriate blank.

Units of activity

Activities are expressed in terms of μM per mg protein per unit time employed. Protein concentrations were determined by a quantitative biuret procedure. If the protein concentration was not accurately measured, activities are expressed as μM change under the conditions described.

Results

pH Optimum for Pyridoxal Phosphate Breakdown

Preliminary experiments showed the pH optimum to be in the range 8 to 10. Veronal buffers (Britton and Robinson[9]) were used in the range 8 to 9, and carbonate-bicarbonate buffers (Delory and King[10]) between 9 and 10. The pH optimum was found to be approx 8.9. The results are illustrated in Fig. 71. It was concluded that Ammediol (2-amino-2-methyl-1, 3-propanediol) buffers (Holmes[11]) should not be used in the range 8 to 10,

[8] G. Gomori, J. Lab. Clin. Med. 27, 955 (1941).

[9] H. T. S. Britton and R. A. Robinson, J. Chem. Soc. 1456 (1931).

[10] G. E. Delory and E. J. King, Biochem. J. 39, 245 (1945).

[11] W. Holmes, Anat. Record 86, 163 (1943).

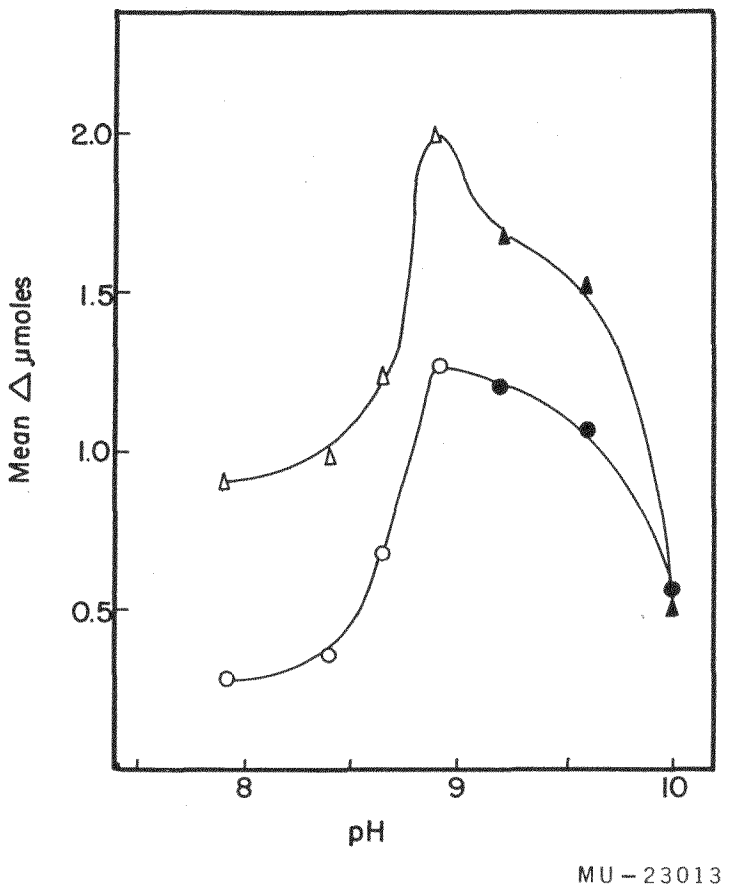

Fig. 71. Effect of pH on pyridoxal phosphate breakdown. Reaction mixtures contained 2.0 ml of 0.04 M buffer; 0.1 ml of approx. 1 mg/ml enzyme solution; 0.4 ml pyridoxal phosphate solution, i.e., containing 0.4 μM; 1.5 ml water or $MgSO_4$ solution. Reactions carried out at 37° for 4 min, then stopped by the addition of 0.5 ml 2.5 N NaOH. Absorption values were read at 300 and 390 mμ, using blanks which contained water in place of substrate. The concentrations of pyridoxal and pyridoxal phosphate present were calculated as described in the text. These values are expressed as the mean of pyridoxal phosphate utilized and free pyridoxal formed. The lower curve represents pyridoxal phosphate breakdown in the presence of 0.2×10^{-2} M $MgSO_4$. Open points (○ and △) indicate results using Veronal buffers. Solid points (● and ▲) indicate the use of Na_2CO_3 - $NaHCO_3$ buffers.

because of differences observed in the absorption spectra of both pyridoxal and pyridoxal phosphate when plotted at pH 10 with Ammediol rather than carbonate-bicarbonate buffer.

Effect of Substrate and Enzyme Concentrations

With use of the standard reaction mixture composition, initial rates of pyridoxal phosphate breakdown at 37° were found to be proportional to the amount of enzyme up to a value of at least 0.16 mg/4 ml. Under similar conditions, with 0.10 mg enzyme, substrate utilization was linear with time up to approx 8 min, and reaction rates remained constant at substrate concentrations above approx 0.5×10^{-4} M, i.e., 0.2 μM per 4 ml (see Table XXVII). At an enzyme concentration of 0.3 mg/4 ml, the variation of substrate concentration between 0.2× and 1.7×10^{-4} M gave a double reciprocal plot (Lineweaver and Burk[12]) indicating a K_m value of approx 0.5×10^{-4} M (see Fig. 72). With p-nitrophenyl phosphate as substrate, and with exactly the same conditions and a similar spectrophotometric assay procedure, a K_m value of approx 0.6×10^{-4} M was obtained.

Effect of Magnesium Ions and Versenol

Magnesium ions were found to increase phosphatase activity when pyridoxal phosphate was used as substrate. The optimum Mg^{2+} ion concentration was found to be approx 0.2×10^{-2} M. (see Table XXVIII). At this concentration, the rate of pyridoxal phosphate breakdown was increased 56%. The pH optimum for phosphatase activity, measured in the presence of Mg^{2+} ions, was the same as that observed in their absence (see Fig. 71).

The metal-chelating agent Versenol (n-hydroxyethyl-ethylene-diamine-trisodium acetate) inhibited pyridoxal phosphate breakdown at all concentrations used, without preincubation with the enzyme (see Table XXVIII).

Effect of Various Compounds on Pyridoxal Phosphate Phosphatase

Pyridoxamine phosphate was found to behave as a competitive inhibitor of pyridoxal phosphate breakdown. Variable inhibitor concentrations were used with two different substrate concentrations, and the breakdown of pyridoxal phosphate was measured spectrophotometrically by the previously described method. Control experiments showed that the possible simultaneous breakdown of inhibitor did not cause any change in absorption at the wave lengths used for the assay procedure. The simple graphical method of Dixon[13] was used to obtain the inhibition constant directly, without calculation; a value of Ki = $p.5\times10^{-4}$ M was found (see Fig. 73). K_m values were also obtained from Fig. 73 by virtue of the fact that the extrapolation of each linear plot cuts the base line at a value of i equal to $-Ki\left(\frac{s}{K_m}+1\right)$ (Dixon and Webb[14]). The K_m values thus derived were 0.8× and 0.6×10^{-4} M. At the higher substrate concentration, and equivalent concentration of

[12] H. Lineweaver and D. Burk, J. Am. Chem. Soc. 56, 658 (1934).

[13] M. Dixon, Biochem. J. 55, 170 (1953).

[14] M. Dixon and E.C. Webb, in Enzymes (Academic Press, Inc., New York, 1958).

Table XXVII. Effect of substrate concentration on pyridoxal phosphate breakdown

The reaction mixtures were of the standard composition described in the text except that substrate concentration was varied as indicated. In each case, 0.1 mg enzyme was present (cf Fig. 72), and incubation was for 4 min at 37°.

Initial substrate concentration (10^4 M)	$\Delta E^{1\text{ cm}}$ 390 mμ	$\Delta E^{1\text{ cm}}$ 300 mμ	Substrate utilized (μmole/mg protein)	Mean Δ substrate and product (μmole/mg protein)
0.28	0.070	0.073	0.45	0.43
0.50	0.090	0.092	0.57	0.54
0.75	0.095	0.100	0.61	0.58
1.00	0.092	0.094	0.59	0.55
1.25	0.085	0.092	0.54	0.53
2.25	0.083	0.103	0.52	0.55

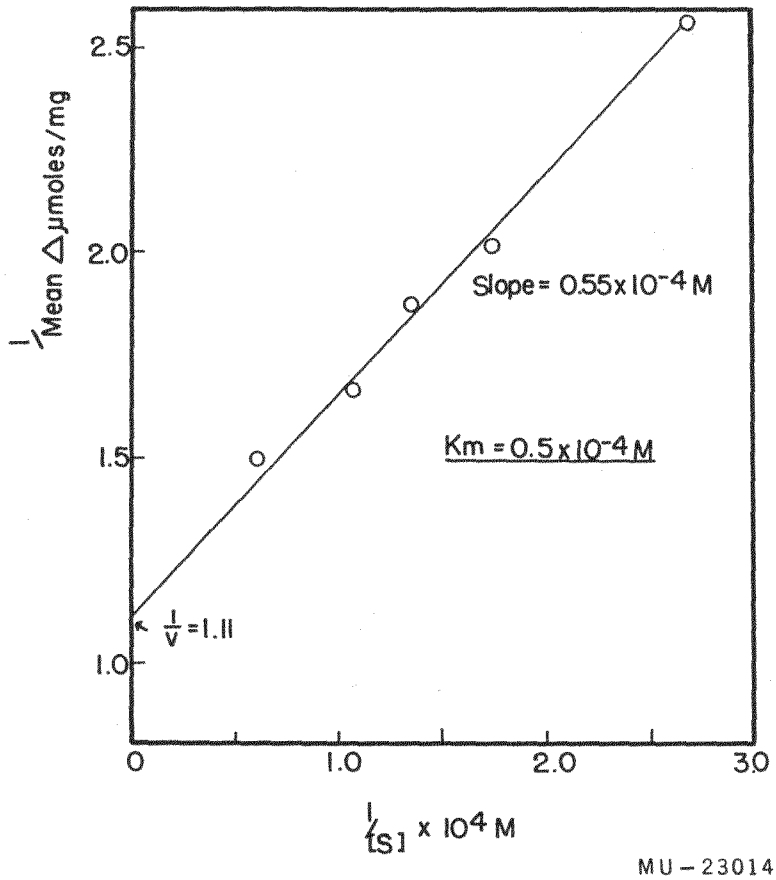

Fig. 72. Effect of substrate concentration on pyridoxal phosphate breakdown. Reaction mixture composition was as described for Fig. 71, except that 0.3 mg enzyme was present, and initial substrate concentration varied as indicated. No metal ions were added. Reaction rates were calculated as described in the text.

Table XXVIII. Effect of magnesium ions, also Versenol, on the hydrolysis of pyridoxal phosphate

Standard reaction mixture composition and conditions were used, and results were calculated as described in the text. In the Mg^{2+} ion experiments, the reaction was started by the addition of substrate, $MgSO_4$ solution and enzyme being allowed to preincubate in buffer for approx 30 min. For Versenol, reactions were started by the addition of enzyme, and no preincubation of of these two components occurred. The Mg^{2+} ion and Versenol experiments were carried out on separate occasions.

Addition	Concentration of addition (M)	Mean Δ substrate and product (μmole)	Activity (%)
Mg^{2+} ions	0	0.108	100
	0.2×10^{-1}	0.144	133
	0.2×10^{-2}	0.168	156
	0.2×10^{-3}	0.148	137
	0.2×10^{-4}	0.134	124
Versenol	0	0.073	100
	0.27×10^{-3}	0.044	60
	0.47×10^{-3}	0.035	48
	0.67×10^{-3}	0.012	17
	0.20×10^{-2}	0.006	8

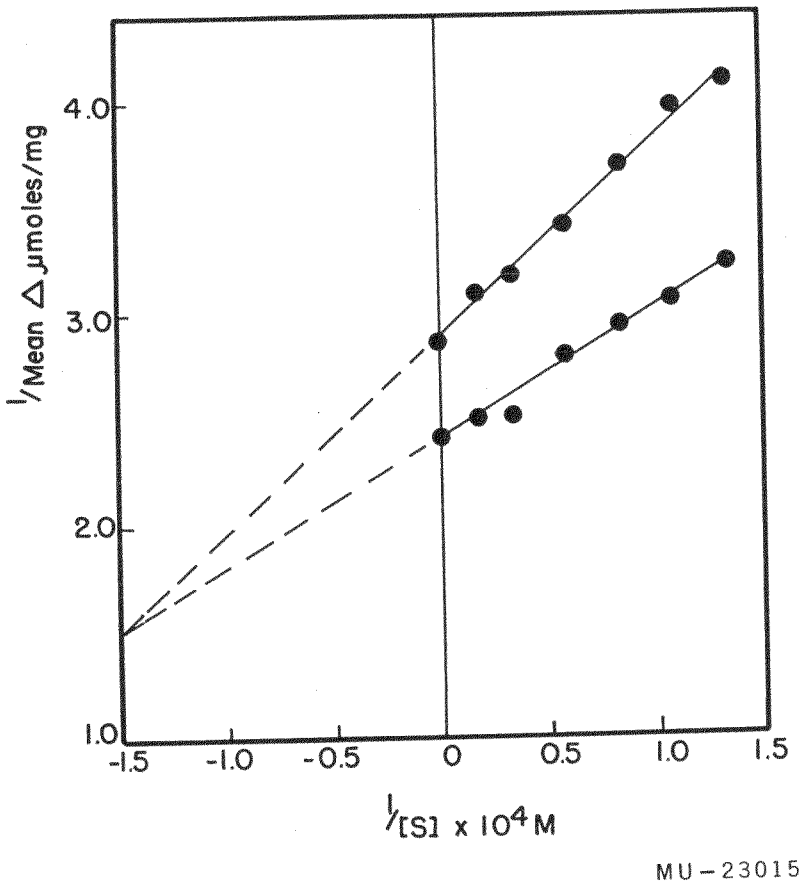

Fig. 73. Effect of pyridoxamine phosphate on phridoxal phosphate breakdown. Reactions were carried out under the standard conditions previously described, with inhibitor concentrations shown. The two substrate concentrations used were 0.67×10^{-4} M (lower plot) and 1.33×10^{-4} M.

pyridoxamine phosphate caused 25% inhibition, at the lower concentration, 18% inhibition.

Under similar conditions pyridoxal had no inhibitory effect on pyridoxal phosphate breakdown when used at concentrations between 0.25× and 1.66× substrate concentration, i.e., 10^{-4} M.

Inorganic orthophosphate inhibited pyridoxal phosphate hydrolysis competitively; the value of Ki was determined, by the method of Dixon,[13] as approx 0.6×10^{-4} M. Under standard reaction conditions, with substrate at a concentration of 10^{-4} M, an equivalent amount of inorganic phosphate caused 43% inhibition.

No effect of NH_4^+ ions on pyridoxal phosphate phosphatase activity could be detected at concentrations between approx 0.17 and 1.66 times the substrate concentration, i.e., 10^{-4} M.

Pyridoxamine Phosphate as Substrate of Alkaline Phosphatase

It was not possible to investigate the breakdown of pyridoxamine phosphate spectrophotometrically. The spectra of the free base and its phosphate ester are similar at all pH values. Accordingly, rates of hydrolysis were measured by assay of the inorganic phosphate produced. The composition of reaction mixtures is described under Experimental Procedure.

Preliminary experiments showed that rapid hydrolysis of pyridoxamine phosphate was catalyzed by the alkaline phosphatase preparation, and that the pH optimum was approx 8.9. A direct comparison of the rates of hydrolysis of pyridoxamine and pyridoxal phosphates showed that the former was approx 1.5 times the latter. Similar ratios, i.e., 1:5 and 1:2, were observed by Pogell[1] using rabbit liver fractions. These results, together with those obtained by using p-nitrophenyl phosphate as a standard, are given as Expt. 1 in Table XXIX.

Specificity of Phosphatase Action

To determine whether or not the same species of enzyme was responsible for the hydrolysis of pyridoxal, pyridoxamine, and p-nitrophenyl phosphates, experiments were carried out using all three substrates, both singly and in pairs. The results are given as Expt. 2 in Table XXIX. Relative reaction velocities for the three substrates were also determined by using an alternative preparation of alkaline phosphatase (Worthington Biochemical Corp.). Preliminary experiments showed that this sample of the enzyme had an absolute requirement for Mg^{2+} ions, and also suggested a lower pyridoxal phosphate phosphatase activity than p-nitrophenyl phosphate. The results of an experiment to determine relative reaction velocities with each enzyme preparation in the presence of Mg^{2+} ions are given in Table XXX.

Table XXIX. Comparative rates of hydrolysis of pyridoxal, pyridoxamine and p-nitrophenyl phosphates

In Experiment 1, the reaction mixture composition was that specified for the assay of phosphatase activity using pyridoxamine phosphate as described in Experimental Procedure. In Experiment 2, however, only 1.5 μM of each substrate was used. Approx 0.1 mg protein was used in each case. To each 4.5 ml of stopped reaction mixture was added 1.25 ml of approx N H_2SO_4, and water to 8.0 ml. Inorganic phosphate was then measured by the method of Gomori (Ref 8). The colorimetric blanks were the controls in which NaOH was added to reaction mixtures before the substrate. A KH_2PO_4 solution was used as standard.

Substrate	Inorganic phosphate formed (μM) after time interval shown 2.5 min	5 min	10 min	Relative reaction velocity (initial)
Experiment 1				
Pyridoxamine phosphate	0.07	0.14	0.22	0.64
Pyridoxal phosphate	0.045	0.09	0.14	0.41
p-Nitrophenyl phosphate	0.11	0.19	0.31	1.00
Experiment 2				
Pyridoxamine phosphate	0.10	-	-	0.67
Pyridoxal phosphate	0.06	-	-	0.40
p-Nitrophenyl phosphate	0.15	-	-	1.00
Pyridoxamine & pyridoxal phosphates	0.06	-	-	0.40
Pyridoxal & p-nitrophenyl phosphates	0.06	-	-	0.40
Pyridoxamine & p-nitrophenyl phosphates	0.12	-	-	0.80

Table XXX. Relative reaction rates for pyridoxal, pyridoxamine, and p-nitrophenyl phosphates with different enzyme preparations

The reaction mixture composition and assay procedure used were the same as described for Table XXIX. Approx 0.1 mg enzyme protein and 2.0 μM substrate were used and the concentration of Mg^{2+} ions was 0.2×10^{-2} M in each case. The source of the enzyme preparations used is indicated by the manufacturer's name.

Substrate	Inorganic phosphate formed (μM) after time interval shown				Relative reaction velocity (initial) Enzyme preparation	
	Enz. A, Armour		Enz. B, Worthington			
	2.5 min	5 min	2.5 min	5 min	A	B
Pyridoxamine phosphate	0.10	0.23	0.11	0.25	0.67	0.73
Pyridoxal phosphate	0.06	0.14	0.05	0.12	0.40	0.33
p-Nitrophenyl phosphate	0.15	0.33	0.15	0.34	1.00	1.00

Discussion

In schemes summarizing vitamin B_6 metabolism (Snell[15] and Braunstein[16]), the hydrolysis of both pyridoxal and pyridoxamine phosphates by phosphatase action has been postulated. No evidence, however, has been published concerning the nature and specificicity of the phosphatases involved. Whereas most enzyme reactions involved in vitamin B_6 metabolism appear to be specific for the heterocyclic ring moiety of the vitamin, the oxidation of pyridoxal to 4-pyridoxic acid has been shown to be catalyzed by the broadly specific mammalian enzyme aldehyde oxidase (Schwartz and Kjeldgaard[17]). From the results presented here, it appears that alkaline phosphatases of apparently broad specificity are involved in vitamin B_6 metabolism. Results obtained by using pairs of mixed substrates (Table XXIX), in which the observed activity was in all cases less than the sum of the individual activities, suggests that a mixture of narrowly specific phosphatases is not involved. The competitive inhibition by pyridoxamine phosphate of pyridoxal phosphate breakdown also supports this view. The slightly different relative reaction velocities observed when different sources of phosphatase preparation were used may mean that each preparation is a mixture of enzymes, each with comparatively broad but quantitatively different specificity.

The K_m value of 0.5×10^{-4} M for pyridoxal phosphate, compared with the value of 0.6×10^{-4} M for p-nitrophenyl phosphate measured under identical conditions, appears to be of the same order as K_m values for other naturally occurring substrates as reported in the literature, although such comparison is difficult because of the influence of pH, buffers, etc. (Roche[18]). Activation by Mg^{2+} ions and inhibition by metal-chelating agents and orthophosphate are common phenomena with mammalian alkaline phosphatases (Roche[18]). The apparent activation by pyridoxal phosphate hydrolysis by NH_4^+ ions, observed by Pogell[1] using Escherichia coli extracts, could not be demonstrated in this work. Nor was the inhibition of phosphatase activity by NH_4^+ ions as reported by Aebi[19] and Motzok and Wynne.[20]

---

[15] E.E. Snell, in Vitamins and Hormones, 16, Ed. by R.S. Harris, G.F. Marrian, and K.V. Thimann (Academic Press Inc., New York, 1958), p. 78.

[16] A.E. Braunstein, in The Enzymes, Vol. 2, Ed. by Boyer, Lardy, and Myback (Academic Press Inc., New York, 1960), p. 113.

[17] R. Schwartz and N.V. Kjeldgaard, Biochem. J. 48, 333 (1951).

[18] J. Roche, in The Enzymes, Vol 1, part 1, Ed. by Sumner and Myrback (Academic Press, Inc., New York, 1950), p. 473.

[19] H. Aebi, Helv. Chim. Acta 32, 464 (1949).

[20] I. Motzok and A.M. Wynne, Biochem. J. 47, 187 (1950).

The possible role of a phosphatase for the coenzyme pyridoxal phosphate in the control of amino acid metabolism has previously been pointed out (Turner and Happold[7]). The role of pyridoxal catalysis in the control and integration of nitrogen metabolism has been discussed by Braunstein.[21]

Summary

1. An intestinal phosphatase preparation, of bovine origin, was found to hydrolize pyridoxal phosphate. At a substrate concentration of 10^{-4} M, the pH optimum is approx 8.9, and at this pH value the K_m is approx 0.5×10^{-4} M. The K_m value measured under identical conditions for p-nitrophenyl phosphate, a commonly used substrate for alkaline phosphatase assays, was found to be 0.6×10^{-4} M.

2. Phosphatase activity was increased by Mg^{2+} ions, the optimum concentration being approx 0.2×10^{-2} M. The presence of Mg^{2+} ions did not affect the pH optimum. Versenol inhibited activity at all concentrations used. Both pyridoxamine phosphate and inorganic orthophosphate inhibited pyridoxal phosphate breakdown competitively, the Ki values being $1.5 \times$ and 0.6×10^{-4} M respectively. Neither pyridoxal nor NH_4^+ ions affected phosphatase activity.

3. The enzyme preparation also hydrolized pyridoxamine phosphate at a pH optimum of 8.9. With the rate of hydrolysis of p-nitrophenyl phosphate used as a standard, the relative reaction velocities for pyridoxal and pyridoxamine phosphates were approx 0.41 and 0.64 respectively. With an alternative preparation of alkaline phosphatase, similar relative reaction rates were observed.

[21] A. E. Braunstein, in Proc. IVth Internatl. Cong. Biochem, Vienna, vol 14 (Trans. of the Plenary Sessions), p. 63. Pergamon Press, London, (1959).

2. A NEW RAPID SAMPLER TO BE USED WITH SUSPENSIONS OF ISOTOPICALLY LABELED CELLS

Karl K. Lonberg-Holm

A new rapid sampler has been constructed to be used in further studies of the transient metabolic behavior of cells in suspension. As in earlier studies,[1] starved cells are to be fed glucose and samples are to be removed at short intervals thereafter. The ultramicro quantities of glycolytic intermediates in these samples may be measured, since the cells will either be labeled with $P^{32}O_4$ or fed C^{14} glucose of high specific activity.

The new sampler works on a different principle from the one that was used previously.[2] In practice it has proved to be more complicated and difficult to use. With it, however, samples have been taken at 0.7-sec intervals, or twice as fast as was possible before.

In principle, the sampler (Figs. 74 and 75) is a small water aspirator made of lucite. The jet (a) is 0.028 in. in diameter and the inlet (b) is 0.18 in. Water passing through the jet under pressure (20 to 50 psi, adjustable) sucks some of the cell suspension (c) along with it into a tube of hot 80% ethanol under the sampler. Depending upon the conditions, up to 20% of the effluent volume has come through inlet (b).

The aspirator is at the end of a hollow steel tube (d) which is rotated by a belt drive on a wheel (e). As (d) rotates, it also turns a cylinder of lucite (f), from which impellers project into the suspension. The impeller is moved by a set screw that projects into a slot, and thus (d) and the aspirator are free to move up and down while turning. The cell suspension is held inside a temperature jacket (j) by a teflon cup (i) which is pulled down against the glass jacket to make a tight seal.

A valve arrangement (g) in the upper supporting plate permits water to flow through the aspirator only when it is in the down position. The aspirator is pushed down (against spring tension) by a 15-lb-thrust solenoid (h) whenever a sample is to be taken. The valve should open just before the aspirator inlet dips below the cell suspension, and down position should be so adjusted that the inlet does not go below the edge of the teflon cup at the bottom of the chamber. The valve (g) is scavenged above and below by aspiration to safeguard against water leakage into the reaction. An O ring is also compressed around the bottom of the aspirator to guard against leakage.

The length of time during which the solenoid fires (and during which a given sample is ejected) is adjustable down to about 0.1 sec (plus or minus one or two cycles). This is done with a thyrotron circuit designed by and built with the assistance of Frank Upham and John Mendez. When the solenoid

[1] K. K. Lonberg-Holm, in Chemistry Division Quarterly Report, UCRL-8141, Dec. 1957.

[2] K. K. Lonberg-Holm, in Chemistry Division Quarterly Report, UCRL-3415, June 1956.

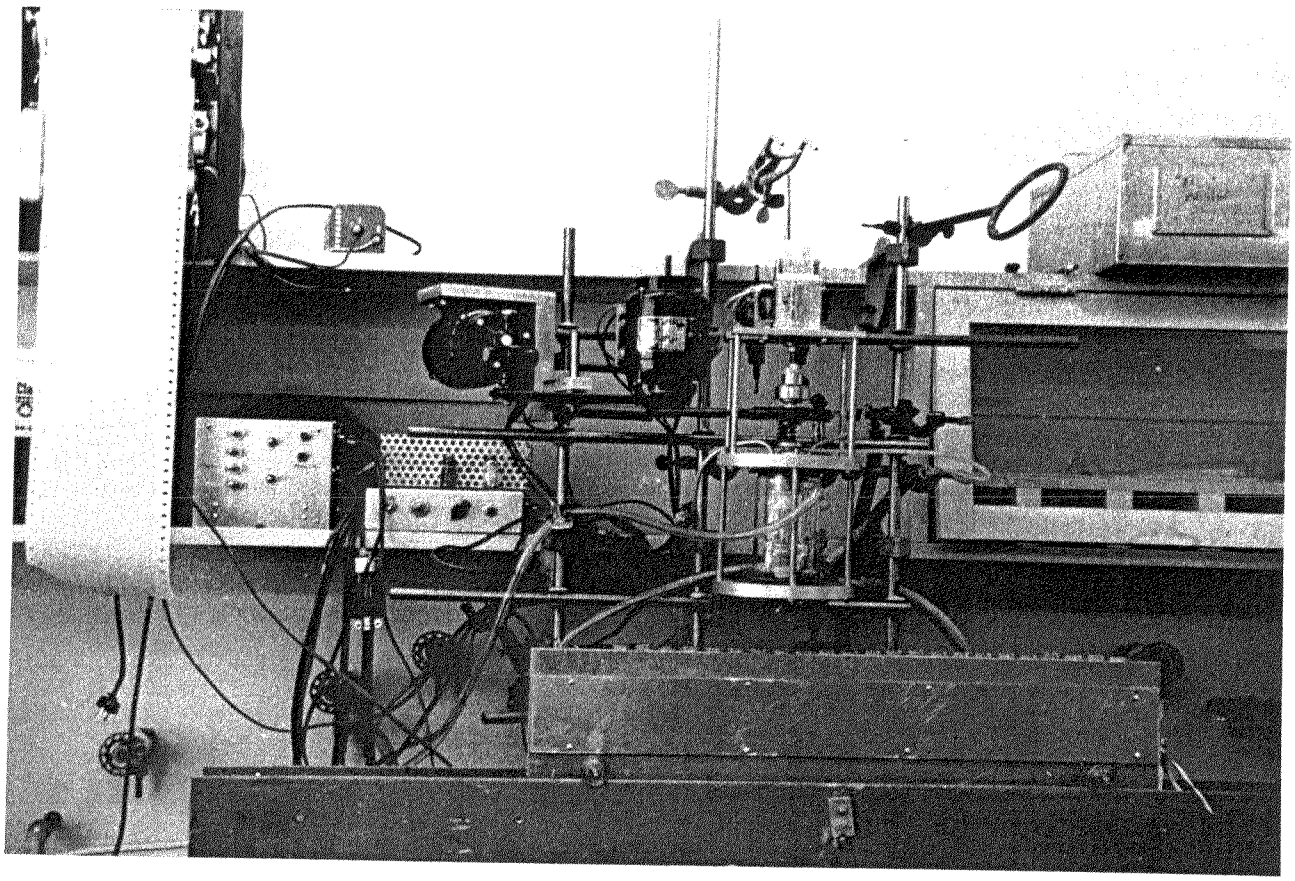

ZN-2784

Fig. 74. Rapid sampler.

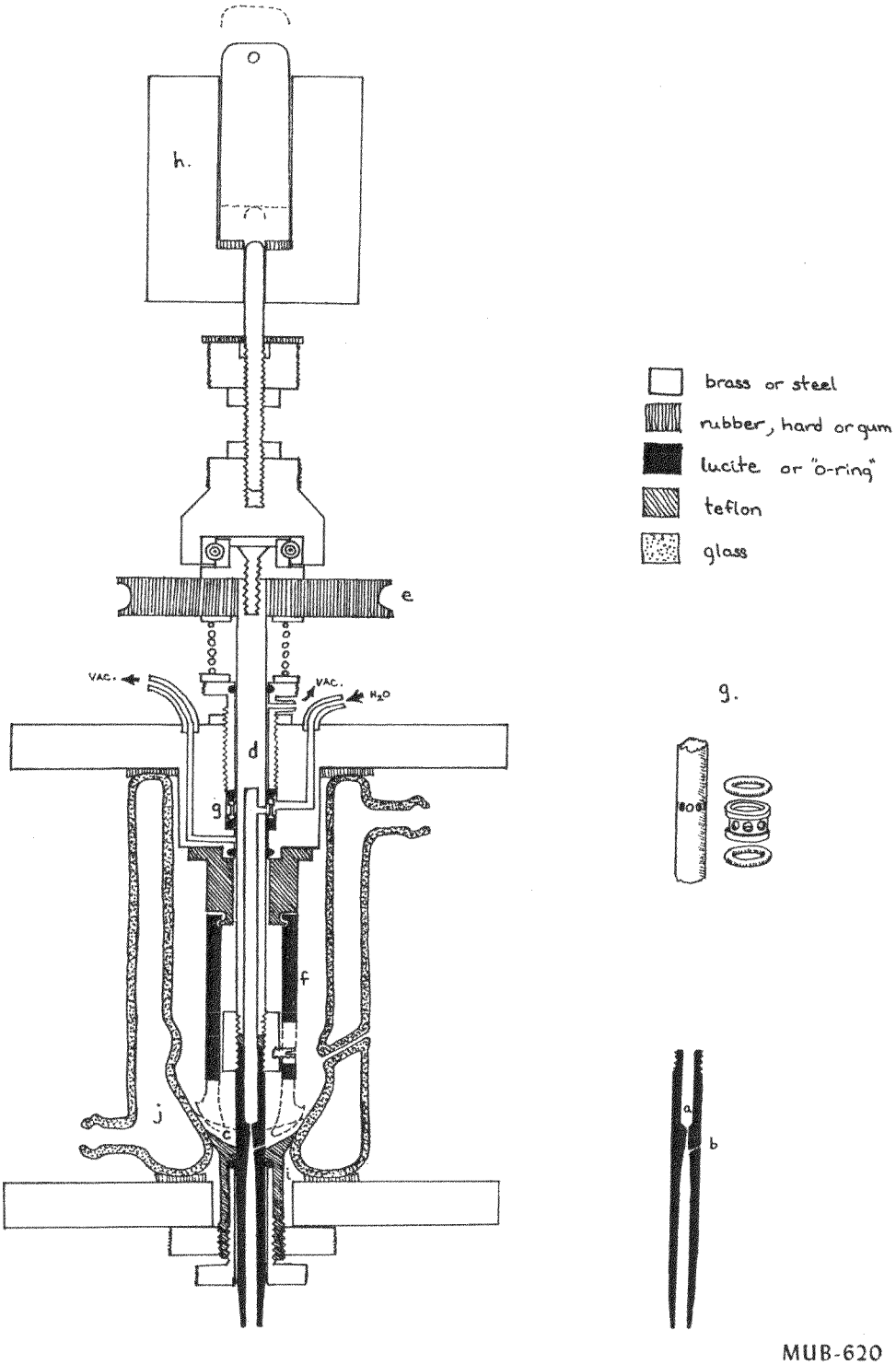

Fig. 75. Detail of rapid sampler.

is fired, a small current is also taken to an Angus recorder on fast drive, and serves to make a permanent time record.

The experiment is run as in the past with inlets into the chamber for gassing, adding the cell suspension, and adding substrate. The arrangement of the recorder, control panel, thyrotron circuit, and sampler is seen in the photograph from left. Also seen is the collecting block, which is made from aluminum and heated electrically. It is driven by direct gear drive from underneath. A machine screw projecting in back of each tube hole fires a microswitch which in turn fires the thyrotron and the solenoid.

The pressure of the water used is regulated by a standard plumber's reducing valve. The water is passed through a 1-in. - diam mixed-bed ion-exchange column before entering the sampler. This seems to cause a drop in effluent pressure by limiting flow during times when many samples are taken in rapid succession, and in the future several columns in parallel will be tried.

The sampler has been used with moderate success. The sample size has varied by 50% during runs, but improvements such as the one mentioned above should decrease this variation. It is too soon to say whether the results obtained in these experiments substantiate those reported in 1957.

I wish to thank Loren Cadra for helping me with the more difficult parts of the machine work and also for helpful discussions on the design.

3. THE MECHANISM OF OXIDATIVE PHOSPHORYLATION

John A. Barltrop

The most effective known process that couples the energy-yielding and the energy-consuming activities of the cell is oxidative phosphorylation. In the oxidation, a pair of electrons, abstracted from a suitable substrate, is passed through an organized sequence of redox coenzymes to molecular oxygen, the over-all effect being the oxidation of the substrate by oxygen. In outline, this may be represented schematically as shown.*

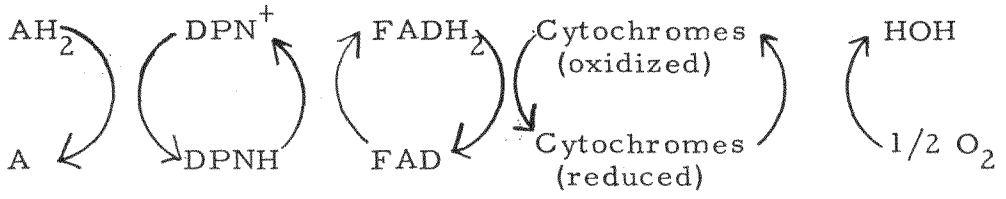

The passage of this pair of electrons from DPNH to molecular oxygen is associated with a decrease in free energy of approx 50 Cals. A large fraction of this energy is trapped by the cell by coupling the oxidation to the conversion of ADP and inorganic phosphate into ATP.

It appears that three molecules of ATP are formed during the passage of two electrons through the redox coenzymes, and that one of these molecules of ATP is formed during the oxidation of DPNH by flavoprotein.

A possible mechanism for coupling ATP synthesis to oxidation at the DPN level is the following

---

*The following abbreviations are used: P, phosphate; PP, pyrophosphate; DPN, diphosphopyridine nucleotide; DPNH, reduced diphosphopyridine nucleotide; ADP, adenosine diphosphate; ATP adenosine triphosphate; EDTA ethylenediamine tetraacetic acid; FAD, flavin adenine dinucleotide.

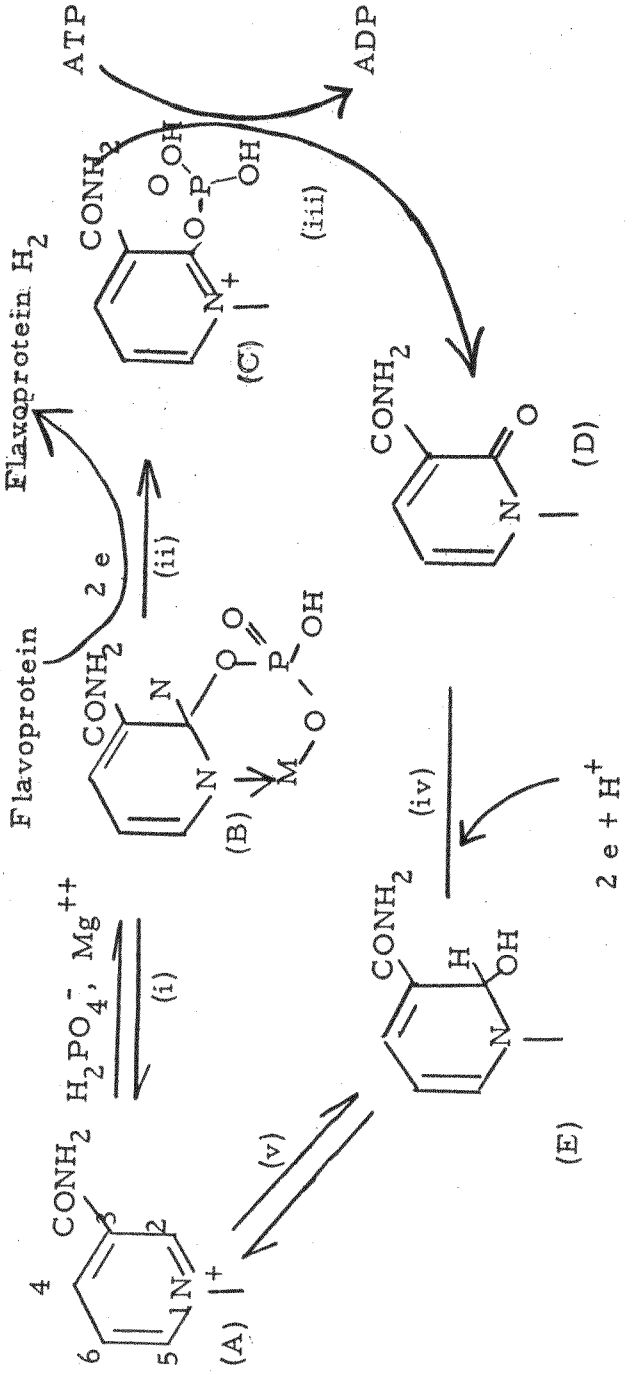
ATP
ADP
Flavoprotein H_2
Flavoprotein
2 e
(i)
(ii)
(iii)
(iv)
(v)
$H_2PO_4^-$, Mg^{++}
2 e + H^+
$CONH_2$
(A)
(B)
(C)
(D)
(E)

A is the nicotinamide residue of DPN, and is susceptible to anionoid attack by phosphate in the 2 or 6 positions. The formation of the adduct B will be assisted by chelation with a metal ion (M^+). Step (ii), the oxidation by flavoprotein, yields a pyridinium phosphate C, which on general grounds would be expected to be a high-energy phosphate capable of phosphorylating ADP to ATP. Such a transformation would lead to the production of the pyridone D of DPN. The reduction (iv) of the pyridone by substrate would yield the pseudobase E, which would be in equilibrium with DPN, A. A single revolution of the cycle would thus lead to the transfer of a pair of electrons from substrate to FAD, and the production of one molecule of ATP which is what the experimental evidence requires. The work here reported describes model experiments designed to test the feasibility of this scheme.

It was already known (unpublished observations by the author) that pyrophosphate links could be produced from systems of type C because the following reaction had been realized.

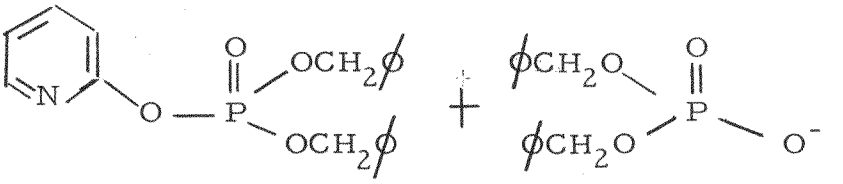

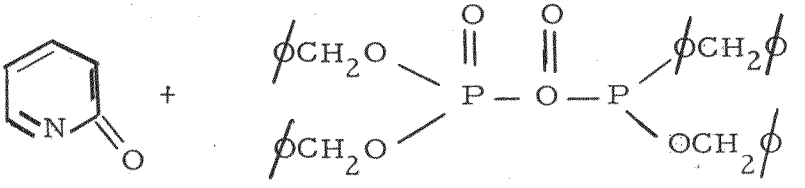

Thus Step (iii) seems to be thermodynamically and mechanistically possible.

We decided to investigate the system more closely by taking various pyridinium systems, A, treating them with P^{32} and a metal ion in order to establish the equilibrium (i), and then oxidizing this mixture in the hope that this would yield C, which should react with the excess phosphate present, giving radioactive pyrophosphate.

The isolation of radioactive pyrophosphate from such experiments would be evidence in support of the over-all scheme, for the chemical reduction of pyridones, D, to the pseudobases E is known, and the pseudobases are known to revert to pyridinium systems.

Experimental Methods and Results

1. Purification of the $P^{32}O_4$ Obtained from Oak Ridge

Carrier-free P^{32} obtained from Oak Ridge was shown by electrophoresis to have seven or eight radioactive components, including pyrophosphate. It was therefore made 1 N with respect to hydrogen ion by adding concentrated HCl and heated in a sealed tube at 110° for periods of 36 to 48 hr. This treatment converted most of the impurities, including the bulk of the pyrophosphate, to $P^{32}O_4$.

2. Electrophoretic Separation of Phosphate and Pyrophosphate

All separations of phosphate and pyrophosphate were effected by electrophoresis. Whatman No. 4 paper, washed with 0.2% disodium ethylenediamine tetraacetic acid (EDTA) and then ten times with deionized water, was soaked in 1 N acetic acid solution saturated with EDTA. The excess solution was removed by blotting between filter papers. The phosphate-pyrophosphate mixture was applied to the damp paper and the electrophoretic separation was conducted for about 2.5 hr under a potential gradient of about 20 v/cm, acetic acid–EDTA solution being present in the electrode compartment. Under these conditions, pyrophosphate migrated approx 35 cm and phosphate approx 24 cm.

3. Pyrophosphate Formation by DPN/Mn(II)/PO_4/Br_2 System.

Four solutions were made up from the components in Columns I, II, and III of Table XXXI.

Table XXXI. Composition of reaction solutions

Solution No.	I	II	III	IV	V (normalized counts/min in PP area)
1	DPN	P	Mn(II)	Br_2/H_2O	252
2	DPN	P	--	Br_2/H_2O	138
3	---	P	Mn(II)	Br_2/H_2O	104
4	DPN	P	Mn(II)	---	94

DPN, 30 μM; Mn(II), 25 μM; P, 35 μM containing approx 1/2 mC of P^{32}. Total volume, 120 μl per tube.

These solutions were adjusted to pH 5 with indicator paper, then allowed to stand at room temperature for 1-1/4 hr to allow the formation of the chelate. Bromine water (250 µl of 1 M) was added to solutions Nos. 1, 2, and 3 to effect oxidation, and water (250 µl) was added to solution No. 4. The mixtures were heated to 70° for 7 min, then treated with a few mg of K_2EDTA to dissolve the precipitates and break up any pyrophosphate complexes.

Aliquots (10 µl) of these mixtures were mixed with approx 2 µl of M/50 PP and applied to a moistened filter paper as in Experiment 2, and separated electrophoretically. Spraying with Hanes-Isherwood spray revealed the phosphate and pyrophosphate as blue spots which were excised, sandwiched between Mylar film, and counted with a Scott tube. The radioactivity in the various pyrophosphate areas, having been corrected for background, was normalized to 10^6 counts/min in the corresponding phosphate areas. In other words, the figures in column V of the table equal

$$\frac{\text{counts/min in pyrophosphate area}}{\text{counts/min in corresponding phosphate area}} \times 10^6 .$$

Examination of the table reveals

(a) that the complete system DPN/Mn(II)/PO_4/Br_2-H_2O (Solution 1) gives much more radioactive pyrophosphate than the other solution;

(b) that Mn(II) has a beneficial effect on the production of radioactive pyrophosphate (cf. Solutions 1 and 2);

(c) that in the absence of DPN, very little pyrophosphate is formed. The actual yield of pyrophosphate is very small (approx 0.01 %), and the possibility exists that it is derived by oxidative breakdown of DPN, liberating "dead" pyrophosphate, which then exchanges with the $P^{32}O_4$, giving rise to radioactive pyrophosphate.

4. Pyrophosphate from DPN/Mg(II)/PO_4/Br_2-H_2O

Four solutions were made up, containing the contents specified in columns I, II, and III of Table XXXII.

Table XXXII. Composition of solutions

Solution No.	I	II	III	IV	V (normalized counts/min
1	DPN	P	Mg	Br_2-H_2O	1798
2	DPN	P	--	Br_2-H_2O	745
3	--	P	Mg	Br_2-H_2O	268
4	DPN	P	Mg	---	17

DPN, 30 μM; P, 50 μM of PO_4 + approx. 1/2 mC of $P^{32}O_4$; Mg(II), 25 μM. Total volume, 125 μl.

The pH was adjusted to 7 with universal indicator. After 30 min, bromine water (250 μl of 1 M) was added to solutions Nos. 1, 2 and 3, and 250 μl of water was added to solution No. 4. The mixtures were then heated at 60° for 10 min. Treatment with K_2EDTA followed by electrophoresis and counting of the radioactive pyrophosphate and phosphate spots gave the results shown in column V of Table XXXII.

The following comments may be pertinent:

(a) Exposing the electrophoretogram to x-ray film showed that the radioactivity in the PP area corresponded exactly with the blue PP spot given by the added ^{31}PP. In other words, the radioactivity in the PP area is due only to pyrophosphate.

(b) The ^{32}PP is not formed by exchange between the ^{31}PP added to the aliquots before electrophoresis and the excess $^{32}P\ O_4$ in the reaction mixture, because the cpm in the PP area was (within the limits of experimental error) independent of whether or not ^{31}PP was added.

(c) Comparison with the preceding experiment, shows an enormous increase in the amount of radioactivity in the PP area corresponding to the solution No. 1 in this experiment. This may be ascribed to replacing Mn(II) by Mg(II) or to changing the pH from 5 to 7, or both.

(d) The yield of PP in this experiment, if it is derived by synthesis from OO_4 , and not by exchange with the PP link of DPN, is approx 0.2%.

(e) The metal ion again exercises a beneficial effect on the yield of PP.

(f) Some ^{32}PP is formed even in the absence of DPN, i.e., from a purely inorganic system of Mg(II)/PO_4/Br_2-H_2O.

5. Pyrophosphate from N-methyl-nicotinamidinium perchlorate/PO_4/Br_2-H_2O

In Experiments 3 and 4 above, the possibility existed that the ^{32}PP formed was derived by oxidative breakdown of the DPN molecule with the liberation of ^{31}PP, which then experienced exchange with the P^{32} to give ^{32}PP. To eliminate this possibility, an experiment was conducted with the methoperchlorate of nicotinamide. The experiment and results are shown in Table XXXIII.

Table XXXIII. Reaction Solutions

Solution No.	I	II	III	IV	V (normalized counts/min in PP areas)
1	N	P	Mg	Br_2-H_2O	366
2	--	P	Mg	Br_2-H_2O	65
3	N	P	--	Br_2-H_2O	116
4	N	P	Mg	---	31
5	N	P	Mg	$Cr_2O_7^{--}$	35

N = nicotinamide methoperchlorate (25.3 μM); P + phosphate (50 μM) + $^{32}PO_4$; Mg(II) (25 μM). Total volume, 125 μl.

This experiment was conducted in the same manner as the previous experiments. The oxidizing agents used were 1 M bromine-water (125 μl) and $Na_2Cr_2O_7$ (50 μl M/10). The volumes of all solutions were equalized by adding water. The solutions were warmed to 60° for 10 min. The radioactivity found in the PP areas after electrophoresis, normalized to 10^6 counts/min in the corresponding P areas, are recorded in column V. We note:

(a) significant amounts of PP were formed in solution No. 1, where all three components were present.

(b) The PP found in these solutions can be formed only from inorganic phosphate.

(c) Omission of the Mg(II) again markedly dropped the yield.

(d) $Cr_2O_7^{--}$ is valueless as an oxidizing agent in this system.

(e) Again, small amounts of PP are formed in a purely inorganic system.

(f) The smaller yield of PP (by comparison with that obtained in Experiment 4) may possibly be partly ascribed to the enhanced effect of chelation with the polydentate system of DPN:

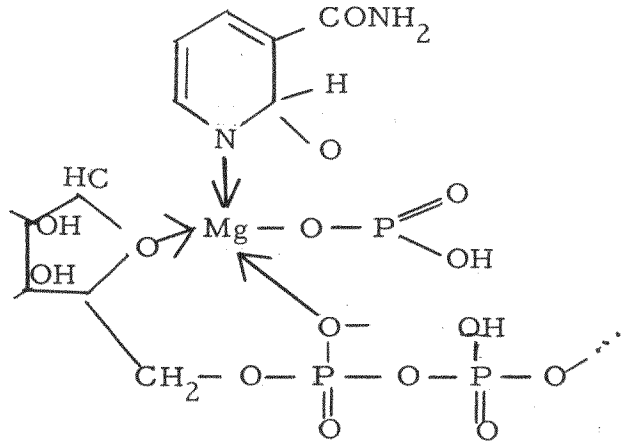

6. Effect of Other Oxidizing Agents on PP Formation in the Nicotinamide System

In all the previous experiments, the oxidative step has been effected with bromine-water. This has the disadvantage that it contains considerable amounts of HBr, so that the pH deviates markedly from 7. Therefore, we decided to examine the effect of other neutral oxidizing agents on the nicotinamide methoperchlorate/phosphate/Mg(II) system.

Solutions were made up, and gave results, as shown in Table XXXIV.

Table XXXIV. Reaction solutions

	I	II	III	IV	V Activity (normalized, counts/min in PP area)	VI (normalized cpm in PP area 2nd oxidation)
No. 1	N	P	Mg	$K_3Fe(CN)_6$	280	283
No. 2	N	P	Mg	H_2O_2	410	--
No. 3	N	P	Mg	H_2O_2/Fe^{II}	1269	2346
No. 4	N	P	Mg	$NaIO_4$	145	203
No. 5	N	P	Mg	$KMnO_4$	248	633
No. 6	N	P	Mg	---	103	

N = nicotinamide methoperchlorate (20 μM); P, 40 μM; Mg(II), 20 μM. Total volume, 100 μl.

The oxidizing agents used were

H_2O_2	100 µl M/10; H_2O_2 ,
$K_3Fe(CN)_6$, $KMnO_4$	100 µl of 1 M;
$NaIO_4$	H_2O_2/Fe(II), (100 µl of 1 M H_2O_2 + a small amount of ferrous ammonium sulfate).

After heating at 60° for 10 min, etc., and electrophoresis, the normalized activities found in the PP area were found to be as in column V. Three days later, the same amounts of the oxidizing agents were added again. Electrophoresis and counting of the P and PP area gave the figures in column VI.

From this experiment we can draw these conclusions.

(a) It appears that all the oxidizing agents tried, with the possible exception of $K_3Fe(CN)_6$, induced the formation of PP in this system.

(b) It appears also that Fenton's reagent is by far the best oxidizing agent.

(c) Control experiments show that the radioactivity in the PP area derived from the use of Fenton's reagent is not formed by exchange between the $^{32}PO_4$ in the reaction mixtures and the ^{31}PP added before electrophoresis.

(d) The possibility, however, remains that significant amounts of the radioactivity found in the PP area derived from the use of Fenton's reagent might arise by some unknown mechanism from the purely inorganic system Mg(II)/PO_4/Fe(II)-H_2O_2 . This possibility is under investigation.

It would seem that we have here a system capable of effecting oxidative phosphorylation in vitro. It remains to define more clearly the parameters controlling the system and to conduct biological experiments to determine whether or not this proposed cycle actually operates in mitochondria. These experiments are in progress.

F. ANIMAL BIOCHEMISTRY

1. EFFECT OF ETHANOL INGESTION ON ALCOHOL DEHYDROGENASE IN LIVERS OF MICE

Marie Hebert and Edward L. Bennett
(in collaboration with Gerald E. McClearn, Dept. of Psychology, University of California)

We have previously shown that the preference for 10% ethanol exhibited by some male mice from highly inbred strains is correlated with the alcohol dehydrogenase (ADH) activity of their livers.[1] Preliminary data suggested that this enzyme activity might be changed if the animals were required to drink 10% ethanol solution by providing them with no other liquid. Eleven male DBA strain (water-preference mice) and nine male C_{57} strain (alcohol-preference mice) were divided into two groups, one group receiving water as their only liquid, and the other group receiving 10% ethanol. At the end of a 2-week period the mice were sacrificed and the ADH activity of their livers was determined.

Method of Analysis

We have modified our analytical method from that reported in June 1960[1] to obtain faster ethanol oxidation.

Mice were sacrificed in random order. Livers were removed, weighed, and immediately homogenized in a Potter-type teflon pestle homogenizer with distilled water at O° C to make a final liver concentration of 50 mg/ml. The homogenates were then centrifuged in an International refrigerated centrifuge at O° C for 30 min at 3000 rmp. The supernatant solution below the top fatty layer was used for assays.

Solutions used:

Buffer: 2.5 parts 0.2 N NaOH,
7 parts 0.1 N glycine in 0.1 N NaCl,
1 part
semicarbazide solution (1.66 g semicarbazide-HCl in 100 ml 0.1 N NaOH),
Final pH ≈ 9.5;

DPN (Diphosphopyridine nucleotide) 10 mg/ml H_2O;

EtOH 2% Ethanol in water.

[1] Edward L. Bennett and Marie Hebert, in Bio-Organic Chemistry Quarterly Report, UCRL-9208, June 1960, p. 125.

The following amounts of the above reagents were mixed in a 1-cm-light-path Beckman DU spectrophotometer cuvette:

3.0 ml Buffer solution

200 µl DPN (3.02 µM)

50 µl 2% EtOH (17.2 µM)

This solution was prewarmed inside the spectrophotometer, which was kept at 37.8°C (by a heating unit attachment) for 10 minutes. Then 50 µl centrifuged liver homogenate was added (2.5 mg liver). Optical density was recorded by an optical density converter and automatic cuvette positioner[2] and rate curves were obtained on a Leeds and Northrup recorder. The average optical density change for the first 10 minutes was determined from the rate curves.

It was found unnecessary to run blanks (runs omitting EtOH), since the rate of the blank reaction was essentially zero after the first few minutes.

In our calculations we assume a stoichiometry of one DPN reduced to one EtOH oxidized.

Experimental Results

As was indicated earlier, the mice forced on ethanol for 2 weeks showed higher ADH activity than those receiving only water (Table XXXV). Although drinking alcohol also raises liver weight, the enzymes level is higher even when expressed on a basis of unit liver weight. Total body weight is not significantly changed by alcohol drinking.

A replication is planned which will triple the number of animals studied in each group. Later, we may study the effect of lengthening and shortening the period of ethanol administration.

Summary

A higher level of alcohol dehydrogenase activity is induced by the ingestion of ethanol for a 2-week period. This increase has been shown for both the DBA (water-preference) and C_{57} (ethanol-preference) strains of mice. There is some indication that the C_{57} strain shows a greater ADH increase.

[2] Gilford Instrument Co., Oberlin, Ohio.

Table XXXV. Rate of oxidation of EtOH by mouse liver homogenates

	C_{57} Mice		DBA Mice	
	drinking EtOH (5 mice)	drinking H_2O (4 mice)	drinking EtOH (5 mice)	drinking H_2O (6 mice)
EtOH oxidized:				
μM/min/g liver	6.29 ± .25[a]	5.42 ± .29	4.93 ± .13	4.36 ± .36
μM/min/liver	8.63 ± .93	6.69 ± 1.15	4.95 ± .81	4.07 ± .12
μM/min/g mouse	.399 ± .036	.290 ± .038	.263 ± .021	.221 ± .012
Average Liver Weights	1.37 ± .19	1.23 ± .32	1.01 ± .18	0.94 ± .12
Average Body Weights	21.71 ± 2.28	22.95 ± 1.42	18.77 ± 2.26	18.47 ± 2.44

[a] Average ± $\bar{\sigma}$; $\bar{\sigma} = \sqrt{\frac{\Sigma x^2}{N-1} - \frac{(\Sigma x)^2}{N(N-1)}}$

2. FACILITATIVE AND DISRUPTIVE EFFECTS OF STRYCHNINE SULPHATE ON MAZE LEARNING

James L. McGaugh*

Several studies have shown that, in rats, injections of depressant drugs administered either shortly before or shortly after training trials impair learning.[1] These results, along with those obtained from studies of the retroactive effects of electroconvulsive shock and anoxia on learning,[2] support the general hypothesis that the amount learned on each trial depends upon the extent of perseveration of the neural activity initiated by the trial.[3] Since disruption of neural activity with central nervous system depressants has been shown to impair learning, it might be possible to facilitate learning by enhancing perseveration with central nervous system stimulants. To date, there have been few investigations of this hypothesis.

Strychnine sulphate is one of the most potent central nervous system stimulants.[4] Physiological studies have shown that in low concentrations strychnine lowers synaptic thresholds whereas high concentrations raise them. If it is assumed that degree of neural perseveration depends upon synaptic thresholds, then low doses of strychnine sulphate might facilitate learning.

In 1917 Lashley reported that low doses of strychnine sulphate facilitated the rate at which rats learned a Watson maze.[5] Recently, McGaugh and Petrinovich reported similar findings using a Lashley III alley maze.[6] A further study of this problem using a complex 14-unit alley maze is reported here.

Experiment I

Subjects

The Ss were 71 naive male hooded rats of the S_{13} strain maintained at the University of California. This strain consists of descendents of crosses between the Tryon maze-bright and maze-dull strains. All subjects (Ss) were between 70 and 80 days old when training was begun.

---

*Present address, Psychology Dept., San Jose State College.

[1] M.R. Rosenzweig, D. Krech, and E.L Bennett, Science 123, 371 (1956); F. Leukel, J. Comp. Physiol. Psychol. 50, 300 (1957); C. Pearlman, S.K. Sharpless, and M.E. Jarvik, Fed. Proc. 18, #1 (1959).

[2] R. Thompson and W.A. Dean, J. Comp. Physiol. Psychol. 48, 488 (1955); R. Thompson and R.S. Pryer, J. Comp. Physiol Psychol. 49, 297 (1956).

[3] G.E. Mueller and A. Pilsecker, Z. Psychol. 1, (1900); D.O. Hebb, The Organization of Behavior (1949).

[4] P. Heinbecker and S.H. Bartley, Am. J. Physiol. 125, 172 (1939).

[5] K.S. Lashley, Psychbiol, 1, 141 (1917).

[6] J.L. McGaugh and L. Petrinovich, Am. J. Psychol. 72, 99 (1959).

Apparatus

A 14-unit automatically recording alley maze was used. Each alley was 4 inches wide, 5 inches high, and 32 inches long and was painted medium gray. Each alley contained two black doors, one on either side of the entrance, hinged at the top and 6 inches from the entrance. Microswitches behind blind-alley doors activated Veeder-Root counters on a control panel. Correct doors swung up to allow Ss to progress through the maze. A bell signaled a S's entry into the goal box.

The pretraining apparatus consisted of the starting unit of the maze and an 8-unit goal box joined by a 48-inch alley containing four doors identical to those in the maze.

Preliminary Training

The Ss were first pretrained for nine days in the straight alley. During this period the Ss learned to operate the doors. Body weights were reduced to and maintained at 85% of their pre-experimental weights following the initial 24-hour food deprivation. A highly palatable wet mash (Simonsen's White Diet) was used as a reward.

Maze Training

On the tenth day and every subsequent day for 14 days each S was given one trial in the maze. Two minutes of feeding in the goal box followed each run, and additional wet mash was given in the home cages after all Ss were run. The order in which the Ss were run was varied systematically from day to day. Errors were automatically recorded on the counters each time a S pushed against an incorrect door.

Design

On the seventh day of pre-training, Ss were assigned to experimental and control groups. On this and each subsequent day, each S was injected intraperitoneally with 1.00 cc per kg of body weight of either a 0.9% saline solution (normal saline) or a strychnine sulphate solution (in normal saline), and was then placed in a retaining cage for 10 minutes before the daily trial.

The 29 control (C) Ss received normal saline. The 13 low-strychnine (LS) Ss received 0.33-mg/cc strychnine sulphate solution and the 29 high-strychnine (HS) Ss received 1.00-mg/cc strychnine sulphate solution.[7]

Results

Twenty-two Ss (7C, 5LS, and 10 HS) were discarded. These Ss displayed excessive emotionality (e.g. urination, defecation, crouching, freezing, biting, and fighting) and were unable to complete all the training. Ss of this strain (S_{13}) displayed similar behavior in other experiments. Consequently, this strain have since been discontinued.

[7] These doses were previously calculated to be about 1/6 and 1/2 of the average lethal amounts for an earlier generation of Ss of the S_{13} strain.

The results of the 49 successful Ss are shown in Fig. 76. As can be seen, the LS Ss were superior to the C Ss, while the HS made more errors than the C Ss. Although these groups did not differ significantly according to a Kruskal and Wallace test,[8] ($0.25 > p > 0.10$), these results suggest that maze learning may possibly be facilitated by a low dose of strychnine and disrupted by a high dose.

An inspection of the individual error scores revealed that the best Ss (i.e., those with the lowest error scores) in the LS group had lower scores than those in either the C or HS groups. To test the significance of this observation each group was divided into subgroups consisting of those above the median in errors for the particular group and those at or below the median. As can be seen in Fig. 76, the best LS Ss averaged fewer errors than the best C Ss while the best HS Ss made more errors, on the average, than the C Ss. A Kruskal and Wallace analysis of these groups was significant at the 0.02 level of significance. Mann-Whitney U Tests[9] indicated that the best LS Ss were significantly superior to both the C Ss ($p < .02$) and the RS Ss ($p < .002$). The C and HS Ss, however, did not differ significantly.

In order to investigate possible disruptive effects of the high strychnine dose, a similar analysis was made of the worst Ss (i.e., those above the median in errors) in each group. As Fig. 76 shows, the worst C Ss averaged fewer errors than either the LS or the HS Ss. Although a Kruskal-Wallace test failed to reach statistical significance ($0.25 > p > 0.10$), a Mann-Whitney U Test indicated that the C and HS Ss differed at the 5% level of significance.

Thus, although an over-all test failed to reveal statistically significant differences among the three groups of Ss, analyses of the best and worst Ss indicate that the learning of some Ss is facilitated by a low dose of strychnine sulphate and that the learning of some Ss is disrupted by a high dose.

---

[8] H. M. Walker and J. Lev, Statistical Inference (1953), 436.

[9] Ibid., 434.

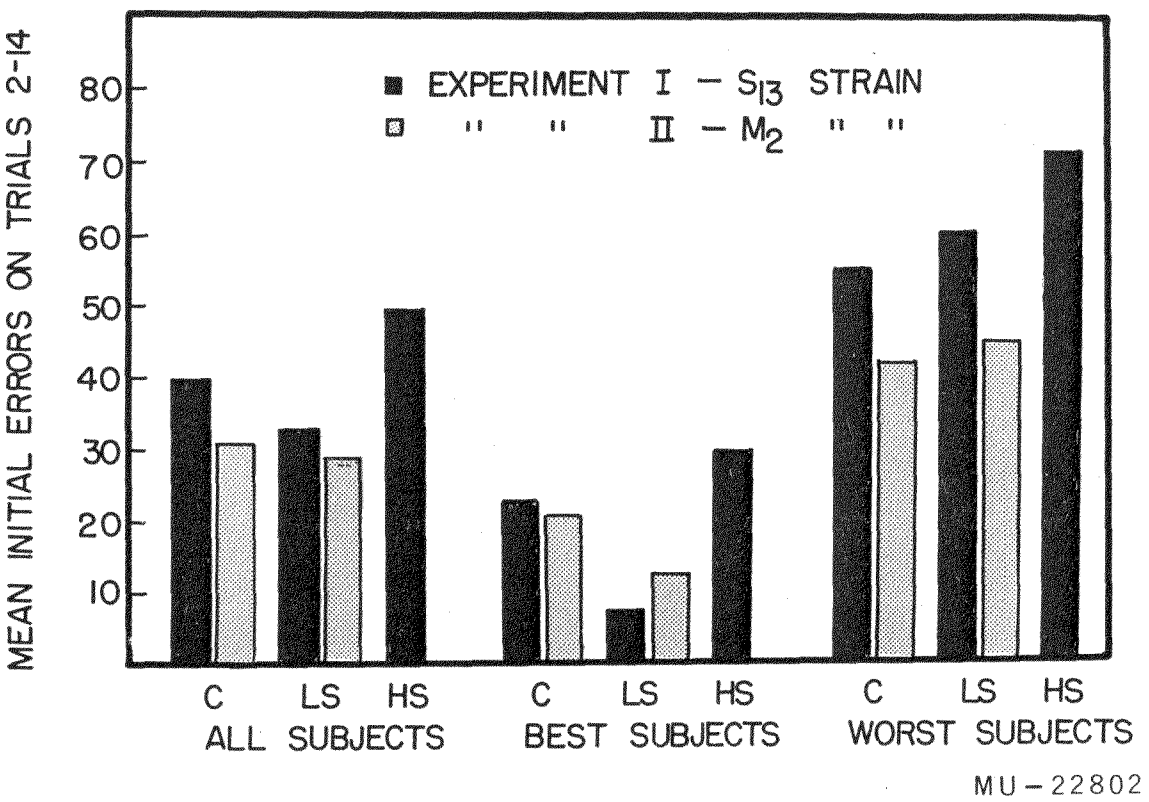

Fig. 76. Mean number of initial errors made by all subjects, the best subjects, and the worst subjects on trials 2 through 14 in the 14-unit maze. Repetitive errors were not recorded, since multiple pushes on the doors and re-entries could not be separately recorded.

Experiment II

Since the particular subgroup analyses reported in Experiment I were suggested by an inspection of the data, and since almost a third of the Ss failed to complete the training, a portion of the experimnet was repeated with Ss from another strain of rats. The number of Ss was limited so that only the C and LS groups were replicated.

Subjects

The Ss were 26 naive male hooded rats of the M_2 strain maintained at the University of California. These Ss were also descendents of crosses between the Tryon maze-bright and maze-dull strains. All Ss were between 70 and 80 days old when the experiment was begun.

Apparatus and Procedure

The same apparatus and procedure were used as in Experiment I. Thirteen Ss were assigned to the C group and 13 were assigned to the LS group.

Results

All 26 Ss completed the training procedure. As can be seen in Fig. 76, the mean number of errors made by the LS Ss was slightly lower than that of the C Ss. The two groups did not differ significantly, however, according to a Mann-Whitney U Test. As in Experiment I, a further analysis was made of the scores of the best and worst Ss in each group. As Fig. 76 shows, the best LS Ss averaged fewer errors than the best C Ss. The difference between the two groups was significant at the 2% level according to a Mann-Whitney U Test. As in Experiment I, the worst Ss in the C and LS groups did not differ significantly.

Thus, the results of Experiment II replicated those of Experiment I; the low dose of strychnine facilitated the learning of some of the animals.

Discussion

The results of these experiments indicate that maze learning is facilitated by a low dose of strychnine and disrupted by a high dose. Although the facilitative and disruptive effects are found in only some of the Ss, the present results are similar to those of other experiments and provide additional support for the hypothesis that facilitation of neural perseveration via central nervous system stimulation facilitates learning.

The finding of impairment with the high dose is consistent with the finding (reported above) that synaptic thresholds are increased by large concentrations of strychnine. The finding that only some animals were affected

by either dose indicates that there are individual differences in susceptibility to the drug.[10]

The mechanism by which strychnine stimulates central nervous system activity is not as yet known. Bradley, Easton, and Eccles have argued that strychnine stimulates indirectly by inhibiting some inhibitory transmitter substance.[11] Another possibility is that facilitation may result from slight accumulation of acetylcholine (ACh) due to an inhibition of the enzyme acetylcholinesterase (ChE). Nachmansohn has shown that strychnine is capable of inhibiting ChE activity in vitro.[12] Since the transmitter substance ACh is a stimulant when present in samll quantities, in some Ss a slight increase in ACh might stimulate central nervous system activity and, hence, increase neural perseveration. This hypothesis is consistent with the evidence that, within the strains used in this study, Ss with low ChE activity are superior to those with high ChE activity.[13] It is also consistent with findings of other experimenters that slight reduction in ChE activity facilitates learning while severe reduction impairs learning.[14]

Although the hypothesis that the effects of strychnine on learning are due to ChE inhibiiton seems to be consistent with a number of studies, the hypothesis that the effects are due to blocking of an inhibitory transmitter substance is also tenable. Since the indirect effects of such inhibition is central nervous system facilitation, either of the proposed interpretations is consistent with the general hypothesis that learning can be facilitated by central nervous system stimulants. Further studies are necessary to determine if facilitation of learning is limited to drugs known to affect the ACh-ChE system. A number of experiments with other stimulants, currently in progress, will be reported shortly.

---

[10] McGaugh and Petrinovich found facilitating effects with the high dose used in this study (1.00 mg/kg) on the learning of Ss from an earlier generation of the S_{13} strain. However, since no animals had to be discarded from their study, whereas 31% of the S_{13} Ss in this study had to be discarded owing to excessive emotionality, it seems highly probable that the S_{13} Ss used in this study were different from the S_{13} Ss used in the study by McGaugh and Petrinovich. This suggests that the effect of the particular high dose used in these studeis depends upon the particular Ss used.

[11] K. Bradley, D.M. Easton, and J.C. Eccles, J. Physiol. 122, 474 (1953).

[12] D. Nachmansohn, Compt. rend soc. biol. 129, 941 (1938).

[13] J.L. McGaugh, Some Neurochemical Factors in Learning (Thesis), University of California, 1959.

[14] C.E. Platt, Thesis, Ohio State University, 1951; R.W. Russell, Sump. Biochemical Process and Behavior, Internatl. Congr. Psychol., Brussels, 1957.

Summary

In Experiment I, two experimental groups injected with different amounts of strychnine sulphate and a control group were trained on a 14-unit maze. In Experiment II, the control and low-strychnine-dose groups of experiment I were replicated with Ss of another strain. The maze performance of the best low-strychnine-dose Ss was superior (in terms of errors) to that of the best control and the best high-strychnine-dose Ss. The maze performance of the worst Ss of the high-strychnine-dose Ss was inferior to that of the worst control Ss. The significance of these finding is discussed.

3. THE SPECTROFLUOROMETRIC MICRODETERMINATION OF SEROTONIN

Hiromi Morimoto and Gordon Pryor

Serotonin (5-hydroxytryptamine)(5-HT) has been implicated as a potentially important neurohumor. Primarily, this is based on its selectively high distribution in brain tissues of biologically uniform systems, and on its ability to increase the permeability of membranes to potassium ions. A further indication is the striking relation between the levels of 5-HT to those of 5-hydroxytryptophane decarboxylase and monoamine oxidase, the enzymes which synthesize and degrade 5-HT. The monoamine oxidase, however, appears to be exclusively intracellular.

Acetylcholine is well known to be important as a neurotransmittor in the peripheral nervous system and it is thought to have this role in the central nervous system. At those synapses in the peripheral nervous system were acetylcholine is not the mediator, other substances, noradrenaline and adrenaline, are the mediator substances. This may also be true in the central nervous system where adrenalin, noradrenalin, serotonin, γ-amino butyric acid, and histamine have been suggested as the active compounds.

Krech, Rosenzweig, and Bennett[1] have demonstrated brain cholinesterase levels (ChE) to be related to behavioral differences among rats. Further, they have shown that ChE levels can be modified by environmental manipulation.[2] Their success prompts the investigation of serotonin in the central nervous system.

Of prime importance in this respect is the posterior hypothalamus, which, when stimulated electrically, produces peripheral autonomic responses. These responses occur as sympathetic nervous system discharges, i.e., increased heart rate, vasconstriction, etc. Also of importance may be the brain stem, where many vegatative centers are found which act via the autonomic nervous system. Both of these areas are high in serotonin content in comparison with the rest of the brain.

Since "experience" has been shown to influence ChE activity in rat brain, it is hypothesized that experience relevant to areas utilizing serotonin will also influence such areas. The experience most likely to do so would be "stress," if the aforementioned connection between brain serotonin and sympathetic output is correct.

The examination of small sections of neural tissues for serotonin has been delayed by lack of a rapid and accurate assay sensitive to the low concentrations found in these fractions. The sensitivity and specificity of the

---

[1] M.R. Rosenzweig, D. Krech, and E.L. Bennett, Psych. Bull 57, 476 (1960).

[2] D. Krech, M.R. Rosenzweig, and E.L. Bennett, J. Comp. Physiol. Psychol. 53 1 (1960).

[3] D.F. Bogdanski, A. Pletscher, B.B. Brodie, and S. Udenfriend, J. Pharmacol. Exptl. Therap. 117, 82 (1956).

known bioassays are uncertain. This report describes the extraction and microdetermination of serotonin by using a modification of Bogdanski's method.[3] In this method, after concentration of the serotonin in an acid solution, the quantity is determined by spectrofluorometry.

Frozen cerebral tissue is homogenized with 4 to 6 ml of 0.1 N HCl in the presence of ascorbic acid. A salt-saturated borate buffer (pH 10) is added to the homogenate and the serotonin is extracted into butanol. With 1 μg of serotonin, the solubility in the salt-saturated buffer is such that only 95% of the serotonin can be extracted into the organic phase. The solubility of serotonin in butanol is then decreased by addition of heptane, and the serotonin is re-extracted into an acidic aqueous phase. Addition of 2 volumes of heptane to the butanol permits nearly quantitative re-extraction of the serotonin into an acidic aqueous phase (Table XXXVI). Serotonin is somewhat more stable when extracted with tissue, and some water dissolved in the butanol precipitates out on addition of heptane. Therefore standards containing known amounts of serotonin are carried through the extraction procedure.

The concentration of serotonin in the acidic aqueous extract is determined spectrofluorometrically using an Aminco-Bowman spectrofluorometer. Serotonin in 3 N HCl fluoresces maximally at 550 mμ upon activation at 305 mμ (Figs. 77 and 78). At pH 4, serotonin fluoresces maximally at 330 mμ. However, at this wave length fluorescence from other materials in the brain interfere with the analyses. The fluorescence is linear from 0.01 μg/ml to 10 μg/ml, but a minimum of 0.25 μg is required for accurate determinations.

Method

Reagents

Borate buffer: 94.2 g boric acid was dissolved in 3 liters of water and 165 ml 10 N NaOH was added. This solution was saturated with n-butanol and NaCl.

n-Butanol and n-heptane: reagent grade solvents were washed with 1 N NaOH in HCl and three times with deionized water.

Procedure

1. Tissues are homogenized in 4 to 6 ml of 0.1 N HCl in the presence of 30 mg of ascorbic acid.

2. The homogenate and 1 ml of 1% EDTA are placed in a 50-ml glass-stoppered centrifuge tube.

3. Approximately 5 g of NaCl and 5 ml of borate buffer are added.

4. After addition of 15 ml BuOH, the tubes are mixed thoroughly.

5. Thirteen ml of the BuOH phase is put into another tube containing 1.0 cc 0.1 N HCl, after which 25 ml of heptane is added. After thorough mixing, the tubes are centrifuged for several minutes at 1200 rpm.

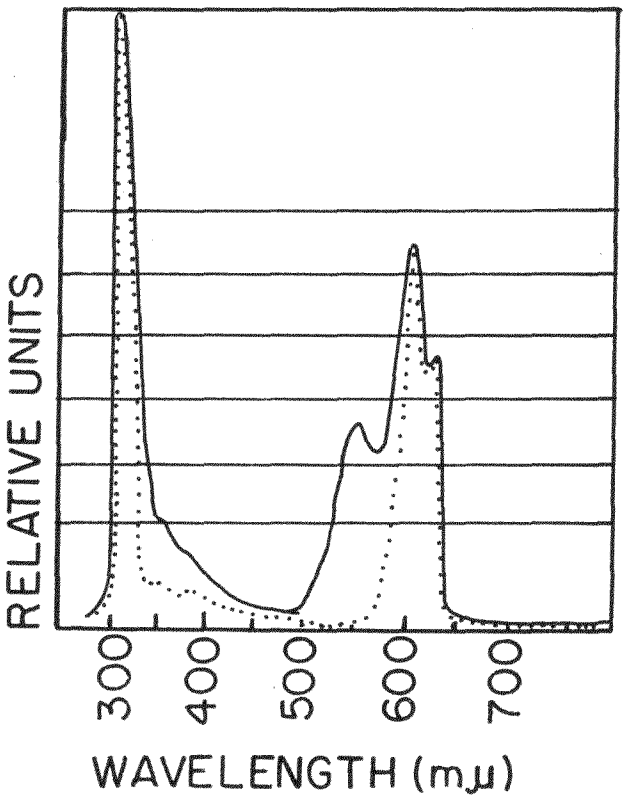

Fig. 77. Fluorescence spectra of serotonin (1 μg/ml) — activation at 305 mμ.

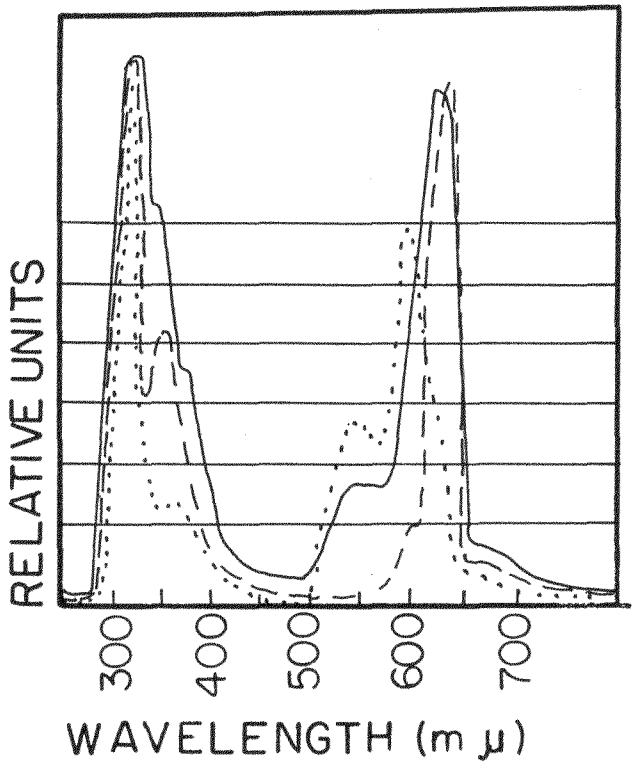

Fig. 78. Fluorescence spectra of serotonin (1 μg/g). Various pH. - - - - at 1/3 the magnitude of the other two curves.

Table XXXVI. Extractability of serotonin

Extraction volume of BuOH (ml)	Aliquot of BuOH taken (ml)	Volume of heptane added (ml)	Extraction (%)
15	8	25	100
15	8	25	93
15	12	25	93
15	12	25	92
15	12	30	90.5
15	12	30	93
15	12	35	92
15	12	35	88

6. The organic solvent is removed by aspiration and discarded and then 1.0 ml of the acid phase is removed and mixed with 0.3 ml conc. HCl.

7. The acid extract is activated at 305 mμ and fluorescence is read at 550 mμ. Literature cites activation wave length as 295 mμ, but maximal fluorescence occurs at 305 in our Aminco-Bowman spectrofluorometer. Slit arrangement number 4 is used.

8. Standards of known serotonin concentration with about 100 mg of cerebellar tissue (very low in serotonin) are run through the extraction procedure with samples.

In order to determine the reproducibility of the method, the brains from four 30-day-old S_1 rats were pooled and aliquot portions analyzed. The concentrations found for whole brain (minus cerebellum) were 0.479, 0.470, and 0.470 μg/g. With 55-day-old rats, the values obtained for hypothalamus, brain stem, and remainder of brain (minus cerebellum) are recorded in Table XXXVII. These values are in good agreement with those reported by Kato,[4] when one makes allowances for dissection differences.

Experiments are now in progress to study the effects of stress (electrical shock) on serotonin levels in various areas of the rat brain.

[4] R. Kato, J. Neurochem. 4, 202 (1959).

Table XXXVII. Serotonin content of 55-day S_1 rat brain (μg/g)

Section	Male			Female		
Hypothalamus	0.76	S.E.M.	0.07	0.98	S.E.M.	0.18
Brain stem	0.87		0.4	0.90		0.04
Remainder	0.56		0.02	0.59		0.02